**Universidade de São Paulo**
Brasil

**Instituto de Química - Departamento de Bioquímica**

**Thiago Cardoso Genaro de Mattos**

# MODIFICAÇÃO DE PROTEÍNAS POR PRODUTOS DE OXIDAÇÃO DO COLESTEROL: MECANISMOS E IMPLICAÇÕES BIOLÓGICAS

**Versão original da Tese a ser defendida**

São Paulo

LOMBADA

Thiago C. G. Mattos

Modificação de proteínas por produtos de oxidação
do colesterol: mecanismos e implicações biológicas

Doutorado
IQ-USP 2014

Data do Depósito na SPG:

**Universidade de São Paulo**
Brasil

**Instituto de Química - Departamento de Bioquímica**

**Thiago Cardoso Genaro de Mattos**

# MODIFICAÇÃO DE PROTEÍNAS POR PRODUTOS DE OXIDAÇÃO DO COLESTEROL: MECANISMOS E IMPLICAÇÕES BIOLÓGICAS

Tese apresentada à secretaria de pós-graduação do Instituto de Química da Universidade de São Paulo para a obtenção do título de doutor em Ciências Biológicas.

Área de concentração: Bioquímica

Orientador: Profa. Dra. Sayuri Miyamoto

São Paulo

Agosto de 2014

Autorizo a reprodução e divulgação total ou parcial deste trabalho, por qualquer meio convencional ou eletrônico, para fins de estudo e pesquisa, desde que citada a fonte.

FOLHA CATALOGRÁFICA

Genaro-Mattos, T. C. Oxiesteróis como potenciais modificadores de proteínas. Tese apresentada ao Instituto de Química da Universidade de São Paulo para a obtenção do título de doutor em Ciências Biológicas.

Aprovado em: _____/_____/_____

Banca examinadora

Prof. Dr. _____ Instituição:_____
Julgamento:_____ Assinatura:_____


Prof. Dr. _____ Instituição:_____
Julgamento:_____ Assinatura:_____


Prof. Dr. _____ Instituição:_____
Julgamento:_____ Assinatura:_____


Prof. Dr. _____ Instituição:_____
Julgamento:_____ Assinatura:_____


Prof. Dr. _____ Instituição:_____
Julgamento:_____ Assinatura:_____

*"To see the world, things dangerous to come, to see behind walls, to draw closer, to find each other and to feel. That's the purpose of life."*

The Secret Life of Walter Mitty, adapted from the *Life* magazine motto.

*"I am among those who think that science has great beauty. A scientist in his laboratory is not only a technician: he is also a child placed before natural phenomena, which impresses him like a fairy tale. We should not allow it to be believed that all scientific progress can be reduced to mechanisms, machines, gearings, even though such machinery also has its beauty."*

Marie Curie

*À minha família e amigos.*

# AGRADECIMENTOS

# SUMMARY

# RESUMO

O colesterol é um importante componente das membranas celulares em eucariotos superiores, desempenhando papéis estruturais e funcionais. O colesterol possui uma insaturação em sua estrutura sendo, portanto, alvo de oxidação mediada por espécies reativas de oxigênio e/ou nitrogênio. A oxidação não enzimática do colesterol gera, como produtos primários, os hidroperóxidos de colesterol. Tais moléculas, por sua vez, são altamente reativas e podem reagir com metais livres e/ou metaloproteínas, trazendo consequências à celula. Neste sentido, o primeiro capítulo deste trabalho tem como objetivo estudar a reação dos hidroperóxidos de colesterol (ChOOH) com o citocromo c (citc), uma heme proteína envolvida no transporte de elétrons na mitocôndria. Análises de espectroscopia no UV-Vis mostraram que o ChOOH promove o bleaching da banda Soret do citc de uma maneira dose-dependente. Mais ainda, esta reação leva à formação de radicais centrados em carbono tanto na proteína como no lipídeo, sugerindo uma redução homolítica do ChOOH. Como consequências, pode-se observar a oligomerização do citc, um processo que pode influenciar no transporte de elétrons bem como na sinalização para a apoptose. A partir da reação do citc com ChOOH podem surgir, direta ou indiretamente, outras espécies reativas, como aldeídos, cetonas e epóxidos. Dentre estas, destacam-se os aldeídos de colesterol, em particular o colesterol secoaldeído (CSec) e o carboxialdeído (ChAld), uma vez que foram encontrados elevados em placas ateroscleróticas e em tecidos cerebrais de pacientes com doenças neurodegenerativas. Tais espécies podem reagir com resíduos de aminoácidos provocando alterações estruturais e funcionais em proteínas. Neste sentido, o segundo capítulo deste trabalho tem como objetivo estudar a reação do ChAld com citc. Usando modelos miméticos de membrana e espectrometria de massas, foi mostrado que o ChAld modifica covalentemente o citc por um mecanismo consistente com a formação de bases de Schiff. Tal modificação ocorre preferencialmente em resíduos de lisina que interagem com a membrana. Estas modificações influenciam na afinidade do citc pela membrana, aumentando sua aderência, o que pode ter influência no transporte de elétrons e sinalização para a apoptose. No terceiro e último capítulo deste trabalho nós buscamos uma ferramente analítica que permitisse analisar modificação de proteínas promovidas por produtos de oxidação de colesterol e outros esteróis. Em um estudo realizado em colaboração com o grupo do professor Porter na Universidade de Vanderbilt, utilizamos ensaios baseados em *click chemistry* para buscar proteínas modificadas. Para isso, foram sintetizados derivados de colesterol e 7-deidrocolesterol (7-DHC, precursor imediato do colesterol) contendo um grupo alquinil na sua cadeia lateral. Este grupo pode ser ligado a um grupo azida por meio de uma reação de cicloadição, em um processo conhecido como *click chemistry*. Após a síntese e caracterização dos derivados lipídicos contendo o grupo alquinil na cadeia lateral, células Neuro2a foram tratadas com o alquinil-7-DHC e o alquinil-colesterol para averiguar seu metabolismo. Análises por HPLC-MS/MS mostraram que ambos derivados contendo o grupo alquinil foram metabolisados e convertdos nos respectivos ésteres. Usando um modelo celular para a doença conhecida como Sindrome de Smith-Lemli-Opitz (SLOS), doença caracterizada pela deficiência na enzima 7-deidrocolesterol redutase, foi mostrado que o acúmulo característico de 7-DHC nos pacientes pode levar a uma maior modificação de proteínas promovidas por seus derivados, o que pode contribuir para o desenvolvimento da doença.

**Palavras chave**: hidroperóxidos - aldeídos - peroxidação lipídica - radicais livres

# ABSTRACT

Cholesterol is an important component of eukaryotic cellular membranes, where it has an influence in the fluidity and stability. Due to the presence of a double bond in its structure, cholesterol can be oxidized by reactive oxygen and nitrogen species. This non-enzymatic oxidation generates, as primary products, cholesterol hydroperoxides. Such molecules, in turn, are highly reactive and can react with free metal ions and/or metalloproteins, affecting cell metabolism. Therefore, the first chapter of the present study aims to investigate the reaction of cholesterol hydroperoxides (ChOOH) with cytochrome c (cytc), a heme protein involved in the mitochondrial electron transport. Spectroscopic analyses in the UV-Vis region showed that ChOOH induces a dose-dependent bleaching of cytc's Soret band. In addition, this reaction leads to the formation of carbon-centered radicals on both protein and lipid, suggesting a homolytic reduction of ChOOH. As consequences, cytc undergoes oligomerization, a process that can influence electron transport and apoptosis signaling. The reaction of cytc and ChOOH can produce, directly or indirectly, reactive species such as epoxides, aldehydes and ketones. Among them, cholesterol aldehydes, such as cholesterol secoaldehyde (CSec) and cholesterol carboxyaldehyde (ChAld), are of particular interest, since they were previously found elevated in atherosclerotic plaques and brain tissue of patients bearing neurodegenerative diseases. These species can also react with amino acid residues leading to protein denaturation and malfunction. With that in mind, the second chapter of this study aims to investigate the reaction of ChAld and cytc. Using mimetic membrane models and mass spectrometry analyses, we showed that ChAld covalently modifies cytc through a mechanism consistent with the formation of Schiff base adducts. Such modification occurs mostly at lysine residues that are known to interact with the membrane. The modifications have an influence in the affinity of cytc to the membrane, where they increase its binding to the membrane, a process that could affect the electron transport and apoptosis signaling. In the last and third chapter of this study we wanted an analytical tool that allowed the investigation of protein adduction promoted by cholesterol and other sterols-derived oxidation products. In a study performed in collaboration with the Porter group from Vanderbilt University, we used analyses based on click chemistry to search for protein adduction. To address that, we first synthesized derivatives of cholesterol and 7-dehydrocholesterol (7-DHC, the immediate precursor of cholesterol) containing an alkynyl group in the side chain. The alkynyl group can be ligated to an azide group through a cycloaddition reaction, in a process known as click chemistry. After the synthesis and characterization of alkynyl derivatives, Neuro2a cells were treated with alkynyl-7-DHC and alkynyl-cholesterol to check their metabolism. HPLC-MS/MS analyses showed that both alkynyl derivatives are metabolized and converted into their respective esters. In addition, using a cell model for Smith-Lemli-Optiz Syndrome (SLOS), a disease characterized by the deficiency in the dehydrocholesterol reductase 7, we showed that the characteristic accumulation of 7-DHC in SLOS patients might be associated with protein adduction promoted by its oxidation products, which might contribute to the development of the disease.

**Keywords**: hydroperoxides - aldehydes - lipid peroxidation - free radicals

# 1. Introduction

## 1.1 Chemical structure and cholesterol oxidation

Cholesterol is an important membrane component in higher eukaryotes, where it modulates cell signaling events and also regulates both membrane fluidity and permeability (Ikonen 2008). Due to its chemical structure – the presence of a $\Delta^{5,6}$ double bond – it can be easily oxidized giving rise to several oxidation products. Cholesterol can be oxidized by both free radical and non-radical species. Free radical species – particularly hydroxyl radicals and radicals derived from lipid peroxidation processes – will abstract the allylic hydrogen from C7 and originate, after secondary reactions, 7-hydroperoxycholesterol (7OOH), 7-hydroxycholesterol (7OH) and 7-ketocholesterol (7K) (for more details on lipid peroxidation see (Augusto and Miyamoto 2011; Yin, Xu et al. 2011)). This process accounts for most cholesterol-derived oxidation products.

Since the beginning of the twentieth century, attention has been given to the reaction between cholesterol and non-radical species, such as ozone ($O_3$) and singlet molecular oxygen ($^1O_2$). Both species are well known oxidizing agents that are capable of reacting with unsaturated molecules leading to the formation of an enormous variety of reactive products. In this study, it will be discussed the reactions of ozone and singlet molecular oxygen with cholesterol, focusing on the production of cholesterol aldehydes. As far as we know, cholesterol aldehydes are only produced when cholesterol is oxidized by such non-radical species, which characterize them as fingerprints of these types of oxidation. It will also be discussed the reactions of cholesterol aldehydes with biomolecules - particularly with peptides and proteins - as well as their biological implications.

*1.2 Cholesterol and the mitochondria*

Cholesterol is found in different amounts among the organelles in the cell (van Meer, Voelker et al. 2008). Differently from the plasma membrane, that is rich in cholesterol, the mitochondrial membrane has a limited pool, corresponding to 0.5 to 3% of the pool found in the plasma membrane (Ikonen 2008; van Meer, Voelker et al. 2008). Since cholesterol plays an important role in the regulation of membrane fluidity and stability, its concentration and distribution in the cell is strictly regulated (Montero, Morales et al. 2008). However, several reports show that mitochondrial cholesterol is elevated in cancer cells as well as in the brain tissue if patients bearing Alzheimer's disease, which could be associated with increased resistance in triggering apoptosis (Feo, Canuto et al. 1973; Montero, Morales et al. 2008; Garcia-Ruiz, Mari et al. 2009). This augment in mitochondrial cholesterol also induces a decrease in the mitochondrial content of glutathione (mGSH), which would increase the oxidative stress and, consequently, lipid peroxidation in the mitochondria (Colell, Fernandez et al. 2009; Garcia-Ruiz, Mari et al. 2009). This whole scenario could increase cholesterol oxidation and, therefore, increase the levels of its oxidation products.

*1.3 Oxidation by ozone*

Ozone is a reactive triatomic species widely known for its protective effect against UV radiation in the upper atmosphere, where its formation depends upon complex reactions involving nitrogen dioxide, hydrocarbons and sunlight. In large urban centers, on the other hand, it is considered noxious, and its production has been associated with increased air pollution (reviewed in (Brunekreef and Holgate 2002)). Ozone toxicity can be attributed to its elevated oxidizing power (+0.89 V for the pair

$O_3/O_3^{\cdot-}$), which gives it the potential to oxidize DNA, proteins and lipids (Buettner 1993). Moreover, ozone can add to double bonds leading to the formation of 1,2,3-trioxolane species, which undergo secondary reactions producing aldehydes, ketones and alcohols. This mechanism was first proposed by Dr. Rudolf Criegee in 1975 and was confirmed in 1998 by an independent group using $^{17}$O-labelled NMR spectroscopy (Criegee 1975; Geletneky and Berger 1998). In the 1980s, great attention was directed to the reaction between ozone and cholesterol, when the group coordinated by Dr. Leland L. Smith published several papers characterizing cholesterol ozonization, giving evidence for the formation of cholesterol-derived aldehydes (Gumulka and Smith 1983; Jaworski and Smith 1988). Cholesterol ozonolysis can be conducted in a variety of solvents and the reaction mechanisms change according to the solvent; it varies from participating and non-participating solvents. For instance, in 2004 Tagiri-Endo and co-workers studied the ozonization of cholesterol in the presence of ethanol (a participating solvent), where they reported the formation of a toxic ethoxyhydroperoxide intermediate (Tagiri-Endo, Nakagawa et al. 2004).

From the biological perspective, very little attention was given to ozone oxidation potential, since no evidence pointed toward its formation in biological systems. It was only at the beginning of the 21$^{st}$ century that ozone formation *in vivo* was reported (Wentworth, McDunn et al. 2002; Babior, Takeuchi et al. 2003; Wentworth, Wentworth et al. 2003). Wentworth's group proposed the participation of ozone at the inflammatory response, being one of the powerful oxidizing agents present at this process. In 2003, the same research group published a study showing the formation of ozone in atherosclerotic arteries, which also provided evidence for

the formation of cholesterol-derived aldehydes *in vivo* (Wentworth, Nieva et al. 2003).

*1.4 Oxidation by singlet molecular oxygen and formation of ChAld*

In biological systems, especially under oxidative stress conditions, cholesterol is oxidized by the generally called reactive oxygen species (ROS), generating more than 80 steroids containing different functional groups like hydroxyl, ketones, aldehydes and epoxides groups, and some of them are toxic for the cell (Girotti 1992; Smith 1996). These oxysterols can also be generated by autoxidation of cholesterol, ozonolysis reaction and photooxidation (Kulig and Smith 1973; Smith 1987; Jaworski and Smith 1988; Girotti and Kriska 2004; Smith 2004).

The photooxidation reaction of cholesterol consists of two competitive reactions: type I and II (Foote 1991). In type I (free radical-mediated), two cholesterol hydroperoxides predominate as major products arouse through a H abstraction at the C-7 position of cholesterol: 3β-hydroxycholest-5-ene-7α-hydroperoxide and 3β-hydroxycholest-5-ene-7β-hydroperoxide. Further products such as dihydroxy, 7-ketone and 5,6-epoxides derivatives are formed with minor amounts (Girotti 1992; Osada and Sevanian 2000; Girotti and Kriska 2004). On the other hand, in type II reaction, characterized by the ene-addition of $^1O_2$, three main products are formed: 3β-hydroxy-5α-cholest-6-ene-5-hydroperoxide (5α-OOH), 3β-hydroxycholest-4-ene-6α-hydroperoxide (6α-OOH), and 3β-hydroxycholest-6β-hydroperoxide (6β-OOH) (Korytowski and Girotti 1999). These hydroperoxide derivatives are called primary oxidation products and can be further oxidized to a variety of bioactive species.

A study conducted in 2003 by Wentworth and collaborators using atherosclerotic plaque from patients with atherosclerosis identified two oxysterols: β-

hydroxy-5-oxo-5,6-secocholestan-6-al (CSec) and 3β-hydroxy-5β-hydroxy-B-norcholestane-6β-carboxaldehyde (ChAld) by identification of hydrazone derivatives, suggesting that ozone is produced endogenously by antibody-catalyzed oxidation of water by singlet dioxygen. Their conclusions were based on the identification - using indigo carmine and derivatives reaction using 2,4-dinitrophynylhydrazine - of "signature products" generated upon ozone oxidation (Wang, Bermudez et al. 1993). Nevertheless, many researchers expressed their reservations about the use of such biomarkers to infer the presence and generation of ozone endogenously (Kettle, Clark et al. 2004; Sies 2004; Smith 2004).

During the past decade, the oxysterols ChAld and CSec were identified as products in photooxidation reactions of cholesterol using methylene blue as photosensitizer (Uemi, Ronsein et al. 2009). There are two suggested mechanisms to explain the formation of these oxysterols in the presence of $^1O_2$, which were discussed in details by Uemi and co-workers (2009) (see **Scheme 1**). Briefly, the first mechanism, involves a process known as Hock Cleavage of the 5α-hydroperoxide (5α-OOH) (Frimer 1979). The Hydroperoxide 5α-OOH, one of the primary products generated by $^1O_2$ oxidation may undergo acid-catalyzed heterolysis, generating after subsequent reactions two carbonyl fragments (Brinkhorst, Nara et al. 2008).The second mechanism involves the formation of a 1,2 dioxetane generated upon a cycloaddition (2 + 2) of $^1O_2$ to the $\Delta^5$ bond of cholesterol (Uemi, Ronsein et al. 2009). The dioxetane is then cleaved generating electronically excited triplet carbonyl species and, finally, ChAld (Uemi, Ronsein et al. 2009).

In general, the involvement of $^1O_2$ in the generation of CSec and ChAld seems to be more plausible then by ozone in biological systems. Tomono and collaborators (2009) related the formation of CSec and ChAld using during the myeloperoxidase-

5

chlorinating activity and they suggest the evolvement of $^1O_2$ (Tomono, Miyoshi et al. 2009). They also demonstrated that CSec and ChAld are formed by PMA-activated human neutrophil-like HL-60 cell in culture as well as activated neutrophils obtained from WT mice (Tomono, Miyoshi et al. 2011).

Both CSec and ChAld were detected in human brain tissue of patients with either Alzheimer's or Lewy body dementia diseases, in which they were suggested to accelerate Aβ amyloidogenesis *in vitro* (Zhang, Powers et al. 2004; Bieschke, Zhang et al. 2006). Moreover, these oxysterols were also able to promote α-synuclein fibrilization, a process involved in the development of Parkinson's disease (Bieschke, Zhang et al. 2006; Bosco, Fowler et al. 2006). These findings suggest that these oxysterols could play an important role on the development of neurodegenerative diseases such as atherosclerosis, Alzheimer's and Parkinson's diseases.
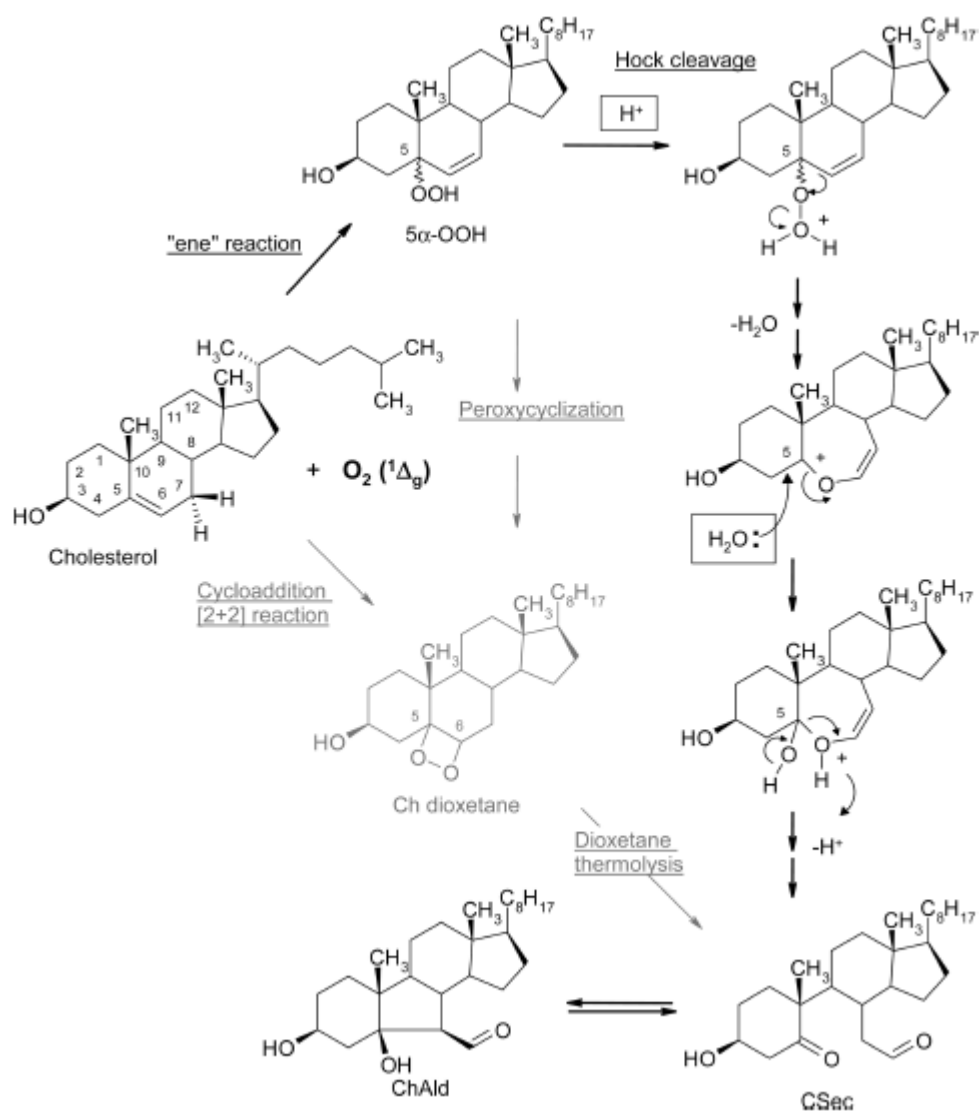
**Scheme 1**: Scheme of formation of oxysterols CSec and ChAld by $^1O_2$. (a) Hock cleavage, (b) cycloaddtion (2 + 2) followed by thermolysis. Scheme removed from (Uemi, Ronsein et al. 2009).

*1.5 Lipid peroxidation and the primary products of cholesterol oxidation*

Lipid peroxidation is an autocatalytic process that generates an enormous variety of products (Augusto and Miyamoto 2011; Yin, Xu et al. 2011). It can be divided into three phases: *i)* initiation, *ii)* propagation and *iii)* termination (**scheme 2**). *i) the initiation phase*: this process usually initiates with the abstraction of a hydrogen

atom from polyunsaturated fatty acids (PUFAs) producing a carbon-centered radical. Chemical reagents, UV-light and ionization radiation can induce the first hydrogen abstraction. From this point, the remaining carbon-centered radical can react with another one and terminate the reaction, a mechanism that will produce lipid dimers. In oxygenated media, however, these carbon-centered radicals combine with oxygen generating the highly reactive peroxyl radical. *ii) the propagation phase*: The peroxyl radical, in turn, has the potential to abstract a hydrogen atom from an adjacent lipid in the membrane, producing a hydroperoxide and another carbon-centered radical. Hydroperoxides can also react with transition metals (i.e. copper and/or iron) producing peroxyl and alkoxyl radicals, which can keep propagating the lipid peroxidation cascade. *iii) the termination phase*: the lipid peroxidation cascade reaches its termination by a series of complex reactions which ends up producing aldehydes, ketones, alcohols and alkanes (reviewed in Yin, Xu et al. 2011).
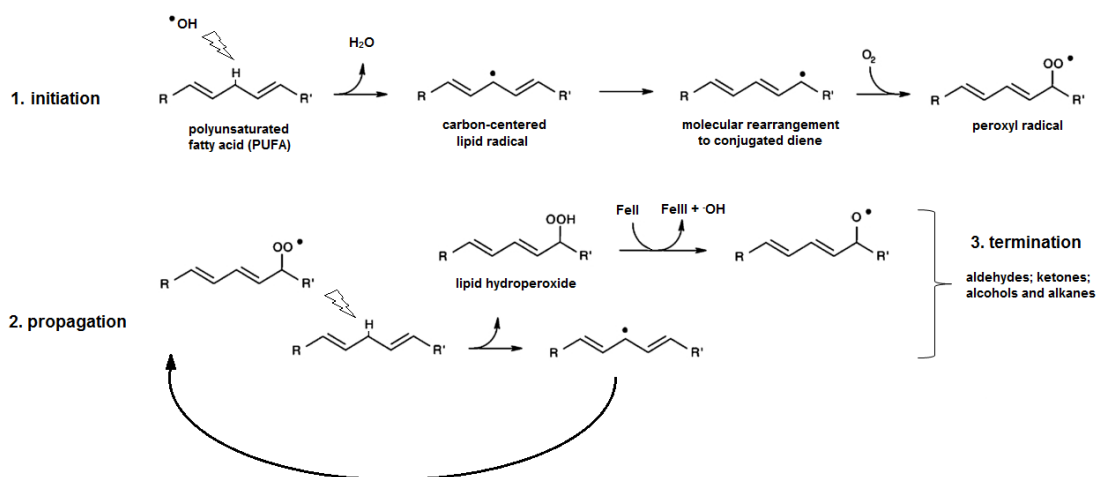


**Scheme 2**. Cascade of reactions involved in lipid peroxidation. TOH is an antioxidant found in elevated levels in the plasma membrane. Double bonds are shown in the *trans* configuration.

In the initial steps of the lipid peroxidation cascade it is produced, as primary products, lipid-derived hydroperoxides. In the specific case of cholesterol, the free

radical oxidation can be initiated by the abstraction of a hydrogen atom from an allylic position or by the addition of a peroxyl radical to the double bond. The abstraction of the allylic hydrogen atom can occur at both C-4 and C-7 positions, although reports from literature suggest that the abstraction at C-4 plays a minor role in cholesterol peroxidation (Yin, Xu et al. 2011). The abstraction at C-7 generates a secondary carbon-centered radical that resonates between the C-5 and C-7 positions and ends up combining with oxygen, in a diffusion-controlled rate, generating a peroxyl radical (see **scheme 3**). This peroxyl radical has the potential to abstract another hydrogen atom, producing a hydroperoxide and a carbon-centered radical on another lipid. Interestingly, analyzing the products of free radical oxidation of cholesterol, the hydroperoxides at the C-5 position are not observed (Brinkhorst, Nara et al. 2008; Uemi, Ronsein et al. 2009). Pratt and co-workers suggest that the rate of the β-fragmentation of the peroxyl radical at this position is higher than the propagation reactions, which would change the equilibrium towards the formation of hydroperoxides at the C-7 position (Pratt, Mills et al. 2003). Hydroperoxides at the C-5 position were only identified using $^1O_2$ as oxidant (see *section 1.4*) (Brinkhorst, Nara et al. 2008; Uemi, Ronsein et al. 2009). The mechanisms for the formation of hydroperoxides on the C-4 position are quite similar to the described for the C-7, with the exception that hydroperoxides at the C-6 position are observed (Yin, Xu et al. 2011). Overall, cholesterol-derived hydroperoxides formed by free radical oxidation are identified at C-4, C6 and C-7 positions.
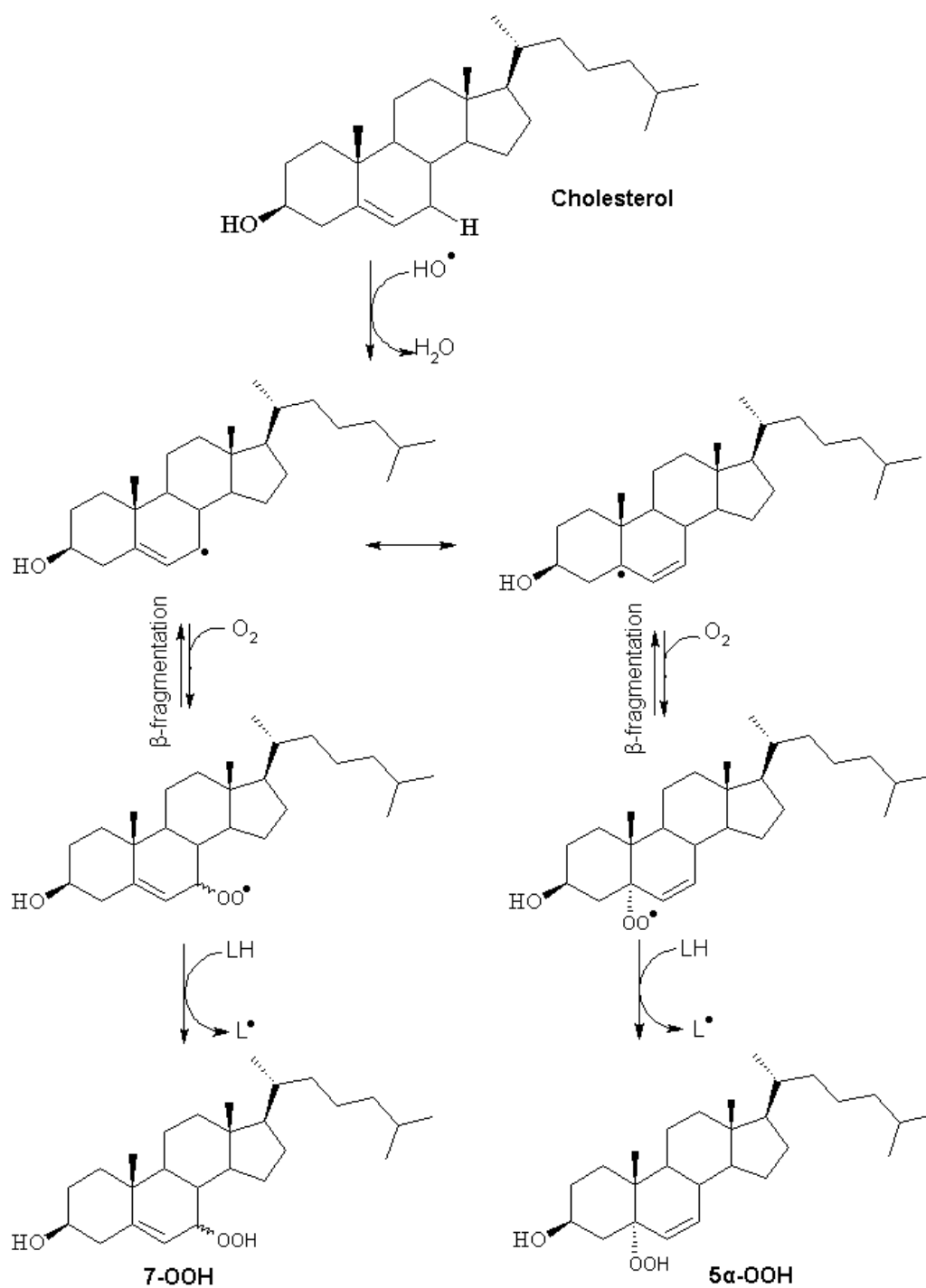
**Scheme 3**. Free radical oxidation of cholesterol. The abstraction of an H atom from the C-7 position is depicted in the scheme. The mechanism is essentially the same for the oxidation at C-4.

Over the past decades, several studies were published showing the capacity of hydroperoxides to react with transition metals and metalloproteins, leading to the formation of reactive free radicals (see **scheme 4** and **5**) (Barr and Mason 1995; Barr, Gunther et al. 1996; Nantes, Faljoni-Alario et al. 2000; Qian, Chen et al. 2002; Belikova, Tyurina et al. 2009). These reactions gained attention due to their ability to change protein structure and promote its inactivation (Barr and Mason 1995; Barr, Gunther et al. 1996; Nantes, Faljoni-Alario et al. 2000).
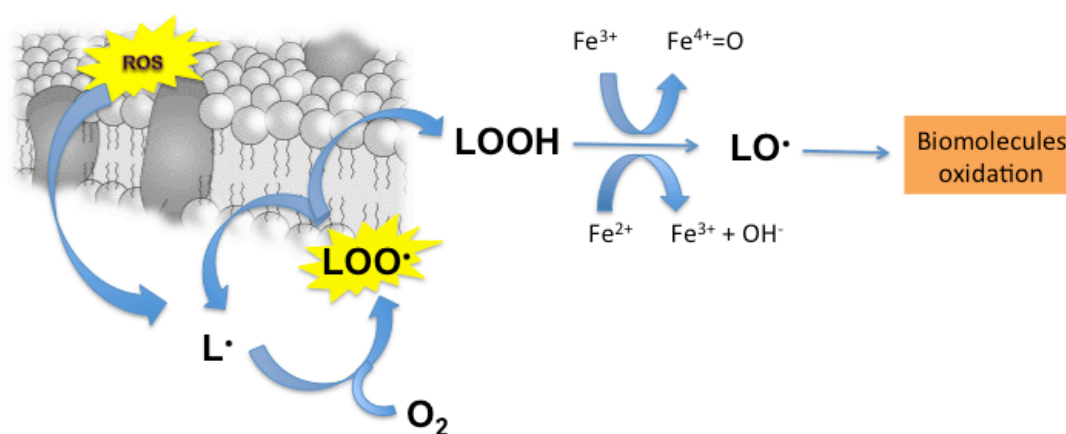


**Scheme 4**. Formation of lipid-derived hydroperoxides (LOOH) followed by reaction with metals or metalloproteins producing reactive free radicals.

One of the classical examples is the reaction of cytochrome *c* (cytc) with peroxides, a reaction that is usually attributed to a peroxidase activity o cytc (Nantes, Faljoni-Alario et al. 2000; Belikova, Tyurina et al. 2009). Several studies characterized the reaction of cytc with $H_2O_2$, showing that the protein cleaves the peroxide bond via a homolytic mechanism, producing the highly reactive hydroxyl radical (Barr and Mason 1995; Barr, Gunther et al. 1996). Moreover, this reaction

leads to the production of carbon-centered radicals on the protein, a situation that has been implicated in protein inactivation (Barr, Gunther et al. 1996). Recently, the Kagan's group published a study showing that cytc reacts differently with lipid-derived hydroperoxides when compared to $H_2O_2$ and other organic peroxides (i.e. *tert*-butil hydroperoxide – *t*-BuOOH) (Belikova, Tyurina et al. 2009). The authors conclude that cytc cleaves lipid-derived hydroperoxides via a heterolytic mechanism, reducing the hydroperoxide to its corresponding alcohol. As conclusions, the authors attribute this reaction to an antioxidant property of cytc in the mitochondria, acting as a classical peroxidase enzyme in the organelle (**scheme 5**). The homolytic mechanism, on the other hand, is highly pro-oxidant, since the hydroperoxide moiety is converted into the highly reactive alkoxyl radical (**scheme 5**). It is not clear yet, what reduction mechanism is the most relevant in the mitochondria, since there is evidence pointing towards both mechanisms (Barr and Mason 1995; Barr, Gunther et al. 1996)(Nantes, Faljoni-Alario et al. 2000; Belikova, Tyurina et al. 2009).
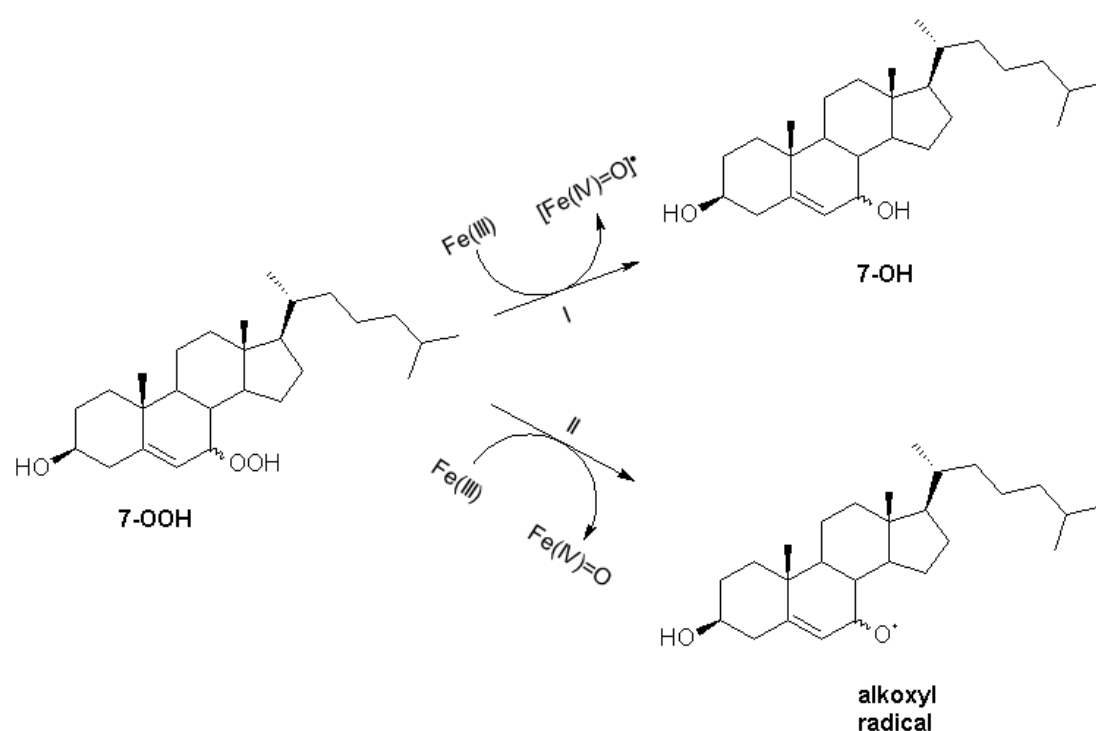
**Scheme 5**. Proposed mechanisms for the reduction of hydroperoxides by cytochrome c. I) Heterolytic reduction of 7-OOH to its corresponding alcohol (7-OH). II) Homolytic reduction of 7-OOH producing an alkoxyl radical. This mechanism is common to other hydroperoxides and the reduction of 7-OOH from cholesterol was used as an example.

*1.6 Methods for detection of ChAld*

Cholesterol-derived aldehydes are known to be very reactive towards biomolecules *in vivo* (Wentworth, Nieva et al. 2003). In this sense, the detection and identification of these compounds in biological samples may help understanding both their physiological and pathological roles in the cell. In the past ten years, great efforts were done to develop new and reliable methods in order to detect these species in biological samples. The methods currently available are mostly based on HPLC separations followed by UV-Vis (Wang, Bermudez et al. 1993; Wentworth, Nieva et al. 2003; Wentworth, Song et al. 2009), mass spectrometry (Uemi, Ronsein et al. 2009; Ronsein, Prado et al. 2010) and/or fluorescence detections (Tomono, Miyoshi et al. 2009; Mansano, Kazaoka et al. 2010).

The first step to identify these aldehydes is to achieve a good chromatographic separation. Most studies that identified these compounds used reversed-phase chromatography using C18 columns, employing gradients to achieve a good separation (Wentworth, Nieva et al. 2003; Uemi, Ronsein et al. 2009; Ronsein, Prado et al. 2010).

Among the methods available for detection, only mass spectrometry is able to detect these aldehydes without any chemical modifications, since both ChAld and CSec do not possess absorbance and/or fluorescence properties in the UV-Vis region.

In order to circumvent these issues and detect such species without using mass spectrometry, derivatization reactions can ligate chromophore or fluorophore tags to these molecules, making them detectable by either UV-Vis or fluorescence spectroscopy (Wang, Bermudez et al. 1993; Wentworth, Nieva et al. 2003; Tomono, Miyoshi et al. 2009; Wentworth, Song et al. 2009; Mansano, Kazaoka et al. 2010). In the work of Tomono and co-workers (2009), for instance, they identified the formation of both ChAld and CSec when cholesterol was reacted with the myeloperoxidase-$H_2O_2$-chloride system. After the reaction, the total lipid content was extracted and then incubated in an acidic media with a fluorescence molecule, in this case, dansyl hydrazine. After the derivatization reaction, the mixtures were analyzed by HPLC followed by fluorescence detection.

Another recent work that used fluorescence molecules to help the identification of these aldehydes is the study conducted by Mansano and co-workers (2010). The authors oxidized cholesterol employing several oxidants, including ozone and singlet molecular oxygen, and then derivatized the mixture with 1-pyrenebutiric hydrazine (PBH). The identification of the aldehydes was assessed by HPLC followed by fluorescence detection. One advantage of the this method is that the derivatization reaction is conducted in a neutral pH, preventing the acid-catalyzed conversion of the 5-α-hydroperoxide (5α-OOH) to ChAld via the Hock cleavage mechanism (Brinkhorst, Nara et al. 2008), which could lead to an inaccurate measurement of its content in biological samples (Mansano, Kazaoka et al. 2010).

The direct detection of ChAld by mass spectrometry can be tricky, since its ionization by electrospray – ESI is not facilitated. The ionization of ChAld for mass spectrometry analyses can be achieved using an alternative ionization source, known as atmospheric pressure chemical ionization (APCI). Recently, two studies employed

this technique to characterize, *in vitro*, the pattern of fragmentation of ChAld by HPLC-MS/MS (Uemi, Ronsein et al. 2009; Ronsein, Prado et al. 2010). In the study of Ronsein and co-workers (2010), the use of dopant agents, such as toluene or acetone, showed to improve the ionization of several oxysterols, including ChAld.

Among those methods discussed herein, those based on either mass spectrometry or fluorescence detection were shown to be the most sensitive ones, being able to detect ChAld in the fmol (Ronsein, Prado et al. 2010) and pmol range (Mansano, Kazaoka et al. 2010). Noteworthy is that "free" cholesterol-derived aldehydes content inside the cell is expected to be very low, since these molecules are great electrophiles and react very fast with amino acids, peptides and proteins (vide *infra*). In this context, the development and improvement of methods with high sensitivity comes in hand, allowing the detection and quantification of these compounds inside the cell.

*1.7 Modification of peptides and proteins by ChAld*

Cholesterol-derived aldehydes have recently been detected in atherosclerotic tissue samples and human brain as important intermediates in the pathogenesis of cardiovascular and neurodegenerative diseases. Several studies show that these oxidized derivatives of cholesterol modify specific proteins in brain, such as the β-amyloid peptide. Such modifications were suggested to induce the formation of neurotoxic aggregates in Alzheimer's disease by covalently modifying basic amino acid residues. These modifications occur more specifically at lysine residues 16 and 28, as well as the N-terminal group of aspartate 1 (Usui et al. 2009; Scheinost et al. 2008; Bieschke et al. 2005; Zhang et al. 2004). There are two mechanisms that can lead to protein modification promoted by oxysterols (**scheme 6**): *i)* formation of imine

bonds with free amino groups from basic amino acids (Lys and/or Arg) and/or to amino groups at the N-terminal portion of the protein – mechanism known as Schiff base formation; *ii)* amino groups of basic amino acids (His, Lys and/or Arg) can promote a nucleophilic addition to a double bond of oxysterols - usually α,β-unsaturated carbonyl groups – mechanism known as Michael addition.
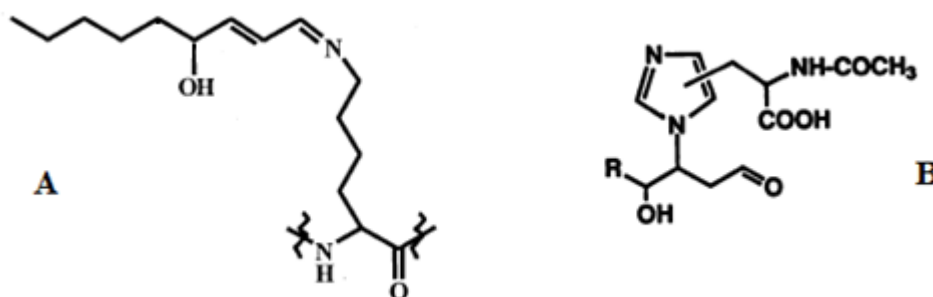


**Scheme 6**. **(A)** Schiff base formation between the aldehyde moiety from HNE with the side chain from a lysine residue. **(B)** Adduct formed from a Michael addiction of a histidine residue to HNE. Scheme adapted from (Uchida and Stadtman 1992) and (Isom, Barnes et al. 2004).

Recently, Bosco and co-workers reported increased levels of cholesterol-derived aldehydes in the cerebral cortex of patients who have dementia related to the formation of Lewy bodies when compared to healthy individuals (Bosco, Fowler et al. 2006). Moreover, the authors showed, using the thioflavin T fluorescence assay, circular dichroism and electron microscopy, that these metabolites were able to induce the aggregation of α-synuclein *in vitro*. Interestingly, replacing the aldehyde moiety for a carboxylic acid also promoted the aggregation of α-synuclein, suggesting that

the formation of the imine bond is not required for the aggregation *in vitro* (Bosco, Fowler et al. 2006).

Nieva and co-workers reported in 2011 that cholesterol-derived aldehydes are able to induce amyloidogenesis and dysfunction of the wild-type protein p53, indicating a link between inflammation and cancer (Nieva, Song et al. 2011). By employing fluorescence and circular dichroism analyses, the authors showed that cholesterol aldehydes, but not other lipid-derived aldehydes, induced amyloidogenesis and conformational changes in p53, which leads to a loss of 85% of its DNA-binding capacity *in vitro*. Finally, the authors suggest that these oxysterols induce p53 amyloidogenesis and loss of function by covalently binding to lysine residues via Schiff bases, a behavior that would contribute to the development of cancer.

Wachtel and co-workers (2006) showed that oxysterols may react with amino groups from phospholipids (i.e. phosphatidylethanolamine) in addition to amino groups from amino acid residues, which could compromise the structure and stability of lipid bilayers. It has also been proposed that aldehydes derived from cholesterol-esters-derived are able to covalently modify proteins, particularly apolipoprotein B100 from LDL particles (Kawai, Saito et al. 2003). This type of modification is expected to be quite common in oxidized lipoproteins, a factor that could contribute to the development of atherosclerosis (Kawai, Saito et al. 2003).

*1.8 Relationship between oxysterols and disease – the case of SLOS*

Palmitoylation, cholesterylation, and S-acylation with both saturated and unsaturated fatty acids are known modes of protein lipidation (Hang and Linder 2011) These modifications affect proteins stability, cellular localizations and their biological activities (Resh 2012) In addition to modifying proteins, lipids themselves are very sensitive to reaction with the molecular oxygen, producing a variety of oxidation

products (Augusto and Miyamoto 2011) Recently, Porter's group at Vanderbilt University provided evidence that 7-dehydrocholesterol (7-DHC), the immediate biosynthetic precursor of cholesterol, is one of nature's most oxidizable lipids.(Xu, Davis et al. 2009) Elevated levels of 7-DHC are a hallmark of Smith-Lemli-Opitz syndrome (SLOS), a disorder that arises from mutations in the gene encoding 7-DHC reductase (Dhcr7), the last enzyme in the cholesterol biosynthesis pathway (Tint, Seller et al. 1995; Kelley and Hennekam 2000; Porter and Herman 2011) As consequence of the mutations, 7-DHC is greatly increased and cholesterol decreased in the blood of SLOS patients (Bukelis, Porter et al. 2007; Haas, Garbade et al. 2007).

It is not clear whether the abnormalities associated with the SLOS pathology are due to 7-DHC buildup, cholesterol deficiency, or some other cause. A plausible hypothesis is that 7-DHC or its peroxidation products are biologically-active and contribute to the pathology of SLOS.(Gaoua, Chevy et al. 1999; Richards, Nagel et al. 2006) In this context, oxysterols derived from 7-DHC peroxidation might react with proteins, leading to protein malfunction and, ultimately, to the development of the disease. One way to address that, is the development of a strategy where one can identify protein adduction induced by oxysterols using a cell model for SLOS (Windsor, Genaro-Mattos et al. 2013). Recently, Vila and co-workers synthesized alkynyl derivatives of 4-hydroxynonenal (HNE) to address protein adduction promoted by this lipid electrophile (Vila, Tallman et al. 2008). α,β-unsaturated aldehydes, such as HNE and trans,trans-2,4-decadienal (DDE), have been shown to covalently modify a variety of proteins, including cytc (Isom, Barnes et al. 2004; Sigolo, Di Mascio et al. 2007). Alkynyl derivatives of HNE (*a*-HNE) were used to address protein adduction using a cell model. Cells were supplemented with either *a*-HNE or the vehicle (control conditions) and then probed for protein adduction with

biotin with an azide tag. The azide moiety of biotin can be ligated to the alkyne one by a 1,3 dipolar cycloaddition reaction, reaction usually referred as click chemistry (Vila, Tallman et al. 2008). This strategy allows the isolation of potentially modified proteins and their visualization using streptavidin-derived fluorophores. By synthesizing sterols and oxysterols containing an alkyne moiety one can try to identify proteins potentially modified by these species, which might help elucidate their physiological and pathological roles in the cell.

## 2. Objectives

With that in mind, we designed a study with the goal of characterizing the reactions of cholesterol-derived hydroperoxides and cholesterol-derived aldehydes, particularly ChAld, with cytc. Literature reports that cytc has the capacity of reacting with hydroperoxides – including lipid-derived hydroperoxides – leading to the formation of free radical species, which, in turn, can modify biomolecules and affect cellular events. Moreover, Kagan's group reported that cytc reacts faster with lipid-derived hydroperoxides when compared to $H_2O_2$ and $t$-BuOOH, showing that these species can be particularly harmful to the cell (Belikova, Tyurina et al. 2009). Therefore, we designed a study to characterize the kinetics and mechanisms of the reaction between cytc and ChOOH. Our results allowed us to re-examine the reaction of this protein with other lipid-derived hydroperoxides. These results are discussed in the first chapter of this thesis.

Due to its small size and unique structure, cytc is an excellent candidate as a model protein for the study of protein adduction promoted by cholesterol-derived aldehydes. The presence of 18 Lys and 3 His residues allows the identification of possible modification sites as well as the mechanisms involved in the protein

adduction. To address that issue, we used mimetic membrane models based on the use of SDS-micelles and cardiolipin-containing liposomes to react ChAld with cytc. These results are discussed in the second chapter of this thesis.

In the third and last chapter of this study, we wanted to use analytical tools with the purpose of identifying cholesterol-derived aldehydes in biological systems. With that in mind, a collaboration with the Porter group at Vanderbilt University was established. The Porter group, in collaboration with the Marnett group, used alkynyl derivatives of lipids (and lipid oxidation products) to probe for protein adduction (Vila, Tallman et al. 2008). We also to sought to examine the potential roles of oxysterols on the development of the neurodevelopmental disease known as SLOS, a field of interest of the Porter group. To pursue that, we synthesized alkynyl derivatives of cholesterol, its immediate precursor 7-DHC and some 7-DHC-derived oxysterols. These molecules were then supplemented to a cell model of the disease and then checked for incorporation and metabolism. Knowing that the alkyne derivatives were not toxic to the cells and that they were being metabolized, we compared protein adduction in control cells with SLOS cells. Our results pointed toward the modification of proteins by oxysterol-derived electrophiles, which could play a role in the development of the disease.

# Chapter 1

Revisiting cytochrome *c* peroxidase activity

using cholesterol hydroperoxides as substrates

**Abstract**

Lipid peroxidation is a well-known process that has been implicated in many diseases. Recent evidence showed that mitochondrial cholesterol is increased under specific conditions, making it an important target for peroxidation inside the mitochondria. Cholesterol peroxidation generates as primary products several hydroperoxides (ChOOH), which can react with transition metals and metalloproteins. In this sense, cytochrome *c* (CYTC), a heme protein largely found in the mitochondria, becomes a candidate to mediate free radical reactions with ChOOH. Using SDS to mimic the mitochondrial membrane, we show that ChOOH induces a dose-dependent Soret band bleaching, indicating that CYTC is using ChOOH as a peroxidase substrate. This reaction leads to protein oligomerization, which suggests the formation of a protein radical that, subsequently, recombines giving dimers, trimers and tetramers. EPR experiments confirmed the production of carbon-centered radicals from both protein and lipid in the presence of ChOOH and LAOOH. Moreover, the reaction is inhibited by pre-incubating CYTC with cyanide, showing that the heme group mediates the reaction. Kinetic experiments show that CYTC-bleaching is faster with ChOOH and LAOOH than with $H_2O_2$, rendering lipid peroxides relevant substrates for CYTC peroxidase activity in biological media. Altogether, these results suggest that CYTC cleaves lipid-derived hydroperoxides via a homolytic mechanism, producing reactive free radical species. In addition, ChOOH may be an important oxidant inside mitochondria, contributing to protein oxidation and cell death.

## Introduction

Cholesterol is a neutral lipid highly enriched in the plasma membrane of eukaryotic cells, where it corresponds to approximately 20-25% of the total lipid pool.[1,2] Its distribution, however, is not uniform among other organelles. In mitochondria, for instance, cholesterol corresponds to only 0.5 to 3% of the total lipid pool under normal conditions.[1] This molecule is synthesized in the endoplasmic reticulum and then transported to the mitochondria, where it is metabolized into many steroids in a process strictly regulated in the cell.[2-5] The protein suggested to be involved in this trafficking process is the steroidogenic acute regulatory protein (StAR), a protein with a motif that targets mitochondria and another one that binds cholesterol.[3,5,6] This protein was recently shown to transport cholesterol-derived hydroperoxides into the mitochondria.[6] Under pathological conditions, such as cancer, Alzheimer's, atherosclerosis and hepatic steatosis, cholesterol has been reported to be increased in the mitochondria.[7-9] This increase could be associated with a malfunction in the trafficking process involving the StAR protein, an event that could lead to the accumulation of cholesterol.[6] Knowing that cholesterol is susceptible to free radical oxidation and that mitochondria are primary sources of various reactive oxygen species (ROS), it is reasonable to assume that cholesterol can become a major target for lipid peroxidation under these conditions.

Lipid peroxidation is an auto-catalytic process that is known to produce several reactive products, including hydroperoxides, epoxides, aldehydes and ketones.[10,11] During the past decade, many studies have been published showing the ability of such products to react with other biomolecules, especially proteins and nucleic acids.[12-15] Previous studies already reported the ability of metal-containing proteins to react with lipid hydroperoxides generating a broad spectrum of products.[16-

[18] Heme proteins, such as cytochrome *c* (CYTC), were shown to mediate free radical reactions with many peroxides including, $H_2O_2$, *t*-BuOOH, cumene hydroperoxide and lipid-derived peroxides.[18-22] The ability of CYTC to react with peroxides is usually attributed to its peroxidase activity, which consists of the reduction of the peroxide moiety via either one or two electrons.[21] These reactions have been reported to produce free radical species such as peroxyl, alkoxyl and hydroxyl radicals.[23-26]

Cholesterol peroxidation generates as primary products several reactive hydroperoxides (**scheme 1**).[10] The production of each species depicted in **scheme 1** depends on several conditions, including which oxidant is being used and whether or not a hydrogen donor is present (see more details at reference [10]). In a scenario where cholesterol accumulates in the mitochondria, the appearance of such hydroperoxides might become a major event. Therefore, their reaction with mitochondrial proteins, such as CYTC, can play an important role in the generation of free radicals inside the organelle.
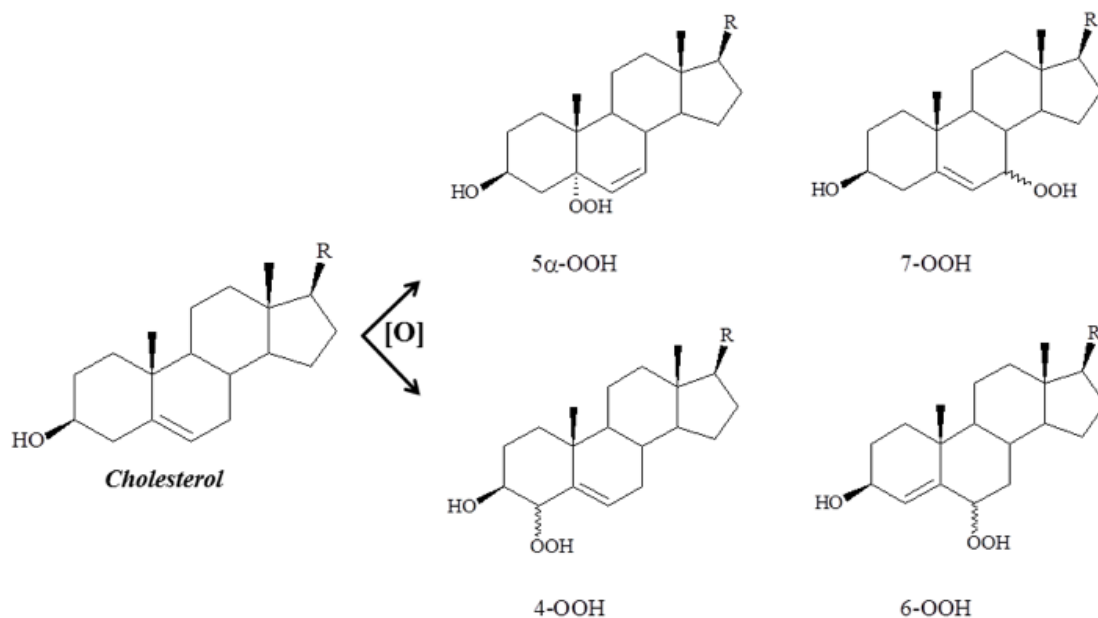


**Scheme 1**. Possible hydroperoxides formed from cholesterol peroxidation. It is depicted only primary products of oxidation that can be produced by different mechanisms (for more details about these mechanisms see reference 10).

With this in mind, we sought to study the reaction of cholesterol-derived hydroperoxides (ChOOH) with CYTC, a heme protein that is found peripherally bound to the mitochondrial inner membrane. Here, we employed SDS micelles as a mimetic model to insert ChOOH and anchor CYTC in a similar way as used previously.[14,27] In this situation, CYTC is assumed to possess similar structure and physicochemical properties as the native species found in the mitochondria.[27] By using electron paramagnetic resonance (EPR), we show that CYTC reacts with ChOOH generating carbon-centered radicals on both lipid and protein. These protein radicals recombine producing high molecular weight species (i.e. dimers, trimers and tetramers). In order to test the relevance of this reaction in biological media, we determined the rate constant and compared it to the reaction of other relevant peroxides, such as $H_2O_2$ and linoleic acid hydroperoxide (LAOOH). Interestingly, rate constants for the reaction of CYTC with ChOOH were higher than $H_2O_2$ and similar to LAOOH, which suggests that this reaction could be relevant *in vivo*.

**Materials and methods**

*Chemicals*

Bovine heart cytochrome *c* (Fe(III)), ammonium bicarbonate ($NH_4HCO_3$), cholesterol (cholest-5-en-3-ol), sodium dodecyl sulfate (SDS), silica gel 60 (230-400 mesh), methylene blue, potassium monobasic phosphate ($KH_2PO_4$), potassium dibasic phosphate ($K_2HPO_4$), potassium chloride (KCl), potassium cyanide (KCN), N-tert-butyl-a-phenylnitrone (PBN), *t*-butyl hydroperoxide (*t*-BuOOH) and hydrogen peroxide ($H_2O_2$) were purchased from Sigma (St. Louis, MO). Isopropanol and acetonitrile were purchased from JTBaker. Dioleoylphosphatidylcholine (DOPC) and

tetraoleoylcardiolipin (TOCL) were obtained from Avanti Polar Lipids (Alabaster, AL). The α-(4-pyridyl-1-oxide)-N-tert-butylnitrone (POBN) was obtained from the OMRF (Oklahoma City, OK). The 3,5-dibromo-4-nitrosobenzene sulfonate (DBNBS) was *synthesized according* to Kaur et al. (1981).[28] All other reagents were of analytical grade. Stock solutions of ammonium bicarbonate buffer (pH 7.4) were freshly prepared in Milli-Q water and the pH adjusted to 7.4 prior to use. CYTC concentration was checked prior to each experiment as described before.[14,29]

*Synthesis of cholesterol hydroperoxides (ChOOH) by the photooxidation of cholesterol*

ChOOH was synthesized as described by Uemi and co-workers (2009).[30] Briefly, cholesterol (200 mg) was dissolved in 20 mL of chloroform in a 100 mL round-bottom flask, and 250 μL of methylene blue solution (10 mM in methanol) were added. The solution was ice-cooled and irradiated using two tungsten lamps (500 and 300 W) for 2.5 h under continuous stirring and in an oxygen-saturated atmosphere. ChOOH was purified by flash column chromatography using silica gel 60 (230-400 mesh). The column was equilibrated with hexane, and a gradient of hexane and ethyl ether was used. After purification, the solvent was evaporated and the hydroperoxides were re-suspended in isopropanol and stored at -80 $^{\circ}$C for further use. ChOOH's identities were confirmed by RP-HPLC.

*Synthesis of linoleic acid hydroperoxides (LAOOH) by photooxidation of linoleic acid*

Linoleic acid hydroperoxide was synthesized as previously described.[31] Briefly, linoleic acid (0.5 g) was dissolved in 25 mL of chloroform in a 50 mL round

bottom flask, and 0.1 mL of methylene blue solution (100 mM) was added. The solution was ice-cooled and irradiated using two tungsten lamps (500 W) for 4.5 h under continuous stirring and in an oxygen-saturated atmosphere. LAOOH was purified by flash column chromatography using a gradient of hexane and ethyl ether. After purification, the solvent was evaporated and LAOOH was re-suspended in methanol, quantified by iodometry and stored at -80 ºC for further use.

*Liposomes preparation*

Unilamellar vesicle liposomes containing cardiolipin and LAOOH or ChOOH were prepared by extrusion technique.[22] Dry films of a mixture containing dioleoylphosphatidylcholine (DOPC) and tetraoleoylcardiolipin (TOCL) were prepared from stock solutions in methanol. The solvent was evaporated under a nitrogen atmosphere and the film formed was left for 1 h under vacuum to remove traces of organic solvents. The lipid films were resuspended in HEPES buffer (20mM) with 400 µM DTPA and mixed for one minute in a vortex. The final lipid concentration in liposomes was 2.0 mM (1 mM DOPC and 1 mM TOCL). Alternatively, lipid hydroperoxides-containing liposomes were prepared at the final lipid concentration of 2.08 mM (1 mM DOPC, 1 mM TOCL, and 0.08 mM LAOOH or ChOOH). Unilamelar vesicles with an approximate diameter of 100 nm were prepared by extrusion through polycarbonate membranes (Avestin). The samples were extruded 21 times through the membrane.

*CYTC incubation with SDS micelles*

The reaction between CYTC and ChOOH in the presence of SDS micelles was performed in the same way as described previously.[14] Briefly, ammonium bicarbonate

buffer (10 mM), pH 7.4, was mixed with SDS (8 mM final concentration) followed by ChOOH (varying concentrations). After 5 min, CYTC (5 μM) was added to the solution and the reaction was carried out at room temperature (25 ± 0.5 °C).

*Spectroscopic determinations*

Spectrophotometric analyses were carried out in a Varian model Cary 50 Bio spectrophotometer in a 10 mm path length cuvette. Incubations were carried out in the presence of bicarbonate buffer (10 mM), pH 7.4, at 25 ± 0.5 °C. CYTC concentrations were determined at 410 nm ($\varepsilon = 106.1$ mM$^{-1}$ cm$^{-1}$) prior to each experiment.[14] Spectra of blanks were subtracted from those of samples.

*Detection of PBN-, POBN- and DBNBS-carbon centered adducts by EPR*

Unless otherwise stated, ammonium bicarbonate buffer (25 mM), pH 7.4, was mixed with SDS (8 mM), cholesterol hydroperoxide (1 mM), DTPA (0.1 mM) and spin traps PBN (50 or 100 mM), POBN (100 mM), DMPO (350 mM) or DBNBS (10 mM). In some experiments, SDS micelles were substituted by cardiolipin-containing liposomes. Reactions were started by CYTC (100 μM) addition and incubated at 25 °C for 5 min before the EPR analysis. Aliquots (100 μL) were transferred to a quartz flat cell and EPR spectra were recorded at room temperature (21 ± 1 °C) on a Bruker ER 200 D-SRC upgraded to an EMX instrument. The instrumental conditions were: frequency, 9.7 GHz; receiver gain, 6.32 x 10$^4$; microwave power, 20 mW; modulation amplitude, 1 G; time constant, 163.84 ms; conversion time, 163.84 ms. Four single scans were accumulated to improve the signal-to-noise ratio. In some experiments, cyanide (10 mM) was pre-incubated with CYTC (1 mM) for 5 min

before its addition in the reaction mixtures in the final concentration of 100 μM. Nitroxide tempol was loaded to calibrate the EPR before the experiments.

*POBN-lipid radical adduct analysis by LC-ESI-MS*

POBN-lipid radical adducts were separated on a C18 column (150 x 3.0 mm, 2.6 um, Kinetex, Phenomenex) using a gradient of acetonitrile (solvent B) and water (solvent A), both containing formic acid (0.1% v/v). For the analysis 10-30 μL of the reaction mixture was injected into the column. Elution was started by keeping 10 % B for 5 min, them increasing from 10 to 27% B in 5 min, 27 to 70 % in 15 min, 70 to 95 % in 3 min and them keeping at 95 % for 17 min, and finally returning to 10 % in 1 min. The flow rate was set to 0.2 mL/min. The eluent was monitored with a UV detector at 270 nm and with the mass spectrometer utilizing electrospray ionization (ESI) in the positive ion mode (Quattro II triple quadrupole, Micromass, Manchester, UK). The initial 10 min of analysis containing unreacted POBN reagent was discarded to avoid overload of POBN into the MS. The source temperature of the mass spectrometer was held at 150 °C, desolvation temperature at 200 °C, and the capillary and the electrode potentials were set to 2.5 and 0.5 kV, respectively. Linoleic acid hydroperoxide-derived POBN adducts were analyzed with cone voltage and collision energy of 20 V and 15 eV, respectively. Cholesterol hydroperoxide-derived POBN adducts were analyzed with cone voltage and collision energy of 40 V and 30 eV, respectively. Full scan data from 100-800 m/z was acquired. Data was processed by means of the Mass Lynx NT data system.

*SDS-polyacrylamide gel electrophoresis (SDS-PAGE)*

The procedure of SDS-PAGE electrophoresis was performed as described previously.[29,32] ENREF_2 Briefly, CYTC incubated in the presence and absence of ChOOH was submitted to electrophoresis in a 15% acrylamide gel under non-reducing conditions. Gels were prepared containing acrylamide (15%), TRIS buffer (0.4M), ammonium persulfate (0.1%) and SDS (0.1%), pH 8.8. Samples were mixed with Laemmli buffer (62 mM TRIS-HCl buffer (pH 6.8), glycerol 10% v/v, SDS 2% w/v and bromophenol blue 0.01% w/v) and heated at 95 $^{\circ}$C for 5 min for denaturation. After the electrophoretic run, the samples were silver stained.

*Transient-state kinetics*

The transient-state kinetic studies were performed with a stopped-flow spectrophotometer (Applied Photophysics SX-18MV) at (25.0 ± 0.5 $^{\circ}$C) using the single-mixing mode. CYTC (0.8 µM) in bicarbonate buffer (25 mM) and in the presence of SDS micelles was allowed to react with various concentrations of ChOOH, which were in excess of at least 5-fold compared with protein to ensure pseudo-first-order kinetics. The decay of CYTC was monitored in Soret band at 407 nm. The rate constants for reaction of CYTC with $H_2O_2$ and LAOOH were determined as experimental control and compared to that reported in literature.[21]

The $k_{obs}$ values were determined using the single curve-fit equation of the instrument software. Six to ten determinations of $k_{obs}$ were performed for each substrate concentration. The apparent second order rate constants were calculated from the slopes using linear least-squares regression analysis. In all experimental conditions, the coefficients of determination ($R^2$) and *p*-values were >0.999 and <0.0001, respectively.

**Results**

*ChOOH induces a dose-dependent bleaching of CYTC Soret band*

CYTC was incubated with ChOOH in bicarbonate buffered media (pH 7.4) and the resulting UV-Vis spectra were recorded after 10 min of incubation (**figure 1**). The Soret band of CYTC has its maximum absorption at 408 nm when CYTC is incubated in the presence of SDS (8 mM).[27] The black line on **figure 1A** represents this condition. The addition of increasing amounts of ChOOH (5 to 100 µM) induces a dose-dependent bleaching of the Soret band centered at 408 nm (**figures 1A** and **1B**), suggesting that the heme group is being disrupted. In addition, heme bleaching was more pronounced at molar ratio of ChOOH/CYTC $\geq$ 5 (**figure 1B**), which suggests that in that conditions a partial conformational change of the protein (*data not show*) and a putative oxidation of axial Met[80] by ChOOH may also cause the enhancement of CYTC-peroxidase activity and, consequently, heme damage.[33] It is noteworthy that no increase in the absorbance at 550 nm was observed in these experiments, suggesting that the heme iron is not being reduced to the ferrous form.[34] These are indications that CYTC is mediating free radical reactions using ChOOH as substrate, a reaction that ends up oxidizing the heme group.

**A**



**B**
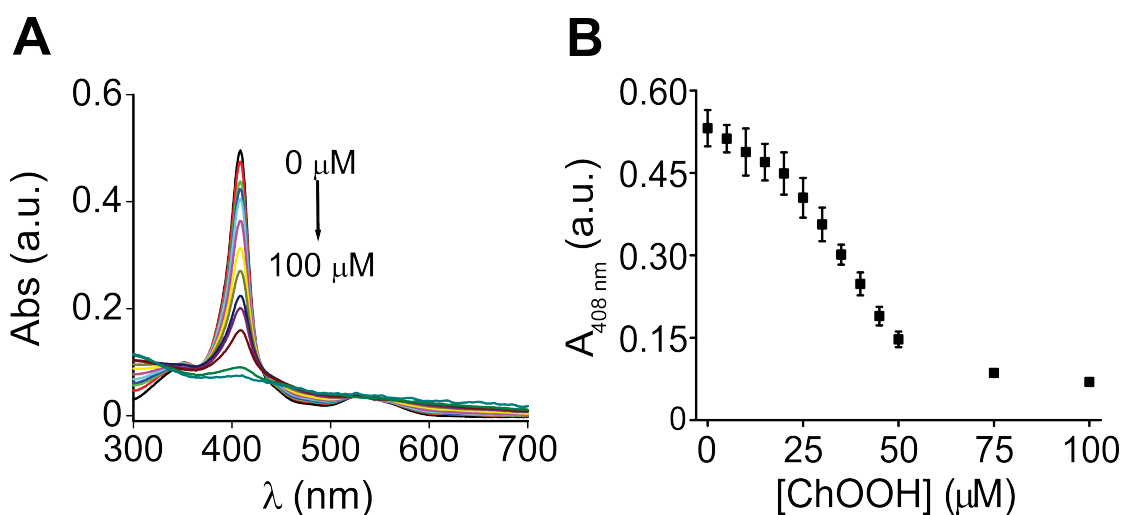
**Figure 1.** UV-Vis scans of CYTC in the presence of different concentrations of ChOOH. All experimental conditions contained bicarbonate buffer (10 mM), pH 7.4, SDS (8 mM) and CYTC (5 μM). ChOOH concentrations ranged from 5 to 100 μM. **Panel A** shows scans of CYTC after 10 min of incubation with ChOOH. Black line represents the control condition (without ChOOH) and subsequent lines represent each concentration of ChOOH used. **Panel B** shows the absorbance values of the Soret band centered at 408 nm *versus* ChOOH concentration. Experiments are performed in triplicate.

*CYTC reacts with ChOOH producing protein and lipid carbon-centered radicals*

We performed EPR spin trapping experiments in an attempt to find if free radicals participate in the CYTC-heme bleaching by ChOOH. The composite EPR spectrum obtained using the spin trap DBNBS (10 mM) is shown in **figure 2**. First, an immobilized nitroxide was detected when the reaction of CYTC/ChOOH was performed in the presence of DBNBS (filled circles, fourth line in **figure 2**), likely by trapping tyrosyl and/or tryptophanyl radicals, similar to DBNBS radical adduct provided from the treatment of CYTC with hydrogen peroxide.[18] More recently it was demonstrated that the CYTC-derived tyrosyl radical was trapped by MNP, leading to a persistent radical adduct at the C-3/C-5 positions of the tyrosine phenyl ring.[35]

**Figure 2.** Spin-trapping of CYTC-derived radicals formed from its peroxidase activity. CYTC (100 μM) was added to SDS-micelles prepared by mixing SDS (8 mM), DBNBS (10 mM), ChOOH (1 mM) and DTPA (0.1 mM) in bicarbonate buffer (25 mM), pH 7.4. The mixture was incubated at 25 ºC. After 5 min, an aliquot was transferred to a quartz flat cell and the EPR spectrum was recorded. In some experiments, CYTC (1 mM) was pre-incubated with cyanide (10 mM) for 5 min before its addition in the reaction mixtures. The filled circles, open circles and crosses mark the spectral lines of protein radical, lipid radical and DBNBS ene addition, respectively. Spectra were accumulated four times and are representative of three independent experiments.

As indicated in the spectra obtained from control experiments (three top lines in **figure 2**), formation of the DBNBS adduct was dependent on the presence of both protein and lipid peroxide. Second, ChOOH reacted with DBNBS to yield an EPR spectrum of a free radical with a coupling constant of aN = aH 13.6 G, which is assigned to DBNBS/ChOOH, a product of the ene reaction between the nitroso group and a double bond,[36] independently of CYTC-peroxidase activity (crosses, third line

in **figure 2**). The addition of CYTC gave lipid-derived adduct radicals mixed to a broad EPR spectrum typical of an immobilized nitroxide. EPR analysis showed an isotropic six-line carbon-centered radical spectrum indicative of an electron interacting with a nitrogen and a β-hydrogen (aN = 14.1 G; aH = 7.7 G) (open circles, third line in **figure 2**).[37] Studies of dependence of ChOOH concentration demonstrated that both lipid- and protein-centered EPR signals were formed upon reaction with CYTC (**figure 3**).
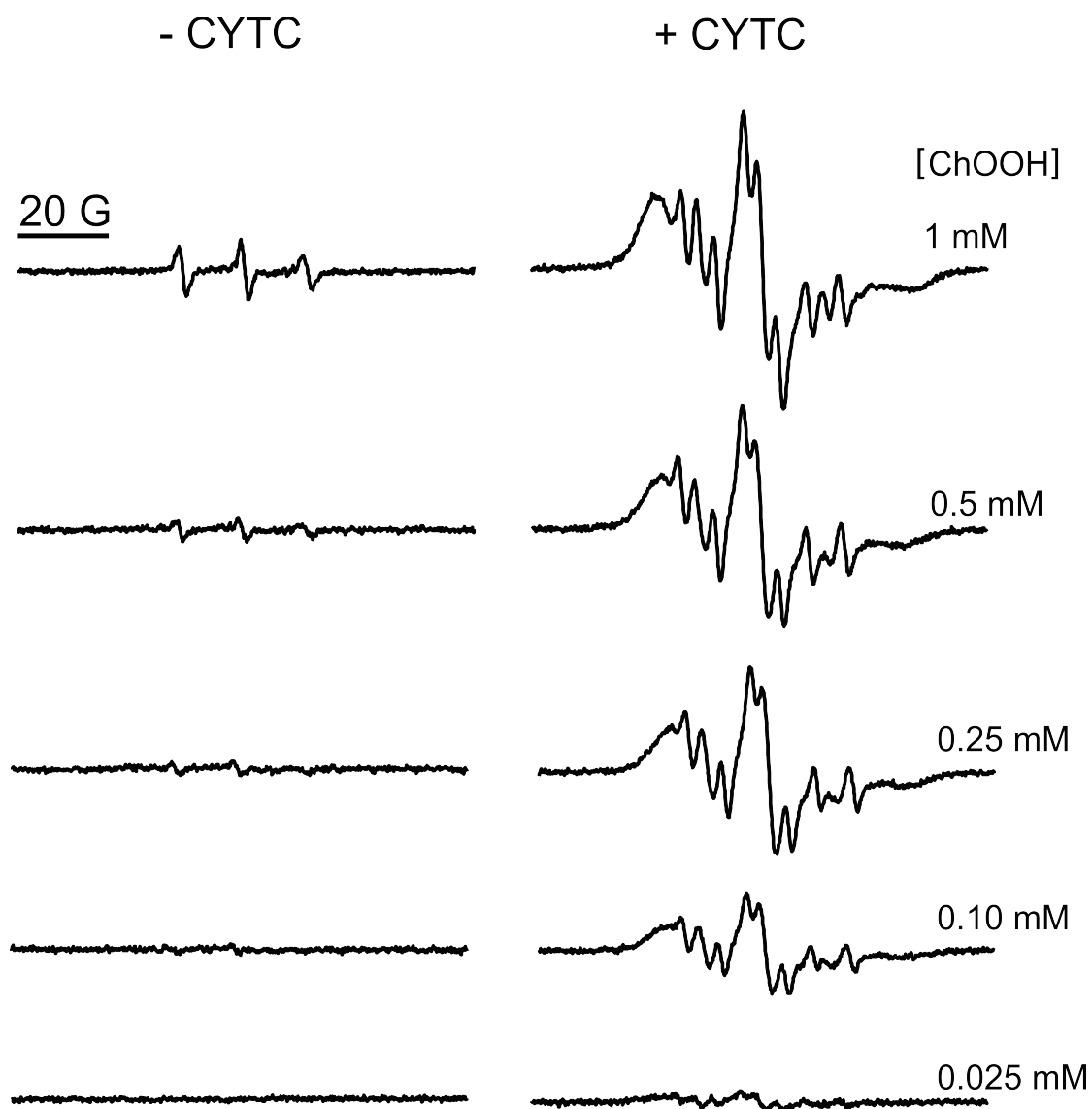


**Figure 3.** ChOOH-concentration dependence on production of DBNBS-CYTC adducts. CYTC (100 μM) was added to SDS-micelles prepared by mixing SDS (8

mM), DBNBS (10 mM), ChOOH (at the specified concentrations) and DTPA (0.1 mM) in bicarbonate buffer (25 mM), pH 7.4. The mixture was incubated at 25 ℃. After 5 min, an aliquot was transferred to a quartz flat cell and the EPR spectrum was recorded. Spectra were accumulated four times and are representative of three independent experiments.

We also used the spin trap PBN due to its high reactivity with lipid-centered radicals.[38] Again, an EPR signal was only detected when ChOOH was incubated with CYTC in the presence of PBN (50 mM) (top four lines at **figure S1**). The signal was represented by a six-line spectrum with hyperfine coupling constants for the PBN spin adducts of aN  = 15.5 G and aH = 4.0 G, suggesting that ChOOH-derived alkyl radicals were also trapped.[39] In addition, increasing PBN concentration to 100 mM allowed the detection of a relatively immobilized double triplet (aN = 15.1 G and aH = 3.1) which was consistent with the assignment of this signal to a trapped carbon-centered radical inserted into micelles (fifth line at **figure S1**).[40]

Further, hydroperoxide-derived radicals were analyzed using another spin trap, POBN, which has been successfully employed for the detection of lipid-centered radicals.[41] CYTC was incubated with ChOOH, LAOOH or *t*-BuOOH in the presence of SDS-micelles and POBN with subsequent EPR detection (**figure 4**). Under control conditions, i.e. in absence of CYTC, a reasonable signal was detected with both ChOOH and LAOOH but not *t*-BuOOH, probably due to a thermal instability of the lipid hydroperoxides. However, addition of CYTC to the mixtures containing hydroperoxides yielded a strong double triplet signal with hyperfine constant (aH = 2.9 G and aN = 15.2 G) characteristic of carbon-centered radical adduct.
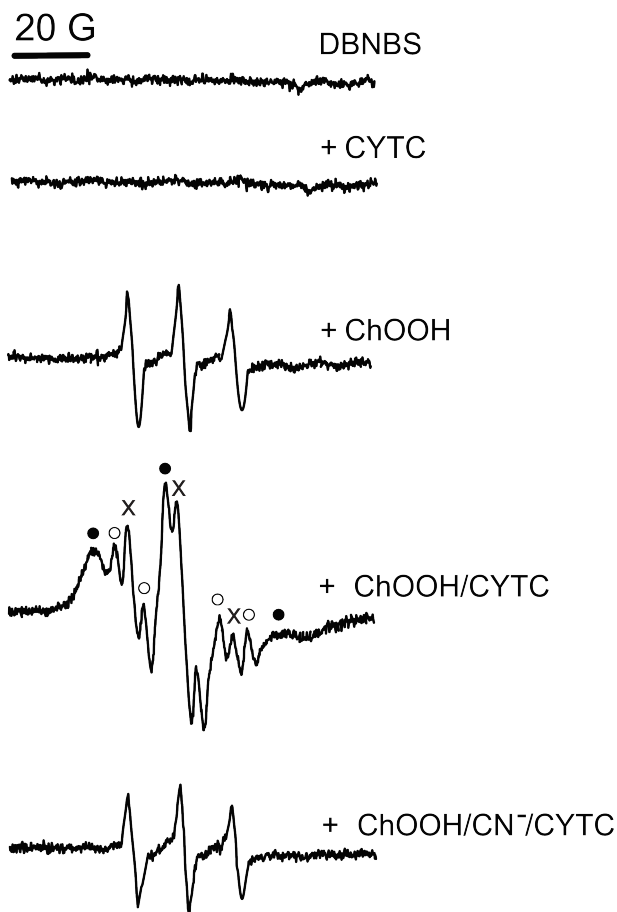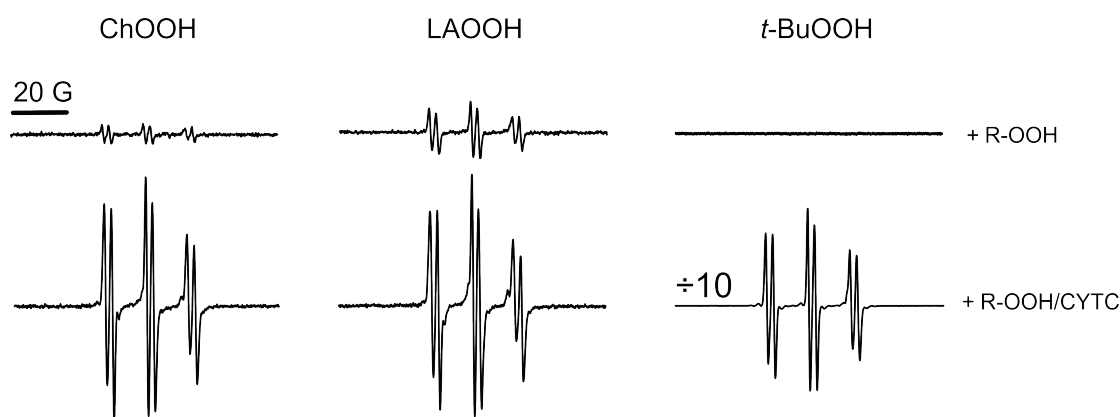
**Figure 4.** Spin-trapping of CYTC-derived radicals formed from its peroxidase activity in SDS micelles. CYTC (100 μM) was added to SDS-micelles prepared by mixing SDS (8 mM), POBN (100 mM), ChOOH (1 mM), LAOOH (1 mM), *t*-BuOOH (1 mM) and DTPA (0.1 mM) in bicarbonate buffer (25 mM), pH 7.4. The mixture was incubated at 25 °C. After 5 min, an aliquot was transferred to a quartz flat cell and the EPR spectrum was recorded. Spectra were accumulated four times and are representative of three independent experiments.

To confirm that these signals are not an "artifact" of the use of SDS-micelles, we repeated these analyses replacing the SDS-micelles by cardiolipin-containing liposomes as done in the study of Belikova and co-workers.[21] The incubation of cardiolipin-containing liposomes with CYTC and lipid peroxides (1 mM) provided similar spectra as those observed with SDS-micelles (**figure 5**). In addition, incubating CYTC with lower concentration of LAOOH (5 μM; condition used by Belikova and co-workers) produced an EPR signal barely distinguishable from noise (**figure 5**). Alternatively, liposomes were also prepared using a combination of DOPC, TOCL, and LAOOH or ChOOH (at final concentration of 0.08 mM). As expected, the addition of CYTC in incubation mixtures containing POBN and liposomes-inserted lipid peroxides also rendered EPR signals with hyperfine constants characteristics of carbon-centered radicals (**figure S2**). Taken together, results from EPR spin-trapping experiments suggest that CYTC in contact with SDS-micelles or to cardiolipin-containing liposomes could split both ChOOH and LAOOH predominantly via the homolytic mechanism (**scheme 3**).

36
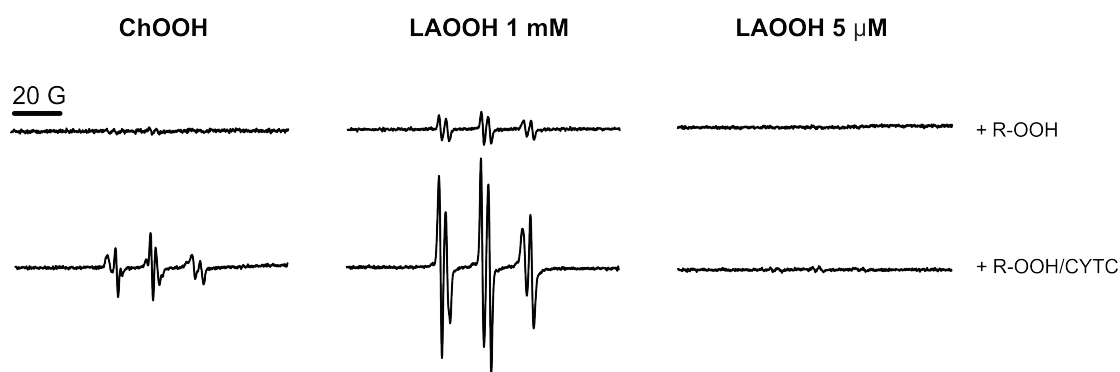
**Figure 5.** Spin-trapping of CYTC-derived radicals formed from its peroxidase activity in liposomes. CYTC (50 µM) was added to cardiolipin-containing liposomes (prepared as described in the *Experimental section*), POBN (100 mM), ChOOH (1 mM), LAOOH (5 µM and 1 mM), and DTPA (0.1 mM) in bicarbonate buffer (25 mM), pH 7.4. The mixture was incubated at 25 ºC. After 5 min, an aliquot was transferred to a quartz flat cell and the EPR spectrum was recorded. Spectra were accumulated four times and are representative of three independent experiments.

To trap primary alkoxyl radicals, DMPO (at a high concentration of 350 mM) was added to CYTC and SDS micelles in the presence of ChOOH (1 mM). In our experimental conditions, DMPO adducts were not detected (*data not shown*). Indeed, Belikova and co-workers also did not trap any EPR signal derived from LAOOH in CYTC/liposomes complexes by employing DMPO (500 mM) as spin trap. These results suggest that a*lkoxyl* radicals derived from ChOOH can *rearrange* to *epoxy* allylic radicals faster than they react with DMPO.[42]

The cyanide ion serves as a high affinity ligand for the ferric state of CYTC by displacing the axial Met[80] ligand, a situation that inhibits heme-catalyzed reactions and ends up preventing CYTC-heme degradation by hydroperoxides.[20,43] Accordingly, adding 100 eq of potassium cyanide/heme before adding ChOOH inhibits the heme-catalyzed reaction and prevents the production of both DBNBS and PBN adducts (see fifth line on both **figures 2** and **S1**). Not surprisingly, only a three-line ESR spectrum with hyperfine coupling constants aN=aH of 13.6 G from ene reaction of nitroso-aromatic spin trap and the lipid hydroperoxide was

37

obtained in the presence of cyanide (**figure 2**). Altogether the data indicate that CYTC is oxidized by micelle-associated ChOOH producing protein-centered radicals that may react with another carbon-centered radical to form cross-linked products.

*Cross-linked species of CYTC are formed upon reaction with ChOOH*

We performed SDS-PAGE experiments in order to support the hypothesis that cross-linked products of CYTC are produced after its reaction with ChOOH (**figure 6**). Native CYTC gives two bands in the SDS-PAGE under reductive conditions, which remained unaltered in our experimental conditions (**figure 6**, first lane). It is noteworthy that the second band on the gels corresponds to a protein dimer, which is already present in small amounts in the purified protein (see reference [14] and reactant brochure at www.sigmaaldrich.com). On the other hand, incubation of CYTC with either 150 or 300 μM of ChOOH induces the appearance of species with higher molecular weights (dimer, trimer and tetramer) in a concentration-dependent manner (**figures 6**, second and third lanes). In conclusion, these results suggest that ChOOH-dependent CYTC peroxidase activity mediates the production of protein-centered radicals that in turn can recombine to form covalent adducts.



**ChOOH**     **ChOOH**
**150 μM**     **300 μM**
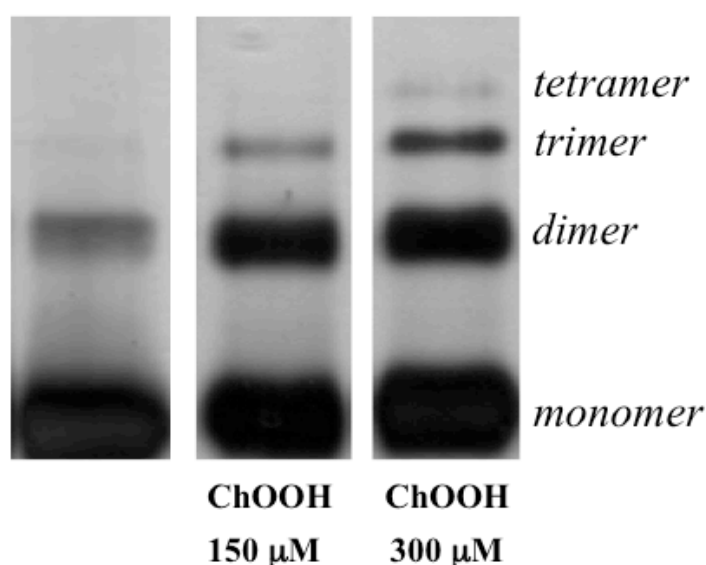
**Figure 6.** Detection of CYTC covalent adducts by SDS-PAGE. Incubation mixtures contained SDS (8 mM), CYTC (30 µM) and DPTA (0,1 mM) in bicarbonate buffer (10 mM), pH 7.4. Reactions were incubated for 10 min at 25 ºC. **First lane** represents control conditions containing only CYTC (without ChOOH). The other two lanes represent the conditions in the presence of 150 and 300 µM ChOOH, respectively. Gels are representative of three independent experiments.

*Identification of the POBN-lipid adducts by LC-MS*

We performed MS analyzes of the mixtures containing either LAOOH or ChOOH with the purpose of identifying POBN-lipid adducts as described previously.[41] Incubation of LAOOH with CYTC in the presence of POBN resulted in the formation of a covalent adduct characteristic of a carbon-centered radical (**figure 7C**). This pseudo-molecular ion with a *m/z* = 489 at 18.9 min can be visualized in the *selected-ion monitoring* (SIM) *chromatogram* (**figure 7A**). MS spectrum corresponding to this peak is depicted in **figure 7B**, where is shown $[M \cdot + H]^+ = 489$, $[M \cdot + H - H_2O]^+ = 471$ and $[M \cdot + H - LAOOH]^+ = 195$. A similar profile is observed in the reaction of ChOOH and CYTC (**figures 7D-7F**). The expected ChOOH-derived POBN adduct is illustrated in **figure 7F**. **Figure 7D** shows an extracted ion chromatogram from the pseudo-molecular ion of *m/z* = 595 at 21.87 min. MS spectrum corresponding to this peak is showed in **figure 7E**, where is possible to identify the following species: $[M \cdot + H]^+ = 595$, $[M \cdot + H - POBN - H_2O]^+ = 383$ and $[M \cdot + H - ChOOH]^+ = 195$. These results suggest that CYTC reacts with ChOOH or LAOOH by the homolytic pathway, generating an alkoxyl radical that rearranges spontaneously to an epoxy-alkyl radical that can be trapped by POBN.[42]
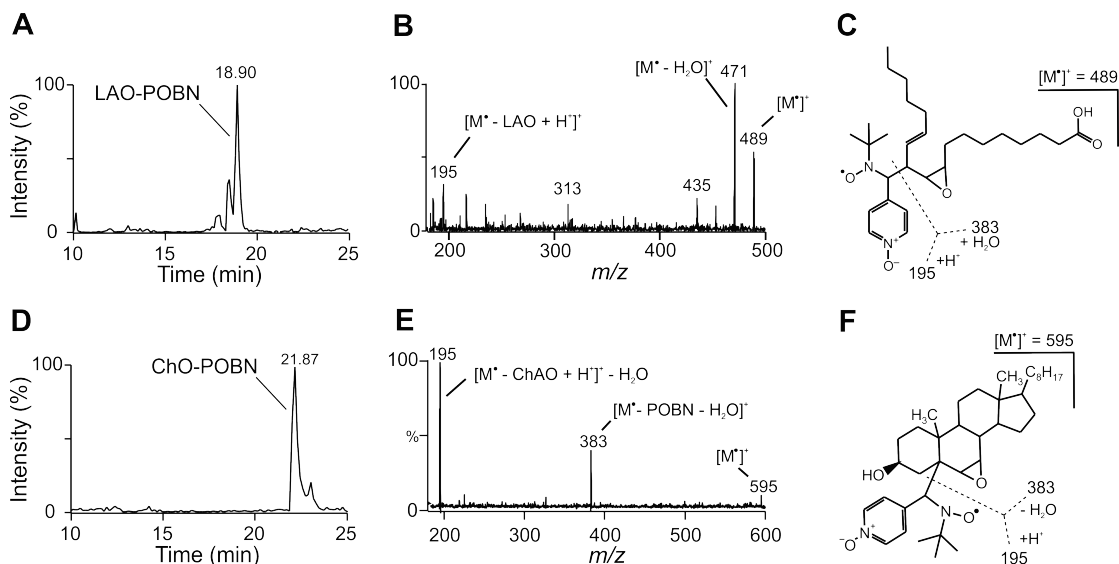
**Figure 7.** MS analyses of POBN-lipid adducts after the reaction with CYTC. Experimental conditions are exactly the same as described in **figure 4**. After the EPR analyses, samples of CYTC with LAOOH or ChOOH were analyzed by LC-MS as described in the *Experimental section*. (**C**) and (**F**) show the expected adducts between LAOOH and ChOOH, respectively. (**A**) Representative extracted ion chromatogram obtained for LAOOH and CYTC. The peak at 18.9 min corresponds to $[M\cdot + H]^+ = 489$, which is the ion corresponding to the epoxy-alkyl radical of LAOOH trapped by POBN. (**B**) Representative MS spectrum from peak at 18.9 min: $[M\cdot + H]^+ = 489$; $[M\cdot + H - H_2O]^+ = 471$; $[M\cdot + H - LAOOH]^+ = 195$. (**C**) Representative extracted ion chromatogram obtained for ChOOh and CYTC. The peak at 21.87 min corresponds to $[M\cdot + H]^+ = 596$, which is the ion corresponding to the epoxy-alkyl radical of ChOOH trapped by POBN. (**E**) Representative MS spectrum from peak at 21.87 min: $[M\cdot + H]^+ = 596$; $[M\cdot + H - POBN - H_2O]^+ = 383$; $[M\cdot + H - ChOOH]^+ = 195$. These experiments were performed in triplicate.

*CYTC reacts with lipid hydroperoxides faster than with $H_2O_2$*

Transient-state kinetic experiments were performed in a stopped-flow spectrophotometer in the single-mixing mode as described in the *Experimental section*.[44] First, we analyzed the kinetic parameters for interaction of CYTC (0.8 μM) and SDS micelles by following the heme absorbance shift from 410 to 408 nm to confirm low-spin state of the protein.[27] The interaction of CYTC and SDS did not follow simple second-order kinetics and the plot of $k_{obs}$ against SDS concentration

was a rectangular hyperbola (**figure S3**). This saturation behavior indicates a binding interaction between CYTC and SDS-micelles. The value of dissociation constant (K) of 3.1 mM was estimated directly from hyperbolic equation using a nonlinear least-square fit to the data. Therefore, we confirmed that SDS concentration of 8 mM used in our experiments was enough to shift CYTC-active site and displace Met[80] from the axial coordination, which generates a species that is more similar to *in vivo* conditions.[27]

In the next step, we determined the reaction of micelles-associated ChOOH (4–10 μM) with CYTC by following heme decay at 408 nm, because the spectroscopic characterization of CYTC compound I and II is possible only in pH extremes.[45] Typical pseudo-first-order kinetics was observed for each ChOOH concentration (**figure 8,** *insert*). Plotting the obtained $k_{obs}$ values against the ChOOH concentration provided a straight line, the slope of which provided the second-order rate constant of the CYTC-bleaching of $k = (2.5 \pm 0.3) \times 10^3$ M$^{-1}$·s$^{-1}$ (pH 7.4, 25 °C) (**figure 8**).
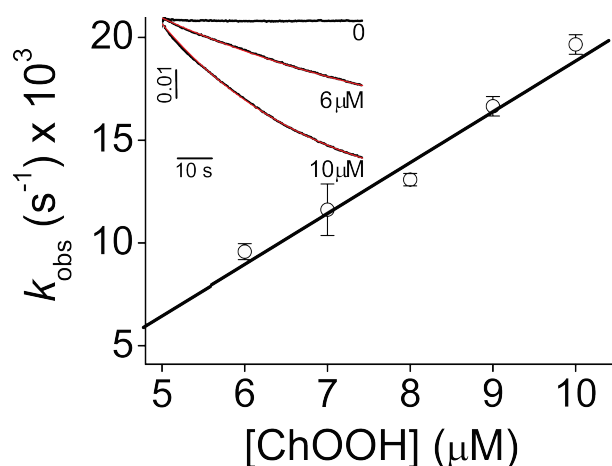


**Figure 8.** Determination of the second-order rate constant of the reaction between ChOOH and CYTC. Pseudo first-order rate constants ($k_{obs}$) were determined upon mixing of CYTC (0.8 μM) with SDS (8 mM), DTPA (0.1 mM), bicarbonate buffer (25 mM), ChOOH (at the indicated concentrations), pH 7.4. The reaction time course was monitored at 408 nm at 25 °C for 60 s. The insert graph shows typical traces

obtained in the absence (0) and presence of ChOOH 6 and 10 μM. The $k_{obs}$ values were determined using the single curve-fit equation of the instrument software (*red line*). The apparent second-order rate constant was calculated from the slope using linear least-square regression analysis (*black line*). The values shown are the means ± S.D. obtained from three independent experiments.

This rate was about two orders of magnitude higher in the presence of ChOOH than H$_2$O$_2$ (**table 1**). As comparisons, we also determined – in our experimental conditions – the rate constant of CYTC-bleaching induced by LAOOH (**figure S4**). By using the competitive method, the authors assumed that the peroxidase cycle is irreversible and the reaction between CYTC and ROOH is the rate-determining step in the whole cycle.[21] To estimate the rate constant of the reaction between CYTC and ROOH by measuring the rate of the bleaching, we also assumed that the cycle is irreversible and that this is the rate-determining step in the whole cascade of reactions. Interestingly, the use of this assumption gave similar rate constants for LAOOH and H$_2$O$_2$ when compared to previous determinations (**table 1**), which shows that our method of determination may be valid for this purpose.[21] Since organic hydroperoxides can oxidize CYTC-heme more effectively than H$_2$O$_2$,[29] we could reason that reaction with lipid hydroperoxides may be yet another important regulatory function of CYTC in mitochondria during respiration and apoptosis.

**Table 1**

Rate constants for the heme-group oxidation promoted by SDS-micelle-associated peroxides.

| R-OOH | $^{\$}$Our determinations k ($M^{-1}s^{-1}$) | $^{\#}$Previous determinations k ($M^{-1}s^{-1}$) |
|:---:|:---:|:---:|
| $H_2O_2$ | $2.09 \pm 0.02 \times 10^1$ | $4.64 \times 10^1$ |
| LAOOH | $1.52 \pm 0.05 \times 10^4$ | $5.20 \times 10^4$ |
| ChOOH | $2.50 \pm 0.20 \times 10^3$ | ND |

$^{\$}$Values correspond to the average of three distinct determinations. Determinations were done as shown in the *experimental section*.
$^{\#}$Values extracted from reference 21. These determinations were done using cardiolipin-containing liposomes.

**Discussion**

CYTC is peripherally bound to the inner membrane of the mitochondria, which increases the possibility of a reaction with lipid-derived hydroperoxides. This reaction can occur via one- or two-electron mechanisms (see **scheme 2**).[21] The first mechanism consists of the homolytic cleavage of the O—O bond, generating the highly reactive alkoxyl radical.[46] The second mechanism consists on the heterolytic cleavage of the O—O bond, a mechanism that reduces the hydroperoxide group to the corresponding alcohol and is known to be the catalytic mechanism of several peroxidase enzymes.[47,48] Indeed, this mechanism was suggested by several authors as an antioxidant mechanism of CYTC in the mitochondria, where it reduces fatty acid hydroperoxides to the corresponding alcohols.[21,49] On the other hand, it is hard to see

the homolytic mechanism as antioxidant, since the product of the cleavage is more reactive than the hydroperoxide itself.[50]
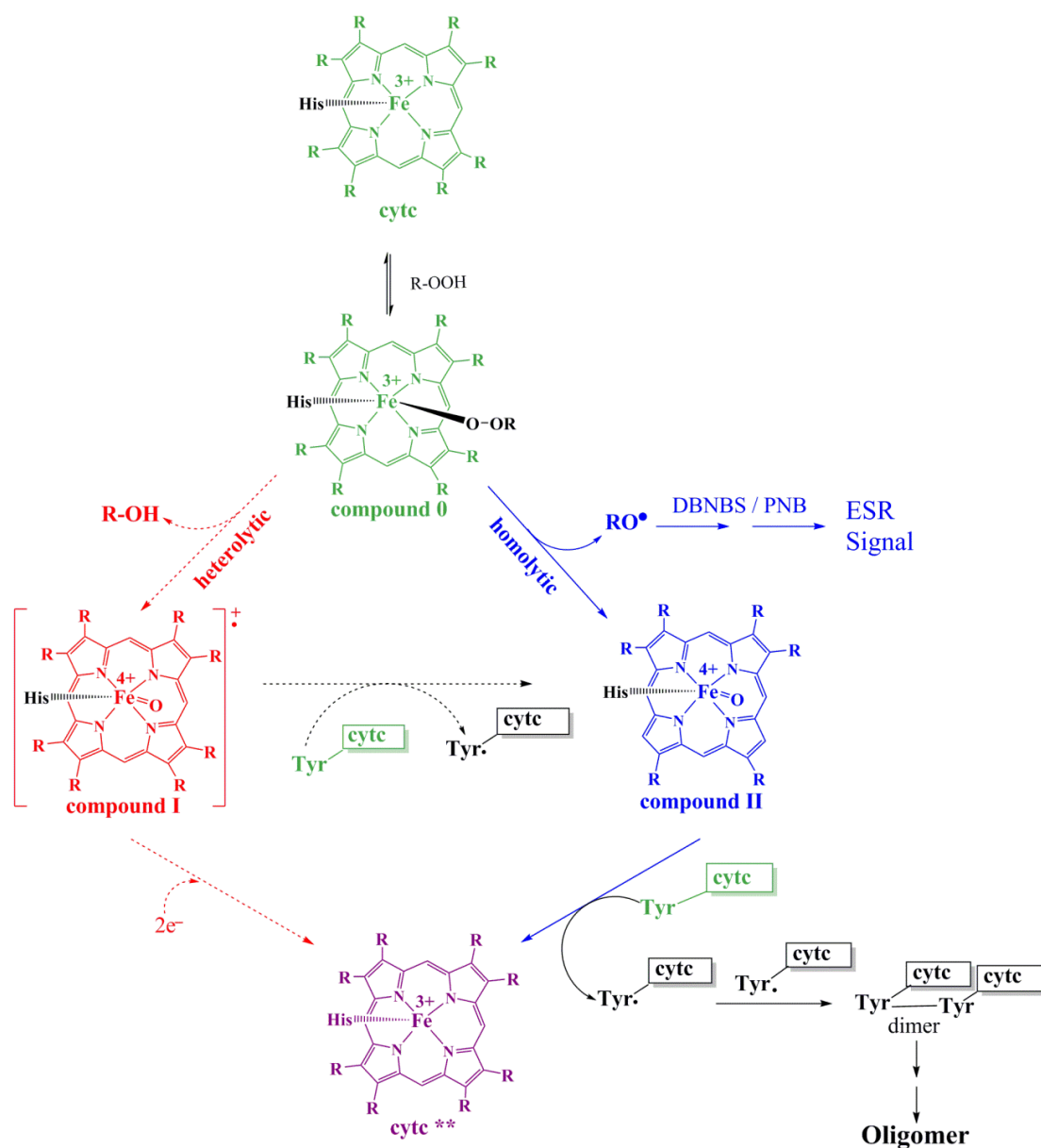


**Scheme 2**. Supposed peroxidase cycle of CYTC upon reaction with hydroperoxides. The reaction can occur via the homolytic (*blue section*) or heterolytic mechanisms (*red section*). After the cycle the heme group is disrupted and the protein is presumably inactivated (species marker with ** at the *purple section*). The alkoxyl radical produced in the homolytic pathway can be trapped by POBN/DBNBS/PBN after rearrangement to the epoxy-alkyl radical shown in **scheme 3**. Tyrosine radicals can recombine producing protein dimers and oligomers.

The reaction between CYTC and ChOOH leads to the formation of carbon-centered radicals on the protein and the lipid (**figures 2**, **3, 4 and 5**). Lipid radicals

can be formed by a homolytic cleavage of the O—O bond, generating an alkoxyl radical allylic to the double bond. This species, in turn, is highly unstable and rearranges spontaneously to the epoxide, generating a carbon-centered radical (see scheme 3).[46,51] This is the species being trapped by PBN, POBN and DBNBS (**figures 2**, **3, 4 and 5**). Since the rearrangement of the alkoxyl radical to the epoxide is much faster than the reaction of alkoxyl radical with spin traps the entrapment of this species is difficult.[46,51,52] Indeed, Belikova and co-workers did not see any alkoxyl radicals in the reaction of CYTC with LAOOH using DMPO (500 mM), probably because LAOOH-derived alkoxyl radicals rapidly rearranges to the epoxide in a similar way as ChOOH (see **scheme 3**).[21] In addition, incubations with DMPO (350 mM) in our experimental conditions did not trap any alkoxyl radicals in the reaction of CYTC and ChOOH (*data not shown*).
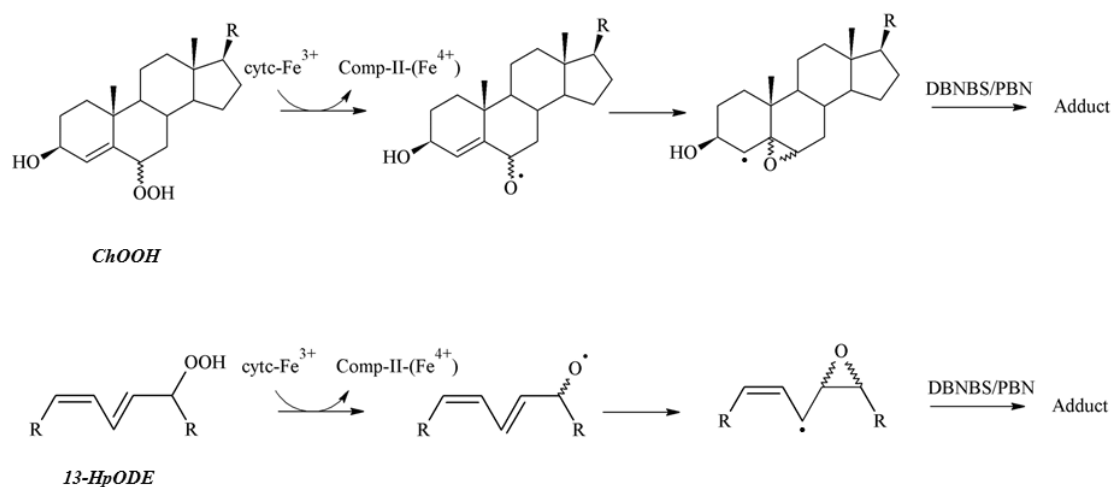


**Scheme 3**. Homolytic cleavage of the O—O bond mediated by CYTC. The hydroperoxide is cleaved generating an alkoxyl radical that rearranges producing a carbon-centered radical. This carbon-centered radical, in turn, can react with a spin trap and be visualized by EPR. The 6-OOH (ChOOH) isomer was chosen as an example, but the reaction mechanism is the same for all isomers shown in **scheme 1**.

Interestingly, Belikova and co-workers did not trap carbon-centered radicals with POBN in the reaction of CYTC with LAOOH.[21] We believe that the inobservance of the EPR signal is associated with the concentration of LAOOH used

in their experiment (5 μM). Observing **figure 5**, it can be seen that incubating CYTC in the presence of cardiolipin-containing liposomes with 5 μM LAOOH yields a signal barely distinguishable from the noise. Increasing LAOOH concentration (1 mM) leads to an intense signal that can be attributed to a carbon-centered lipid-derived radical, which reinforces the idea that 5 μM of LAOOH is not enough to provide a detectable signal. Altogether, these data suggest that CYTC reacts with lipid-derived peroxides via a homolytic mechanism.

Protein radicals were identified using DBNBS and PBN as spin trapping (**figures 2**, **3 and S1**) and can be explained by both hetero- and homolytic cleavages of the O—O bond. The homolytic mechanism occurs with the one-electron oxidation of CYTC to compound II ($Fe^{4+}$) (**scheme 2**). Since CYTC is not a peroxidase enzyme *per se*, the return to the native form is not as effective as other peroxidases. Moreover, the recovery of the native protein after a "peroxidase cycle" was never possible. Literature shows that CYTC ends the "peroxidase cycle" with either the heme group oxidized (bleaching of the Soret band) or with amino acids oxidized (i.e. tyrosine residues).[18,35] This is an indication that compounds I and II of CYTC are not stable and their reduction to the native form ($Fe^{3+}$) occurs with the oxidation of the protein chain. Indeed, spectroscopic studies of CYTC were only able to identify the compounds I and II in extreme pHs.[45] This hypothesis is supported by the results depicted in **figure 1**, where the incubation of CYTC with increasing concentrations of ChOOH promoted a dose-dependent bleaching of the Soret band. In parallel, increasing concentrations of ChOOH also promoted a dose-dependent increase in the EPR signal of both lipid and protein radicals (**figure 3**), suggesting that oxidation of the heme group and appearance of the lipid and protein radicals are co-dependent processes. This hypothesis is further supported by the experiments where CYTC was

pre-incubated with CN⁻, an ion that replaces Met[80] and prevents the reaction with ChOOH (**figures 2** and **S1**). Tyrosine residues were previously identified to be oxidized and dimerized upon reaction with peroxides.[18,35] Oxidation of tyrosine residues generates a phenoxyl radical that, in turn, resonates in the aromatic ring giving carbon-centered radicals.[53] These radicals, in turn, can follow many pathways, including: *i)* entrapment by spin traps and visualization by EPR as in **figures 2**, **3, S1** and **S2** (which was also confirmed by MS as shown in **figure 7**) or; *ii)* recombination generating protein dimers and, subsequently, oligomers as in **figure 6**.[53]

The heterolytic mechanism occurs via a two-electron oxidation of CYTC to compound I ($Fe^{4+}=O$) (see **scheme 2**). Analogously, the reduction of compound I to the native form is not effective for CYTC, and the heme group would end up oxidizing amino acid residues also producing protein radicals. Interestingly, from a thermodynamic point of view, the compound II of HRP has a slightly higher oxidizing potential than the compound I.[50,54] Since this determination cannot be made for CYTC, we speculate that compounds I and II of CYTC would behave similarly, with compound II being a stronger oxidant than compound I. Although both mechanisms explain the formation of protein radicals, we suggest that, due to the identification of lipid-derived carbon-centered radicals, these reactions occur, preferentially, via the homolytic mechanism.

The reactions of CYTC-bleaching by lipid-derived hydroperoxides have higher rate constants when compared with $H_2O_2$ (**table 1**).[21] In our experimental conditions, ChOOH presented a rate constant comparable to LAOOH. One of the possible explanations for this kinetic difference is that, due to the hydrophobicity of lipid-derived hydroperoxides (including ChOOH), they stay immersed in the membrane and/or in the SDS-micelles, a condition that facilitates the interaction of

the peroxide group with the membrane-bound CYTC. This condition would also increase the concentration of the lipid-derived hydroperoxides at the interface of the membrane, which would increase the reaction rate.

Overall, our results corroborate available data showing that CYTC reacts with lipid-derived hydroperoxides with higher rate constants than with other peroxides (i.e. $H_2O_2$). Due to the elevated rate constant, ChOOH might be an important substrate for CYTC, contributing to the free radical production in the mitochondria. As opposite to classic peroxidases (i.e. HRP), our data suggest that these reactions occur via a homolytic mechanism, a situation that leads to the formation of lipid and protein radicals and induces CYTC inactivation and oligomerization. From an evolutionary perspective, CYTC evolved to transport electrons in the mitochondria through a redox cycle that only involves the reduction and re-oxidation of the heme-iron ($Fe^{3+}/Fe^{2+}/Fe^{3+}$). In a situation of enhanced oxidative stress in the mitochondria, the hydroperoxides production would be increased and these reactions would be more likely to occur. We speculate that, instead of an antioxidant mechanism, CYTC would contribute to increase the oxidative stress in the mitochondria and, ultimately, to apoptosis signaling. In this context, could this inactive form of CYTC be the one that is released in the initial steps of the apoptosis signaling?

**ASSOCIATED CONTENT**

*Supporting information*

Figures corresponding to EPR spectra using PBN and POBN, kinetic data of the interaction of SDS with CYTC and kinetic data of the reaction of $H_2O_2$ with

CYTC are found in the supporting information. This material is available free of charge via the Internet at http://pubs.acs.org.

*Abbreviations*

ChOOH, cholesterol-derived hydroperoxides; CYTC, cytochrome *c*; SDS, sodium dodecyl sulfate; StAR, steroidogenic acute regulatory protein; *t*-BuOOH, *tert*-butil hydroperoxide; LAOOH, linoleic acid-derived hydroperoxides; ROOH, hydroperoxides used in the study; ROS, reactive oxygen species; EPR, electron paramagnetic resonance; TOCL, tetraoleoylcardiolipin; DOPC, dioleoylphosphatidylcholine; CL, cardiolipin; DTPA, Diethylenetriaminepentaacetic acid; PBN, alpha-phenyl N-tertiary-butyl nitrone; DMPO, 5,5-dimethyl-pyrroline N-oxide; DBNBS, 3,5-Dibromo-4-nitrosobenzenesulfonic acid; POBN, α-(4-pyridyl-1-oxide)-N-tert-butylnitrone; KCN, potassium cyanide; MNP, 2-methyl-2-nitrosopropane; LC-MS, liquid chromatography coupled with mass spectrometry; ESI, electrospray ionization; SDS-PAGE, SDS-polyacrylamide gel electrophoresis; HRP, horseradish peroxidase; 13-HpODE, 13-hydroperoxy-linoleic acid.

**References**

(1)     Garcia-Ruiz, C.; Mari, M.; Colell, A.; Morales, A.; Caballero, F.; Montero, J.; Terrones, O.; Basanez, G.; Fernandez-Checa, J. C. *Histol Histopathol* **2009**, *24*, 117.

(2)     Ikonen, E. *Nature Reviews Molecular Cell Biology* **2008**, *9*, 125.

(3)     Miller, W. L. *Biochimica Et Biophysica Acta-Molecular and Cell Biology of Lipids* **2007**, *1771*, 663.

(4)     Maxfield, F. R.; Tabas, I. *Nature* **2005**, *438*, 612.

(5)     van Meer, G.; Voelker, D. R.; Feigenson, G. W. *Nature Reviews Molecular Cell Biology* **2008**, *9*, 112.

(6)    Korytowski, W.; Pilat, A.; Schmitt, J. C.; Girotti, A. W. *J. Biol. Chem.* **2013**, *288*, 11509.

(7)    Colell, A.; Fernandez, A.; Fernandez-Checa, J. C. *Journal of Bioenergetics and Biomembranes* **2009**, *41*, 417.

(8)    Fernandez, A.; Llacuna, L.; Fernandez-Checa, J. C.; Colell, A. *Journal of Neuroscience* **2009**, *29*, 6394.

(9)    Montero, J.; Morales, A.; Llacuna, L.; Lluis, J. M.; Terrones, O.; Basanez, G.; Antonsson, B.; Prieto, J.; Garcia-Ruiz, C.; Colell, A.; Fernandez-Checa, J. C. *Cancer Research* **2008**, *68*, 5246.

(10)   Yin, H. Y.; Xu, L. B.; Porter, N. A. *Chem. Rev.* **2011**, *111*, 5944.

(11)   Xu, L. B.; Korade, Z.; Porter, N. A. *J. Am. Chem. Soc.* **2010**, *132*, 2222.

(12)   Bartesaghi, S.; Wenzel, J.; Trujillo, M.; Lopez, M.; Joseph, J.; Kalyanaraman, B.; Radi, R. *Chem. Res. Toxicol.* **2010**, *23*, 821.

(13)   Isom, A. L.; Barnes, S.; Wilson, L.; Kirk, M.; Coward, L.; Darley-Usmar, V. *J. Am. Soc. Mass Spectrom.* **2004**, *15*, 1136.

(14)   Genaro-Mattos, T. C.; Appolinario, P. P.; Mugnol, K. C.; Bloch, C., Jr.; Nantes, I. L.; Di Mascio, P.; Miyamoto, S. *Chem Res Toxicol* **2013**, *26*, 1536.

(15)   Marnett, L. J. *Carcinogenesis* **2000**, *21*, 361.

(16)   Chamulitrat, W.; Takahashi, N.; Mason, R. P. *J. Biol. Chem.* **1989**, *264*, 7889.

(17)   Kalyanaraman, B.; Mottley, C.; Mason, R. P. *J. Biol. Chem.* **1983**, *258*, 3855.

(18)   Barr, D. P.; Gunther, M. R.; Deterding, L. J.; Tomer, K. B.; Mason, R. P. *J Biol Chem* **1996**, *271*, 15498.

(19)   Chen, Y. R.; Chen, C. L.; Chen, W. G.; Zweier, J. L.; Augusto, O.; Radi, R.; Mason, R. P. *Journal of Biological Chemistry* **2004**, *279*, 18054.

(20)     Dyer, C.; Schubert, A.; Timkovich, R.; Feinberg, B. A. *Biochimica Et Biophysica Acta* **1979**, *579*, 253.

(21)     Belikova, N. A.; Tyurina, Y. Y.; Borisenko, G.; Tyurin, V.; Samhan Arias, A. K.; Yanamala, N.; Furtmuller, P. G.; Klein-Seetharaman, J.; Obinger, C.; Kagan, V. E. *J Am Chem Soc* **2009**, *131*, 11288.

(22)     Miyamoto, S.; Nantes, I. L.; Faria, P. A.; Cunha, D.; Ronsein, G. E.; Medeiros, M. H.; Di Mascio, P. *Photochem Photobiol Sci* **2012**, *11*, 1536.

(23)     Davies, M. J. *Biochim Biophys Acta* **1988**, *964*, 28.

(24)     Barr, D. P.; Mason, R. P. *J Biol Chem* **1995**, *270*, 12709.

(25)     Iwahashi, H.; Nishizaki, K.; Takagi, I. *Biochem J* **2002**, *361*, 57.

(26)     Nantes, I. L.; Faljoni-Alario, A.; Nascimento, O. R.; Bandy, B.; Gatti, R.; Bechara, E. J. *Free Radic Biol Med* **2000**, *28*, 786.

(27)     Mugnol, K. C.; Ando, R. A.; Nagayasu, R. Y.; Faljoni-Alario, A.; Brochsztain, S.; Santos, P. S.; Nascimento, O. R.; Nantes, I. L. *Biophys J* **2008**, *94*, 4066.

(28)     Kaur, H. *Free Radic Res* **1996**, *24*, 409.

(29)     Oellerich, S.; Lecomte, S.; Paternostre, M.; Heimburg, T.; Hildebrandt, P. *Journal of Physical Chemistry B* **2004**, *108*, 3871.

(30)     Uemi, M.; Ronsein, G. E.; Miyamoto, S.; Medeiros, M. H.; Di Mascio, P. *Chem Res Toxicol* **2009**, *22*, 875.

(31)     Miyamoto, S.; Martinez, G. R.; Rettori, D.; Augusto, O.; Medeiros, M. H. G.; Di Mascio, P. *P Natl Acad Sci USA* **2006**, *103*, 293.

(32)     Laemmli, U. K. *Nature* **1970**, *227*, 680.

(33)     Chen, Y. R.; Deterding, L. J.; Sturgeon, B. E.; Tomer, K. B.; Mason, R. P. *J Biol Chem* **2002**, *277*, 29781.

(34)     Hill, B. C.; Nicholls, P. *Biochem. J.* **1980**, *187*, 809.

(35)    Qian, S. Y.; Chen, Y. R.; Deterding, L. J.; Fann, Y. C.; Chignell, C. F.; Tomer, K. B.; Mason, R. P. *Biochem J* **2002**, *363*, 281.

(36)    Hiramoto, K.; Hasegawa, Y.; Kikugawa, K. *Free Radic Res* **1994**, *21*, 341.

(37)    Kalyanaraman, B.; Joseph, J.; Kondratenko, N.; Parthasarathy, S. *Biochim Biophys Acta* **1992**, *1126*, 309.

(38)    Pou, S.; Ramos, C. L.; Gladwell, T.; Renks, E.; Centra, M.; Young, D.; Cohen, M. S.; Rosen, G. M. *Anal. Biochem.* **1994**, *217*, 76.

(39)    Novakov, C. P.; Feierman, D.; Cederbaum, A. I.; Stoyanovsky, D. A. *Chem. Res. Toxicol.* **2001**, *14*, 1239.

(40)    Buettner, G. R. *Free Radic Biol Med* **1987**, *3*, 259.

(41)    Shan, Z.; Yu, Q.; Purwaha, P.; Guo, B.; Qian, S. Y. *Free Radic Res* **2009**, *43*, 13.

(42)    Wilcox, A. L.; Marnett, L. J. *Chem Res Toxicol* **1993**, *6*, 413.

(43)    Blumenthal, D. C.; Kassner, R. J. *J. Biol. Chem.* **1980**, *255*, 5859.

(44)    Isin, E. M.; Guengerich, F. P. *J. Biol. Chem.* **2007**, *282*, 6863.

(45)    Orii, Y.; Shimada, H. *Journal of Biochemistry* **1978**, *84*, 1543.

(46)    Wilcox, A. L.; Marnett, L. J. *Chem. Res. Toxicol.* **1993**, *6*, 413.

(47)    Rodriguez-Lopez, J. N.; Lowe, D. J.; Hernandez-Ruiz, J.; Hiner, A. N. P.; Garcia-Canovas, F.; Thorneley, R. N. F. *J. Am. Chem. Soc.* **2001**, *123*, 11838.

(48)    Rodriguez-Lopez, J. N.; Smith, A. T.; Thorneley, R. N. *J Biol Chem* **1996**, *271*, 4023.

(49)    Belikova, N. A.; Vladimirov, Y. A.; Osipov, A. N.; Kapralov, A. A.; Tyurin, V. A.; Potapovich, M. V.; Basova, L. V.; Peterson, J.; Kurnikov, I. V.; Kagan, V. E. *Biochemistry* **2006**, *45*, 4998.

(50)    Buettner, G. R. *Arch. Biochem. Biophys.* **1993**, *300*, 535.

(51)     Dix, T. A.; Marnett, L. J. *J. Biol. Chem.* **1985**, *260*, 5351.

(52)     Stolze, K.; Udilova, N.; Nohl, H. *Acta Biochim Pol* **2000**, *47*, 923.

(53)     Shchepin, R.; Moller, M. N.; Kim, H. Y.; Hatch, D. M.; Bartesaghi, S.; Kalyanaraman, B.; Radi, R.; Porter, N. A. *J Am Chem Soc* **2010**, *132*, 17490.

(54)     Hayashi, Y.; Yamazaki, I. *J Biol Chem* **1979**, *254*, 9101.

# Revisiting cytochrome *c* peroxidase activity

# using cholesterol hydroperoxides as substrates
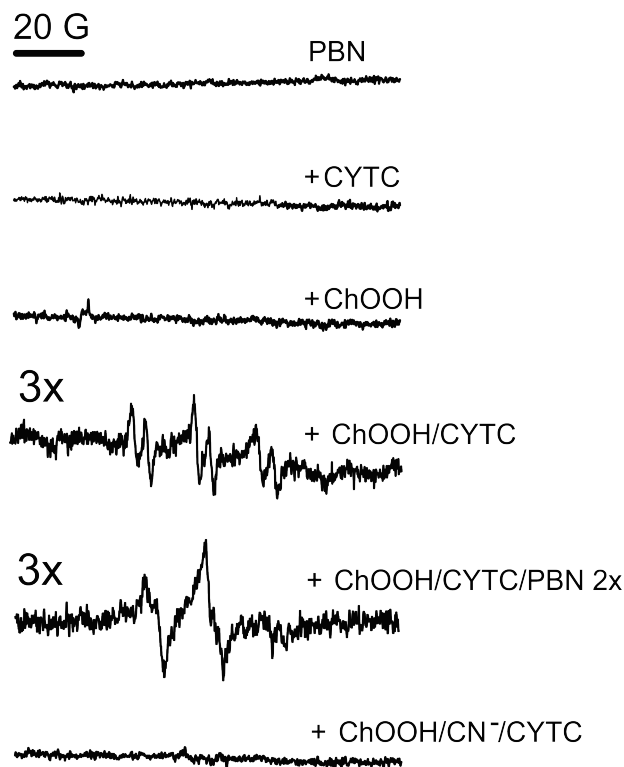
**Figure S1.** Production of lipid radicals in the CYTC-peroxidase activity. SDS-micelles were prepared by mixing SDS (8 mM), PBN (50 mM), ChOOH (1 mM) and DTPA (0.1 mM) in bicarbonate buffer (25 mM), pH 7.4. CYTC (100 μM) was added to the mixture and incubated at 25 °C. After 5 min, an aliquot was transferred to a quartz flat cell and the EPR spectrum was recorded. In some experiments, cyanide (10 mM) was pre-incubated with CYTC (1 mM) for 5 min before its addition in the reaction mixtures. In the fifth line, PBN 2x indicates that its concentration was twice. Spectra were accumulated four times and are representative of three independent experiments.

ChOOH          LAOOH

20 G

+ R-OOH

+ R-OOH/CYTC
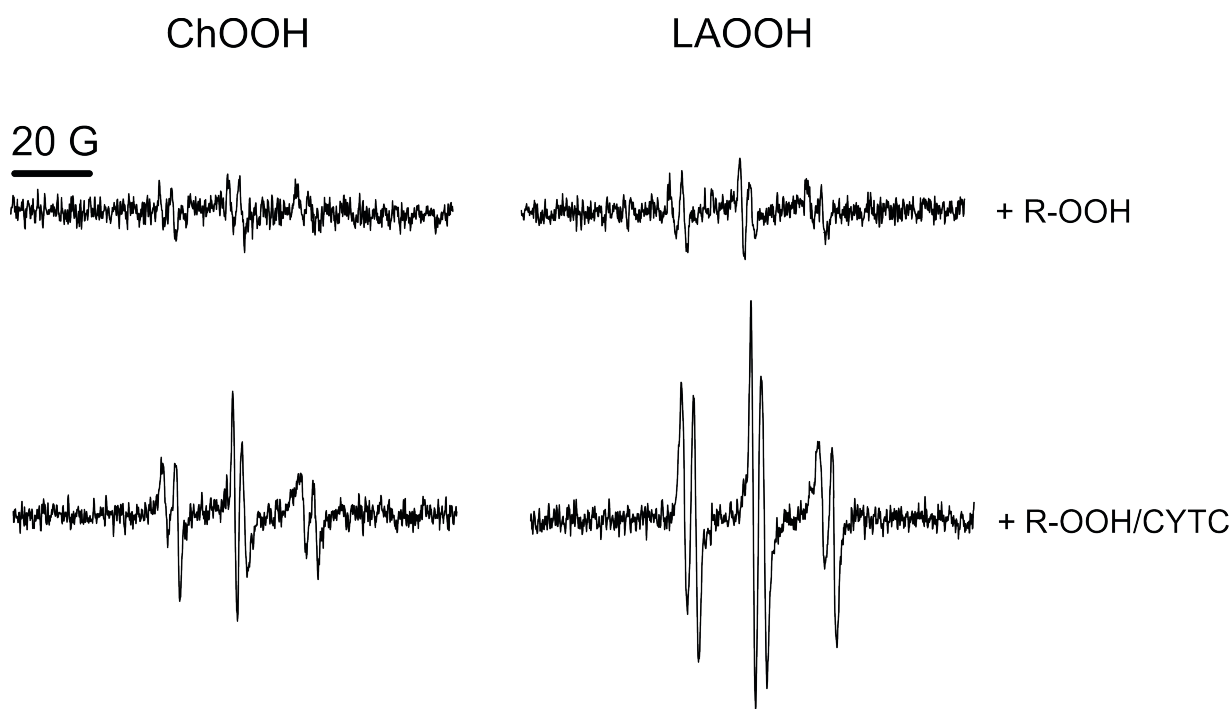
**Figure S2.** Spin-trapping of CYTC-derived radicals formed from its peroxidase activity in liposomes. CYTC (50 μM) was added to cardiolipin-containing liposomes already containing LAOOH (80 μM) and ChOOH (80 μM) (prepared as described in the *Experimental section*), POBN (100 mM) and DTPA (0.1 mM) in bicarbonate buffer (25 mM), pH 7.4. The mixture was incubated at 25 ºC. After 5 min, an aliquot was transferred to a quartz flat cell and the EPR spectrum was recorded. Spectra were accumulated four times and are representative of three independent experiments.
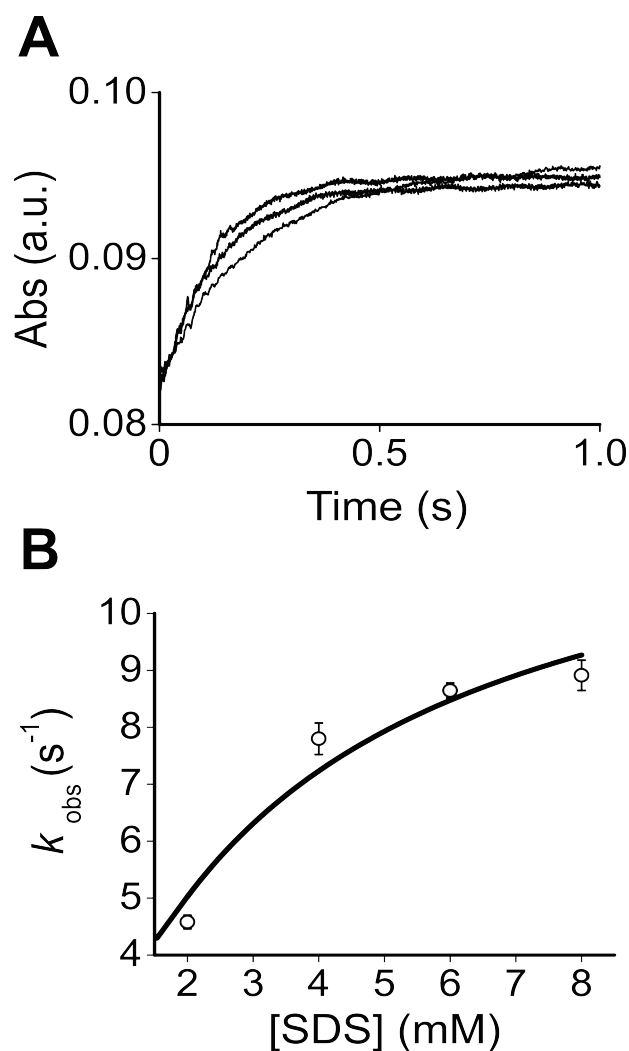
**Figure S3.** Determination of the kinetic constants of the interaction of SDS with CYTC. SDS-micelles were prepared by mixing SDS (at the specified concentrations), DTPA (0.1 mM) in bicarbonate buffer (25 mM), pH 7.4. Following, CYTC (100 μM) was allowed to mix with SDS-micelle. (**A**) The reaction time course was monitored at 408 nm at 25 °C for 1 s. The graph shows typical traces obtained in the presence of SDS 2 and 8 mM. The $k_{obs}$ values were determined using the single curve-fit equation of the instrument software. (**B**) Kinetic constants were obtained by *hyperbolic* nonlinear *regression oh the data (black line).* The values shown are the means ± S.D. obtained from three independent experiments.
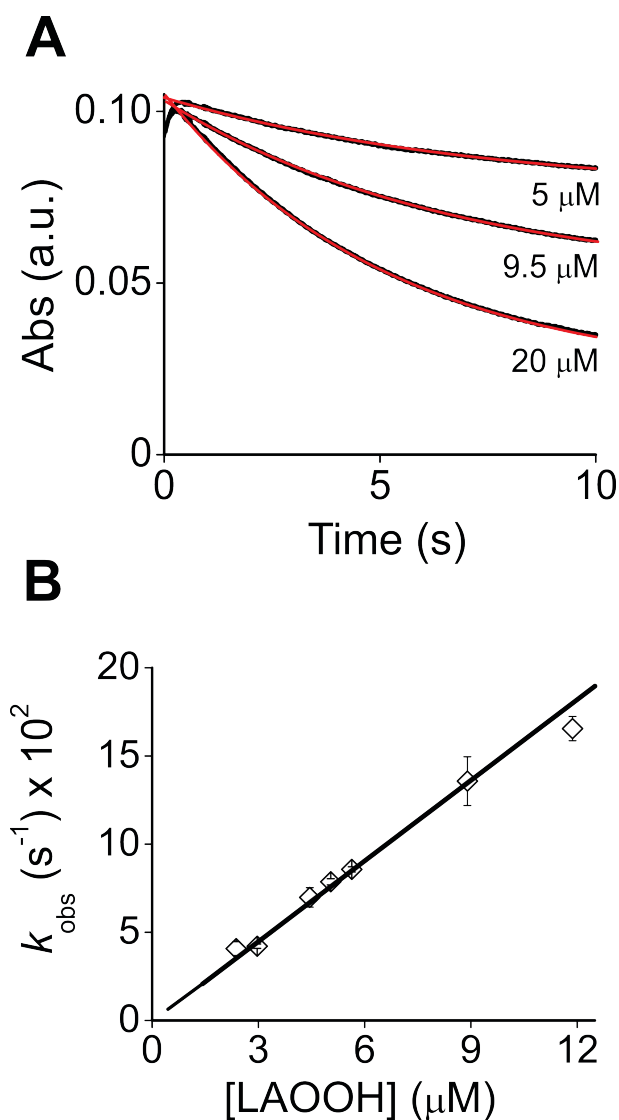
**Figure S4**. Determination of the second-order rate constant of the reaction of LAOOH with CYTC. Pseudo first-order rate constants ($k_{obs}$) for reaction of LAOOH with CYTC were determined upon mixing of CYTC (0.8 µM) with SDS (8 mM), DTPA (0.1 mM), bicarbonate buffer (25 mM), LAOOH (at the specified concentrations), pH 7.4. (**A**) The reaction time course was monitored at 408 nm at 25 ºC for 30 s. The graph shows typical traces obtained in the presence of LAOOH 5, 9.5 and 20 µM. The $k_{obs}$ values were determined using the single curve-fit equation of the instrument software. (**B**) The apparent second-order rate constant was calculated from the slope using linear least-square regression analysis (*black line*). The values shown are the means ± S.D. obtained from three independent experiments.

# Chapter 2

## Covalent Binding and Anchoring of Cytochrome *c* to Mitochondrial Mimetic Membranes Promoted by Cholesterol Carboxyaldehyde

# Covalent Binding and Anchoring of Cytochrome *c* to Mitochondrial Mimetic Membranes Promoted by Cholesterol Carboxyaldehyde

Thiago C. Genaro-Mattos,[†] Patricia P. Appolinário,[†] Katia C. U. Mugnol,[‡] Carlos Bloch Jr.,[§]
Iseli L. Nantes,[‡] Paolo Di Mascio,[†] and Sayuri Miyamoto*,[†]

[†]Departamento de Bioquímica, Instituto de Química, Universidade de São Paulo, São Paulo, SP, Brazil
[‡]Centro de Ciências Naturais e Humanas, Universidade Federal do ABC, Santo Andre, SP, Brazil
[§]Laboratório de Espectrometria de Massas, Embrapa Recursos Genéticos e Biotecnologia, Brasília, DF, Brazil

**S** Supporting Information

**ABSTRACT:** Mitochondrial cholesterol has been reported to be increased under specific pathological conditions associated with enhanced oxidative stress parameters. In this scenario, cholesterol oxidation would be increased, leading to the production of reactive aldehydes, including cholesterol carboxyaldehyde (ChAld). By using SDS micelles as a mitochondrial mimetic model, we have demonstrated that ChAld covalently modifies cytochrome *c* (cytc), a protein known to participate in electron transport and apoptosis signaling. This mimetic model induces changes in cytc structure in the same way as mitochondrial membranes do. Tryptic digestion of the cytc-ChAld adduct followed by MALDI-TOF/TOF analyses revealed that modifications occur at Lys residues (K22) localized at cytc site L, a site involved in protein−protein and protein−membrane interactions. Interestingly, ChAld ligation prevented cytc detachment from liposomes even under high ionic strength conditions. Overall, it can be concluded that ChAld ligation to Lys residues at site L creates a hydrophobic tail at cytc, which promotes cytc anchoring to the membrane. Although not investigated in detail in this study, cytc adduction to cholesterol derived aldehydes could have implications in cytc release from mitochondria under apoptotic stimuli.
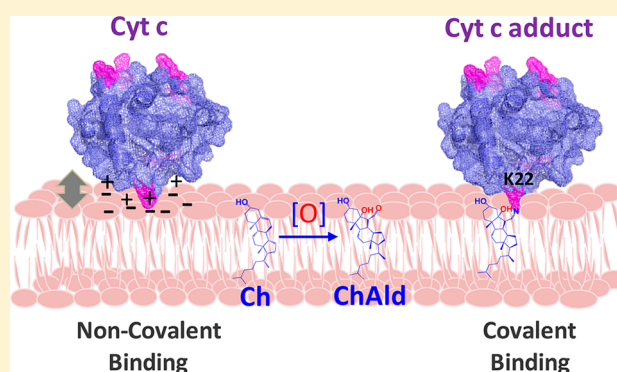
## INTRODUCTION

Cytochrome *c* (cytc) is a small heme protein attached to the external side of the inner mitochondrial membrane where it is responsible for the electron transport between cytochrome *c* reductase and cytochrome *c* oxidase.[1] The electron transport mediated by cytc occurs through a lateral diffusion of this protein on the external side of the membrane, where it interacts with phospholipids.[2] The interaction between cytc and the mitochondrial membrane is mostly mediated by electrostatic interactions between lysine residues and the phosphate groups of phospholipids, especially cardiolipin.[2−4] It has also been proposed that an acyl chain from cardiolipin penetrates in a hydrophobic core of the protein and contributes for the protein anchorage to the membrane.[5,6] In specific situations and under the proper stimuli, cytc is released to the cytosol where it is involved in apoptosis signaling.[1,7,8]

Cholesterol is a neutral amphiphilic lipid widely found in the cell membrane of eukaryotes where it plays an important role by maintaining lipid organization and fluidity.[9−11] It is enriched in specific membrane regions known as lipid rafts.[12−14] These regions are recognized to act as scaffolds to membrane-bound proteins and to have an influence in signaling transduction.[12,14,15] Unlike the cell plasma membrane that is rich

in cholesterol, the mitochondrial inner membrane has a very small pool of this lipid, corresponding to 0.5 to 3% of the amount found in the cell membrane.[11,16] However, several studies reported elevated cholesterol levels (2−10-folds higher concentration) in the mitochondria of cancerous cells[17−19] and in nervous tissues of patients with Alzheimer's disease,[9,20] which makes cholesterol a major target for lipid peroxidation. In addition, the increased cholesterol levels in the mitochondria are described to deplete mitochondrial glutathione (mGSH), probably by impairing the cytosolic mGSH influx through the mitochondrial membranes.[20,21] Since mitochondria are primary sources of reactive oxygen species (ROS), this depletion in mGSH could increase the oxidative stress and, consequently, lipid peroxidation inside the mitochondria.

Cholesterol oxidation promoted by reactive oxygen species generates several products including hydroperoxides and aldehydes.[22−26] In the last 10 years, studies have identified the formation of cholesterol-derived aldehydes, namely, the 3β-hydroxy-5-oxo-5,6-secocholestan-6-al (CSec) and its aldolization product 3β-hydroxy-5β-hydroxy-*B*-norcholestane-6β-car-
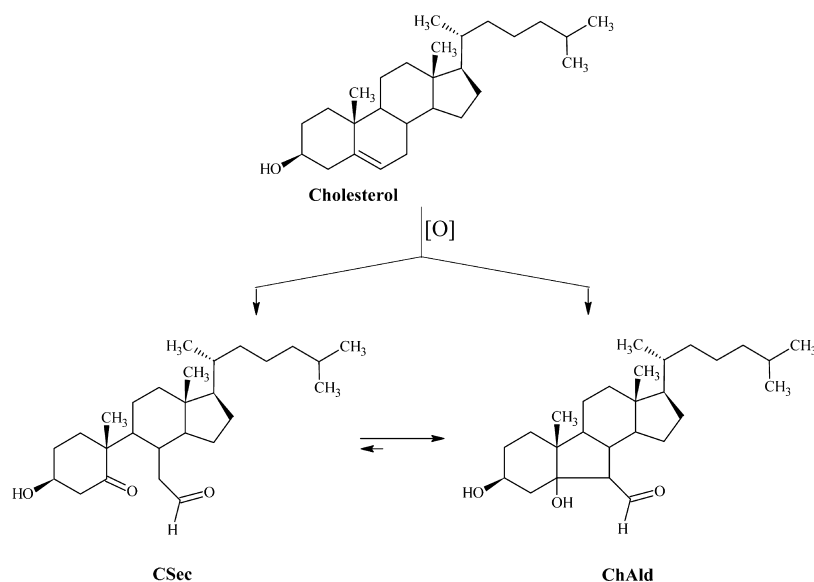
**Figure 1.** Chemical structures of 3β-hydroxy-5-oxo-5,6-secocholestan-6-al (CSec) and its aldolization product 3β-hydroxy-5β-hydroxy-*B*-norcholestane-6β-carboxaldehyde (ChAld). Both compounds have a molecular weight of 418.65 g/mol.

boxaldehyde (ChAld) during cholesterol oxidation mediated by ozone $(O_3)$[25,26] and/or singlet molecular oxygen $(^1O_2)$[23,24] (see Figure 1 for the aldehydes chemical structures). Wentworth Jr. and co-workers reported the formation of cholesterol aldehydes in atherosclerotic plaques *in vivo* and associated their presence with the formation of ozone in human arteries.[25] However, later studies have demonstrated that singlet molecular oxygen can also generate cholesterol aldehydes, in particular ChAld.[23,24] Indeed, this aldehyde was detected as the major aldehyde product both *in vitro* and *in vivo*.[27] In this sense, singlet molecular oxygen can be generated by a number of biologically relevant chemical pathways involving hydrogen peroxide and lipid hydroperoxides.[28−30] Among these pathways, we have recently demonstrated that the interaction of cytc with cardiolipin (CL) generates singlet oxygen,[31] indicating that this excited species can be generated in mitochondria where it can contribute to the oxidation of mitochondrial lipids.

ChAld exerted cytotoxic effects in different cell types present within atheromatous arteries. These aldehydes were also able to trigger a loss of secondary structure of apolipoprotein B-100 upon binding to LDL.[25] Moreover, ChAld was implicated in proatherogenic processes and was also reported to induce amyloidogenesis in several biological relevant proteins.[32] Since ChAld is believed to be the major cholesterol aldehyde found *in vivo*,[25] in the present study we investigated only the effect of this cholesterol derivative.

Several studies on cytc modification have been published demonstrating the ability of aldehydes derived from lipid peroxidation to react with basic amino acids of the protein.[33−35] For instance, the covalent addition of both 4-hydroxynonenal (HNE)[33] and 2,4-decadienal (DDE)[34] to cytc was reported. The addition mechanisms were either a condensation reaction, formation of a Schiff base adduct, or a Michael addition. From a biological point of view, several critiques can be made to studies using cytc adduction by lipid electrophiles in solution. Cytc is a membrane-bound protein that displays different conformation and physicochemical properties when bound to membranes when compared to the "free" protein in solution. Hence, depending on how the protein anchors to the membrane, the

adduction may occur at different portions on the protein (e.g., to different amino acid residues) and by different mechanisms. In this sense, the use of membrane models to mimic the interaction between cytc and the membrane will induce the expected conformation and physicochemical alterations to the protein, inducing the adduction at a more biologically relevant site on the protein. In addition, this approach may also help understand the biological implications of these adductions.

In the present study, we used micelles of sodium dodecyl sulfate (SDS) to mimic the inner mitochondrial membrane by providing the anchor base to cytc. The interactions between cytc and SDS micelles have been extensively characterized by Mugnol and co-workers.[36] The authors showed that, upon interaction with the micelles, cytc changes its tertiary structure and assumes an alternative low spin state, in which it holds the same structure and physicochemical properties as the cytc bound to the mitochondrial membrane.[36] In our study, the use of this particular model comes in handy since in addition to the alterations induced on the protein, it also behaves as a membrane model, preventing protein aggregation and sterol precipitation. Therefore, by using this model we were able to bring together ChAld and cytc in a manner similar to that presumed to occur in the mitochondrial membrane. Another convenience of using this model is that, unlike polyunsaturated fatty acids, SDS cannot be oxidized, which makes it a simpler model for elucidating the mechanisms proposed in this work. By doing that, we showed that cytc is covalently modified by ChAld in either the presence or the absence of the mimetic membrane. Relevantly, in the presence of mimetic membranes cytc modification was residue-specific and occurred primarily at Lys22, a residue situated in site L, a pH-dependent binding site of the protein. Interestingly, release of cytc from ChAld-containing liposomes is impaired when compared to cholesterol-containing ones, suggesting that covalent adduction could possibly influence cellular events involving cytc mobility. To our best knowledge, this is the first study to use this approach to elucidate the mechanisms of protein adduction induced by cholesterol electrophiles. Possible implications of these modifications to electron transport and apoptosis signaling are also discussed.
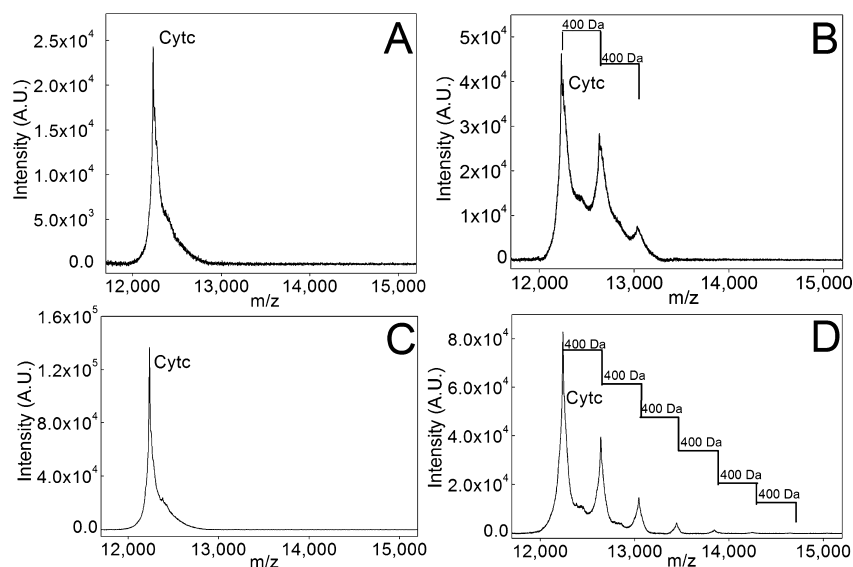
**Figure 2.** MALDI-TOF MS of cytc before and after 24 h of reaction with ChAld in the presence (panels A and B) and absence (panels C and D) of SDS micelles. Reactions were conducted in bicarbonate buffered media (10 mM, pH 7.4) containing 8 mM SDS (when present), 100 $\mu$M cytc, and 1 mM ChAld. Panels A and C show the control conditions performed in the absence of ChAld. Panels B and D represent the incubations conducted in the presence of 1 mM ChAld. The addition of ChAld leads to the appearance of peaks separated by 400 Da. Two and six ChAld additions can be observed at panels B and D, respectively.

## ■ EXPERIMENTAL PROCEDURES

**Chemicals.** Bovine heart cytochrome *c* (Fe(III)), ammonium bicarbonate (NH$_4$HCO$_3$), cholesterol (cholest-5-en-3-ol), sodium dodecyl sulfate (SDS), silica gel 60 (230−400 mesh), methylene blue, potassium monobasic phosphate (KH$_2$PO$_4$), potassium dibasic phosphate (K$_2$HPO$_4$), potassium chloride (KCl), and deuterated chloroform (CDCl$_3$) were purchased from Sigma (St. Louis, MO). Tetraoleoylcardiolipin (TOCL) and dipalmitoylphosphatidylcholine (DPPC) were from Avanti Polar Lipids, Inc. Isopropanol and acetonitrile were purchased from JTBaker. Trypsin Gold (mass spectrometry grade) was purchased from Promega. All other reagents were of analytical grade. The K22A cytc mutant was prepared exactly as described in Kawai et al.[37] Stock solutions of ammonium bicarbonate buffer (pH 7.4) were freshly prepared in Milli-Q water and the pH adjusted to 7.4 prior to use.

**Synthesis of 3-Hydroxy-5-hydroxy-$\beta$-norcholestane-6-carboxaldehyde (ChAld) by the Photooxidation of Cholesterol.** ChAld was synthesized as described by Uemi and co-workers.[23] Briefly, cholesterol (200 mg) was dissolved in 20 mL of chloroform in a 100 mL round-bottomed flask, and 250 $\mu$L of methylene blue solution (10 mM in methanol) was added. The solution was ice-cooled and irradiated using two tungsten lamps (500 and 300 W) for 2.5 h under continuous stirring and in an oxygen-saturated atmosphere. ChAld was purified by flash column chromatography using silica gel 60 (230−400 mesh). The column was equilibrated with hexane, and a gradient of hexane and ethyl ether was used. After purification, the solvent was evaporated, and the aldehyde was resuspended in isopropanol and stored at −80 °C for further use. ChAld's identity was confirmed by NMR spectroscopy, and its concentration was determined using propionaldehyde as an internal standard.

**Cytc Incubation with SDS Micelles.** The reaction between cytc and ChAld in the presence of SDS micelles was done in the presence of 10 mM ammonium bicarbonate buffer (pH 7.4). SDS (8 mM final concentration) was added prior to ChAld and cytc. After the addition of SDS, ChAld was added, and the mixture was agitated. After 5 min, cytc was added to the solution, and the reaction was carried out at 37 °C under constant agitation. The reaction in the absence of SDS was conducted exactly in the same way without adding SDS.

**Tryptic Digestion of Cytochrome *c*.** Cytc samples incubated in the absence and presence of ChAld were digested for 18 h with proteomic grade trypsin (Promega) in a 1:50 (w/w) ratio at 37 °C.

The reaction medium contained 50 mM ammonium bicarbonate (pH 8.0) and 1 mM CaCl$_2$.

**MALDI-TOF MS.** Cytc samples incubated in the absence and presence of ChAld were analyzed by MALDI-TOF mass spectrometry. Samples were mixed in a 1:4 (v/v) ratio with a saturated solution of $\alpha$-cyano-4-hydroxycinnamic acid (HCCA) in 50% acetonitrile/0.1% aqueous trifluoroacetic acid (1:1, v/v). Approximately 0.5 $\mu$L of the resulting mixture was spotted onto a MALDI target and analyzed by MALDI-TOF MS. The analyses were performed in the linear, positive ion mode in an UltrafleXtreme spectrometer (Bruker Daltonics, Germany) using an acceleration voltage of 25 kV. The resulting spectra were analyzed by flexAnalysis software (Bruker Daltonics, Germany). The instrument was calibrated using an external calibration mixture containing cytochrome *c* and myoglobin as standards (Protein Standard I from Bruker Daltonics). For MALDI-TOF analysis of digested protein, the samples were passed through a C18 ZipTip column (Millipore) and then prepared as described above. Approximately 0.5 $\mu$L of the resulting mixture was spotted onto a MALDI target and analyzed by MALDI-TOF MS. Analyses of the digest were performed in reflector mode in an UltrafleXtreme spectrometer. The spectra were analyzed using the flexAnalysis software (Bruker, Germany) aided by the Biotools and Sequence editor software.

**Circular Dichroism (CD).** CD measurements were carried out in a Jasco J-720 spectropolarimeter (Easton, MD) using quartz cuvettes of 0.1 cm optical path. The instrument parameters were bandwidth, 1.0 nm; scanning speed, 200 nm/min; response time, 0.25 s; and accumulations, 6. Protein concentration was determined spectrophotometrically at 410 nm ($\varepsilon_{410\ nm}$ 106.1 mM$^{-1}$·cm$^{-1}$) prior to the spectral acquisition.

**Spectroscopic Determinations.** Spectrophotometric analyses were carried out in a Varian model Cary 50 Bio spectrophotometer in a 10 mm path length cuvette. Incubations were carried out in the presence of 10 mM bicarbonate buffer (pH 7.4) at 37 °C under constant stirring. Incubation times are given in the figure legends. Cytochrome *c* concentrations were determined at 410 nm.[38] Spectra of blanks were subtracted from those of samples.

**Vesicle Preparation and Binding Experiments.** Dry films of a mixture containing dipalmitoylphosphatidylcholine (DPPC), tetraoleoylcardiolipin (TOCL), and either cholesterol (Ch) or ChAld were prepared from stock solutions in methanol. The solvent was evaporated under nitrogen gas (N$_2$), and the resulting mixture was
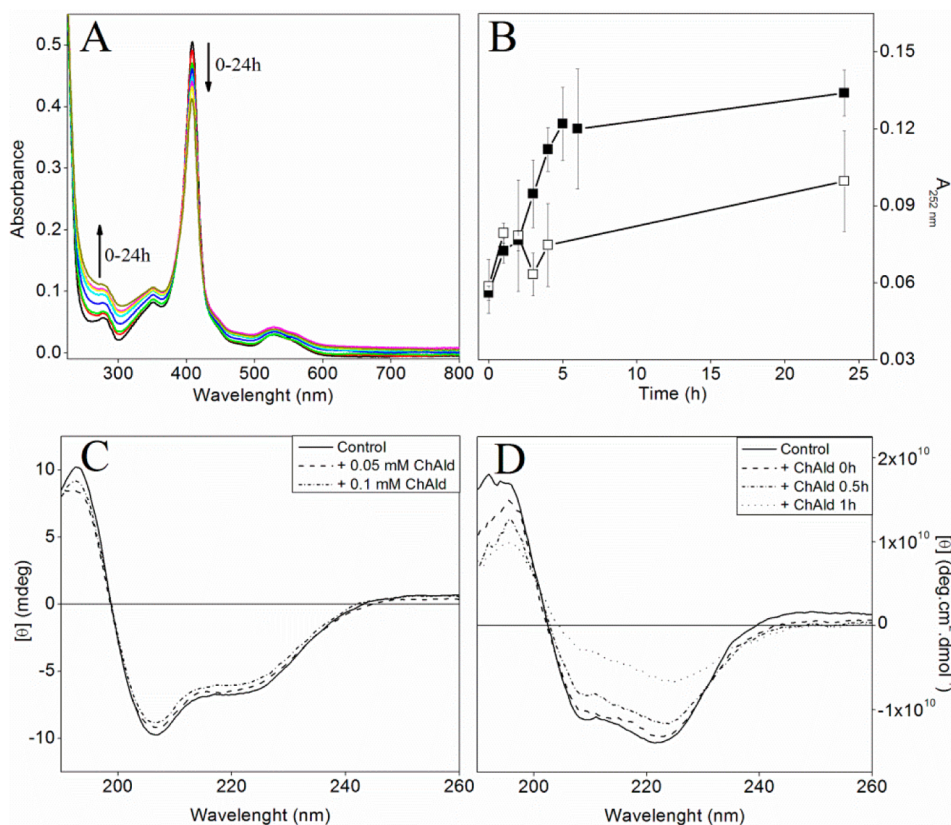
**Figure 3.** Spectroscopic determinations of cytochrome after the reaction with ChAld. Analyses were conducted in a SDS micelles-containing medium (except for panel D, which was conducted in the absence of SDS micelles) in the presence and absence of ChAld. Incubations were conducted in bicarbonate buffered media (10 mM, pH 7.4) containing 8 mM SDS (except for panel D). Panel A shows scans (190 to 800 nm) of cytc in the presence of ChAld. Experimental conditions: 5 $\mu$M cytc and 50 $\mu$M ChAld (when present). Incubations were conducted for 24 h with the absorbance values recorded hourly in the first 6 h. Panel B depicts the absorbance values recorded at 252 nm along the incubation time in the presence (■) and absence (□) of ChAld. Panels C and D show far-UV CD analyses of cytc before (control) and after incubation with ChAld. In panel C, incubations were conducted for 24 h at 37 °C, under constant agitation. No differences from the time-zero reaction were observed in all experimental conditions. Panel D depicts an initial period of the reaction (up to 1 h) in which major alterations in the protein's secondary structure are observed. The reaction media also contained 10 $\mu$M cytc and 100 $\mu$M ChAld. The spectrum marked cytc control corresponds to the incubation conducted in the absence of ChAld, which remained unaltered through the entire incubation period. Spectrum marked + ChAld 0 h was recorded immediately after the addition of cytc to the medium. All spectra are representative of 3 different analyses.

left under vacuum for 1 h to remove traces of the organic solvents. The lipid films were resuspended in phosphate buffer (50 mM) and agitated for a few minutes. The final lipid concentration was 1 mM (0.7 mM DPPC, 0.1 mM TOCL, and 0.2 mM Ch or ChAld). Unilamellar vesicles with a diameter of about 100 nm were prepared by extrusion through polycarbonate membranes (Avestin). Samples were passed through the membrane 21 times.

Cytc binding to liposomes was measured as described by Oellerich and co-workers.[38] Briefly, cytc was incubated with either Ch or ChAld-containing liposomes for 24 h. The samples were then submitted to ultracentrifugation at 104,000g for 4 h at 4 °C using a Beckman Optima TLX ultracentrifuge. Binding was evaluated by the residual content of cytc in the supernatant. Cytc concentration was determined spectrophotometrically at 410 nm.

**SDS–Polyacrylamide Gel Electrophoresis (SDS–PAGE).** The procedure of SDS–PAGE was adapted from Laemmli.[39] Briefly, cytc incubated in the presence and absence of ChAld was subjected to electrophoresis in 15% acrylamide gel under nonreducing conditions. Gels were prepared with 15% acrylamide, 0.4 M TRIS buffer (pH 8.8), 0.1% ammonium persulfate, and 0.1% SDS. Samples were mixed with the sample buffer (62 mM Tris-HCl buffer (pH 6.8), 10% v/v glycerol, 2% w/v SDS, and 0.01% w/v bromophenol blue) and placed at 95 °C for 5 min for heat denaturation. After the electrophoretic run, the samples were silver stained.

## ■ RESULTS

**ChAld Covalently Modifies Cytochrome c.** Cytc was incubated with ChAld in buffered media (pH 7.4) and then analyzed by MALDI-TOF mass spectrometry. The incubation was conducted in the presence of SDS in order to mimic the interaction between cytc and the mitochondrial membrane. ChAld was incorporated in the micelle according to the protocol described by Rawat and Chattopadhyay,[40] and then cytochrome c was added to the suspension of ChAld-containing SDS micelles. This incubation led to the formation of two modified cytc species differing by 400 Da, as evidenced by the appearance of two additional peaks in the MS spectrum (Figure 2B). This result is consistent with the addition of either one or two ChAld molecules to cytc. The same experiment conducted in the absence of SDS micelles revealed a much more aggressive modification pattern, in which cytc molecules presenting up to six covalent additions of ChAld were identified (Figure 2D). In the absence of ChAld, no addition was observed either in the presence or in the absence of SDS (Figures 2A and C, respectively). Importantly, ChAld has a molecular weight of 418 Da, and each addition corresponds to 400 Da, indicating a loss of one water molecule. This type of addition is consistent with the formation of Schiff base adducts between the aldehyde
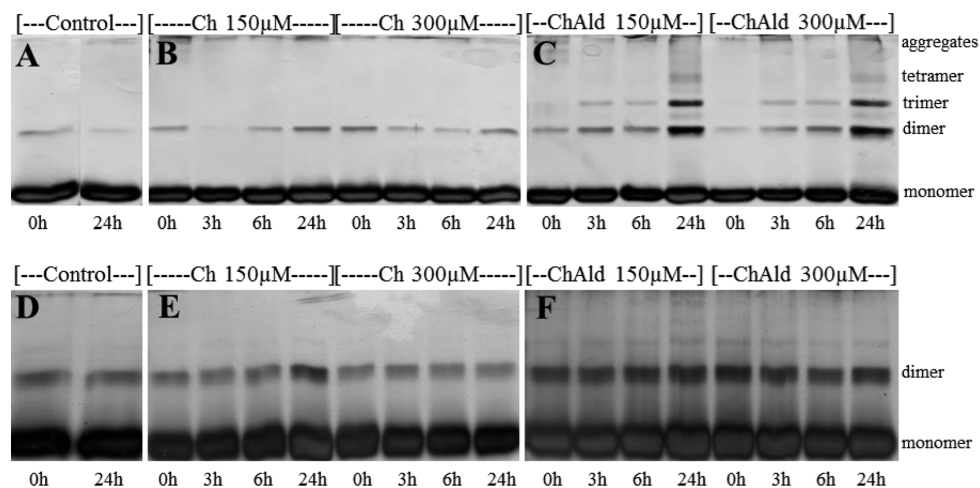
**Figure 4.** SDS–PAGE of cytc in the absence and presence of SDS. All experimental conditions contain 10 mM bicarbonate buffer (pH 7.4) and 30 $\mu$M cytc. Panels A to C represent the incubations conducted in the absence of SDS micelles. Panels D to F represent the incubations conducted in the presence of SDS micelles (8 mM SDS). Panels A and D are control conditions containing only cytc. Panels B and E represent the conditions in the presence of cholesterol. Panels C and F represent the conditions containing ChAld. Cholesterol was used as a control to show that the aggregation is not associated with the presence of a hydrophobic molecule in solution. Cholesterol and ChAld concentrations are depicted above each gel. Incubation times are shown below each lane. The results are representative of, at least, 3 repetitions.

group and the side chain of basic amino acid residues such as lysine and/or arginine.[33]

**Schiff Base Adducts and Cytc Conformational Changes.** Schiff base adducts (imine bond) are known to absorb light when irradiated at 252 nm.[41] In order to attest the formation of Schiff base adducts between ChAld and cytc, we monitored the reaction for 24 h. Simultaneously, we observed the cytc Soret band. The Soret band had a 2 nm blue shift upon incubation with the SDS micelles, being now centered at 408 nm.[36] In the presence of ChAld, a slight bleaching of the Soret band was observed (Figure 3A). The bleaching was accompanied by the increase of the absorbance at 252 nm, consistent with the formation of Schiff base adducts (Figure 3B). An isosbestic point can be observed at 385 nm, suggesting that the bleaching is a consequence of the formation of the Schiff base adducts. Unlike the cytochrome c samples incubated with ChAld (closed squares) that presented the progressive increase of absorbance at 252 nm, the incubation of cytochrome c in the control conditions (open squares) led to no significant difference within 24 h. Altogether, these observations strongly suggest that ChAld covalently modifies cytc through a Schiff base mechanism. It is worth mentioning that we were unable to use this spectroscopic approach to study the reaction in the absence of SDS because cytc precipitated upon reaction with ChAld. This is an indication that cytc undergoes aggregation upon reaction with ChAld (discussed in more detail below).

Chemical modifications of amino acids are known to induce conformational changes in both secondary and tertiary structures of proteins. We assessed these features by employing CD and fluorescence spectroscopies. CD spectra in the far-UV region showed that the secondary structure of cytc remained unaltered upon incubation with two different concentrations of ChAld for 24 h in the presence of SDS (Figure 3C). Furthermore, intrinsic tryptophan fluorescence experiments revealed that the chemical environment of the fluorophore did not change upon incubation with ChAld and that the amino acid fluorescence remained quenched due to the proximity to the heme iron (Figure S1, Supporting Information).[36]

However, CD analyses revealed that, in the absence of SDS micelles, cytc had its secondary structure severely altered upon reaction with ChAld (Figure 3D). The major alterations include a loss of $\alpha$-helix and a gain in $\beta$-sheet structures, which may suggest the formation of high molecular weight species. Besides the modifications induced by ChAld, the secondary structure of cytc changes upon incubation with SDS (control conditions at Figures 3C and D), a behavior already observed and discussed by Mugnol and co-workers.[36]

**Cytc Aggregates in the Absence of SDS Micelles.** The incubation of cytc with ChAld for 1 h in the absence of SDS micelles leads to the formation of a red precipitate. In order to characterize the aggregation pattern, we performed SDS–PAGE electrophoresis. The experiments were done with two different cytc/ChAld ratios (1:5 and 1:10), and aliquots were taken along the incubation time and analyzed. Cytc itself appears in the gel as two bands, one corresponding to the monomer and the other to the dimer (see reactant information brochure at www.sigmaaldrich.com). This electrophoretic pattern remained unchanged along the 24 h of incubation in the control conditions (Figure 4A). In order to test the hypothesis that cholesterol itself could induce cytc aggregation, we incubated cytc with the same amounts of either cholesterol (Ch) or ChAld. The presence of cholesterol did not change cytc electrophoretic pattern under all conditions tested (Figure 4B). However, bands corresponding to species with higher molecular weight appeared when cytc was incubated with ChAld (Figure 4C), correlating aggregation with the reaction with the aldehyde. Cytc aggregation was further confirmed via dynamic light scattering (DLS). This technique revealed that aggregates are formed when cytc is mixed with ChAld (Figure S2, Supporting Information). In addition, making use of FESEM, we observed that amorphous cytc aggregates are formed under these conditions (Figures S3A–D, Supporting Information).

In contrast to the above-described scenario, when cytc is incubated with ChAld in the presence of SDS micelles, no aggregation was observed (Figures 4D to F). The cytc electrophoretic pattern remained unaltered in all experimental

conditions in the presence of SDS micelles, suggesting that aggregation would only occur in conditions in which the modified cytc molecules are released from the mimetic membrane and move randomly in solution.

**Cytc Is Modified in Specific Lysine Residues.** In order to further characterize these modifications, we attempted to identify the specific amino acid residues that are modified by ChAld. Cytc samples incubated in the presence of SDS micelles, either in the presence or absence of ChAld, were digested with trypsin, and the resulting peptides were analyzed by MALDI-TOF mass spectrometry (Figure 5, upper panel).
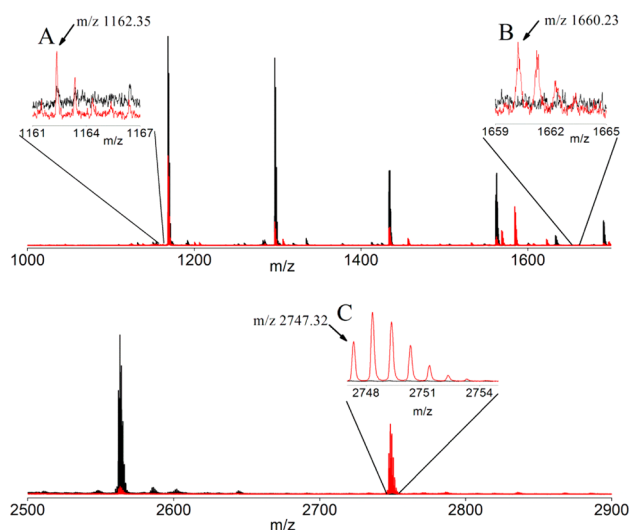


**Figure 5.** Sections of MALDI-TOF-MS of the peptides resulting from the tryptic digestion of cytc before (black spectra) and after (red spectra) incubation with ChAld. Typical reactions contained bicarbonate buffer (10 mM, pH 7.4), 8 mM SDS, 50 $\mu$M cytc and 500 $\mu$M ChAld. Spectra are representative of, at least, 3 different experiments. The upper panel shows the tryptic digestion of the wild type cytc. The lower panel shows the tryptic digestion of the K22A mutant. Panels A and B show mass peaks ($m/z$ 1162.35 and 1660.36) found only after the incubation of WT cytc with ChAld. Panel C shows a mass peak with $m/z$ 2747.32 found only after the incubation of ChAld with K22A cytc. Note that in the control conditions (black spectra in panels A−C) no peaks were detected. See Table 1 for more details concerning the tryptic digestion of cytc.

The peptides from each sample were analyzed using the peptide mass fingerprinting (PMF) approach. Briefly, PMF consists of matching the experimental peptides to theoretical peptides generated from protein digestion, usually aided by computer software (in this case, MASCOT, Matrix Science Inc., Boston, MA, USA).[42] PMF analyses revealed that two peptides in the native protein sequence were covalently modified by ChAld

(see Table 1 for more details). The unmodified peptides have $m/z$ ratios of 762.49 and 1260.58, and the corresponding peaks were identified in the mass spectrum (see Table 1). Incubation with ChAld leads to the appearance of a new peak with $m/z$ 1162.35 corresponding to the modified peptide K*IFVQK (residues 8−13) and another peak with $m/z$ 1660.36 corresponding to the modified peptide CAQCHTVEK*GGK (residues 14−25) (Figure 5A and B, respectively). An MS/MS analysis of the peptide containing Lys22 revealed that this residue is covalently modified by ChAld (Figure S4, Supporting Information). In order to confirm that Lys22 is indeed the modified residue (see Table 1 for more details) in this sequence, we performed the same experiments with a K22A cytc mutant, in which Lys22 was replaced by Ala (Figure 5, lower panel, and Figure S6, Supporting Information). These results show that the peptide mentioned above (residues 14−25) is no longer modified at any of its residues. However, a new covalent addition of ChAld was observed at Lys13 of the K22A cytc mutant, which replaced the modification at Lys22 (Figure 5C).

In addition to the modification observed in Lys13, a modification in Lys8 was also observed at incubations of ChAld with K22A cytc. The mass peak observed in Figure 5C corresponds to the sequence KIFVQKCAQCHTVEAGGK (residues 8 to 25 in the K22A cytc mutant), in which the lysine residues at positions 8 and 13 are covalently modified by ChAld (see Figure S5, Supporting Information, for the theoretical simulation of the observed mass peak in Figure 5C). Another evidence that the residues mentioned above (Lys 8, 13, and 22) are indeed modified by ChAld is that they were not recognized by trypsin, characterizing missing cleavage sites. Since trypsin cleaves after K and R residues, a modification would render them unrecognizable by the enzyme.

**ChAld Impairs Cytc Release from Liposomes.** In order to study the effect of these covalent additions on cytc binding to membranes, we performed experiments using a liposome model and making use of ultracentrifugation, as described by Oellerich and co-workers.[38] Briefly, liposomes containing 10% mol/mol TOCL, 70% mol/mol DPPC, and either ChAld (20% mol/mol) or cholesterol (as a control condition 20% mol/mol) were incubated with cytc for 24 h. After the incubation time, samples were centrifuged at 104,000g for 4 h, and the absorbance of the supernatant was recorded at 410 nm. The results presented in Figure 6 show that cytc binds to the liposome containing TOCL in the presence of either cholesterol or ChAld, as revealed by the decrease in cytc concentration in the supernatant after centrifugation (in both conditions, 22% of cytc was released from the liposome). An increase in the ionic strength before centrifugation (by adding 250 mM KCl) released cytc from cholesterol-containing

**Table 1. Modified Peptides Identified by MALDI-TOF MS after Tryptic Digestion**[a]

| sequence[b] | residues | unmodified[c] $m/z$ | expected[d] $m/z$ | observed[e] $m/z$ |
|---|---|---|---|---|
| K*IFVQK | 8−13 | 762.49 | 1162.82 | 1162.35 |
| CAQCHTVEK*GGK | 14−25 | 1260.58 | 1660.91 | 1660.36 |
| K*IFVQK*CAQCHTVE<u>A</u>GGK | 8−25 | 1946.99 | 2747.66 | 2747.34 |

[a]All $m/z$ depicted at the table correspond to the $[M + H]^+$ values. It is worth noticing that another suggestion that the residues marked with * are indeed modified by ChAld is that they were not recognized by trypsin. Note that trypsin cleaves the peptide bond after K and/or R residues. [b]Sequence of the modified peptide. Residues marked with * were covalently modified by ChAld. The alanine residue underlined in the third sequence corresponds to the K22A mutation. [c]Values correspond to the theoretical $m/z$ for the unmodified peptide. [d]Values correspond to the expected $m/z$ for the ChAld-modified peptide. [e]Values correspond to the observed $m/z$ for the ChAld-modified peptide.
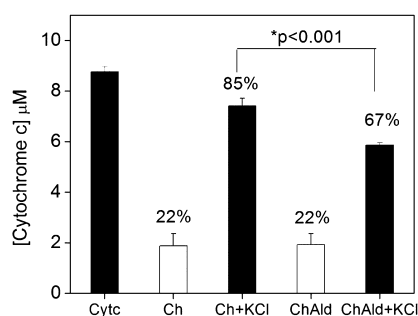
**Figure 6.** Binding of cytc to ChAld-containing liposomes. Incubations were conducted in phosphate buffered media (10 mM, pH 7.4) at 37 °C. After 24 h of incubation, samples were centrifuged at 104,000g for 4 h at 4 °C. The final lipid content was 1 mM (700 $\mu$M of DPPC, 100 $\mu$M of TOCL, and 200 $\mu$M of either ChAld or cholesterol (Ch)), 10 $\mu$M cytc, and 250 mM KCl (when present). The first condition (Cytc) refers to the incubation conducted in absence of the liposomes. The second condition (Ch) refers to the incubation conducted in the presence of cholesterol-containing liposomes. The third condition (Ch + KCl) is the same as Ch with the addition of KCl after 24 h of incubation and prior to centrifugation. The fourth (ChAld) and fifth (ChAld + KCl) conditions were equal to Ch and Ch + KCl, respectively, where cholesterol was replaced by ChAld.

liposomes (85% of total cytc was released upon treatment with KCl), showing that the interaction between the protein and the vesicle is mostly electrostatic. However, the increase in ionic strength in liposomes containing ChAld had a smaller effect in releasing cytc from the membrane (only 67% of total cytc was released upon treatment with KCl), suggesting that the covalent modification is preventing its release from liposomes.

## ■ DISCUSSION

Oxidative stress is known to be associated with pathological conditions such as cancer and Alzheimer's and Parkinson's diseases, situations recognized to produce increased amounts of lipid peroxidation products, including reactive aldehydes.[20,21,25] Proteins are excellent targets for modification by lipid aldehydes, mainly by covalent addition to nucleophilic amino acid residues.[33−35] Among these aldehydes, ChAld is of major interest since it is reported to be increased *in vivo* in cells under pathological conditions.[43] ChAld can react with several proteins, including those attached to the inner mitochondrial membrane, such as cytc. Since cytc integrity is vital for many physiological processes, its modification upon reaction with ChAld could have implications to the cell, including impairment of both electron transport and apoptosis signaling.

The production of ChAld *in vivo* can occur by three different mechanisms, in which cholesterol is oxidized by ozone and/or singlet molecular oxygen.[23,25] Briefly, ChAld can be formed by (i) Hock cleavage of cholesterol 5α-hydroperoxide;[24] (ii) ozonolysis;[25] and (iii) [2 + 2] cycloaddition to cholesterol followed by dioxetane thermolysis, originating CSec and, ultimately, ChAld.[44] In this sense, quantitative analysis of human arterial plaque extracts revealed the presence of approximately 32 ± 15 pmol/mg tissue.[27] Moreover, these aldehydes have also been detected at nanomolar levels in stimulated neutrophils.[45]

Cytc modification has been previously studied using other lipid-derived aldehydes, such HNE,[33] DDE,[34] and trans-2-hexenal.[46] In the study with HNE-induced cytc modification, Isom and co-workers, making use of mass spectrometry,

identified three covalent additions of HNE, where the modified residues were His33, Arg38, and Lys87. In the study regarding DDE-induced cytc modification, Sigolo and co-workers reported up to seven time-dependent covalent additions of DDE to cytc (H18, K22, K25, K73, K86, K87, and K99 were the supposed modified sites), a behavior similar to that observed in this study in the absence of SDS micelles. Moreover, the authors also identified Lys22 as a possible modified residue, which is the same residue found modified by ChAld using the SDS mimetic model, a residue known to participate in protein−protein and protein−membrane interactions. It is worth mentioning, however, that all studies mentioned above characterized cytc modifications promoted by lipid aldehydes in experiments conducted in the absence of mimetic membranes. In this situation, cytc is moving randomly in the solution, and therefore, the modification sites are spread along the entire sequence of the protein.[46] In our conditions the aldehyde was inserted in the SDS micelles which, in turn, bind cytc at specific sites on its surface. In this situation, cytc is approximated to the aldehyde, which guides the reaction to specific residues, particularly residues situated at the binding sites of cytc.

Since cytc is positively charged (isoeletric point 10.2), the interaction between this protein and lipid membranes carrying negatively charged phospholipids is initially guided by electrostatic interactions.[2,47,48] These interactions are assumed to occur through three sites in the protein surface, named A, C, and L sites, corresponding to 30% of the protein surface.[6,47,48] Site A comprises a basic portion on the protein containing the positively charged Lys72 and Lys73 residues and is characterized as contributing to electrostatic and lipid-extended interactions between cytc and phospholipid membranes.[49,50] Site C, in turn, is assumed to interact through a hydrogen bond between the invariant Asn52 and protonated phospholipids in the membrane exposed to acidic media.[6,48] Site L has its interaction with acidic phospholipids modulated by the pH of the medium, in which lysine residues 22 and 27 play a pivotal role in the attachment of cytc to membranes.[4] These two lysine residues have their side chain in a convergent position toward the membrane, which induces a lowering of their ε-amino p$K_a$ values (around 6.0).[4] The p$K_a$ values of lysine residues of cytc site L indicate that these residues are predominantly protonated at the inner mitochondrial membrane interface when the medium is acidified by proton pumping to the intermembrane space. However, the increase of pH in the intermembrane space promoted by the loss of pH gradient changes the acid−base equilibrium of these ε-amino groups to the deprotonated base conjugated form.[4] In this sense, the identification of Lys22 as a modified residue can be partially explained by the low p$K_a$ value of Lys22 since the reaction between the amino group and the aldehyde can only occur when the amino group is deprotonated.

Cholesterol overload to the mitochondria is suggested to decrease mGSH levels, increasing oxidative stress inside the organelle and favoring, for instance, lipid peroxidation processes.[9,21] In this situation, cholesterol aldehyde production could be enhanced, and the reaction with proteins, including cytc, would be more likely to occur. The result presented in Figure 6 reveals that the release of cytc from cardiolipin-containing liposomes is impaired when ChAld is added to the liposome. The increase in ionic strength (i.e., by adding 250 mM KCl) is known to disrupt the electrostatic interactions between the protein and the membrane, releasing cytc to the

bulk solution. In the presence of ChAld, however, less cytc is released into solution, suggesting that adduction could interfere with the release of cytc by keeping it covalently attached to the aldehyde under oxidative stress conditions. Other types of aldehydes, such as aldehydes formed from phospholipids (e.g., cardiolipin) could also contribute to covalently anchor cytc to the membrane. This hypothesis is under investigation in the laboratory. Although not further investigated in this study, cytc adduction to membrane lipids could have an impact on apoptosis signaling, contributing, for instance, for the resistance of cancerous cells to undergo apoptosis.

In conclusion, our data indicate that cytc can be a potential target for cholesterol-aldehyde-induced protein modification. When cytc is bound to mimetic biological membranes, the modifications are more restricted and occur at specific lysine residues in the protein, namely, Lys22 located at a pH-sensitive binding site of cytc. Although protein adduction seems to occur through a Schiff base formation (formation of an imine bond), further characterization is needed in order to confirm this mechanism. We were also able to demonstrate that these modifications impair cytc detachment under high ionic strength conditions by keeping this protein covalently bound to the aldehyde present in the membrane. The extension of the biological implications of these modifications is still unknown. However, several hypotheses can be made based on the results reported herein, including impairment of the electron transport and cytc release under an apoptosis stimulus. Further experiments are underway in order to find out the implications of these adductions to the cell.

## ■ ASSOCIATED CONTENT

### Ⓢ Supporting Information

Experimental procedures for FESEM, DLS, and fluorescence spectroscopy and figures of fluorescence spectroscopy, DLS, FESEM, MS/MS spectrum of the modified peptide, simulation of the MS peak corresponding to the modified peptide in the K22A cytc mutant, and an expanded version of the MS spectrum shown in Figure 5. This material is available free of charge via the Internet at http://pubs.acs.org.

## ■ AUTHOR INFORMATION

### Corresponding Author

*Departamento de Bioquímica, Instituto de Química, Universidade de São Paulo, Avenida professor Lineu Prestes, 748, Bloco 10 Superior, sala 1074, São Paulo, SP, Brazil 05508-000. Tel: +55113091-9113. E-mail: miyamoto@iq.usp.br.

### Notes

The authors declare no competing financial interest.

## ■ ABBREVIATIONS

ChAld, 3$\beta$-hydroxy-5$\beta$-hydroxy-B-norcholestane-6$\beta$-carboxaldehyde; cytc, cytochrome $c$; SDS, sodium dodecyl sulfate; mGSH, mitochondrial reduced glutathione; ROS, reactive oxygen species; CSec, 3$\beta$-hydroxy-5-oxo-5,6-secocholestan-6-al; $O_3$, ozone; $^1O_2$, singlet molecular oxygen; CL, cardiolipin; LDL, low density lipoprotein; HNE, 4-hydroxynonenal; DDE, 2,4-decadienal; MALDI, matrix assisted laser desorption ionization; TOF, time-of-flight; MS, mass spectrometry; HCCA, alpha-cyano-4-hydroxycinnamic acid; CD, circular dichroism; DPPC, dipalmitoylphosphatidylcholine; TOCL, tetraoleoylcardiolipin; Ch, cholesterol; FESEM, field emission scanning electron microscopy; DLS, dynamic light scattering; SDS–PAGE, SDS–polyacrylamide gel electrophoresis; PMF, peptide mass fingerprinting

## ■ REFERENCES

(1) Ow, Y. P., Green, D. R., Hao, Z., and Mak, T. W. (2008) Cytochrome c: functions beyond respiration. *Nat. Rev. Mol. Cell Biol. 9*, 532−542.

(2) Hanske, J., Toffey, J. R., Morenz, A. M., Bonilla, A. J., Schiavoni, K. H., and Pletneva, E. V. (2012) Conformational properties of cardiolipin-bound cytochrome c. *Proc. Natl. Acad. Sci. U.S.A. 109*, 125−130.

(3) Sorice, M., Manganelli, V., Matarrese, P., Tinari, A., Misasi, R., Malorni, W., and Garofalo, T. (2009) Cardiolipin-enriched raft-like microdomains are essential activating platforms for apoptotic signals on mitochondria. *FEBS Lett. 583*, 2447−2450.

(4) Kawai, C., Prado, F. M., Nunes, G. L., Di Mascio, P., Carmona-Ribeiro, A. M., and Nantes, I. L. (2005) pH-Dependent interaction of cytochrome c with mitochondrial mimetic membranes: the role of an array of positively charged amino acids. *J. Biol. Chem. 280*, 34709−34717.

(5) Kalanxhi, E., and Wallace, C. J. (2007) Cytochrome c impaled: investigation of the extended lipid anchorage of a soluble protein to mitochondrial membrane models. *Biochem. J. 407*, 179−187.

(6) Rytomaa, M., and Kinnunen, P. K. (1994) Evidence for two distinct acidic phospholipid-binding sites in cytochrome c. *J. Biol. Chem. 269*, 1770−1774.

(7) Liu, X., Kim, C. N., Yang, J., Jemmerson, R., and Wang, X. (1996) Induction of apoptotic program in cell-free extracts: requirement for dATP and cytochrome c. *Cell 86*, 147−157.

(8) Li, P., Nijhawan, D., Budihardjo, I., Srinivasula, S. M., Ahmad, M., Alnemri, E. S., and Wang, X. (1997) Cytochrome c and dATP-dependent formation of Apaf-1/caspase-9 complex initiates an apoptotic protease cascade. *Cell 91*, 479−489.

(9) Garcia-Ruiz, C., Mari, M., Colell, A., Morales, A., Caballero, F., Montero, J., Terrones, O., Basanez, G., and Fernandez-Checa, J. C. (2009) Mitochondrial cholesterol in health and disease. *Histol. Histopathol. 24*, 117−132.

(10) Liu, J. P., Tang, Y., Zhou, S., Toh, B. H., McLean, C., and Li, H. (2010) Cholesterol involvement in the pathogenesis of neurodegenerative diseases. *Mol. Cell. Neurosci. 43*, 33−42.

(11) Ikonen, E. (2008) Cellular cholesterol trafficking and compartmentalization. *Nat. Rev. Mol. Cell. Biol. 9*, 125−138.

(12) Simons, K., and Ikonen, E. (1997) Functional rafts in cell membranes. *Nature 387*, 569−572.

(13) Lingwood, D., Kaiser, H. J., Levental, I., and Simons, K. (2009) Lipid rafts as functional heterogeneity in cell membranes. *Biochem. Soc. Trans. 37*, 955−960.

(14) Pike, L. J. (2004) Lipid rafts: heterogeneity on the high seas. *Biochem. J. 378*, 281−292.

(15) Edidin, M. (2003) The state of lipid rafts: from model membranes to cells. *Annu. Rev. Biophys. Biomol. Struct. 32*, 257−283.

(16) van Meer, G., Voelker, D. R., and Feigenson, G. W. (2008) Membrane lipids: where they are and how they behave. *Nat. Rev. Mol. Cell Biol. 9*, 112−124.

(17) Feo, F., Canuto, R. A., Bertone, G., Garcea, R., and Pani, P. (1973) Cholesterol and phospholipid composition of mitochondria and microsomes isolated from morris hepatoma 5123 and rat liver. *FEBS Lett.* 33, 229–232.

(18) Montero, J., Morales, A., Llacuna, L., Lluis, J. M., Terrones, O., Basanez, G., Antonsson, B., Prieto, J., Garcia-Ruiz, C., Colell, A., and Fernandez-Checa, J. C. (2008) Mitochondrial cholesterol contributes to chemotherapy resistance in hepatocellular carcinoma. *Cancer Res.* 68, 5246–5256.

(19) Lucken-Ardjomande, S., Montessuit, S., and Martinou, J. C. (2008) Bax activation and stress-induced apoptosis delayed by the accumulation of cholesterol in mitochondrial membranes. *Cell. Death Differ.* 15, 484–493.

(20) Fernandez, A., Llacuna, L., Fernandez-Checa, J. C., and Colell, A. (2009) Mitochondrial cholesterol loading exacerbates amyloid beta peptide-induced inflammation and neurotoxicity. *J. Neurosci.* 29, 6394–6405.

(21) Colell, A., Fernandez, A., and Fernandez-Checa, J. C. (2009) Mitochondria, cholesterol and amyloid beta peptide: a dangerous trio in Alzheimer disease. *J. Bioenerg. Biomembr.* 41, 417–423.

(22) Brown, A. J., and Jessup, W. (1999) Oxysterols and atherosclerosis. *Atherosclerosis* 142, 1–28.

(23) Uemi, M., Ronsein, G. E., Miyamoto, S., Medeiros, M. H. G., and Di Mascio, P. (2009) Generation of cholesterol carboxyaldehyde by the reaction of singlet molecular oxygen [$O_2$ ($^1\Delta_g$)] as well as ozone with cholesterol. *Chem. Res. Toxicol.* 22, 875–884.

(24) Brinkhorst, J., Nara, S. J., and Pratt, D. A. (2008) Hock cleavage of cholesterol 5 α-hydroperoxide: an ozone-free pathway to the cholesterol ozonolysis products identified in arterial plaque and brain tissue. *J. Am. Chem. Soc.* 130, 12224–12225.

(25) Wentworth, P., Jr., Nieva, J., Takeuchi, C., Galve, R., Wentworth, A. D., Dilley, R. B., DeLaria, G. A., Saven, A., Babior, B. M., Janda, K. D., Eschenmoser, A., and Lerner, R. A. (2003) Evidence for ozone formation in human atherosclerotic arteries. *Science* 302, 1053–1056.

(26) Jaworski, K., and Smith, L. L. (1988) Ozonization of cholesterol in nonparticipating solvents. *J. Org. Chem.* 53, 545–554.

(27) Wentworth, A. D., Song, B. D., Nieva, J., Shafton, A., Tripurenani, S., and Wentworth, P., Jr. (2009) The ratio of cholesterol 5,6-secosterols formed from ozone and singlet oxygen offers insight into the oxidation of cholesterol in vivo. *Chem. Commun.* 21, 3098–3100.

(28) Miyamoto, S., Martinez, G. R., Martins, A. P. B., Medeiros, M. H. G., and Di Mascio, P. (2003) Direct evidence of singlet molecular oxygen production in the reaction of linoleic acid hydroperoxide with peroxynitrite. *J. Am. Chem. Soc.* 125, 4510–4517.

(29) Miyamoto, S., Martinez, G. R., Medeiros, M. H. G., and Di Mascio, P. (2003) Singlet molecular oxygen generated from lipid hydroperoxides by the Russell mechanism: Studies using $^{18}$O-labeled linoleic acid hydroperoxide and monomol light emission measurements. *J. Am. Chem. Soc.* 125, 6172–6179.

(30) Miyamoto, S., Martinez, G. R., Rettori, D., Augusto, O., Medeiros, M. H. G., and Di Mascio, P. (2006) Linoleic acid hydroperoxide reacts with hypochlorous acid, generating peroxyl radical intermediates and singlet molecular oxygen. *Proc. Natl. Acad. Sci. U.S.A.* 103, 293–298.

(31) Miyamoto, S., Nantes, I. L., Faria, P. A., Cunha, D., Ronsein, G. E., Medeiros, M. H. G., and Di Mascio, P. (2012) Cytochrome c-promoted cardiolipin oxidation generates singlet molecular oxygen. *Photochem. Photobiol. Sci.* 11, 1536–1546.

(32) Nieva, J., Song, B. D., Rogel, J. K., Kujawara, D., Altobel, L., III, Izharrudin, A., Boldt, G. E., Grover, R. K., Wentworth, A. D., and Wentworth, P., Jr. (2011) Cholesterol secosterol aldehydes induce amyloidogenesis and dysfunction of wild-type tumor protein p53. *Chem. Biol.* 18, 920–927.

(33) Isom, A. L., Barnes, S., Wilson, L., Kirk, M., Coward, L., and Darley-Usmar, V. (2004) Modification of Cytochrome c by 4-hydroxy-2-nonenal: evidence for histidine, lysine, and arginine-aldehyde adducts. *J. Am. Soc. Mass Spectrom.* 15, 1136–1147.

(34) Sigolo, C. A., Di Mascio, P., and Medeiros, M. H. G. (2007) Covalent modification of cytochrome c exposed to trans,trans-2,4-decadienal. *Chem. Res. Toxicol.* 20, 1099–1110.

(35) Uchida, K., and Stadtman, E. R. (1992) Modification of histidine residues in proteins by reaction with 4-hydroxynonenal. *Proc. Natl. Acad. Sci. U.S.A.* 89, 4544–4548.

(36) Mugnol, K. C., Ando, R. A., Nagayasu, R. Y., Faljoni-Alario, A., Brochsztain, S., Santos, P. S., Nascimento, O. R., and Nantes, I. L. (2008) Spectroscopic, structural, and functional characterization of the alternative low-spin state of horse heart cytochrome c. *Biophys. J.* 94, 4066–4077.

(37) Kawai, C., Pessoto, F. S., Rodrigues, T., Mugnol, K. C., Tortora, V., Castro, L., Milicchio, V. A., Tersariol, I. L., Di Mascio, P., Radi, R., Carmona-Ribeiro, A. M., and Nantes, I. L. (2009) pH-sensitive binding of cytochrome c to the inner mitochondrial membrane. Implications for the participation of the protein in cell respiration and apoptosis. *Biochemistry* 48, 8335–8342.

(38) Oellerich, S., Lecomte, S., Paternostre, M., Heimburg, T., and Hildebrandt, P. (2004) Peripheral and integral binding of cytochrome c to phospholipids vesicles. *J. Phys. Chem. B* 108, 3871–3878.

(39) Laemmli, U. K. (1970) Cleavage of structural proteins during the assembly of the head of bacteriophage T4. *Nature* 227, 680–685.

(40) Rawat, S. S., and Chattopadhyay, A. (1999) Structural transition in the micellar assembly: a fluorescence study. *J. Fluoresc.* 9, 233–244.

(41) Prieto, T., Marcon, R. O., Prado, F. M., Caires, A. C., Di Mascio, P., Brochsztain, S., Nascimento, O. R., and Nantes, I. L. (2006) Reaction route control by microperoxidase-9/CTAB micelle ratios. *Phys. Chem. Chem. Phys.* 8, 1963–1973.

(42) Hollemeyer, K., Altmeyer, W., Heinzle, E., and Pitra, C. (2008) Species identification of Oetzi's clothing with matrix-assisted laser desorption/ionization time-of-flight mass spectrometry based on peptide pattern similarities of hair digests. *Rapid Commun. Mass Spectrom.* 22, 2751–2767.

(43) Bosco, D. A., Fowler, D. M., Zhang, Q., Nieva, J., Powers, E. T., Wentworth, P., Lerner, R. A., and Kelly, J. W. (2006) Elevated levels of oxidized cholesterol metabolites in Lewy body disease brains accelerate [alpha]-synuclein fibrilization. *Nature Chem. Biol.* 2, 249–253.

(44) Timmins, G. S., dos Santos, R. E., Whitwood, A. C., Catalani, L. H., Di Mascio, P., Gilbert, B. C., and Bechara, E. J. H. (1997) Lipid peroxidation-dependent chemiluminescence from the cyclization of alkylperoxyl radicals to dioxetane radical intermediates. *Chem. Res. Toxicol.* 10, 1090–1096.

(45) Tomono, S., Miyoshi, N., Shiokawa, H., Iwabuchi, T., Aratani, Y., Higashi, T., Nukaya, H., and Ohshima, H. (2011) Formation of cholesterol ozonolysis products in vitro and in vivo through a myeloperoxidase-dependent pathway. *J. Lipid Res.* 52, 87–97.

(46) Zidek, L., Dolezel, P., Chmelik, J., Baker, A. G., and Novotny, M. (1997) Modification of horse heart cytochrome c with trans-2-Hexenal. *Chem. Res. Toxicol.* 10, 702–710.

(47) Kagan, V. E., Bayir, H. A., Belikova, N. A., Kapralov, O., Tyurina, Y. Y., Tyurin, V. A., Jiang, J., Stoyanovsky, D. A., Wipf, P., Kochanek, P. M., Greenberger, J. S., Pitt, B., Shvedova, A. A., and Borisenko, G. (2009) Cytochrome c/cardiolipin relations in mitochondria: a kiss of death. *Free Radical Biol. Med.* 46, 1439–1453.

(48) Rytomaa, M., and Kinnunen, P. K. (1995) Reversibility of the binding of cytochrome c to liposomes. Implications for lipid-protein interactions. *J. Biol. Chem.* 270, 3197–3202.

(49) Tuominen, E. K., Wallace, C. J., and Kinnunen, P. K. (2002) Phospholipid-cytochrome c interaction: evidence for the extended lipid anchorage. *J. Biol. Chem.* 277, 8822–8826.

(50) Rytomaa, M., Mustonen, P., and Kinnunen, P. K. (1992) Reversible, nonionic, and pH-dependent association of cytochrome c with cardiolipin-phosphatidylcholine liposomes. *J. Biol. Chem.* 267, 22243–22248.

1544

dx.doi.org/10.1021/tx4002385 | *Chem. Res. Toxicol.* 2013, 26, 1536–1544

# Covalent binding and anchoring of cytochrome c to mitochondrial mimetic membranes promoted by cholesterol carboxyaldehyde

*Thiago C. Genaro-Mattos†, Patricia P. Appolinário†, Katia C.U. Mugnol‡, Carlos Bloch Jr.§,*

*Iseli L. Nantes‡, Paolo Di Mascio†, Sayuri Miyamoto†\**

**Table of contents**

**Experimental section**

*Field Emission Scanning Electron Microscopy (FESEM)*

Protein aggregates were observed using a JSM-7401F scanning electron microscope (JEOL Ltd, Japan). The samples were spotted onto a brass "stub" and the images obtained were of secondary electrons when operated at 5 kV.

*Dynamic Light Scattering (DLS)*

DLS measurements were performed in a Wyatt Dynapro equipment in a 100 μL cuvette. Incubations were carried out in the presence of 10 mM bicarbonate buffer (pH 7.4) at 37 $^o$C under constant stirring. Data were recorder after 1h incubation.

*Fluorescence spectroscopy*

Intrinsic tryptophan fluorescence measurements were carried out in a Fluorescence Spectrophotometer F-2500 (Hitachi, Singapore) at room temperature. Equipment parameters were: excitation wavelength 292 nm; slit 10.0 nm; scan range, 300 to 410 nm.
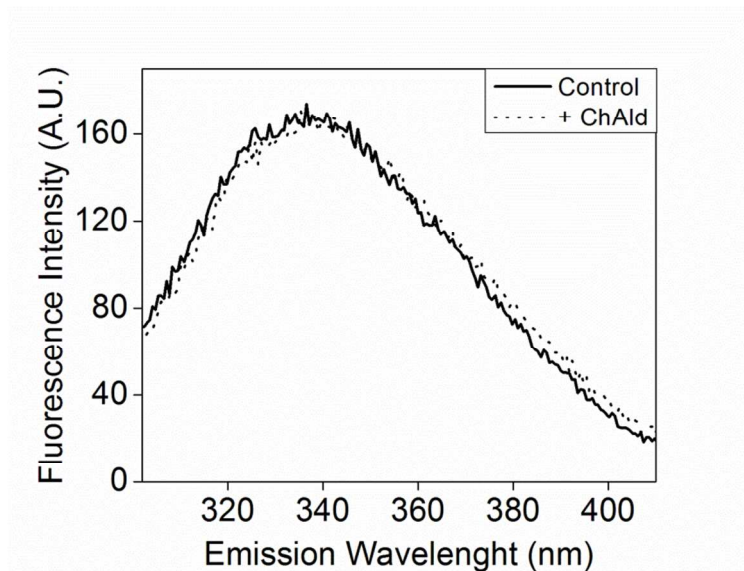
**Figure S1**. Intrinsic tryptophan fluorescence of cytc before and after reaction with ChAld in a SDS micelle containing medium. Incubations were conducted in bicarbonate buffered media (10 mM, pH 7.4) for 24 h at 37 $^{o}$C, under constant agitation. All incubations contained SDS 8 mM and 10 μM cytc. ChAld was present as 100 μM. The Trp fluorescence did not alter along the incubation time, remaining constant through the entire incubation period. Spectra are representative of 3 different analyses.
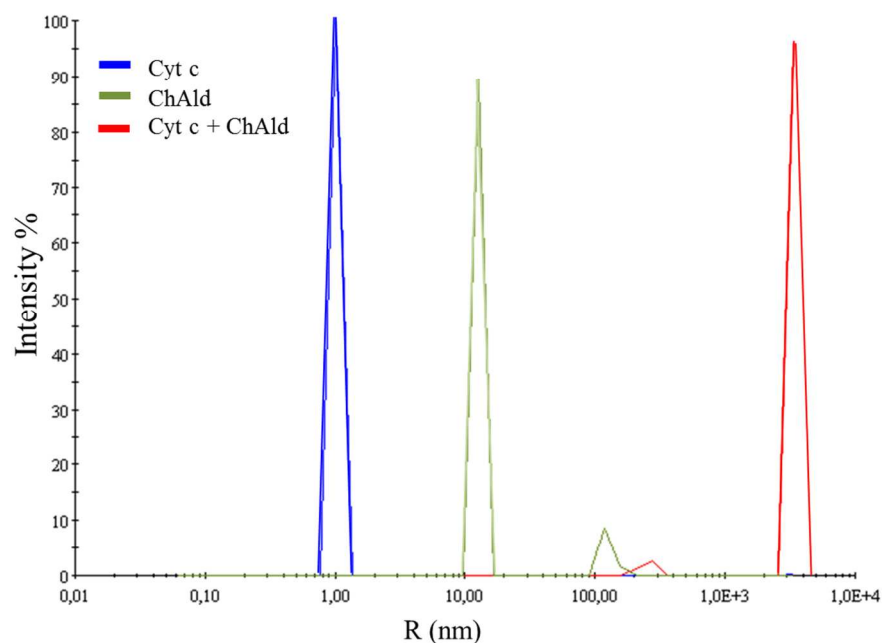
**Figure S2.** Dynamic light scattering analyses of the aggregates formed by the reaction of cytc and ChAld. Reactions were carried out in bicarbonate buffered media (10 mM, pH 7.4) at 37 °C, under constant agitation and contained 0.25 mM cytc and 1.0 mM ChAld. Spectra were acquired after 24h incubation and are representative of 2 different analyses. The experimental condition shown in blue consists of only cytc and has an average hydrodynamic radius of 1.0 nm. The green one consists of only ChAld and has an average hydrodynamic radius of 10.0 nm. The condition shown in red consists of the incubation between cytc and ChAld, in which the average hydrodynamic radius increases to approximately 5 µm.
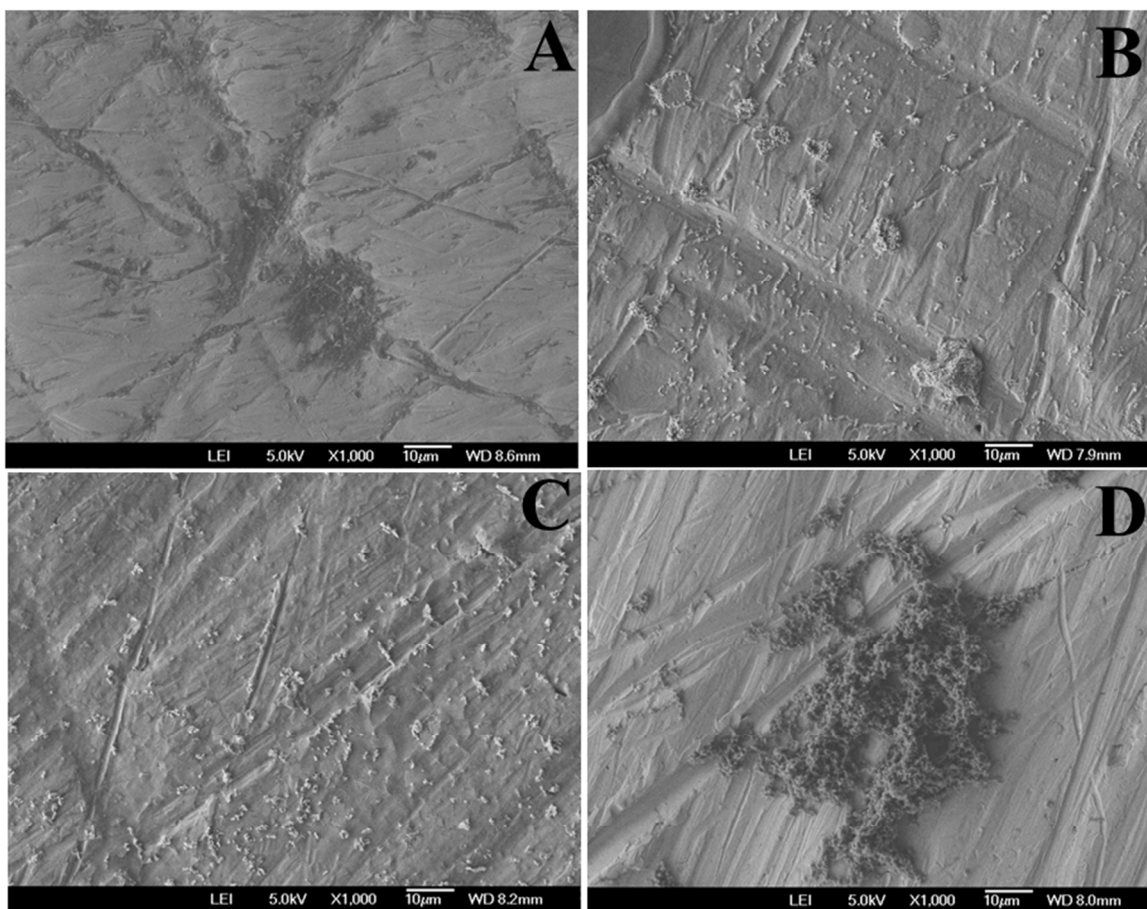
**Figure S3.** Electron microscopy images of cytc incubated in the presence and absence of ChAld after 24h. Typical reactions contained bicarbonate buffer (10 mM, pH 7.4), 10 µM cytc and 100 µM of either cholesterol or ChAld. **Panel A** shows the blank reaction (bicarbonate buffer plus ChAld). **Panel B** shows a control reaction (buffer plus cytc). **Panel C** shows the reaction between cytc and cholesterol. **Panel D** shows the reaction between cytc and ChAld. All images are in the same scale and are representative of 3 different experiments. A large cytc aggregate can be observed only in **panel D**.
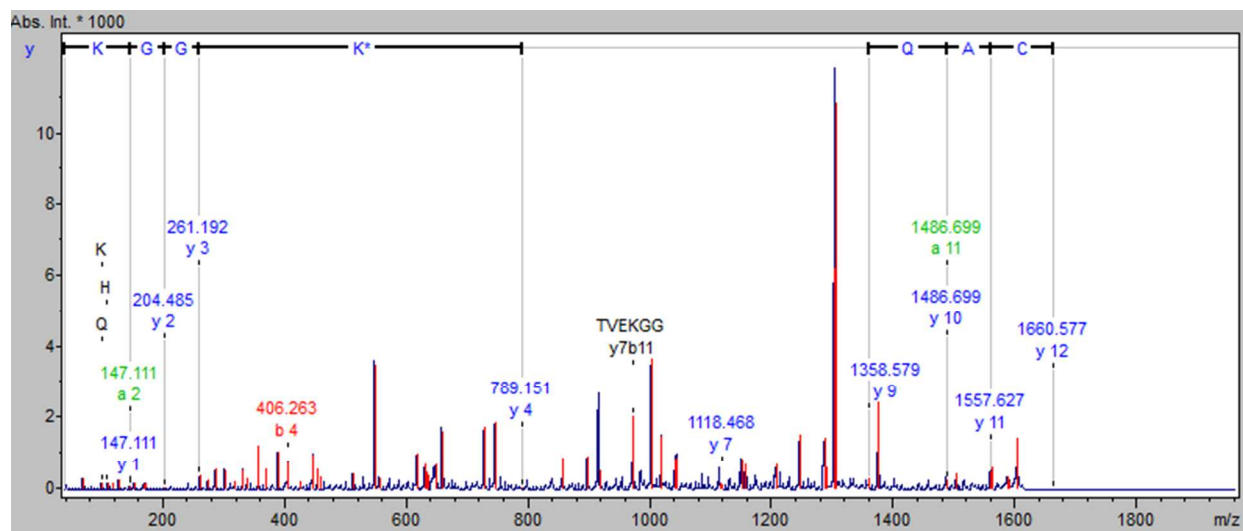
**Figure S4.** MS/MS analyses of the peptide CAQCHTVE**K**\*GGK modified at Lys22 (underlined residue marked with "*" at the sequence).
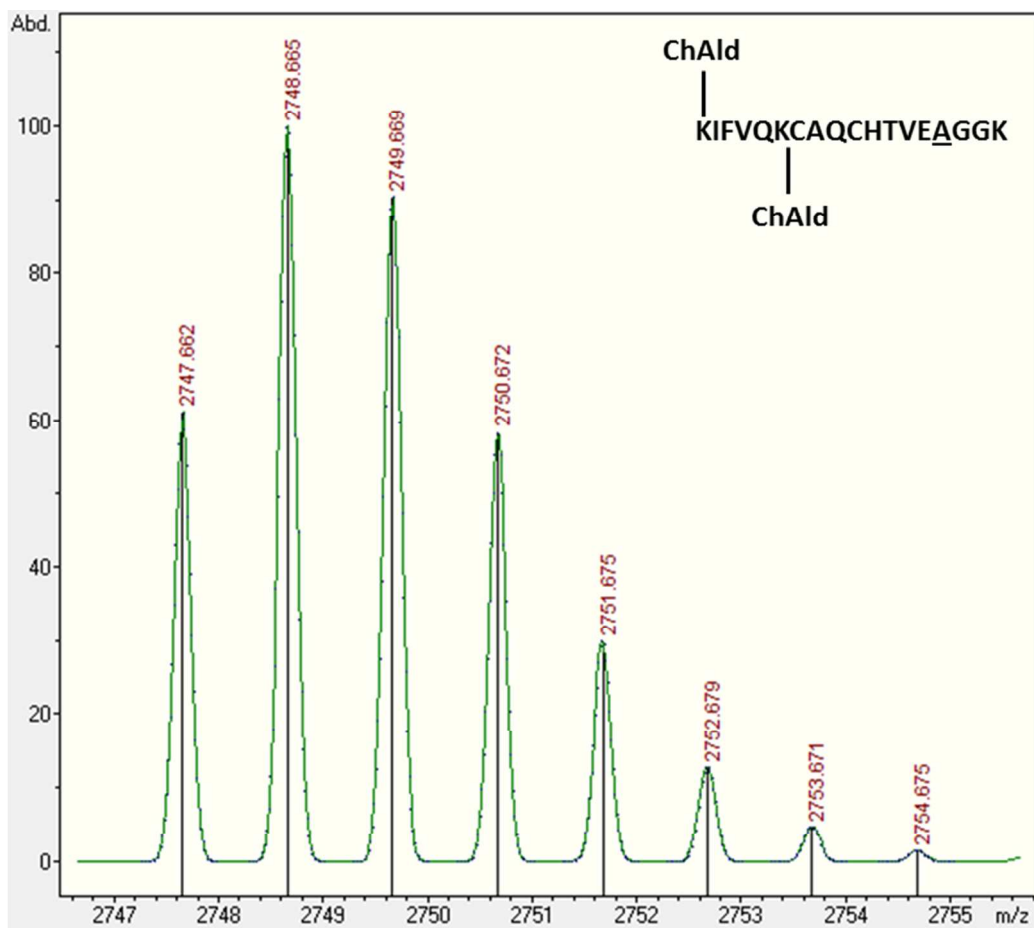
**Figure S5.** Simulation of the isotopic distribution of the mass peak shown in **figure 5C**. This peak corresponds to the peptide added by two molecules of ChAld through the formation of a Schiff base adduct. The simulation was done using the software *IsotopePattern* from Bruker Daltonics.
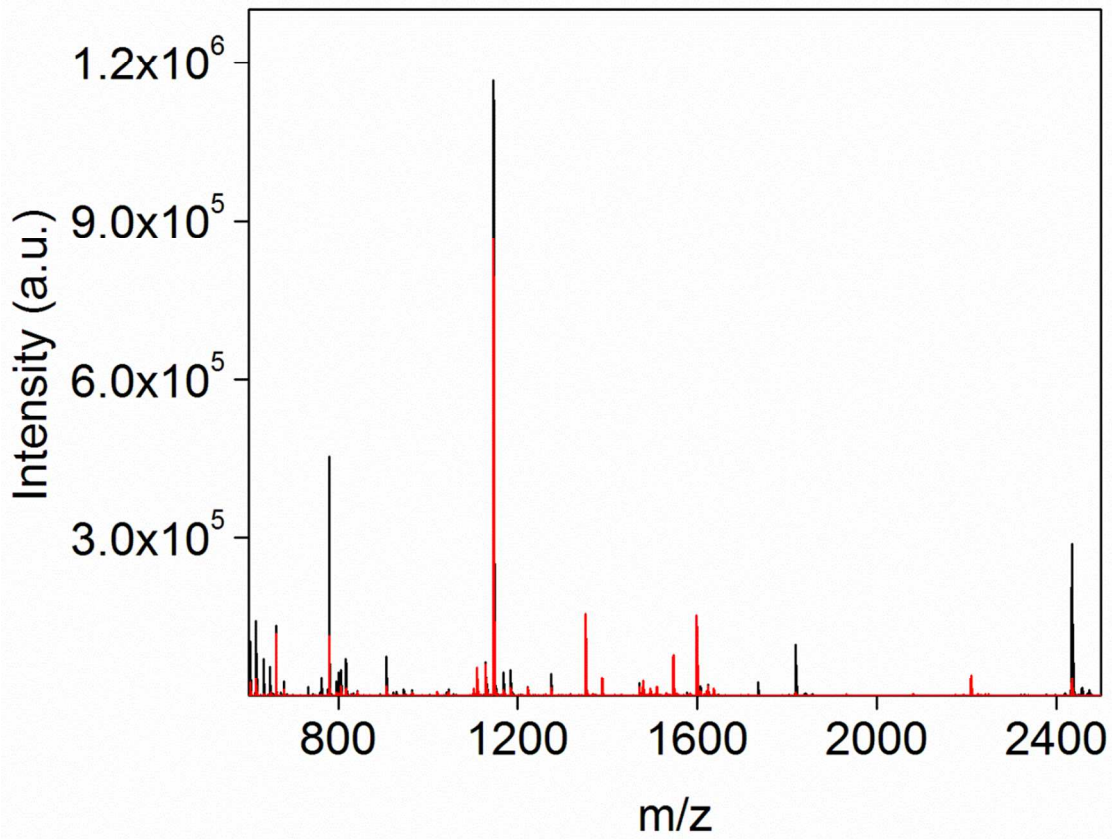
**Figure S6.** Expanded MALDI-TOF-MS of the peptides resulted from the tryptic digestion of K22A cytc mutant before (*black spectra*) and after (*red spectra*) incubation with ChAld (correspond to the expanded spectra shown in **Figure 5**). Typical reactions contained bicarbonate buffer (10 mM, pH 7.4), SDS 8 mM, cytc 50 μM, ChAld 500 μM. Spectra are representative of, at least, 3 different experiments. *Upper panel* shows the tryptic digestion of the wild type cytc.

# Chapter 3

# Probing lipid-protein adduction with alkynyl surrogates: application to Smith-Lemli-Opitz syndrome

# Probing lipid-protein adduction with alkynyl surrogates: application to Smith-Lemli-Opitz syndrome[s]

Katherine Windsor,* Thiago C. Genaro-Mattos,*,† Hye-Young H. Kim,*,§ Wei Liu,*
Keri A. Tallman,* Sayuri Miyamoto,† Zeljka Korade,**,†† and Ned A. Porter[1],*,††,§§

Departments of Chemistry,* Biochemistry,§ and Psychiatry,** Vanderbilt Kennedy Center for Research on Human Development,†† and Vanderbilt Institute of Chemical Biology,§§ Vanderbilt University, Nashville, TN; and Departamento de Bioquímica,† Instituto de Química, Universidade de São Paulo, São Paulo, SP, Brazil

**Abstract   Lipid modifications aid in regulating (and misregulating) protein function and localization. However, efficient methods to screen for a lipid's ability to modify proteins are not readily available. We present a strategy to identify protein-reactive lipids and apply it to a neurodevelopmental disorder, Smith-Lemli-Opitz syndrome (SLOS). Alkynyl surrogates were synthesized for polyunsaturated fatty acids, phospholipids, cholesterol, 7-dehydrocholesterol (7-DHC), and a 7-DHC-derived oxysterol. To probe for protein-reactive lipids, we used click chemistry to biotinylate the alkynyl tag and detected the lipid-adducted proteins with streptavidin Western blotting. In Neuro2a cells, the trend in amount of protein adduction followed known rates of lipid peroxidation (7-DHC >> arachidonic acid > linoleic acid >> cholesterol), with alkynyl-7-DHC producing the most adduction among alkynyl lipids. 7-DHC reductase-deficient cells, which cannot properly metabolize 7-DHC, exhibited significantly more alkynyl-7-DHC-protein adduction than control cells. Model studies demonstrated that a 7-DHC peroxidation product covalently modifies proteins. We hypothesize that 7-DHC generates electrophiles that can modify the proteome, contributing to SLOS's complex pathology.🔓 These probes and methods would allow for analysis of lipid-modified proteomes in SLOS and other disorders exhibiting 7-DHC accumulation. More broadly, the alkynyl lipid library would facilitate exploration of lipid peroxidation's role in specific biological processes in numerous diseases.**—Windsor, K., T. C. Genaro-Mattos, H-Y. H. Kim, W. Liu, K. A. Tallman, S. Miyamoto, Z. Korade, and N. A. Porter. **Probing lipid-protein adduction with alkynyl surrogates: application to Smith-Lemli-Opitz syndrome.** *J. Lipid Res.* 2013. **54:** 2842–2850.

Palmitoylation, *N*-myristoylation, cholesterylation, and glycosylphosphatidylinositol-anchor addition are a few of several known modes of protein lipidation (1, 2). These modifications affect a protein's stability, cellular localization, and biological activities (3, 4). In addition to directly modifying proteins, lipids are susceptible to reaction with molecular oxygen, yielding oxidation products that also have diverse biological effects. We recently provided evidence that 7-dehydrocholesterol (7-DHC), the immediate biosynthetic precursor of cholesterol (5), is one of Nature's most oxidizable lipids (6). Elevated levels of 7-DHC are a hallmark of Smith-Lemli-Opitz syndrome (SLOS), a disorder that arises from mutations in the gene encoding 7-DHC reductase (Dhcr7), the last enzyme in the cholesterol biosynthesis pathway (7–9). This defect in cholesterol biosynthesis causes a broad array of phenotypical, physiological, and neurological abnormalities (7, 9, 10). It is not clear whether the abnormalities are due to 7-DHC buildup, cholesterol deficiency, or some other cause. A plausible hypothesis is that 7-DHC or its peroxidation products are biologically active and contribute to the pathology of SLOS (11–14).

Our analytical studies provided evidence that 7-DHC undergoes free-radical chain oxidation to yield 5α, 6α-epoxide (DHCEp) as well as a variety of other oxysterol products, some of which are derived by either nonenzymatic or enzymatic reactions within cells (15–18). For example, DHCEp can metabolize to 3β,5α-dihydroxycholest-7-en-6-one

Abbreviations: 7-DHC, 7-dehydrocholesterol; *a*-7-DHC, alkynyl 7-dehydrocholesterol; *a*-AA, *19a*-arachidonic acid; *a*-Chol, alkynyl cholesterol; *a*-DHCEp, alkynyl DHC epoxide; *a*-DPPC, 1-palmitoyl-2-*15a*-palmitoyl-*sn*-glycero-phosphocholine; *a*-HNE, *8a*-4-hydroxynonenal; *a*-LA, *17a*-linoleic acid; *a*-OA, *17a*-oleic acid; *a*-PA, *15a*-palmitic acid; *a*-PLPC, 1-palmitoyl-2-*17a*-linoleoyl-*sn*-glycero-phosphocholine; *a*-POPC, 1-*15a*-palmitoyl-2-oleoyl-*sn*-glycero-phosphocholine; APCI, atmospheric pressure chemical ionization; Chol, cholesterol; cyt *c*, cytochrome *c*; DHCEO, 3β,5α-dihydroxycholest-7-en-6-one; DHCEp, 7-dehydrocholesterol 5α, 6α-epoxide; Dhcr7, 7-dehydrocholesterol reductase; HNE, 4-hydroxynonenal; SLOS, Smith-Lemli Opitz syndrome; SRM, selected reaction monitoring.

[1] To whom correspondence should be addressed.
    e-mail: n.porter@vanderbilt.edu

[s] The online version of this article (available at http://www.jlr.org) contains supplementary data in the form of four figures and seven schemes.

(DHCEO), a biomarker of oxidative stress in SLOS models, as shown in **Fig. 1**. DHCEp is very reactive, with the epoxide moiety undergoing hydrolysis in aqueous environments and ring-opening in the presence of alcohols.

While peroxidation of cholesterol and 7-DHC generates oxysterols, peroxidation of polyunsaturated fatty acids, such as arachidonic acid (20:4, ω-6) and linoleic acid (18:2, ω-6), results in different assorted by-products, including the electrophilic 4-hydroxynonenal (HNE) (19). HNE has been shown to react with nucleophilic protein residues to afford stable covalent adducts (20–22). Protein modification with HNE may be involved in the development of various diseases, including Parkinson's disease, Alzheimer's disease, and atherosclerosis, in addition to altered cell signaling (23–26). HNE-protein adduction has been studied extensively, with protein targets of modification and sites of adduction within modified proteins identified (21, 27).

An effective strategy that we have developed to study protein modification involves incorporating an alkyne functional group into a lipid by organic synthesis, thus generating a surrogate for the naturally occurring compound (21, 28, 29). We report here on the preparation of a library of synthetic alkynyl fatty acids, phospholipids, and sterols and the incubation of these lipid surrogates in Neuro2a cells. Subsequent Huisgen-Sharpless cycloaddition (click reaction) (30, 31) of cell lysates with an azido-biotin reagent (21) enabled us to visualize adducted proteins by streptavidin Western blotting, thereby showing the overall level of proteome modification by the alkynyl lipid. A comparison of protein adduction by alkynyl 7-DHC (*a*-7-DHC) in control and SLOS model cells reveals increased protein adduction in the SLOS model. Model peptide and protein adduction studies suggest one potential 7-DHC oxidation product likely to be responsible for covalent protein modification in the SLOS model cell culture.

## MATERIALS AND METHODS

### Synthetic procedures

$^1$H and $^{13}$C NMR spectra were collected on a 300 or 400 MHz NMR. High-resolution mass spectrometry (HRMS) analyses were carried out at the University of Notre Dame. Purification by column chromatography was carried out on silica gel, and TLC plates were visualized with phosphomolybdic acid. The synthesis of *a*-HNE (21), *a*-PA, *a*-DPPC, and *a*-PLPC have been previously published (28). The synthesis of *a*-LA and *a*-AA were previously reported (28), but an improved synthetic route is described

here. Full synthetic procedures for the remaining alkynyl lipids in **Fig. 2A** are included in the supplementary data.

### Cell cultures

Neuroblastoma cell line Neuro2a was purchased from American Type Culture Collection (Rockville, MD). Neuro2a cells were maintained in DMEM (Life Technologies) and supplemented with L-glutamine, 10% FBS (Thermo Scientific HyClone), and penicillin/streptomycin at 37°C and 5% $CO_2$. According to the vendor, the FBS contained cholesterol at concentrations of 32 mg/100 ml. This translates into a final cholesterol concentration of 32 μg/ml in our culture medium. To evaluate the role of exogenous cholesterol on gene expression, cells were also cultured with medium containing 10% cholesterol-deficient serum (Thermo Scientific HyClone Lipid Reduced FBS). This FBS medium did not have detectable cholesterol levels. The Neuro2a cells were subcultured once a week, and the culture medium was changed every two days. Neuro2a cells were cultured for two days before transfections. Cells were transfected with Dhcr7 pGIPZ plasmids using a Nucleofector instrument and Nucleofector kit V (Amaxa GmbH, Cologne, Germany) optimized for use with Neuro2a cells. Briefly, $2 \times 10^6$ cells were resuspended in 100 μl of transfection buffer, shRNA was added, and cells were electroporated using program T-24. The cells were grown for 24 h following transfection, and the stable cell line was established using puromycin as selection marker. The expression of Dhcr7 was monitored by quantitative RT-PCR, and the amount of 7-DHC, with MS.

### Cell viability assay

Neuro2a cells were plated 6,000/well in 96-well plates and allowed to adhere on the plate for 24 h. The medium was removed, and the cells were treated with lipids of interest at different concentrations dissolved in 2% FBS DMEM. After 24 h of incubation, the medium was removed, and the cells were washed once with cold PBS. Cell viability was then evaluated using the CellTiter 96® AQueous One Solution Cell Proliferation Assay (Promega), a colorimetric method for determining the number of viable cells in proliferation or cytotoxicity (see supplementary data for further details). A premixed solution of 2% FBS DMEM containing CellTiter 96® AQueous One Solution Reagent (5/1 v/v of medium to assay reagent) was added to culture wells (120 μl/well). After 1 h of incubation at 37°C, the absorbance at 490 nm was recorded using a 96-well plate reader. The absorbance at 490 nm is directly proportional to the number of living cells in culture.

### Alkynyl lipid treatment in Neuro2a cells

Neuro2a cells were grown in DMEM supplemented with L-glutamine, 10% FBS, and penicillin/streptomycin at 37°C and 5% $CO_2$. Cells were plated $2 \times 10^6$ in 10 cm plates, then allowed to settle and grow for 24 h. The cells were then incubated in the presence of alkynyl probes (20 μM) in 2% FBS DMEM for 24 h. The harvested cells were centrifuged at 800 $g$ for 5 min, then washed with cold PBS, pH 7.4. Cell pellets were stored at −40°C
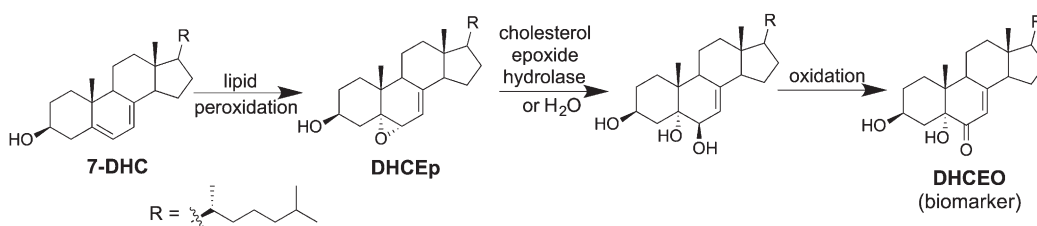


**Fig. 1.** Conversion of 7-DHC to DHCEO in SLOS cells and tissues. Lipid peroxidation and enzymatic oxidation yield the oxysterol DHCEO, which is a biomarker of oxidative stress in SLOS.
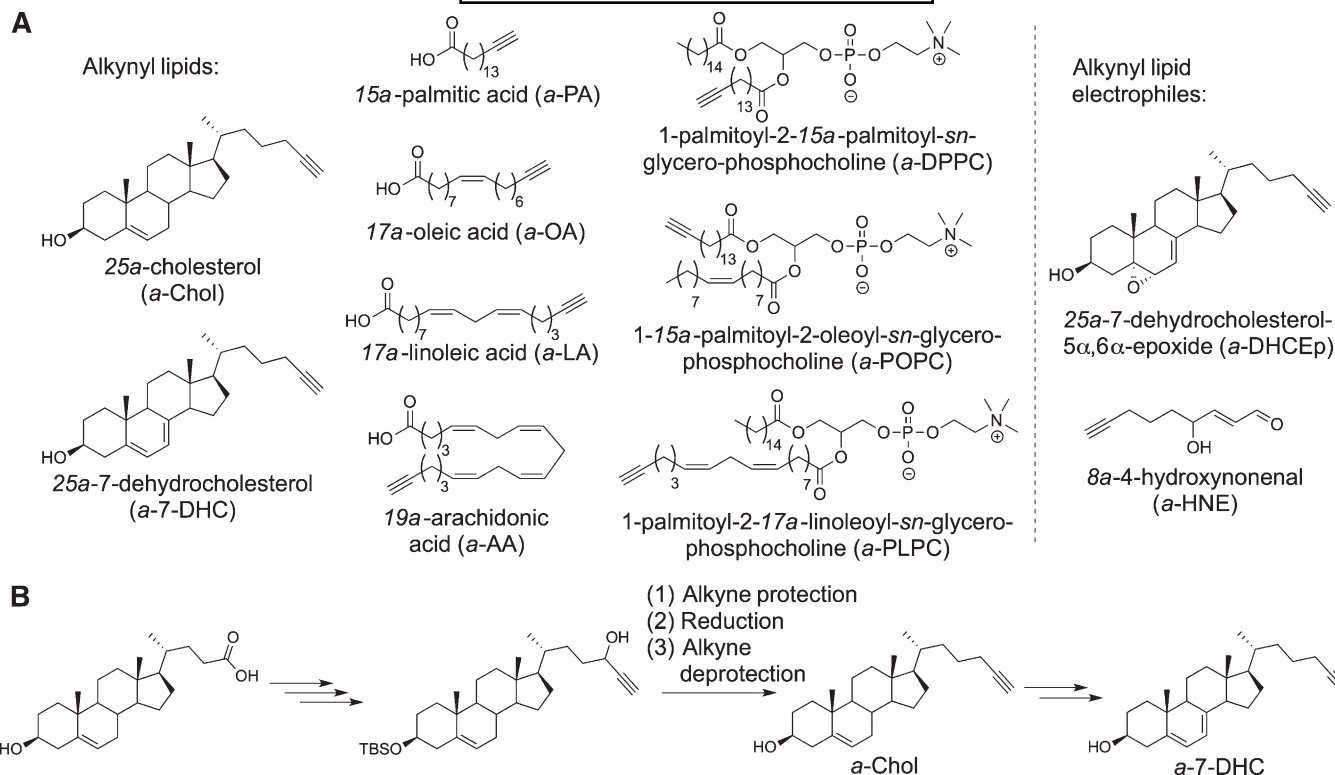
**Fig. 2.** Library of alkynyl lipid probes. A: Synthesized probes include fatty acids, phospholipids, and sterols that were tested for adduction to the Neuro2a proteome. B: Overview of synthetic route to *a*-Chol and *a*-DHC.

until further processing (either lipid extraction and HPLC-MS analysis or protein biotinylation).

### Extraction, separation, and HPLC-MS analysis of free sterols and sterol esters

To the cell pellets was added Folch solution [5 ml chloroform/methanol (2/1) containing 0.001M BHT and PPh$_3$], followed by the addition of NaCl aqueous solution (0.9%, 1 ml). $d_7$-7-DHC, $d_7$-7-DHC-LA, $d_7$-Chol, and $d_7$-Chol-LA were added as internal standards. The resulting mixture was vortexed for 1 min and centrifuged for 5 min. The lower organic phase was recovered, dried under a stream of nitrogen, redissolved in methylene chloride, and subjected to separation with NH$_2$-SPE [500 mg cartridge; the column was conditioned with 4 ml of hexane, and the neutral lipids containing oxysterols were eluted with 4 ml of chloroform/2-propanol (2/1, v/v)]. The eluted fractions were then dried under nitrogen and reconstituted for HPLC-MS analysis. All processed samples were analyzed by a Thermofinnigan TSQ Quantum Ultra equipped with a Finnigan Surveyor Autosampler Plus. Reverse-phase HPLC was performed on a Phenomenex Luna C18 column (150 × 2 mm, 3 µM), preequilibrated in MeCN (solvent A)/CH$_2$Cl$_2$ (solvent B) (87.5/12.5). The samples were injected and eluted (0.2 ml/min) with an increasing concentration of solvent B [time (min)/per percentage of solvent B: 4/12.5, 7/47.5, 28/50.0, 32/12.5, 35/12.5] (32). The MS was operated in the positive-ion mode using atmospheric pressure chemical ionization (APCI) in the selected reaction monitoring (SRM) mode. MS parameters were optimized for $d_7$-7-DHC and $d_7$-7-DHC-LA and were as follows: auxiliary gas pressure was set at 5 psi, sheath gas pressure was 30 psi, utilizing nitrogen for both. Discharge current was set at 20 eV, and the vaporizer temperature was set at 230°C. Collision-induced dissociation was optimized at 16 eV under 1.0 mTorr of argon. Data acquisition and analysis were performed using Xcalibur software, version 2.0

(San Jose, CA). Assignment of the oleate, palmitate, and arachidonate sterol esters was previously established using independently synthesized standards (32).

### Biotinylation of alkynyl lipid-adducted proteins in Neuro2a cells

Cell pellets were lysed on ice for 20 min in 1 ml of cold lysis buffer supplemented with 150 mM NaCl, protease inhibitor mixture, and phosphatase inhibitor mixture (1.0 mM sodium fluoride, 1.0 mM sodium molybdate, 1.0 mM sodium orthovanadate, 10.0 mM β-glycerophosphate) for each plate. The lysate was cleared by centrifugation at 10,000 $g$ for 10 min to remove cellular debris. The total protein concentration was determined using standard BCA assay (Pierce). To detect the alkynyl lipid-modified proteins in Neuro2a, cell lysates from alkynyl probe-treated cells were reduced with sodium borohydride, 5 mM final concentration, for 1 h at room temperature. Sodium borohydride reduction was employed to stabilize any protein-lipid electrophile adducts that may form reversibly, such as Michael and Schiff base adducts. Then the sodium borohydride was quenched by acidifying to pH 6. Subsequently, all click reagents were added to the reduced cell lysates, azido-biotin (21) (0.2 mM), tris(3-hydroxy-propyltriazolylmethyl)amine (THPTA) (33) (0.2 mM), CuSO$_4$ (1 mM), and sodium ascorbate (1 mM), and the reaction was vortexed and allowed to react at room temperature for 2 h. The reaction mixture was precipitated using cold acetone (acetone/water, 6/1, v/v) to remove all excess chemicals. The cell pellets were reconstituted in 100 µl of LDS sample buffer including DTT (50 mM).

### Immunoblot analysis of protein adducts with alkyne probes

The reconstituted proteins were resolved using 10% NuPAGE Novex BisTris® gel (Invitrogen, Carlsbad, CA). Precision Plus

Protein™ Kaleidoscope™ standards (10–250 kDa, Bio-Rad) were run on the same gel for reference. The proteins were electrophoretically transferred to a polyvinylidene difluoride membrane (Invitrogen) and probed with streptavidin conjugated with Alexa Fluor 680®. Biotinylated proteins were visualized using Odyssey Infrared Imaging System™ and Odyssey software as described by the manufacturer (Licor, Lincoln, NE). Integrated intensities were obtained with the Odyssey software and can be found in the supplementary data.

### Modification of AcTpepK (Ac-AVAGKAGAR) by 7-DHCEp and *a*-DHCEp

A solution of AcTpepK (1 mM) and 7-DHCEp or *a*-7-DHCEp (5 mM) in pH 7.4 phosphate buffer:CH$_3$CN (100 µl, 1:1 by volume) was incubated at 37°C for 1 h. The reaction mixture was reduced with 2 M NaBH$_4$ (5 µl), then neutralized with 10% HCl (10 µl) for HPLC/MS analysis. Reverse-phase HPLC was performed on a Supelco Discovery C18 column (150 × 2.1 mm, 5 µM) using a mobile phase consisting of A: 0.05% TFA in H$_2$O and B: 0.05% TFA in CH$_3$CN. The unreacted peptide and adducts were eluted with a gradient of 5% to 35% B over 20 min, then to 100% B over 5 min and held for 20 min, and back to 5% B over 5 min. The MS was operated in the positive-ion mode using electrospray ionization with conditions optimized for the AcTpepK.

### Modification of cytochrome *c* by 7-DHC/7-DHCEp

Cytochrome c (cyt *c*; from equine heart, 40 µM) was incubated in the presence of 7-DHC (1.25 mM) or 7-DHCEp (400 µM) in 10 mM ammonium bicarbonate buffer (pH 7.4) at room temperature overnight with stirring. For the 7-DHC experiment, 10% MeCN was added to aid in lipid solubilization, and the reaction was performed under O$_2$ (1 atm). After stirring overnight, samples were stored at −40°C until MALDI-TOF MS analysis.

### MALDI-TOF MS analysis of sterol-modified cyt *c*

Modified cyt *c* sample (0.5 µl) and a saturated solution of sinapinic acid (3,5-dimethoxy-4-hydroxycinnamic acid) in CH$_3$CN/H$_2$O/TFA (50/50/0.1, v/v/v) (1 µl) were spotted onto a MALDI target plate, immediately mixed by pipetting up and down twice, and allowed to dry before analysis. MALDI-TOF MS analyses were performed with a PerSeptive Biosystems Voyager-DE STR MALDI-TOF equipped with a pulsed N$_2$ laser. Protein spectra were collected in positive ion linear mode with an accelerating voltage of 20 kV. Each spectrum was the accumulation of 1,000 laser shots, with a laser intensity of 2,200–2,300 that was optimized for each spectrum to provide the best signal-to-noise ratio. The MALDI-TOF MS spectra were processed using the Data Explorer software.

### *a*-7-DHC treatment in control versus Dhcr7-deficient Neuro2a cells

Neuro2a cells were maintained in DMEM and supplemented with L-glutamine, 10% FBS (Thermo Scientific HyClone), and penicillin/streptomycin at 37°C and 5% CO$_2$. Cells were plated $7.5 \times 10^5$ in 6 cm plates, then allowed to settle and grow for 24 h. Both control and Dhcr7-deficient Neuro2a cells were treated with *a*-7-DHC at concentrations ranging 0–5 µM in DMEM with N-2 supplement. After incubation at 37°C for 24 h, cells were harvested and lysed, and the total protein concentration was determined using standard BCA assay (Pierce). The lysate was reduced with NaBH$_4$ (5 mM) to stabilize any adducts that may have formed and neutralized. Subsequently, all click reagents were added to the reduced cell lysates, azido-biotin (21) (0.2 mM), THPTA (33) (0.2 mM), CuSO$_4$ (1 mM), and sodium ascorbate (1 mM), and the reaction was vortexed and allowed to react at room temperature for 2 h.

## RESULTS

### Synthesis of alkynyl lipid probes

Analogs of several lipids and lipid electrophiles have been synthesized with an alkyne group introduced as a functional tag (Fig. 2A). For each lipid, the alkyne is incorporated in a terminal chain position, facilitating a subsequent click reaction (21). For the alkynyl fatty acids and phospholipids, this triple bond substitution results in a net loss of four hydrogens from the naturally occurring lipid. In the alkynyl sterols and oxysterols prepared, the triple bond replaces the C24 isopropyl group.

While full synthetic procedures for all alkynyl lipids are included in the supplementary data [and synthetic approaches to some of the alkynyl analogs have been published previously (21, 28)], we highlight efficient syntheses of the novel alkynyl cholesterol (*a*-Chol), *a*-7-DHC (Fig. 2B), and *a*-DHCEp here. *a*-Chol was prepared starting from commercially available 3β-hydroxy-5-cholenic acid; a key synthetic step was the deoxygenation of the propargyl alcohol intermediate to the corresponding alkyne. Traditional reductive methods resulted in undesired side reactions: elimination of water to yield an enyne and isomerization of the alkyne to an allene. One-pot cobalt protection of the alkyne, acid-catalyzed borane reduction, and final deprotection of the alkyne afforded *a*-Chol in good yield (34). *a*-Chol was smoothly converted to *a*-7-DHC via oxidation to alkynyl 7-ketocholesterol and a subsequent Shapiro reaction to form the diene. *m*CPBA oxidation of *a*-7-DHC provided *a*-DHCEp, the alkynyl analog of DHCEp.

### Alkynyl compounds show cellular metabolism comparable to their naturally occurring analogs

Since the naturally occurring lipid and its alkynyl analog are structurally very similar, we expected to observe minimal perturbation of the lipid's cellular metabolism. The suitability of *a*-Chol and *a*-7-DHC as surrogates for cholesterol and 7-DHC, respectively, was tested by comparing their cellular toxicity, incorporation, and esterification. Neuro2a neuroblastoma cells were treated with cholesterol, *a*-Chol, 7-DHC, and *a*-7-DHC, and cellular viability was determined after 24 h (supplementary Fig. I). *a*-Chol and cholesterol were nontoxic at all concentrations tested (≤40 µM). Although more toxic than cholesterol and *a*-Chol, *a*-7-DHC exhibited similar toxicity to its natural analog, 7-DHC.

To test the incorporation and metabolism of the compounds of interest, Neuro2a cells were treated with *a*-Chol or *a*-7-DHC using a concentration that does not affect cell viability (2.5 µM), and cell extracts were analyzed after 24 h by reverse-phase HPLC-MS with SRM. Upon treatment with *a*-Chol, cells incorporate and esterify the alkynyl analog (supplementary Fig. II). Similarly, upon incubation with *a*-7-DHC, cells successfully incorporate the alkynyl lipid (**Fig. 3A**). Using methods previously established in our

group, we were able to separate and analyze endogenous cholesterol, *a*-Chol, *a*-7-DHC, and their corresponding esters in one chromatographic run (32). Under these analytical conditions, cholesterol and its esters fragment to give a common ion having $m/z$ 369, generated by loss of water or the fatty ester tail, respectively. Accordingly, *a*-Chol and its esters fragment to afford a carbocation with $m/z$ 351, and *a*-7-DHC and its esters undergo fragmentation to yield a carbocation with $m/z$ 349. The fatty acid constituent profiles of *a*-Chol esters and the endogenous cholesterol esters (displayed in Fig. 3E, F) are comparable, indicating that the alkynyl probe is metabolized similarly to natural cholesterol. Most of the *a*-7-DHC is converted to *a*-Chol (Fig. 3B) and its corresponding alkynyl cholesteryl esters (Fig. 3E), exhibiting metabolism typical of the naturally occurring 7-DHC. There are no *a*-7-DHC esters formed at this concentration of treatment (Fig. 3D). Both the cell viability and incorporation results confirm that the alkynyl derivatives are suitable surrogates for the naturally occurring sterols.

## Biotinylation allows for detection of Neuro2a cellular proteome modification with alkynyl lipid probes

The unique characteristic of the lipid analogs used in this study is the presence of a terminal alkyne moiety, which enables the click reaction with an azido-biotin reagent (**Fig. 4**) (21, 27, 35). With evidence that *a*-Chol and *a*-7-DHC incorporate into cells and with previous work demonstrating that alkynyl fatty acid and alkynyl phospholipid probes can be incorporated and metabolized as well (28, 29), Neuro2a cells were treated with each of our alkynyl fatty acids, phospholipids, and sterols shown in Fig. 2A. An overview of the procedure is outlined in Fig. 4, with details described in Materials and Methods. To visualize the biotinylated adducts (alkynyl lipid-modified proteins with biotin tag), we used Western blotting, employing a
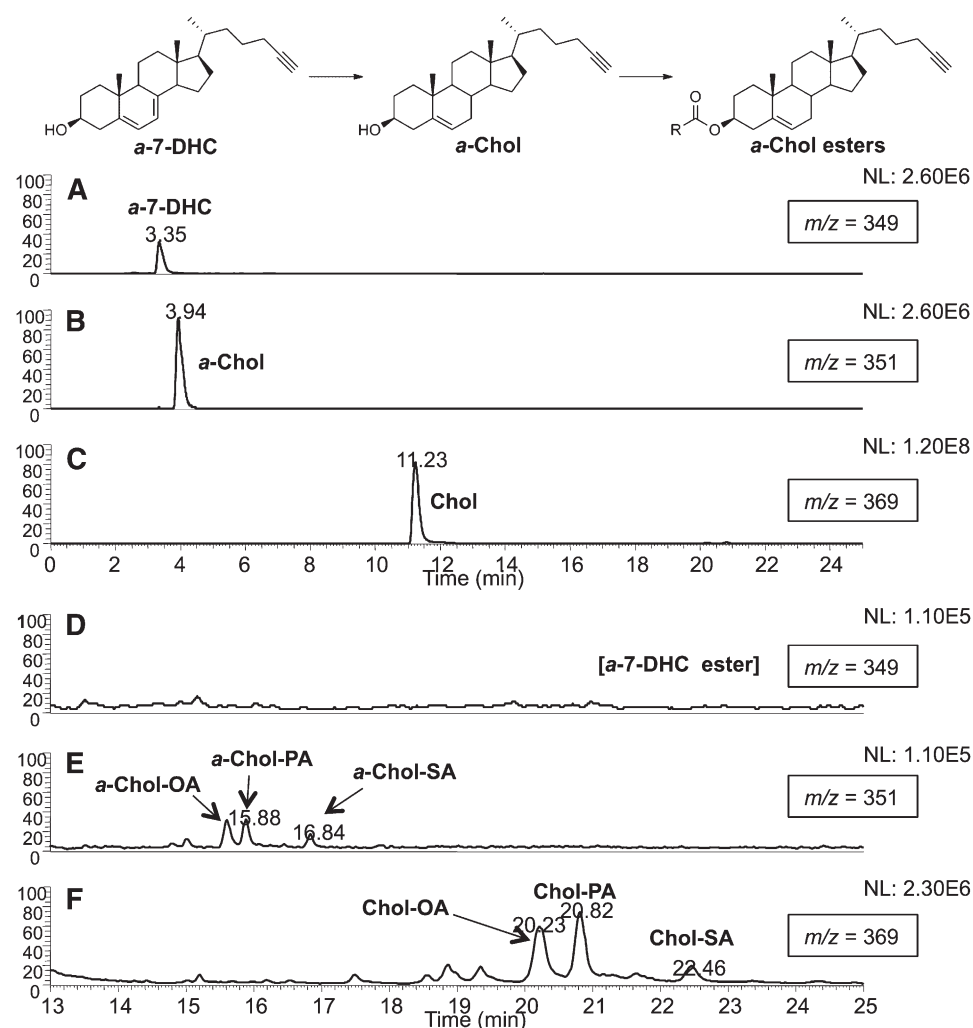


**Fig. 3.** Incorporation and metabolism of *a*-7-DHC in Neuro2a cells. Neuro2a cells were incubated in the presence of 2.5 µM *a*-7-DHC for 24 h in 2% FBS DMEM. Free sterols and sterol esters were analyzed by HPLC-MS operated in SRM mode. A–C: Chromatograms showing free sterols. D–F: Chromatograms showing sterol esters (expansions of A–C, respectively). A and D: Molecules that fragment to give an ion with $m/z$ 349, *a*-7-DHC, and its esters. B and E: Molecules that fragment to give an ion with $m/z$ 351, *a*-Chol, and its esters OA, oleate; PA, palmitate; SA, stearate. C and F: Molecules that fragment to give $m/z$ 369, cholesterol, and its esters.
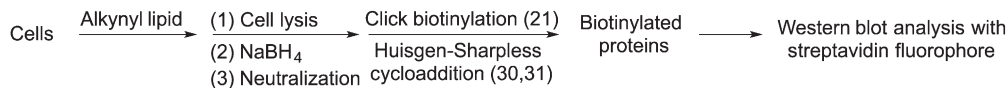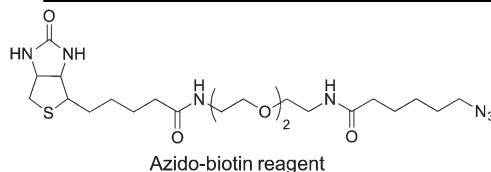
**Fig. 4.** General experimental workflow, including the azido-biotin reagent used for click biotinylation of alkynyl lipid-modified proteins.

fluorescent streptavidin conjugate (**Fig. 5**). Integrated intensities from the Western blot analyses of Neuro2a protein adduction with the alkynyl lipid probes indicated the degree of alkynyl lipid modification of the Neuro2a proteome (supplementary Fig. III).

*a*-7-DHC exhibited the greatest amount of Neuro2a proteome adduction among all alkynyl lipids (Fig. 5A). Because *a*-7-DHC led to a significant amount of protein adduction, an alkynyl analog of DHCEp (*a*-DHCEp), a major product of 7-DHC peroxidation, was prepared and tested for protein adduction. *a*-DHCEp also showed a considerable amount of protein modification, demonstrating that 7-DHC oxidation products can act as reactive electrophiles. *a*-Chol afforded negligible protein adduction.

As shown in Fig. 5B, within the alkynyl fatty acid class, the amount of protein adduction followed: *19a*-arachidonic acid (*a*-AA) > *17a*-linoleic acid (*a*-LA) > *17a*-oleic acid (*a*-OA) ≈ *15a*-palmitic acid (*a*-PA). The alkynyl phospholipids yielded little adduction relative to the ethanol control (data not shown). The oxidizability of each lipid correlates with the amount of Neuro2a proteome modification by each lipid: a higher rate of lipid peroxidation generally results in a greater amount of lipid-protein adduction (6).

### Direct evidence for model peptide and protein adduction

To confirm that alkynyl lipids covalently bind proteins, we used in vitro studies, incubating lipids with a peptide and small protein; the two lipid species giving the greatest amount of Neuro2a proteome modification (*a*-7-DHC and *a*-DHCEp) were utilized in these model studies. When DHCEp or *a*-DHCEp is reacted with a model peptide containing one nucleophilic site, we observed compounds by HPLC-MS that have masses corresponding to the respective peptide-oxysterol adduct (supplementary Fig. IV).

Cyt *c*, a 12 kDa protein containing 19 lysine residues and 3 histidine residues, was chosen as an illustrative protein for DHCEp (400 Da) adduction studies. Cyt *c* (40 μM) was incubated with DHCEp (400 μM) at room temperature for 18 h and subsequently analyzed by MALDI-MS (**Fig. 6A**). Focusing on the region displaying doubly charged cyt *c* species, a protein-DHCEp adduct shifted +200 *m/z* units from the unmodified protein was observed. A peak representing cyt *c*-oxysterol adduction plus loss of the cyt *c* heme group during MS analysis was also seen, providing further support for modification.



**Fig. 5.** Neuro2a protein adduction with alkynyl lipids. Neuro2a cells were incubated in the presence of alkynyl lipid (20 μM) for 24 h in 2% FBS DMEM. Proteins adducted with alkynyl lipid were ligated with biotin via click reaction. The degree of adduction is determined by Western blotting using the streptavidin-AlexaFluor 680 conjugate. The fluorophore was detected using the Odyssey Infrared Imaging System (Licor). A: Western blot comparison of Neuro2a proteome modification by alkynyl sterols. Chol was used as a control treatment. B: Western blot comparison of Neuro2a proteome modification by alkynyl fatty acids. Ethanol was used as a control treatment.



**Fig. 6.** Reaction of cyt *c* with 7-DHCEp and 7-DHC. MALDI-MS analysis of (A) protein adduct with 7-DHCEp and (B) protein adduct with 7-DHC.

Alkynyl lipids incorporate into cellular proteome **2847**

A similar adduction experiment employing the highly oxidizable 7-DHC, rather than one of its preformed oxysterols (DHCEp), was performed. Cyt $c$ (40 $\mu$M) was incubated with 7-DHC (384 Da) (1.25 mM) under an oxygen atmosphere (1 atm) at room temperature for 18 h and subsequently analyzed by MALDI-MS (Fig. 6B). 7-DHC showed an adduction profile similar to that of DHCEp. A peak in the range of doubly charged cyt $c$ species with a $m/z$ shift of +200 appeared after incubation with 7-DHC. This result is consistent with 7-DHC undergoing lipid peroxidation to form an electrophilic oxysterol (384 Da + 16 Da), such as DHCEp, which subsequently modifies cyt $c$. A peak representi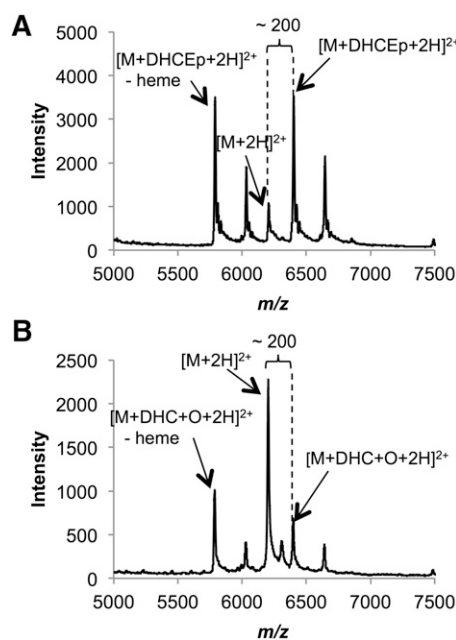ng cyt $c$-7-DHC oxysterol adduction and subsequent loss of the heme group during MS analysis was also observed. These model experiments verified that we are able to monitor the modification of a single protein or peptide by an oxysterol.

### Protein adduction increases in the cellular SLOS model

In SLOS, mutations in the gene encoding Dhcr7 result in an inactive enzyme and an accumulation of 7-DHC (36). Here, we tested whether increased 7-DHC and the presence of 7-DHC-derived oxysterols would lead to increased lipidation of a cellular proteome. Dhcr7-deficient Neuro2a cells were generated as described previously and utilized as a model for SLOS study (37). Using the $a$-7-DHC probe, the extent of protein modification in control Neuro2a cells and Dhcr7-deficient Neuro2a cells was compared. Biotinylated proteins were visualized using streptavidin Western blotting (**Fig. 7**). At treatment concentrations ⩾ 2.5 $\mu$M of $a$-7-DHC, Dhcr7-deficient cells clearly showed an increased amount of protein adduction relative to control Neuro2a cells. Control Neuro2a cells treated with $a$-7-DHC at 0–5 $\mu$M showed little protein adduction, because at these concentrations, $a$-7-DHC is effectively being converted to $a$-Chol. These results suggest that increased lipid



**Fig. 7.** $a$-7-DHC protein adduction in control Neuro2a versus Dhcr7-deficient Neuro2a cells. Neuro2a cells were incubated in the presence of $a$-7-DHC (0–5 $\mu$M) or $a$-Chol (20 $\mu$M) for 24 h. Alkynyl lipid-adducted proteins were ligated with biotin via click reaction. The degree of adduction is determined by Western blotting using the streptavidin-AlexaFluor 680 conjugate. The fluorophore was detected using the Odyssey Infrared Imaging System (Licor).

peroxidation affects the cellular proteome. Future proteomics studies will identify the $a$-7-DHC-modified proteins in SLOS models.

## DISCUSSION

Because of the potent biological activities of a variety of lipids and their corresponding oxidation products, we have designed several alkynyl lipid and alkynyl lipid electrophile probes to survey their reactivity with proteins. Employing an alkyne functional group as the tag generally results in minimal perturbation of the lipid's biological activity, as the naturally occurring lipid and the alkynyl analog are structurally very similar. Upon incubating cells in the presence of an alkynyl lipid, an azido-biotin reagent (21) is clicked to any alkynyl lipid-modified proteins, and subsequent Western blotting with streptavidin fluorophore detection indicates the relative level of protein adduction.

Cell incorporation experiments validate $a$-7-DHC and $a$-Chol as appropriate biological surrogates for their respective nonalkynyl analogs. When comparing the relative amounts of protein adduction by all alkynyl lipids, the results mirror the rates of peroxidation: 7-DHC >> arachidonic acid > linoleic acid >> cholesterol (Fig. 5) (6). 7-DHC is known to be 10-fold more oxidizable than arachidonic acid (6). Correspondingly, significantly more protein adduction is observed in cells treated with $a$-7-DHC than in cells treated with $a$-AA and the other fatty acids. For fatty acids and phospholipids, the relative amount of protein adduction is dependent on the number of bis-allylic methylene centers in the lipid [arachidonic acid (3 centers) > linoleic acid (1) > oleic acid (0) ≈ palmitic acid (0)]. While the amount of protein adduction seems to be influenced by the oxidizability of the lipid probe, there are additional mechanisms of modification that should be considered when analyzing our results. $S$-acylation with palmitic acid and other longer chain fatty acids, both saturated and unsaturated, cholesterylation, and cysteine-alkyne reaction[2] are a few known modes of protein adduction that may contribute to the overall modification of the Neuro2a proteome (1, 38, 39). Nonetheless, the substantial amounts of protein adduction observed for $a$-AA, $a$-7-DHC, and $a$-DHCEp (the two lipids in our study most susceptible to peroxidation and an electrophilic $a$-7-DHC oxidation product) imply that lipid oxidizability is a significant factor in assessing a lipid's propensity to modify proteins.

Modification of proteins with cholesterol-derived oxysterols has been associated with a number of diseases, including multiple sclerosis, antibody light chain misfolding disorders, and neurodegenerative disorders (40–43).
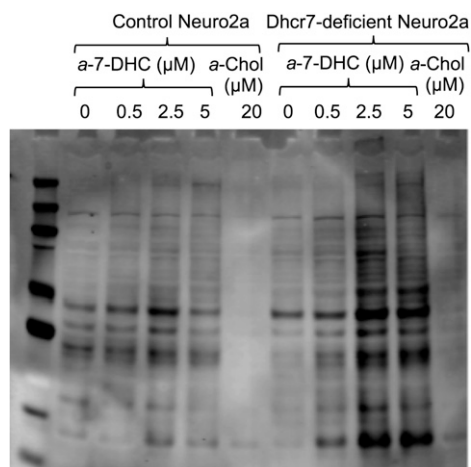
---

[2]The cysteine-alkyne reaction described by Ekkebus et al. (39) was highly selective, occurring in de-ubiquinating enzymes. If this type of proteome modification is operating in our system, it would be reasonable to expect a similar amount of cysteine-alkyne protein lipidation for all of our alkynyl probes, resulting in a similar level of background in each lane of the Western blots; because this mode of lipidation is likely not specific to any alkynyl probe, it should not interfere with our efforts to identify lipids that show increased amounts of protein adduction.

Free-radical oxidation of 7-DHC provides assorted oxysterols, which have been shown to have important biological effects, such as cytotoxicity (15). In the context of SLOS, a mixture of 7-DHC-derived oxysterols induced changes in gene expression in control Neuro2a cells that are similar to those identified in Dhcr7-deficient Neuro2a cells (44). DHCEp is a major product of 7-DHC peroxidation and can metabolize to another oxysterol, DHCEO, a biomarker for 7-DHC oxidation that can affect neural development in a SLOS model mouse (16, 45). Because some of the 7-DHC-derived oxysterols are electrophilic, such as DHCEp, it seems reasonable to consider covalent modification of proteins as a contributing factor in the pathogenesis of SLOS.

Two key experiments directly correlate 7-DHC peroxidation and oxysterol formation to protein adduction. In the first experiment, incubation of 7-DHC or 7-DHCEp in the presence of a single protein, cyt *c*, provides a similar adduction profile. Because the adduction behavior is comparable, this suggests that 7-DHC autoxidizes to form oxysterols, such as DHCEp, which subsequently modify cyt *c* (Fig. 6). In the second experiment, 7-DHC shows greater amounts of protein adduction in Dhcr7-deficient Neuro2a than in control Neuro2a cells (Fig. 7). In deficient cells, the enzyme that converts 7-DHC to cholesterol is inactivated, resulting in a buildup of oxidizable 7-DHC. Treatment with a higher concentration of *a*-7-DHC (20 µM) in control Neuro2a cells led to protein adduction (Fig. 5A), suggesting that Dhcr7 is overwhelmed under these conditions and that *a*-7-DHC is accumulating. These experiments directly correlate accumulation of 7-DHC to increased protein modification, supporting the hypothesis that these covalent modifications may be involved in the mechanism of SLOS. We will report in due course on *a*-7-DHC-adducted proteins in Neuro2a cells using our photocleavable azido-biotin pulldown protocol (21). Any differential adduction of specific proteins between Dhcr7-deficient and control Neuro2a cells may shed light on the pathogenesis of SLOS. Protein adduction by 7-DHC oxysterols may also have bearing on the progression of other diseases that show elevated levels of 7-DHC, such as X-linked dominant chondrodysplasia punctata (CDPX2), cerebrotendinous xanthomatosis (CTX), and breast cancer (8, 46, 47).

In conclusion, the general strategy of using alkynyl probes in conjunction with click biotinylation and streptavidin Western blot visualization is an efficient way to assay the relative propensity of lipids to modify proteins. The rapid readout of results and ease of the azido-biotin tagging process make this an appealing approach for studying protein adduction in any system of interest. In our study of an alkynyl lipid library, *a*-7-DHC showed the greatest amount of Neuro2a protein modification, a finding that may have implications in the pathogenesis of SLOS. Current work is underway to identify and isolate any *a*-7-DHC-adducted proteins in control and Dhcr7-deficient Neuro2a cells and determine the sites of modification.▮

## REFERENCES

1. Nadolski, M. J., and M. E. Linder. 2007. Protein lipidation. *FEBS J.* **274:** 5202–5210.
2. Hang, H. C., and M. E. Linder. 2011. Exploring protein lipidation with chemical biology. *Chem. Rev.* **111:** 6341–6358.
3. Resh, M. D. 2012. Targeting protein lipidation in disease. *Trends Mol. Med.* **18:** 206–214.
4. Triola, G., H. Waldmann, and C. Hedberg. 2012. chemical biology of lipidated proteins. *ACS Chem. Biol.* **7:** 87–99.
5. Nes, W. D. 2011. Biosynthesis of cholesterol and other sterols. *Chem. Rev.* **111:** 6423–6451.
6. Xu, L., T. A. Davis, and N. A. Porter. 2009. Rate constants for peroxidation of polyunsaturated fatty acids and sterols in solution and in liposomes. *J. Am. Chem. Soc.* **131:** 13037–13044.
7. Tint, G. S., M. Seller, R. Hughes-Benzie, A. K. Batta, S. Shefer, D. Genest, M. Irons, E. Elias, and G. Salen. 1995. Markedly increased tissue concentrations of 7-dehydrocholesterol combined with low levels of cholesterol are characteristic of the Smith-Lemli-Opitz syndrome. *J. Lipid Res.* **36:** 89–95.
8. Porter, F. D., and G. E. Herman. 2011. Malformation syndromes caused by disorders of cholesterol synthesis. *J. Lipid Res.* **52:** 6–34.
9. Kelley, R. I., and R. C. M. Hennekam. 2000. The Smith-Lemli-Opitz syndrome. *J. Med. Genet.* **37:** 321–335.
10. Lee, R. W. Y., and E. Tierney. 2011. Hypothesis: the role of sterols in autism spectrum disorder. *Autism Res. Treat.* **2011:** 653570.
11. Sikora, D. M., K. Pettit-Kekel, J. Penfield, L. S. Merkens, and R. D. Steiner. 2006. The near universal presence of autism spectrum disorders in children with Smith-Lemli-Opitz syndrome. *Am. J. Med. Genet. A.* **140:** 1511–1518.
12. Gaoua, W., F. Chevy, C. Roux, and C. Wolf. 1999. Oxidized derivatives of 7-dehydrocholesterol induce growth retardation in cultured rat embryos: a model for antenatal growth retardation in the Smith-Lemli-Opitz syndrome. *J. Lipid Res.* **40:** 456–463.
13. Richards, M. J., B. A. Nagel, and S. J. Fliesler. 2006. Lipid hydroperoxide formation in the retina: correlation with retinal degeneration and light damage in a rat model of Smith-Lemli-Opitz syndrome. *Exp. Eye Res.* **82:** 538–541.
14. Valencia, A., A. Rajadurai, A. B. Carle, and I. E. Kochevar. 2006. 7-Dehydrocholesterol enhances ultraviolet A-induced oxidative stress in keratinocytes: roles of NADPH oxidase, mitochondria, and lipid rafts. *Free Radic. Biol. Med.* **41:** 1704–1718.
15. Xu, L., Z. Korade, and N. A. Porter. 2010. Oxysterols from free radical chain oxidation of 7-dehydrocholesterol: product and mechanistic studies. *J. Am. Chem. Soc.* **132:** 2222–2232.
16. Xu, L., Z. Korade, D. A. Rosado, W. Liu, C. R. Lamberson, and N. A. Porter. 2011. An oxysterol biomarker for 7-dehydrocholesterol oxidation in cell/mouse models for Smith-Lemli-Opitz syndrome. *J. Lipid Res.* **52:** 1222–1233.
17. Xu, L., W. Liu, L. G. Sheflin, S. J. Fliesler, and N. A. Porter. 2011. Novel oxysterols observed in tissues and fluids of AY9944-treated rats: a model for Smith-Lemli-Opitz syndrome. *J. Lipid Res.* **52:** 1810–1820.
18. Xu, L., Z. Korade, D. A. Rosado, K. Mirnics, and N. A. Porter. 2013. Metabolism of oxysterols derived from nonenzymatic oxidation of 7-dehydrocholesterol in cells. *J. Lipid Res.* **54:** 1135–1143.
19. Schneider, C., N. A. Porter, and A. R. Brash. 2008. Routes to 4-hydroxynonenal: fundamental issues in the mechanisms of lipid peroxidation. *J. Biol. Chem.* **283:** 15539–15543.
20. Sayre, L. M., D. Lin, Q. Yuan, X. Zhu, and X. Tang. 2006. Protein adducts generated from products of lipid oxidation: focus on HNE and ONE*. *Drug Metab. Rev.* **38:** 651–675.
21. Vila, A., K. A. Tallman, A. T. Jacobs, D. C. Liebler, N. A. Porter, and L. J. Marnett. 2008. Identification of protein targets of 4-hydroxynonenal using click chemistry for ex vivo biotinylation of azido and alkynyl derivatives. *Chem. Res. Toxicol.* **21:** 432–444.
22. Codreanu, S. G., B. Zhang, S. M. Sobecki, D. D. Billheimer, and D. C. Liebler. 2009. Global analysis of protein damage by the lipid electrophile 4-hydroxy-2-nonenal. *Mol. Cell. Proteomics.* **8:** 670–680.
23. Perluigi, M., R. Coccia, and D. A. Butterfield. 2012. 4-Hydroxy-2-nonenal, a reactive product of lipid peroxidation, and neurodegenerative diseases: a toxic combination illuminated by redox proteomics studies. *Antioxid. Redox Signal.* **17:** 1590–1609.
24. Zarkovic, K. 2003. 4-Hydroxynonenal and neurodegenerative diseases. *Mol. Aspects Med.* **24:** 293–303.
25. Leonarduzzi, G., E. Chiarpotto, F. Biasi, and G. Poli. 2005. 4-Hydroxynonenal and cholesterol oxidation products in atherosclerosis. *Mol. Nutr. Food Res.* **49:** 1044–1049.
26. Jacobs, A. T., and L. J. Marnett. 2010. Systems analysis of protein modification and cellular responses induced by electrophile stress. *Acc. Chem. Res.* **43:** 673–683.

27. Kim, H-Y. H., K. A. Tallman, D. C. Liebler, and N. A. Porter. 2009. An azido-biotin reagent for use in the isolation of protein adducts of lipid-derived electrophiles by streptavidin catch and photorelease. *Mol. Cell. Proteomics.* **8:** 2080–2089.

28. Milne, S. B., K. A. Tallman, R. Serwa, C. A. Rouzer, M. D. Armstrong, L. J. Marnett, C. M. Lukehart, N. A. Porter, and H. A. Brown. 2010. Capture and release of alkyne-derivatized glycerophospholipids using cobalt chemistry. *Nat. Chem. Biol.* **6:** 205–207.

29. Tallman, K. A., M. D. Armstrong, S. B. Milne, L. J. Marnett, H. A. Brown, and N. A. Porter. 2013. Cobalt carbonyl complexes as probes for alkyne-tagged lipids. *J. Lipid Res.* **54:** 859–868.

30. Rostovtsev, V. V., L. G. Green, V. V. Fokin, and K. B. Sharpless. 2002. A stepwise huisgen cycloaddition process: copper(I)-catalyzed regioselective "ligation" of azides and terminal alkynes. *Angew. Chem. Int. Ed. Engl.* **41:** 2596–2599.

31. Thirumurugan, P., D. Matosiuk, and K. Jozwiak. 2013. Click chemistry for drug development and diverse chemical-biology applications. *Chem. Rev.* **113:** 4905–4979.

32. Liu, W., L. Xu, C. R. Lamberson, L. S. Merkens, R. D. Steiner, E. R. Elias, D. Haas, and N. A. Porter. 2013. Assays of plasma dehydrocholesteryl esters and oxysterols from Smith-Lemli-Opitz syndrome patients. *J. Lipid Res.* **54:** 244–253.

33. Hong, V., S. I. Presolski, C. Ma, and M. G. Finn. 2009. Analysis and optimization of copper-catalyzed azide-alkyne cycloaddition for bioconjugation. *Angew. Chem. Int. Ed. Engl.* **48:** 9879–9883.

34. McComsey, D. F., A. B. Reitz, C. A. Maryanoff, and B. E. Maryanoff. 1986. Deoxygenation of acetylenic carbinols. reduction of cobalt carbonyl adducts with borane-methyl sulfide and trifluoroacetic acid. *Synth. Commun.* **16:** 1535–1549.

35. Aluise, C. D., K. Rose, M. Boiani, M. L. Reyzer, J. D. Manna, K. Tallman, N. A. Porter, and L. J. Marnett. 2013. Peptidyl-prolyl cis/trans-isomerase A1 (Pin1) Is a target for modification by lipid electrophiles. *Chem. Res. Toxicol.* **26:** 270–279.

36. Witsch-Baumgartner, M., J. Löffler, and G. Utermann. 2001. Mutations in the human DHCR7 gene. *Hum. Mutat.* **17:** 172–182.

37. Korade, Z., A. K. Kenworthy, and K. Mirnics. 2009. Molecular consequences of altered neuronal cholesterol biosynthesis. *J. Neurosci. Res.* **87:** 866–875.

38. Liang, X., A. Nazarian, H. Erdjument-Bromage, W. Bornmann, P. Tempst, and M. D. Resh. 2001. Heterogeneous fatty acylation of Src family kinases with polyunsaturated fatty acids regulates raft localization and signal transduction. *J. Biol. Chem.* **276:** 30987–30994.

39. Ekkebus, R., S. I. van Kasteren, Y. Kulathu, A. Scholten, I. Berlin, P. P. Geurink, A. de Jong, S. Goerdayal, J. Neefjes, A. J. R. Heck, et al. 2013. On terminal alkynes that can react with active-site cysteine nucleophiles in proteases. *J. Am. Chem. Soc.* **135:** 2867–2870.

40. Cygan, N. K., J. C. Scheinost, T. D. Butters, and P. Wentworth. 2011. Adduction of cholesterol 5,6-secosterol aldehyde to membrane-bound myelin basic protein exposes an immunodominant epitope. *Biochemistry.* **50:** 2092–2100.

41. Nieva, J., A. Shafton, L. J. Altobell, S. Tripuraneni, J. K. Rogel, A. D. Wentworth, R. A. Lerner, and P. Wentworth. 2008. Lipid-derived aldehydes accelerate light chain amyloid and amorphous aggregation. *Biochemistry.* **47:** 7695–7705.

42. Zhang, Q., E. T. Powers, J. Nieva, M. E. Huff, M. A. Dendle, J. Bieschke, C. G. Glabe, A. Eschenmoser, P. Wentworth, R. A. Lerner, et al. 2004. Metabolite-initiated protein misfolding may trigger Alzheimer's disease. *Proc. Natl. Acad. Sci. USA.* **101:** 4752–4757.

43. Bosco, D. A., D. M. Fowler, Q. Zhang, J. Nieva, E. T. Powers, P. Wentworth, Jr., R. A. Lerner, and J. W. Kelly. 2006. Elevated levels of oxidized cholesterol metabolites in Lewy body disease brains accelerate alpha-synuclein fibrilization. *Nat. Chem. Biol.* **2:** 249–253.

44. Korade, Z., L. Xu, R. Shelton, and N. A. Porter. 2010. Biological activities of 7-dehydrocholesterol-derived oxysterols: implications for Smith-Lemli-Opitz syndrome. *J. Lipid Res.* **51:** 3259–3269.

45. Xu, L., K. Mirnics, A. B. Bowman, W. Liu, J. Da, N. A. Porter, and Z. Korade. 2012. DHCEO accumulation is a critical mediator of pathophysiology in a Smith-Lemli-Opitz syndrome model. *Neurobiol. Dis.* **45:** 923–929.

46. Payré, B., P. de Medina, N. Boubekeur, L. Mhamdi, J. Bertrand-Michel, F. Tercé, I. Fourquaux, D. Goudounèche, M. Record, M. Poirot, et al. 2008. Microsomal antiestrogen-binding site ligands induce growth control and differentiation of human breast cancer cells through the modulation of cholesterol metabolism. *Mol. Cancer Ther.* **7:** 3707–3718.

47. de Sain-van der Velden, M. G. M., A. Verrips, B. H. C. M. T. Prinsen, M. de Barse, R. Berger, and G. Visser. 2008. Elevated cholesterol precursors other than cholestanol can also be a hallmark for CTX. *J. Inherit. Metab. Dis.* **31(Suppl. 2):** S387–S393.

# SUPPLEMENTARY DATA


# Probing lipid-protein adduction with alkynyl surrogates: application to Smith-Lemli-Opitz syndrome

Katherine Windsor*, Thiago C. Genaro-Mattos*§, Hye-Young H. Kim*‡, Wei Liu*, Keri A. Tallman*, Sayuri Miyamoto§, Zeljka Korade**‖, Ned A. Porter*†‖[1]


Department of Chemistry*, Department of Biochemistry‡, Department of Psychiatry**, Vanderbilt Institute of Chemical Biology†, Vanderbilt Kennedy Center for Research on Human Development‖, Vanderbilt University, Nashville, Tennessee 37235

Departamento de Bioquímica§, Instituto de Química, Universidade de São Paulo, São Paulo, SP, Brazil


[1]**Corresponding Author**: Ned A. Porter, PhD, Chemistry Department, 7962 Stevenson Center, Vanderbilt University, Nashville, TN 37235, Phone: 615-343-2693, Fax: 615-343-7262, Email: n.porter@vanderbilt.edu
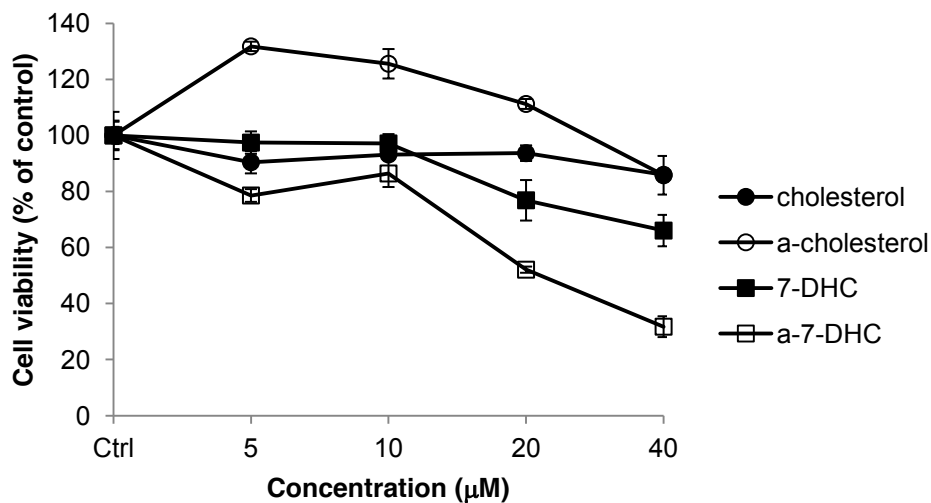
Figure S1. Cellular toxicities of *a*-7-DHC and *a*-Chol and their naturally-occurring analogues. Neuro2a cells were grown in the presence of different concentrations of 7-DHC, *a*-7-DHC, cholesterol, or *a*-Chol for 24 h. The *x*-axis shows concentration of compounds and the *y*-axis shows the percentage of live cells compared to DMSO-treated control cells. The bars are standard errors.
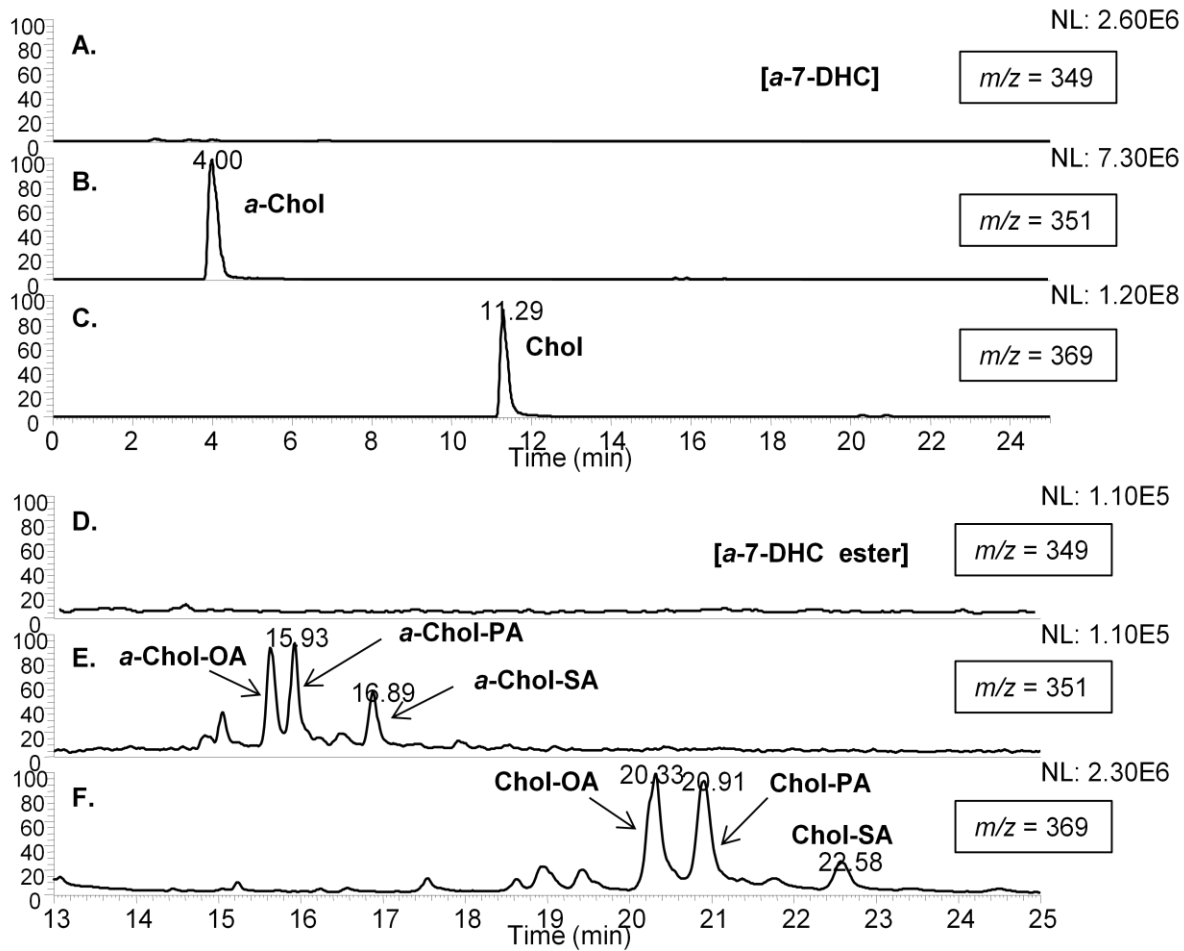
Figure S2. Incorporation and metabolism of *a*-Chol in Neuro2a cells. Neuro2a cells were incubated in the presence of 2.5 μM *a*-Chol for 24 h in 2% FBS DMEM. Free sterols and sterol esters were analyzed by HPLC-MS operated in SRM mode. A-C: Chromatograms showing free sterols. D-F: Chromatograms showing sterol esters (expansions of A-C, respectively). A and D: Molecules that fragment to give an ion with $m/z$ = 349, *a*-7-DHC and its esters. B and E: Molecules that fragment to give an ion with $m/z$ = 351, *a*-Chol and its esters (OA=oleate; PA=palmitate; SA=stearate). C and F: Molecules that fragment to give $m/z$ = 369, cholesterol and its esters.
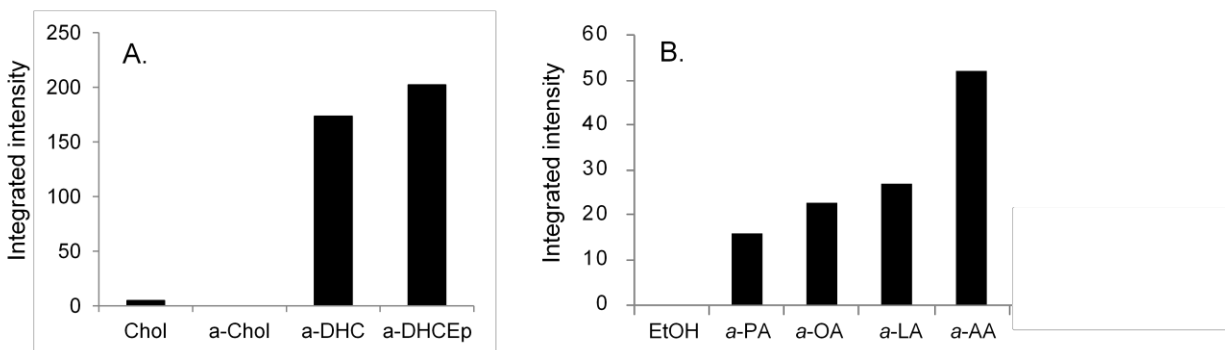
Figure S3. Integrated intensities from western blot analysis of Neuro2a protein adduction with alkynyl lipids. Alkynyl lipid-adducted proteins were ligated with biotin via click reaction and labeled with the streptavidin-AlexaFluor 680 conjugate. The fluorophore was detected and integrated intensities were obtained using the Odyssey Infrared Imaging System and Application Software. For each western blot, the lane with the lowest integrated intensity was set to 0. A: Comparison of Neuro2a proteome modification by alkynyl sterols. B: Comparison of Neuro2a proteome modification by alkynyl fatty acids.
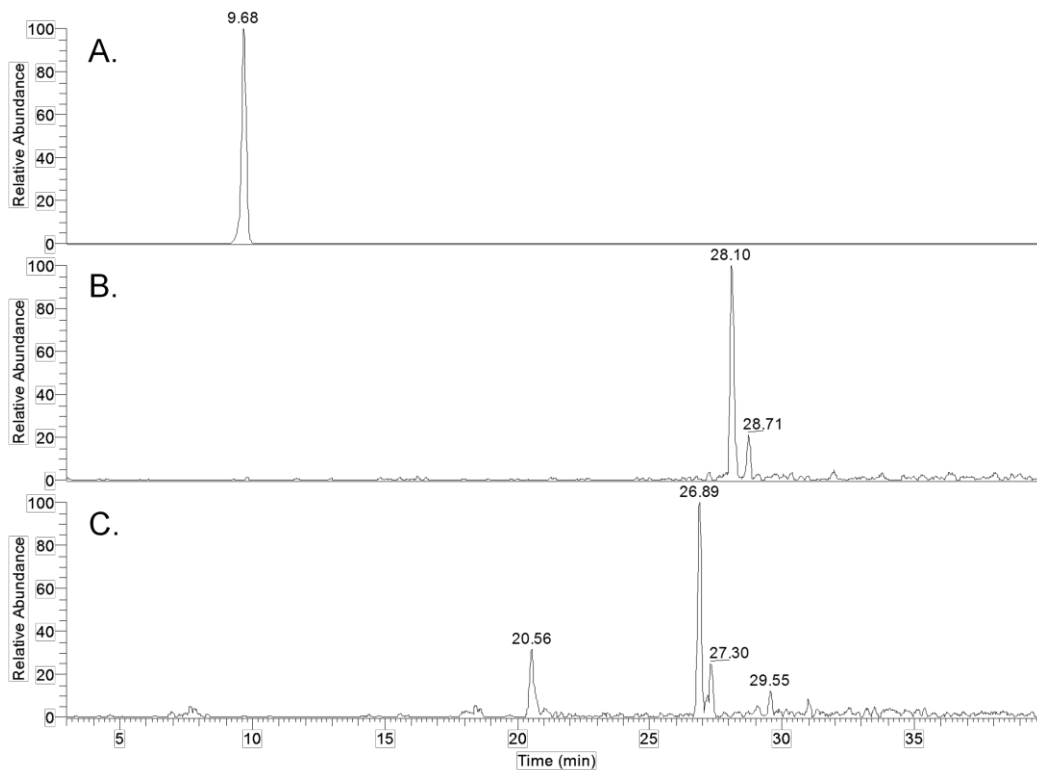
Figure S4. Reaction of AcTpepK (Ac-AVAGKAGAR) with 7-DHCEp and its alkynyl analog *a*-DHCEp. The peptide (1 mM) was incubated in the presence of the electrophile (5 mM) at 37 °C for 1 h. The reaction mixture was then reduced with NaBH$_4$, neutralized, and analyzed by RP-HPLC-MS. Extracted ion chromatograms of A: AcTpepK ([M + 2H]$^{2+}$ = 422) at 9.7 min. B: Peptide adduct with 7-DHCEp ([M + 2H]$^{2+}$ = 622) at 28.1 min. C: Peptide adduct with *a*-7-DHCEp ([M + 2H]$^{2+}$ = 613) at 26.9 min.

**CellTiter 96® AQueous One Solution Cell Proliferation Assay**

The CellTiter 96® Aqueous One Solution contains a tetrazolium compound [3-(4,5-dimethylthiazol-2-yl)-5-(3-carboxymethoxyphenyl)-2-(4-sulfophenyl)-2H-tetrazolium, inner salt; MTS] and an electron coupling reagent (phenazine ethosulfate; PES). The MTS tetrazolium compound (Owen's reagent) is bioreduced by cells into a colored formazan product that is soluble in tissue culture medium. This conversion is presumably accomplished by NADPH or NADH produced by dehydrogenase enzymes in metabolically active cells. Assays are performed by adding a small amount of the CellTiter 96® AQueous One Solution Reagent directly to culture wells, incubating for 1–4 h and then recording the absorbance at 490 nm with a SPECTRA Fluor Plus plate reader (Tecan, Austria). The quantity of formazan product as measured by the absorbance at 490 nm is directly proportional to the number of living cells in culture.

## Synthetic procedures

*Preparation of alkynyl sterols*

Scheme S1.  Synthesis of *a*-Chol
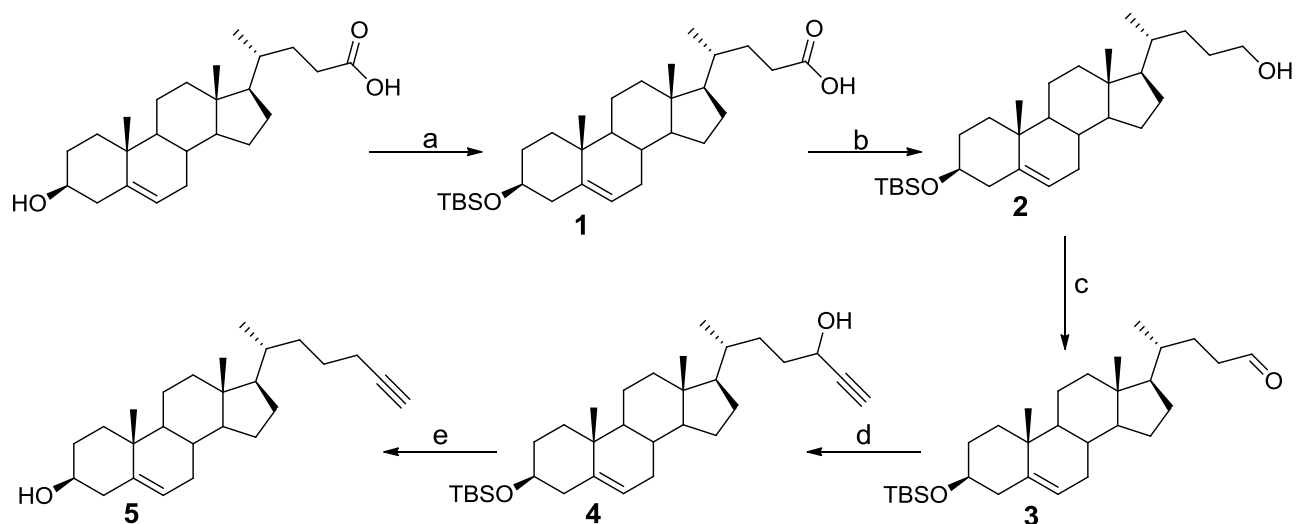


Reagents:  a) TBDMSCl, im, DMAP, DMF; b) LiAlH$_4$, THF; c) PCC, silica gel, CH$_2$Cl$_2$; d) ethynyl magnesium bromide, THF; e) i. Co$_2$(CO)$_8$, CH$_2$Cl$_2$, ii. BH$_3$-Me$_2$S, TFA, iii. Fe(NO$_3$)$_3$, CH$_3$CN/MeOH.

*Synthesis of TBS-cholenic acid* **1** (1).  Imidazole (0.445 g, 6.54 mmol), DMAP (0.200 g, 1.64 mmol), and TBSCl (0.370 g, 2.45 mmol) were added to a solution of 3β-hydroxy-5-cholenic acid (0.305 g, 0.814 mmol) in DMF (7 mL) at 0 °C.  After stirring overnight at room temperature, the reaction was quenched with 1 M HCl (5 mL) and extracted with EtOAc.  The organic layer was washed with brine and dried over MgSO$_4$.  The product was used in the next step without purification.  To a solution of the crude product in MeOH (7 mL) and THF (7 mL) was added a solution of K$_2$CO$_3$ (10% w/w, 4 mL) in water.  After stirring for 1 h, the reaction mixture was concentrated under reduced pressure to remove excess THF and MeOH.  Brine was added.  The solution was acidified to pH 3 with 1 M HCl and extracted with EtOAc.  The organic layer was dried over MgSO$_4$, and the product was isolated as a white solid (0.373 g, 94%).  The NMR data

was consistent with published data. $^1$H NMR (CDCl$_3$) δ 5.33-5.30 (m, 1H), 3.48 (app septet, 1H, J = 4.8 Hz), 2.45-2.35 (m, 1H), 2.31-2.21 (m, 2H), 2.20-2.13 (m, 1H), 2.03-1.93 (m, 2H), 1.91-1.67 (m, 4H), 1.64-1.24 (m, 10H), 1.20-0.96 (m, 4H), 1.00 (s, 3H), 0.94 (d, 3H, J = 6.5 Hz), 0.89 (s, 9H), 0.68 (s, 3H), 0.056 (s, 6H); $^{13}$C NMR (CDCl$_3$) δ 180.3, 141.8, 121.3, 72.9, 57.0, 56.0, 50.4, 43.0, 42.6, 40.0, 37.6, 36.8, 35.5, 32.3, 32.1 (×2), 31.2, 31.0, 28.3, 26.2 (×3), 24.5, 21.3, 19.6, 18.51, 18.50, 12.1, −4.4 (×2).

*Synthesis of TBS-cholenol* **2** (2). A solution of **1** (0.341 g, 0.698 mmol) in THF (20 mL) was added dropwise to a slurry of LiAlH$_4$ (0.106 g, 2.79 mmol) in THF (5 mL) at 0 °C. The reaction mixture was allowed to warm to room temperature and stirred for 1.5 h. At 0 °C, the reaction is quenched with successive dropwise addition of 106 µL of water, 106 µL of 15% NaOH solution, and 318 µL of water. After 1 h, the granular salt is filtered off. The filtrate is dried over MgSO$_4$. Purification by column chromatography (10-20% EtOAc/hexanes) afforded the product as a white solid (0.260 g, 78%). The NMR data was consistent with published data. $^1$H NMR (CDCl$_3$) δ 5.34-5.30 (m, 1H), 3.61 (m, 2H), 3.48 (app septet, 1H, J = 4.7 Hz), 2.31-2.22 (m, 1H), 2.16 (ddd, 1H, J = 13.3, 5.0, 2.1 Hz), 2.03-1.92 (m, 2H), 1.89-1.77 (m, 2H), 1.75-1.37 (m, 12H), 1.32-0.96 (m, 8H), 1.00 (s, 3H), 0.94 (d, 3H, J = 6.5 Hz), 0.89 (s, 9H), 0.68 (s, 3H), 0.056 (s, 6H); $^{13}$C NMR (CDCl$_3$) δ 141.5, 121.1, 72.6, 63.5, 56.7, 55.9, 50.1, 42.7, 42.3, 39.7, 37.3, 36.5, 35.5, 32.0, 31.9, 31.83, 31.77, 29.3, 28.2, 25.9 (×3), 24.2, 21.0, 19.4, 18.6, 18.2, 11.8, −4.7 (×2); HRMS (ESI) calculated 497.3785 (M + Na), observed 497.3763.

*Synthesis of TBS-aldehyde* **3**. A solution of alcohol **2** (0.300 g, 0.632 mmol) in CH$_2$Cl$_2$ (3 mL) was added slowly to a slurry of PCC (0.204 g, 0.946 mmol) and silica gel (0.20 g) in CH$_2$Cl$_2$ (7 mL) at 0 °C. The reaction was stirred at room temperature for 2 h. The dark brown reaction

mixture was filtered through a silica gel plug and rinsed with additional $CH_2Cl_2$. The aldehyde was isolated as an off-white solid (0.265 g, 89%) and used without further purification. The NMR data was consistent with published data (2). ^{1}H NMR (CDCl$_3$) δ 9.77 (t, 1H, J = 1.9 Hz), 5.34-5.30 (m, 1H), 3.53-3.44 (app septet, 1H, J = 4.7 Hz), 2.51-2.41 (m, 1H), 2.40-2.23 (m, 2H), 2.17 (ddd, 1H, J = 13.3, 5.0, 2.1 Hz), 2.03-1.93 (m, 2H), 1.91-1.68 (m, 4H), 1.65-1.39 (m, 8H), 1.39-1.25 (m, 2H), 1.22-0.95 (m, 5H), 1.00 (s, 3H), 0.93 (d, 3H, J = 6.6 Hz), 0.89 (s, 9H), 0.68 (s, 3H), 0.061 (s, 6H); ^{13}C NMR (CDCl$_3$) δ 203.4, 141.8, 121.3, 72.8, 57.0, 56.0, 50.4, 43.0, 42.6, 41.2, 40.0, 37.6, 36.8, 35.6, 32.3, 32.1 (×2), 28.4, 28.2, 26.2 (×3), 24.5, 21.3, 19.6, 18.6, 18.5, 12.1, −4.4 (×2); HRMS (ESI) calculated 495.3629 (M + Na), observed 495.3613.

*Synthesis of TBS-24-hydroxy-aChol* **4**. A solution of aldehyde **3** (0.610 g, 1.29 mmol) in THF (10 mL) was added slowly to a solution of ethynylmagnesium bromide (3.40 mL of 0.5 M in THF, 1.7 mmol) in THF (3 mL) at 0 °C. After stirring at 0 °C for 30 min, the reaction was allowed to stir overnight at room temperature. The reaction was quenched with saturated NH$_4$Cl and extracted with EtOAc. The organic layer was washed with water and brine and dried over MgSO$_4$. The product was purified by column chromatography (5% EtOAc/hexanes) and isolated as a white solid (0.623 g, 97%). ^{1}H NMR (CDCl$_3$) δ 5.33-5.29 (m, 1H), 4.33 (app q, 1H, J = 5.9 Hz), 3.48 (app septet, 1H, J = 4.8 Hz), 2.46 (t, 1H, J = 2.2 Hz), 2.31-2.22 (m, 1H), 2.20-2.13 (m, 1H), 2.04-1.92 (m, 3H), 1.91-1.37 (m, 15H), 1.35-0.91 (m, 7H), 1.00 (s, 3H), 0.94 (d, 3H, J = 6.6 Hz), 0.89 (s, 9H), 0.68 (s, 3H), 0.057 (s, 6H); ^{13}C NMR (CDCl$_3$) δ 141.5, 121.1, 85.1, 85.0, 72.8, 72.7, 72.6, 62.7, 62.6, 56.7, 55.7, 50.1, 42.7, 42.3, 39.7, 37.3, 36.5, 35.3, 35.2, 34.2, 34.1, 32.0, 31.8, 31.8, 31.0, 30.9, 28.1, 25.9 (×3), 24.2, 21.0, 19.4, 18.6, 18.6, 18.2, 11.8, −4.7 (×2); HRMS (ESI) calculated 521.3785 (M + Na), observed 521.3801.

*Synthesis of a-Chol* **5**. $Co_2(CO)_8$ (0.630 g, 1.84 mmol) was added to a solution of propargyl alcohol **4** (0.832 g, 1.67 mmol) in $CH_2Cl_2$ (8.3 mL). After stirring for 2 h, the reaction was cooled to 0 °C. Borane dimethyl sulfide (2.00 mL, 1.0 M in $CH_2Cl_2$, 2.00 mmol) was added via syringe. After stirring at 0 °C for 5 min, TFA (0.830 mL) was added via syringe. The reaction was allowed to stir for 30 min at 0 °C, then quenched with water (8.3 mL). After stirring for 15 min, the organic layer was separated off, washed with water, and concentrated under reduced pressure. The brownish-red residue was redissolved in $CH_2Cl_2$/MeOH (1:1, 10 mL total). Ferric nitrate (3.373 g, 8.35 mmol) was added, and the reaction was allowed to stir for 5 h to enable decomplexation and complete TBS deprotection. The reaction mixture was diluted with $CH_2Cl_2$, washed with 0.1 M HCl and brine, and dried over $MgSO_4$. Purification by column chromatography (5-10% EtOAc/hexanes) afforded the white solid product (0.430 g) in 70% yield. $^1H$ NMR ($CDCl_3$) δ 5.37-5.33 (m, 1H), 3.53 (m, 1H), 2.33-2.08 (m, 4H), 2.04-1.94 (m, 2H), 1.94 (t, 1H, $J$ = 2.6 Hz), 1.89-1.79 (m, 3H), 1.67-1.36 (m, 12H), 1.33-1.22 (m, 1H), 1.20-0.95 (m, 6H), 1.01 (s, 3H), 0.93 (d, 3H, $J$ = 6.5 Hz), 0.68 (s, 3H); $^{13}C$ NMR ($CDCl_3$) δ 140.7, 121.6, 84.8, 71.7, 68.0, 56.7, 55.9, 50.0, 42.3, 42.2, 39.7, 37.2, 36.4, 35.3, 35.0, 31.8 (×2), 31.6, 28.1, 25.1, 24.2, 21.0, 19.3, 18.7, 18.6, 11.8; HRMS (ESI) calculated 391.2971 (M + Na), observed 391.2956.

Scheme S2. Synthesis of 7-keto-*a*-Chol, *a*-7-DHC, and *a*-DHCEp
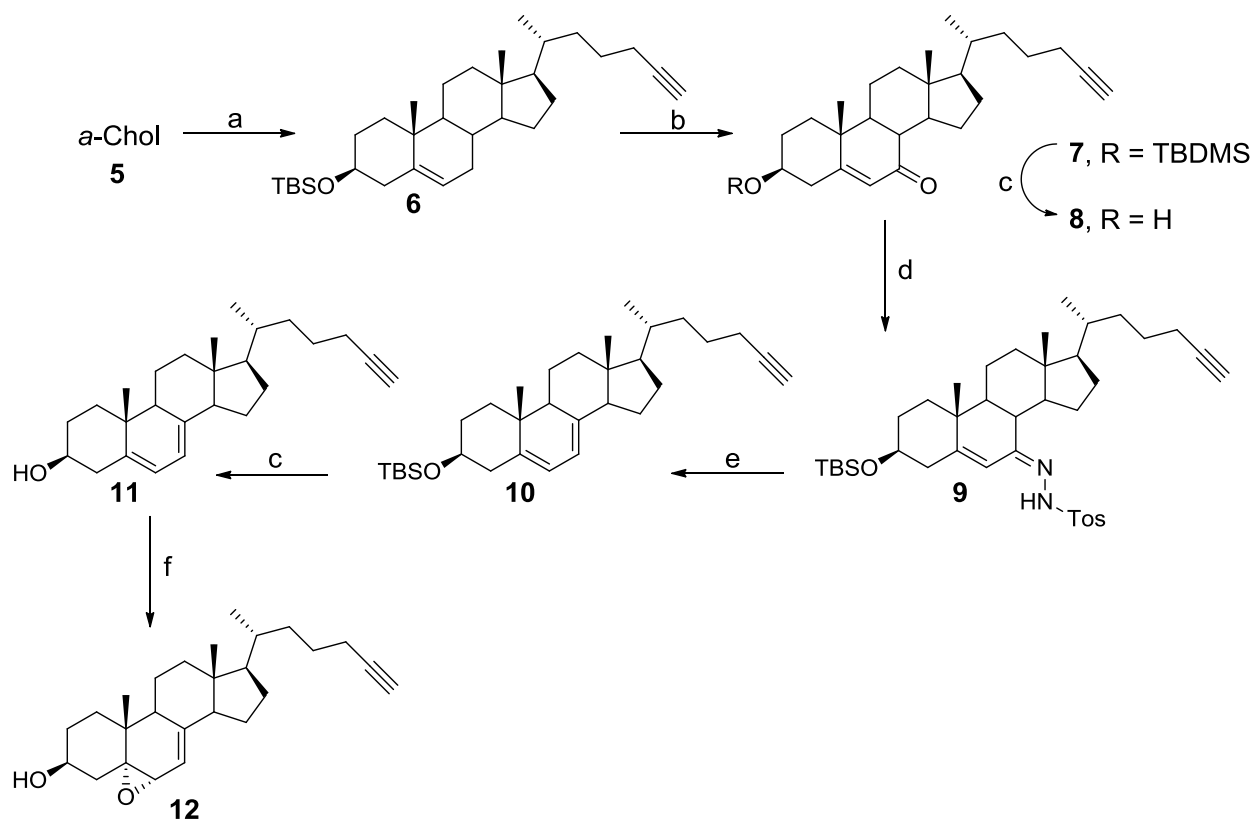


Reagents: a) TBDMSCl, im, DMF; b) CrO₃, pyr, CH₂Cl₂; c) TBAF, THF; d)Tosylhydrazide, THF, reflux; e) NaH, toluene, 100 °C; f) *m*CPBA, Na₂CO₃, CH₂Cl₂/H₂O.

*Synthesis of TBS-a-Chol* **6**. TBDMSCl (0.60 g, 4.0 mmol) and imidazole (0.60 g, 8.8 mmol) were added to a solution of *a*-Chol (1.2 g, 3.3 mmol) in DMF (8 mL). After 1 h, the reaction mixture was diluted with EtOAc and washed with H₂O and brine. The organics were dried over MgSO₄, filtered, and concentrated. The product was purified by column chromatography (10% EtOAc/hexanes) and isolated as a white powder (1.2 g, 78%). ¹H NMR (CDCl₃) δ 5.30-5.28 (m, 1H), 3.45 (app septet, 1H, J = 5.0 Hz), 2.29-2.18 (m, 1H), 2.17-2.09 (m, 3H), 2.00-1.96 (m, 2H), 1.91 (t, 1H, J = 2.6 Hz), 1.85-1.66 (m, 4H), 1.57-1.39 (m, 10H), 1.26-1.01 (m, 7H), 0.97 (s, 3H), 0.90 (d, 3H, J = 6.5 Hz), 0.87 (s, 9H), 0.65 (s, 3H), 0.030 (s, 6H); ¹³C NMR (CDCl₃) δ 141.5, 121.1, 84.8, 72.6, 68.0, 56.7, 55.9, 50.1, 42.8, 42.3, 39.7, 37.3, 36.5, 35.3, 35.1, 32.0, 31.9, 28.1,

25.9, 25.1, 24.2, 21.0, 19.4, 18.8, 18.6, 18.2, 11.8, -4.6; HRMS (ESI) calculated 505.38.3 (M + Na), observed 505.3856.

*Synthesis of TBS-7-keto-a-Chol* **7**.  Pyridine (13 mL, 160 mmol) was added to a suspension of CrO$_3$ (6.5 g, 65 mmol) in CH$_2$Cl$_2$ (90 mL).  After 10 min, a solution of **6** (1.2 g, 2.5 mmol) in CH$_2$Cl$_2$ (10 mL) was added.  After the reaction was allowed to stir overnight, it was diluted with EtOAc and filtered through a pad of Celite.  The filtrate was sequentially washed with H$_2$O, 10% HCl, saturated NaHCO$_3$, brine, and dried over MgSO$_4$.  Purification by column chromatography (5% EtOAc/hexanes) yielded the product as a white powder (0.74 g, 59%).  $^1$H NMR (CDCl$_3$) δ 5.63 (d, 1H, J = 1.0 Hz), 3.56 (app septet, 1H, J = 5.3 Hz), 2.40-2.35 (m, 3H), 2.20 (t, 1H, J = 11.6 Hz), 2.11 (app septet, 2H, J = 3.6 Hz), 2.01-1.95 (m, 1H), 1.90 (t, 1H, J = 2.6 Hz), 1.85-1.72 (m, 2H), 1.58-1.04 (m, 16H), 1.15 (s, 3H), 0.90 (d, 3H, J = 6.5 Hz), 0.85 (s, 9H), 0.64 (s, 3H), 0.028 (s, 6H); $^{13}$C NMR (CDCl$_3$) δ 202.3, 165.8, 125.7, 84.7, 71.3, 68.1, 54.5, 49.9, 45.3, 43.0, 42.5, 38.6, 38.3, 36.4, 35.2, 35.1, 31.7, 28.4, 26.2, 25.8, 25.1, 21.1, 18.8, 18.1, 17.2, 11.9, -4.7; HRMS (ESI) calculated  497.3809 (M + H), observed 497.3785.

*Synthesis of 7-keto-a-Chol* **8**.  TBAF (0.30 mL, 0.30 mmol) was added to a solution of **7** (0.11 g, 0.22 mmol) in THF (1 mL).  After 1 h, the reaction mixture was diluted with EtOAc and washed with H$_2$O, brine, and dried over MgSO$_4$.  The product was purified by column chromatography (30 to 40% EtOAc/hexanes) and isolated as a white powder (65 mg, 76%).  $^1$H NMR (CDCl$_3$) δ 5.64 (d, 1H, J = 1.5 Hz), 3.62 (m, 1H), 2.56 (br s, 1H), 2.50-2.43 (m, 1H), 2.40-2.31 (m, 2H), 2.19 (t, 1H, J = 11.1 Hz), 2.10 (app septet, 2H, J = 3.4 Hz), 2.00-1.84 (m, 4H), 1.90 (t, 1H, J = 2.6 Hz), 1.60-1.20 (m, 12H), 1.15 (s, 3H), 1.13-1.03 (m, 3H), 0.89 (d, 3H, J = 6.5 Hz), 0.64 (s, 3H); $^{13}$C NMR (CDCl$_3$) δ 202.4, 165.6, 125.9, 84.8, 70.3, 68.1, 54.5, 49.9, 49.8, 45.3, 43.1, 41.8,

38.6, 38.2, 36.3, 35.2, 35.0, 31.0, 28.4, 26.2, 25.1, 21.1, 18.7, 17.3, 11.9; HRMS (ESI) calculated 383.2945 (M + H), observed 383.2927.

*Synthesis of hydrazone* **9**.   4-Toluenesulfonyl hydrazide (0.41 g, 2.2 mmol) was added to a solution of the ketone **8** (0.74 g, 1.5 mmol) in THF (4 mL), then the reaction mixture was heated to reflux.  After 6 h, the reaction mixture was cooled and concentrated.  Purification by column chromatography (10% EtOAc/hexanes) yielded the product as a white foam (0.85 g, 86%).  $^1$H NMR (CDCl$_3$) δ 7.89 (br s, 1H), 7.81 (d, 2H, J = 8.2 Hz), 7.25 (d, 2H, J = 8.2 Hz), 5.95 (s, 1H), 3.44 (app septet, 1H, J = 5.4 Hz), 2.39 (s, 3H), 2.35-2.10 (m, 5H), 1.92 (t, 1H, J = 2.6 Hz), 1.84-1.36 (m, 12H), 1.23-1.09 (m, 8H), 1.01 (s, 3H), 0.89 (d, 3H, J = 6.4 Hz), 0.81 (s, 9H), 0.60 (s, 3H), -0.04 (s, 6H); $^{13}$C NMR (CDCl$_3$) δ 157.6, 157.1.43.6, 135.6, 129.2, 128.2, 112.6, 84.8, 71.8, 68.1, 54.5, 50.1, 49.6, 42.8, 42.6, 39.3, 38.6, 38.4, 36.4, 35.2, 35.2, 31.6, 28.3, 26.7, 25.8, 25.2, 21.6, 20.7, 18.9, 18.8, 18.0, 17.9, 12.2, -4.7, -4.8; HRMS (ESI) calculated 665.4167 (M + H), observed 665.4180.

*Synthesis of TBS-a-7-DHC* **10**.  NaH was washed with hexanes several times.  The hexanes was decanted and the NaH dried under vacuum.  A solution of the hydrazone **9** (0.85 g, 1.3 mmol) in toluene (6 mL) was added to a suspension of NaH (0.30 g, 13 mmol) in toluene (6 mL), then the reaction mixture was heated to 100 °C.  After 30 min, the reaction mixture was cooled and quenched with H$_2$O.  The mixture was extracted with EtOAc, and the organic layer washed with brine and dried over MgSO$_4$.  The product was purified by column chromatography (5% EtOAc/hexanes) and isolated as a white foam (0.35 g, 58%).  The ketone (0.18 g), which resulted from hydrolysis of the hydrazone, was also recovered.  $^1$H NMR (CDCl$_3$) δ 5.53 (d, 1H, J = 5.5 Hz), 5.36 (dt, 1H, J = 2.5, 5.2 Hz), 3.57 (m, 1H), 2.30 (d, 2H, J = 7.8 Hz), 2.17-2.02 (m, 4H),

1.92 (t, 1H, J = 2.6 Hz), 1.85-1.12 (m, 18H), 0.93 (d, 3H, J = 6.5 Hz), 0.91 (s, 3H), 0.87 (s, 9H), 0.59 (s, 3H), 0.045 (s, 6H); $^{13}$C NMR (CDCl$_3$) δ 141.0, 140.7, 119.2, 116.3, 84.7, 71.2, 68.1, 55.6, 54.4, 46.3, 42.9, 41.3, 39.2, 38.5, 37.0, 35.7, 35.0, 32.4, 29.7, 28.0, 25.9, 25.1, 23.0, 21.1, 18.8, 18.2, 16.3, 11.8, -4.6.

*Synthesis of a-7-DHC* **11**.  TBAF (1.0 mL, 1.0 mmol) was added to a solution of **10** (0.35 g, 0.73 mmol) in THF (4 mL).  After 3 h, the reaction mixture was diluted with EtOAc and washed with H$_2$O, brine, and dried over MgSO$_4$.  The product was purified by column chromatography (20% EtOAc/hexanes) and isolated as a white powder (0.16 g, 60%).  $^1$H NMR (CDCl$_3$) δ 5.54 (dd, 1H, J = 2.3, 5.6 Hz), 5.36 (dt, 1H, J = 2.6, 5.4 Hz), 3.60 (m, 1H), 2.44 (ddd, 1H, J = 1.9, 4.5, 14.3 Hz), 2.30-2.20 (m, 1H), 2.16-2.02 (m, 4H), 1.92 (t, 1H, J = 2.6 Hz), 1.88-1.82 (m, 5H), 1.72-1.15 (m, 14H), 0.92 (d, 3H, J = 7.1 Hz), 0.91 (s, 3H), 0.59 (s, 3H); $^{13}$C NMR (CDCl$_3$) δ 141.2, 139.8, 119.5, 116.3, 84.8, 70.3, 68.1, 55.6, 54.4, 46.2, 42.9, 40.7, 39.1, 38.3, 36.9, 35.7, 35.0, 31.9, 28.0, 25.1, 23.0, 21.0, 18.8, 16.2, 11.8; HRMS (ESI) calculated  405.2554 (M + K), observed 405.2550.

*Synthesis of a-DHCEp* **12**.  A solution of *m*CPBA (38 mg, 0.22 mmol) in CH$_2$Cl$_2$ (1.5 mL) was added dropwise to a vigorously stirred solution of **11** (62 mg, 0.17 mmol) and Na$_2$CO$_3$ (36 mg, 0.34 mmol) in a mixture of CH$_2$Cl$_2$ and H$_2$O (3 mL, 1:1).  After 15 min, the reaction was quenched with saturated Na$_2$SO$_3$ and extracted with EtOAc.  The organic layer was washed with saturated NaHCO$_3$, brine, and dried over MgSO$_4$.  The product was purified by column chromatography (50% EtOAc/hexanes) and isolated as a white foam (52 mg, 80%).  $^1$H NMR (CDCl$_3$) δ 5.40 (dt, 1H, J = 2.8, 3.9 Hz), 3.92 (m, 1H), 2.97 (d, 1H, J = 4.1 Hz), 2.26-2.18 (m, 2H), 2.12 (app septet, 2H, J = 3.5 Hz), 2.04-1.94 (m, 2H), 1.91 (t, 1H, J = 2.6 Hz), 1.89-1.82 (m,

3H), 1.82-1.18 (m, 16H), 0.98 (s, 3H), 0.89 (d, 3H, J = 6.5 Hz), 0.51 (s, 3H); $^{13}$C NMR (CDCl$_3$)

δ 147.8, 114.8, 84.7, 68.3, 68.1, 66.9, 55.5, 54.5, 53.9, 42.2, 41.3, 39.7, 38.7, 35.6, 34.9, 33.4,

31.1, 27.6, 25.1, 23.1, 20.9, 18.73, 18.67, 16.4, 11.7; HRMS (ESI) calculated 405.2764 (M +

Na), observed 405.2762.

*Preparation of alkynyl fatty acids and phospholipids.*

Scheme S3.  Synthesis of TBS-nonynal for aOA.
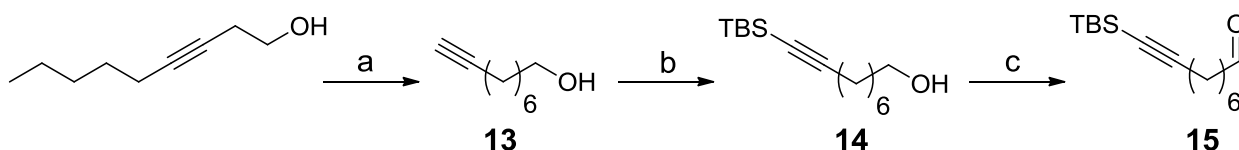


Reagents:  a) NaH, 1,3-diaminopropane; b) i. *n*BuLi, TBSCl, THF; ii. HOAc/H$_2$O; c) PCC, CH$_2$Cl$_2$.

Scheme S4.  Synthesis of alkynyl oleic acid.
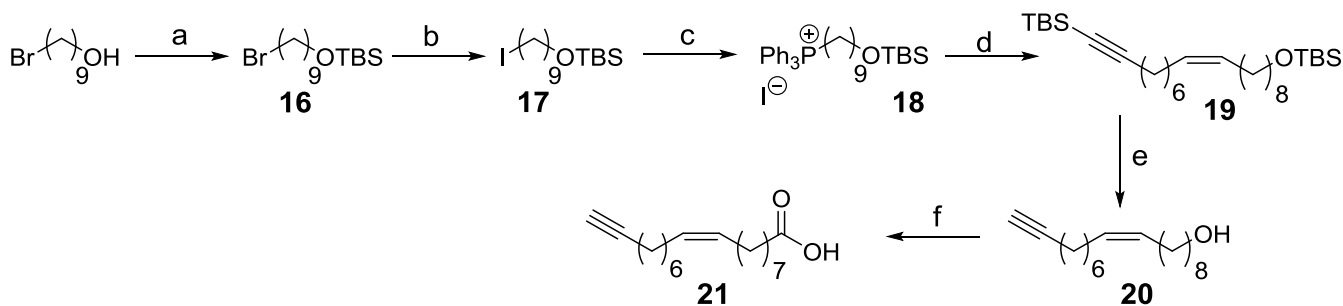


Reagents:  a) TBSCl, im, THF; b) NaI, acetone, reflux; c) PPh$_3$, CH$_3$CN, reflux; d) *n*BuLi, THF/HMPA, **15**; e) TBAF, THF; f) i. Dess-Martin periodinane, ii. Jones oxidation.

*Synthesis of 8-nonyn-1-ol **13** (3).*  1,2-Diaminopropane (70 mL) was added slowly to NaH (3.6 g,

0.15 mol), then heated to 70 °C.  The NaH was washed with hexanes several times and then

dried under vacuum prior to use.  After 1 h, 3-nonyn-1-ol (4.0 g, 0.029 mol) was added and the

temperature lowered to 55 °C. After overnight, the reaction mixture was cooled, cautiously quenched with $H_2O$, and extracted with ether. The organic layer was washed with 10% HCl, brine, and dried over $MgSO_4$. The product (3.11 g) was isolated in 78% yield as an orange liquid and was of sufficient purity for the next reaction. The NMR data was consistent with published data. $^1$H NMR (CDCl$_3$) δ 3.57 (t, 2H, J = 6.6 Hz), 2.13 (dt, 2H, J = 2.6, 6.9 Hz), 1.89 (t, 1H, J = 2.6 Hz), 1.82 (br s, 1H), 1.53-1.45 (m, 4H), 1.38-1.28 (m, 6H); $^{13}$C NMR (CDCl$_3$) δ 84.6, 68.1, 62.8, 32.6, 28.8, 28.6, 28.3, 25.5, 18.3.

*Synthesis of TBS-nonynol 14*. *n*BuLi (42 mL, 2.5 M/hexanes, 0.11 mol) was added to a solution of **13** (6.4 g, 0.046 mol) in THF (100 mL) at 0 °C. After 30 min, a solution of TBSCl (15.8g, 0.10 mol) in THF (10 mL) was added. After 1 h, the reaction mixture was quenched with $H_2O$ and extracted with EtOAc. The organic layer was washed with brine, dried over $MgSO_4$, and concentrated. The crude product was resuspended in HOAc:$H_2O$ (100 mL, 2:1) and heated to 80 °C. After 1 h, the reaction mixture was cooled and extracted with toluene. The organic layer was washed with $H_2O$, saturated $NaHCO_3$, brine, and dried over $MgSO_4$. The product (7.08 g, 61%) was purified by column chromatography (20% EtOAc/hexanes) and isolated as a yellow liquid. $^1$H NMR (CDCl$_3$) δ 3.60 (t, 2H, J = 6.5 Hz), 2.19 (t, 2H, J = 6.8 Hz), 1.56-1.44 (m, 4H), 1.40-1.30 (m, 6H), 0.89 (s, 9H), 0.042 (s, 6H); $^{13}$C NMR (CDCl$_3$) δ 108.1, 82.4, 62.9, 32.6, 28.8, 28.6, 28.5, 26.1, 25.6, 19.7, 16.5, -4.5; HRMS (ESI) calculated 277.1958 (M + Na), observed 277.1932.

*Synthesis of TBS-nonynal 15*. PCC (7.20 g, 0.033 mol) was added to a solution of **14** (7.08 g, 0.028 mol) in CH$_2$Cl$_2$ (100 mL). After 1 h, the reaction mixture was diluted with ether and filtered through a pad of silica. Purification by column chromatography (10% EtOAc/hexanes)

yielded the product (5.27 g) as a colorless liquid in 75% yield. $^1$H NMR (CDCl$_3$) δ 9.73 (t, 1H, J = 1.8 Hz), 2.40 (dt, 2H, J = 1.8, 7.3 Hz), 2.20 (t, 2H, J = 6.8 Hz), 1.61 (pentet, 2H, J = 7.6 Hz), 1.49-1.23 (m, 6H), 0.89 (s, 9H), 0.044 (s, 6H); $^{13}$C NMR (CDCl$_3$) δ 202.7, 107.8, 82.5, 43.8, 28.9, 28.5, 28.3, 26.1, 21.9, 19.7, 16.5, -4.5; HRMS (ESI) calculated 275.1802 (M + Na), observed 275.1833.

*Synthesis of bromide 16* (4).   TBSCl (2.5 g, 0.017 mol) and imidazole (1.4 g, 0.021 mol) were added to a solution of 9-bromononan-1-ol (3.2 g, 0.014 mol) in THF (70 mL).   A white precipitate formed immediately.   After 3.5 h, the reaction mixture was diluted with EtOAc and washed with H$_2$O, brine, and dried over MgSO$_4$.   The product (4.69 g, 97%) was isolated a colorless liquid with no purification necessary.   The NMR data was consistent with published data.  $^1$H NMR (CDCl$_3$) δ 3.57 (t, 2H, J = 6.5 Hz), 3.38 (t, 2H, J = 6.8 Hz), 1.83 (pentet, 2H, J = 6.9 Hz), 1.50-1.46 (m, 2H), 1.42-1.37 (m, 2H), 1.35-1.27 (m, 8H), 0.87 (s, 9H), 0.023 (s, 6H); $^{13}$C NMR (CDCl$_3$) δ 63.2, 34.0, 32.8, 29.4, 29.3, 28.7, 28.1, 25.9, 25.7, 18.3, -5.3.

*Synthesis of iodide 17*.   NaI (4.3 g, 0.029 mol) was added to a solution of the bromide **16** (4.69 g, 0.014 mol) in acetone (70 mL), then the reaction mixture was heated to reflux.   After 3 h, the reaction mixture was cooled and concentrated to remove most of the acetone.   The residue was diluted with EtOAc and washed with H$_2$O, brine, and dried over MgSO$_4$.   The product (4.75 g, 89%) was isolated as a yellow liquid and used in the next reaction without purification.  $^1$H NMR (CDCl$_3$) δ 3.57 (t, 2H, J = 6.6 Hz), 3.16 (t, 2H, J = 7.1 Hz), 1.79 (pentet, 2H, J = 7.1 Hz), 1.50-1.46 (m, 2H), 1.41-1.27 (m, 10H), 0.87 (s, 9H), 0.023 (s, 6H); $^{13}$C NMR (CDCl$_3$) δ 63.2, 33.5, 32.8, 30.4, 29.34, 29.27, 28.4, 25.9, 25.7, 18.3, 7.3, -5.3.

*Synthesis of phosphonium iodide 18*.  PPh$_3$ (3.1 g, 0.012 mol) was added to a solution of the iodide **17** (4.75 g, 0.012 mol) in CH$_3$CN (24 mL), then the reaction mixture was heated to reflux.  After refluxing overnight, the reaction mixture was concentrated and dried under vacuum.  The product (7.72 g) was isolated in 97% yield as a white sticky foam.  $^1$H NMR (CDCl$_3$) δ 7.77-7.62 (m, 15H), 3.53-3.51 (m, 2H), 3.49 (t, 2H, J = 6.6 Hz), 1.56-1.55 (m, 4H), 1.40-1.33 (m, 2H), 1.20-1.15 (m, 8H), 0.79 (s, 9H), -0.049 (s, 6H); $^{13}$C NMR (CDCl$_3$) δ 135.1 (d, J = 3.0 Hz), 133.6 (d, J = 9.8 Hz), 130.6 (d, J = 12.8 Hz), 118.0 (d, J = 85.5 Hz), 63.2, 32.7, 30.5, 30.3, 29.2, 29.1, 25.9, 25.6, 23.4, 22.7, 22.5, 18.3, -5.3; HRMS (ESI) calculated  519.3207 (M - I), observed 519.3069.

*Synthesis of 19*.  *n*BuLi (6.0 mL, 2.5M/hexanes, 0.015 mol) was added to a solution of the phosphonium iodide **18** (7.72 g, 0.012 mol) in a mixture of THF (50 mL) and HMPA (10 mL) at -78 °C.  After 30 min, the aldehyde **15** (3.80 g, 0.015 mol) was added at -78 °C and the reaction mixture was allowed to warm to room temperature.  After stirring overnight, the reaction mixture was quenched with H$_2$O and extracted with CH$_2$Cl$_2$.  The organic layer was dried over MgSO$_4$, filtered, and concentrated.  Purification by column chromatography (5% EtOAc/hexanes) yielded the product (4.68 g) as a yellow liquid in 80% yield.  $^1$H NMR (CDCl$_3$) δ 5.38-5.29 (m, 2H), 3.57 (t, 2H, J = 6.6 Hz), 2.20 (t, 2H, J = 6.8 Hz), 2.02-1.98 (m, 4H), 1.50-1.47 (m, 4H), 1.31-1.24 (m, 16H), 0.90 (s, 9H), 0.87 (s, 9H), 0.055 (s, 6H), 0.024 (s, 6H); $^{13}$C NMR (CDCl$_3$) δ 129.9, 129.7, 108.1, 82.3, 63.3, 32.8, 29.7, 29.6, 29.5, 29.4, 29.2, 28.7, 28.6, 27.2, 27.1, 26.1, 26.0, 25.9, 25.8, 19.8, 18.3, 16.5, -4.5, -5.3; HRMS (ESI) calculated  515.4075 (M + Na), observed 515.4088.

*Synthesis of 20*.  TBAF (28 mL, 1 M/THF, 28 mmol) was added to a solution of **19** (4.68 g, 9.5 mmol) in THF (50 mL).  After the reaction mixture was stirred overnight, it was diluted with $H_2O$ and extracted with EtOAc.  The organic layer was washed with brine and dried over $MgSO_4$.  The product (2.19 g, 87%) was isolated as a colorless liquid after purification by column chromatography (20% EtOAc/hexanes).  $^1H$ NMR ($CDCl_3$) δ 5.31 (dt, 2H, J = 1.5, 3.9 Hz), 3.59 (t, 2H, J = 6.6 Hz), 2.14 (dt, 2H, J = 2.6, 6.9 Hz), 2.01-.97 (m, 4H), 1.90 (t, 1H, J = 2.6 Hz), 1.54-1.44 (m, 4H), 1.32-1.26 (m, 16H); $^{13}C$ NMR ($CDCl_3$) δ 129.9, 129.7, 84.7, 68.0, 62.9, 32.7, 29.7, 29.5, 29.44, 29.35, 29.2, 28.7, 28.6, 28.4, 27.13, 27.06, 25.6, 18.3; HRMS (ESI) calculated  287.2345 (M + Na), observed 287.2387.

*Synthesis of a-OA (21)*.  Dess-Martin periodinane (0.91 g, 2.2 mmol) was added to a solution of the alcohol **20** (0.45 g, 1.7 mmol) in $CH_2Cl_2$ (8 mL).  After 1 h, the reaction mixture was diluted with EtOAc and filtered.  Purification by column chromatography (10% EtOAc/hexanes) yielded the aldehyde (0.30 g, 67%) as a colorless liquid.  A cooled solution of $CrO_3$ (0.13 g, 1.3 mmol) in $H_2O$ (0.75 mL) and $H_2SO_4$ (0.25 mL) was added to a solution of the aldehyde (0.30 g, 1.2 mmol) in acetone (6 mL) at 0 °C.  After 30 min, the reaction mixture was diluted with EtOAc and washed with $H_2O$, brine, and dried over $MgSO_4$.  The *a-OA* (0.22 g, 67%) was isolated as a colorless liquid after purification by column chromatography (20% EtOAc/hexanes).  A two-step oxidation method was necessary to avoid allylic oxidation.  $^1H$ NMR ($CDCl_3$) δ 10.8 (br s, 1H), 5.31 (app t, 2H, J = 4.7 Hz), 2.31 (t, 2H, J = 7.5 Hz), 2.14 (dt, 2H, J = 2.6, 6.9 Hz), 2.02-1.95 (m, 4H), 1.90 (t, 1H, J = 2.6 Hz), 1.62-1.54 (m, 2H), 1.51-1.45 (m, 2H), 1.37-1.28 (m, 14H); $^{13}C$ NMR ($CDCl_3$) δ 180.5, 129.8, 129.7, 84.6, 68.1, 34.1, 29.6, 29.5, 29.1, 29.00, 28.97, 28.7, 28.6, 28.4, 27.09, 27.06, 24.6, 18.3; HRMS (ESI) calculated  301.2138 (M + Na), observed 301.2184.

Scheme S5. Synthesis of alkynyl linoleic acid.
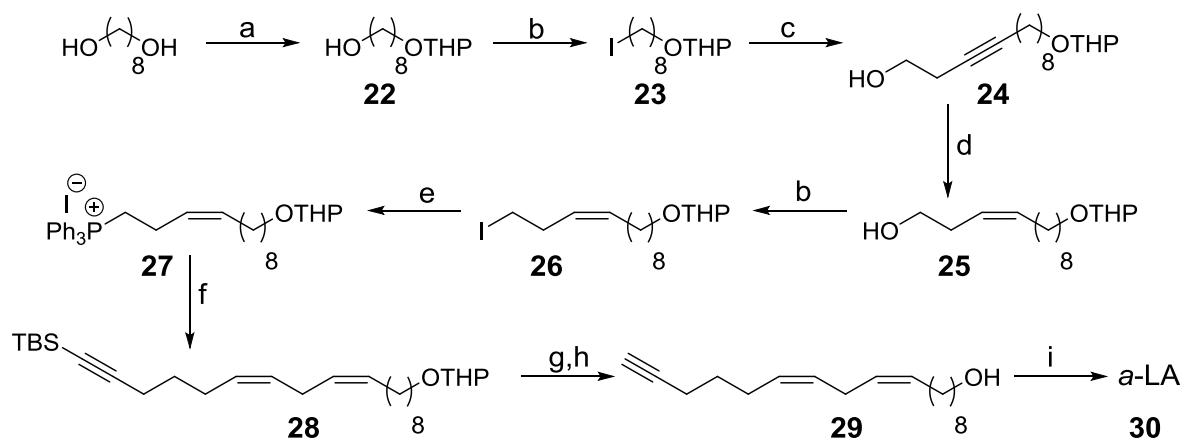


Reagents: a) DHP, TsOH, CH₂Cl₂; b) PPh₃, I₂, im, CH₂Cl₂; c) 3-butyn-1-ol, nBuLi, THF/HMPA; d) H₂, EDA, Pd/BaSO₄; e) PPh₃, CH₃CN, reflux; f) i. *n*BuLi, THF/HMPA, ii. TBS-hexynal, ; g) TBAF, THF; h) TsOH, MeOH; i) i. Dess-Martin periodinane, CH₂Cl₂, ii. Jones oxidation.

*Synthesis of 22* (5).  A solution of 3,4-dihydro-2H-pyran (13 mL, 0.14 mol) in CH₂Cl₂ (250 mL) was added dropwise to a solution of 1,8-octanediol (20.0 g, 0.14 mol) and toluenesulfonic acid (5.3 g, 0.028 mol) in CH₂Cl₂ (250 mL).   After 3 h, the reaction mixture was washed with saturated NaHCO₃ and dried over MgSO₄.  Column chromatography (2:1 to 1:1 hexanes:EtOAc) yielded the product as a colorless liquid (19.2 g, 61%).  The NMR data was consistent with published data.  ¹H NMR (CDCl₃) δ 4.53 (t, 1H, J = 2.7 Hz), 3.86-3.79 (m, 1H), 3.68 (dt, 1H, J = 6.9, 9.6 Hz), 3.58 (t, 2H, J = 6.6 Hz), 3.49-3.42 (m, 1H), 3.34 (dt, 1H, J = 6.6, 9.6 Hz), 1.81-1.45 (m, 10H), 1.34-1.26 (m, 8H).

*Synthesis of iodide 23* (5).  Iodine (15.8 g, 0.062 mol) was added in portions to a solution of **22** (12 g, 0.052 mol), PPh₃ (16 g, 0.063 mol), and imidazole (5.3 g, 0.078 mol) in CH₂Cl₂ (200 mL). After 30 min, the reaction mixture was diluted with ether and filtered through a pad of silica. Higher  purity  product  was  obtained  as  a  colorless  liquid  (14.5  g,  83%)  after  column

chromatography (10% EtOAc/hexanes).  The NMR data was consistent with published data.  $^1$H

NMR (CDCl$_3$) δ 4.55 (t, 1H, J = 2.7 Hz), 3.88-3.81 (m, 1H), 3.71 (dt, 1H, J = 6.9, 9.6 Hz), 3.51-

3.44 (m, 1H), 3.36 (dt, 1H, J = 6.6, 9.6 Hz), 3.16 (t, 2H, J = 6.9 Hz), 1.84-1.73 (m, 4H), 1.60-

1.47 (m, 6H), 1.39-1.26 (m, 8H).

*Synthesis of alkyne 24 (5).*  *n*BuLi (69 mL, 2.5 M/hexanes, 0.17 mol) was added to a solution of

3-butyn-1-ol (6.5 mL, 0.086 mol) in a mixture of THF (70 mL) and HMPA (20 mL) at -78 °C.

After 30 min, a solution of the iodide **23** (14.5 g, 0.043 mol) in THF was added to the reaction

mixture at -78 °C.    After allowing the reaction to stir overnight and warming to room

temperature, the mixture was quenched with H$_2$O and extracted with EtOAc.  The organic layer

was washed with brine and dried over MgSO$_4$.   The product was purified by column

chromatography (20% EtOAc/hexanes) and isolated as a colorless liquid (7.62 g, 64%).   The

NMR data was consistent with published data.  $^1$H NMR (CDCl$_3$) δ 4.54 (t, 1H, J = 2.7 Hz),

3.86-3.80 (m, 1H), 3.74-3.69 (m, 1H), 3.63 (app q, 2H, J = 6.0 Hz), 3.48-3.44 (m, 1H), 3.35 (dt,

1H, J = 6.6, 9.6 Hz), 2.46-2.37 (m, 2H), 2.14-2.10 (m, 2H), 1.96-1.91 (m, 2H), 1.71-1.50 (m,

8H), 1.48-1.29 (m, 8H).

*Synthesis of alkene 25 (5).*   Ethylenediamine (0.2 mL, 2%/wt) and reduced Pd/BaSO$_4$ (1.57 g,

20%/wt) were added to a solution of **24** (7.62 g, 0.027 mol) in EtOAc (135 mL), then the

reaction flask was charged with a balloon of H$_2$. The progress of the reaction was monitored by

GC.   After 2.5 h, the reaction mixture was filtered through a pad of Celite.   Column

chromatography (20% EtOAc/hexanes) yielded the product as a colorless liquid (6.71 g, 87%).

The NMR data was consistent with published data.  $^1$H NMR (CDCl$_3$) δ 5.55-5.49 (m, 1H), 5.37-

5.31 (m, 1H), 4.55 (t, 1H, J = 3.0 Hz), 3.88-3.81 (m, 1H), 3.70 (dt, 1H, J = 6.9, 9.5 Hz), 3.61

(app q, 2H, J = 6.3 Hz), 3.51-3.45 (m, 1H), 3.35 (dt, 1H, J = 6.6, 9.5 Hz), 2.30 (app q, 2H, J = 6.6 Hz), 2.03 (app q, 2H, J = 6.8 Hz), 1.83-1.46 (m, 8H), 1.40-1.20 (m, 10H).

*Synthesis of iodide 26* (5).  Iodine (7.3 g, 0.029 mol) was added in portions to a solution of the alcohol 25 (6.71 g, 0.024 mol), imidazole (2.5 g, 0.037 mol), and PPh$_3$ (7.6 g, 0.029 mol) in CH$_2$Cl$_2$ (120 mL).  After 30 min, the reaction mixture was diluted with ether and filtered through a pad of silica.  The product was obtained as a colorless liquid (7.66 g, 82%) after column chromatography (10% EtOAc/hexanes).  The NMR data was consistent with published data.  $^1$H NMR (CDCl$_3$) δ 5.54-5.46 (m, 1H), 5.33-5.24 (m, 1H), 4.55 (t, 1H, J = 2.8 Hz), 3.88-3.81 (m, 1H), 3.70 (dt, 1H, J = 6.9, 9.5 Hz), 3.51-3.44 (m, 1H), 3.35 (dt, 1H, J = 6.6, 9.5 Hz), 3.10 (t, 2H, J = 7.3 Hz), 2.60 (app q, 2H, J = 7.1 Hz), 1.99 (app q, 2H, J = 6.7 Hz), 1.83-1.51 (m, 8H), 1.40-1.20 (m, 10H).

*Synthesis of phosphonium iodide 27* (5).  PPh$_3$ (5.0 g, 0.019 mol) was added to a solution of the iodide 26 (7.66 g, 0.019 mol) in CH$_3$CN (40 mL), then the reaction mixture was heated to reflux. After refluxing overnight, the reaction mixture was concentrated then dried under vacuum.  The product was isolated as a thick yellow oil (13 g, 100%).  The NMR data was consistent with published data.  $^1$H NMR (CDCl$_3$) δ 7.81-7.73 (m, 9H), 7.71-7.65 (m, 6H), 5.55-5.46 (m, 1H), 5.39-5.30 (m, 1H), 4.52 (t, 1H, J = 4.2 Hz), 3.85-3.78 (m, 1H), 3.71-3.54 (m, 3H), 3.48-3.39 (m, 1H), 3.32 (dt, 1H, J = 6.6, 9.5 Hz), 2.44-2.33 (m, 2H), 1.80-1.60 (m, 4H), 1.54-1.40 (m, 6H), 1.30-1.10 (m, 10H).

*Synthesis of 6-TBS-hexynal* (6).  *n*BuLi (40 mL, 0.10 mol) was added to a solution of 5-hexyn-1-ol (5.0 mL, 0.045 mol) in THF (100 mL) at 0 °C.  After 30 min, a solution of TBSCl (15.2 g, 0.10 mol) in THF (10 mL) was added and the reaction allowed to warm to room temperature.

After stirring overnight, the reaction mixture was quenched with $H_2O$ and extracted with EtOAc. The organic layer was washed with brine and dried over $MgSO_4$. The crude product mixture was dissolved in $HOAc;H_2O$ (100 mL, 2:1) and heated to 80 °C. After 1 h, the reaction mixture was cooled and extracted with toluene. The organic layer was washed with saturated $NaHCO_3$, brine, and dried over $MgSO_4$. The TBS-hexyn-1-ol (8.59 g, 89%) was isolated as a colorless liquid after column chromatography (20% EtOAc/hexanes). PCC (10.3 g, 0.048 mol) was added to a solution of the TBS-hexyn-1-ol (8.59 g, 0.040 mol) in $CH_2Cl_2$ (100 mL). After 1 h, the reaction mixture was diluted with ether and filtered through a pad of silica. The TBS-hexynal (5.47 g, 64%) was purified by column chromatography (10% EtOAc/hexanes) and isolated as a colorless liquid. The NMR data was consistent with published data. $^1$H NMR ($CDCl_3$) δ 9.78 (t, 1H, J = 1.3 Hz), 2.57 (dt, 2H, J = 1.2, 7.3 Hz), 2.28 (t, 2H, J = 6.8 Hz), 1.81 (pentet, 2H, J = 7.0 Hz), 0.89 (s, 9H), 0.05 (s, 6H).

*Synthesis of 28*. *n*BuLi (10 mL, 2.5 M/hexanes, 0.025 mol) was added to a solution of the phosphonium iodide **27** (13 g, 0.020 mol) in a mixture of THF (75 mL) and HMPA (25 mL) at -78 °C. After 30 min, a solution of 6-TBS-hexynal (5.4 g, 0.026 mol) in THF was added at -78 °C. After overnight and allowing the reaction to warm to room temperature, it was quenched with $H_2O$ and extracted with EtOAc. The organic layer was washed with brine and dried over $MgSO_4$. Column chromatography (5% EtOAc/hexanes) yielded the product as a pale yellow liquid (6.56 g, 71%). $^1$H NMR ($CDCl_3$) δ 5.40-5.27 (m, 4H), 4.55 (t, 1H, J = 2.7 Hz), 3.88-3.81 (m, 1H), 3.70 (dt, 1H, J = 6.9, 9.5 Hz), 3.51-3.44 (m, 1H), 3.35 (dt, 1H, J = 6.7, 9.6 Hz), 2.76 (t, 2H, J = 5.9 Hz), 2.25 (t, 2H, J = 7.0 Hz), 2.18-2.13 (m, 2H), 2.05-1.98 (m, 2H), 1.83-1.79 (m, 2H), 1.72-1.46 (m, 8H), 1.40-1.28 (m, 10H), 0.90 (s, 9H), 0.053 (s, 6H); $^{13}$C NMR ($CDCl_3$) δ 130.3, 129.1, 128.7, 127.7, 107.8, 98.8, 82.6, 67.6, 62.3, 30.7, 29.7, 29.6, 29.5, 29.4, 29.2, 28.6,

27.2, 26.2, 26.0, 25.6, 25.5, 19.6, 19.3, 16.5, -4.5; HRMS (ESI) calculated 483.3629 (M + Na), observed 483.3643.

*Synthesis of 29*. TBAF (20 mL, 1M/THF, 0.020 mol) was added to a solution of **28** (6.56 g, 0.014 mol) in THF (70 mL). After 3 h, the reaction mixture was diluted with $H_2O$ and extracted with EtOAc. The organic layer was washed with brine and dried over $MgSO_4$. The alkyne was isolated as a colorless liquid (4.57 g, 93%) after column chromatography (5% EtOAc/hexanes). ^{1}H NMR (CDCl$_3$) δ 5.38-5.25 (m, 4H), 4.55 (t, 1H, J = 2.7 Hz), 3.88-3.80 (m, 1H), 3.70 (dt, 1H, J = 6.9, 9.5 Hz), 3.50-3.43 (m, 1H), 3.35 (dt, 1H, J = 6.6, 9.5 Hz), 2.76 (t, 2H, J = 6.1 Hz), 2.20-2.12 (m, 4H), 2.02 (app q, 2H, J = 6.4 Hz), 1.92 (t, 1H, J = 2.6 Hz), 1.84-1.66 (m, 2H), 1.59-1.51 (m, 8H), 1.35-1.23 (m, 10H); ^{13}C NMR (CDCl$_3$) δ 130.3, 129.2, 128.6, 127.7, 98.8, 84.3, 68.3, 67.6, 62.3, 30.7, 29.7, 29.6, 29.4, 29.2, 28.3, 27.2, 26.2, 26.1, 25.63, 25.58, 25.5, 19.6, 17.8; HRMS (ESI) calculated 369.2764 (M + Na), observed 369.2778.

Toluenesulfonic acid (0.58 g, 0.0030 mol) was added to a solution of this alkyne (4.57 g, 0.013 mol) in MeOH (65 mL). After 2 h, the reaction mixture was concentrated to remove most of the MeOH. The residue was dissolved in EtOAc and washed with saturated $NaHCO_3$, brine, and dried over $MgSO_4$. Column chromatography (20% EtOAc/hexanes) yielded the deprotected alcohol **29** as a colorless liquid (2.69 g, 78%). ^{1}H NMR (CDCl$_3$) δ 5.38-5.25 (m, 4H), 3.59 (t, 2H, J = 6.6 Hz), 2.76 (t, 2H, J = 5.9 Hz), 2.19-2.11 (m, 4H), 2.03 (app q, 2H, J = 6.4 Hz), 1.92 (t, 1H, J = 2.6 Hz), 1.61-1.51 (m, 4H), 1.35-1.25 (m, 10H); ^{13}C NMR (CDCl$_3$) δ 130.2, 129.2, 128.6, 127.7, 84.3, 68.3, 62.9, 32.7, 29.6, 29.4, 29.3, 29.2, 28.3, 27.2, 26.1, 25.7, 25.6, 17.8; HRMS (ESI) calculated 263.2369 (M + H), observed 263.2381.

*Synthesis of a-LA 30*.  Dess-Martin periodinane (5.1 g, 0.012 mol) was added to a solution of **29** (2.69 g, 0.010 mol) in $CH_2Cl_2$ (50 mL).  After 30 min, the reaction mixture was diluted with EtOAc and washed with $H_2O$, brine, and dried over $MgSO_4$.  The aldehyde (2.0 g, 75%) was isolated as a colorless liquid after column chromatography (10% EtOAc/hexanes).  $^1H$ NMR $(CDCl_3)$ δ 9.73 (t, 1H, J = 1.8Hz), 5.40-5.27 (m, 4H), 2.76 (t, 2H, J = 5.8Hz), 2.39 (dt, 2H, J = 1.8, 7.3 Hz), 2.19-2.11 (m, 4H), 2.04-1.98 (m, 2H), 1.92 (t, 1H, J = 2.6 Hz), 1.65-1.51 (m, 4H), 1.35-1.28 (m, 8H); $^{13}C$ NMR $(CDCl_3)$ δ 202.8, 130.1, 129.1, 128.6, 127.8, 84.3, 68.3, 43.8, 29.5, 29.2, 29.1, 29.0, 28.3, 27.1, 26.1, 25.6, 22.0, 17.8; HRMS (ESI) calculated  261.2213 (M + H), observed 261.2202.

A cooled solution of $CrO_3$ (0.13 g, 1.30 mmol) in $H_2O$ (0.75 mL) and $H_2SO_4$ (0.25 mL) was added to a solution of the aldehyde (0.30 g, 1.15 mmol) in acetone (6 mL) at 0 °C.  After 30 min, the reaction mixture was diluted with EtOAc and washed with $H_2O$, brine, and dried over $MgSO_4$.  Column chromatography yielded the *a*-LA (0.22 g, 67%) as a colorless oil.  Residual chromium salts, indicated by a pale green color, were removed with charcoal.  $^1H$ NMR $(CDCl_3)$ δ 9.52 (br s, 1H), 5.40-5.26 (m, 4H), 2.76 (t, 2H, J = 5.8 Hz), 2.32 (t, 2H, J = 7.4 Hz), 2.20-2.12 (m, 4H), 2.05-2.00 (m, 2H), 1.92 (t, 1H, J = 2.6 Hz), 1.62-1.52 (m, 4H), 1.35-1.29 (m, 8H); $^{13}C$ NMR $(CDCl_3)$ δ 180.1, 130.1, 129.2, 128.6, 127.8, 84.3, 68.3, 34.1, 29.5, 29.1, 29.0, 28.9, 28.3, 27.1, 26.1, 25.6, 24.6, 17.8; HRMS (ESI) calculated  277.2162 (M + H), observed 277.2139.

Scheme S6. Synthesis of alkynyl arachidonic acid.
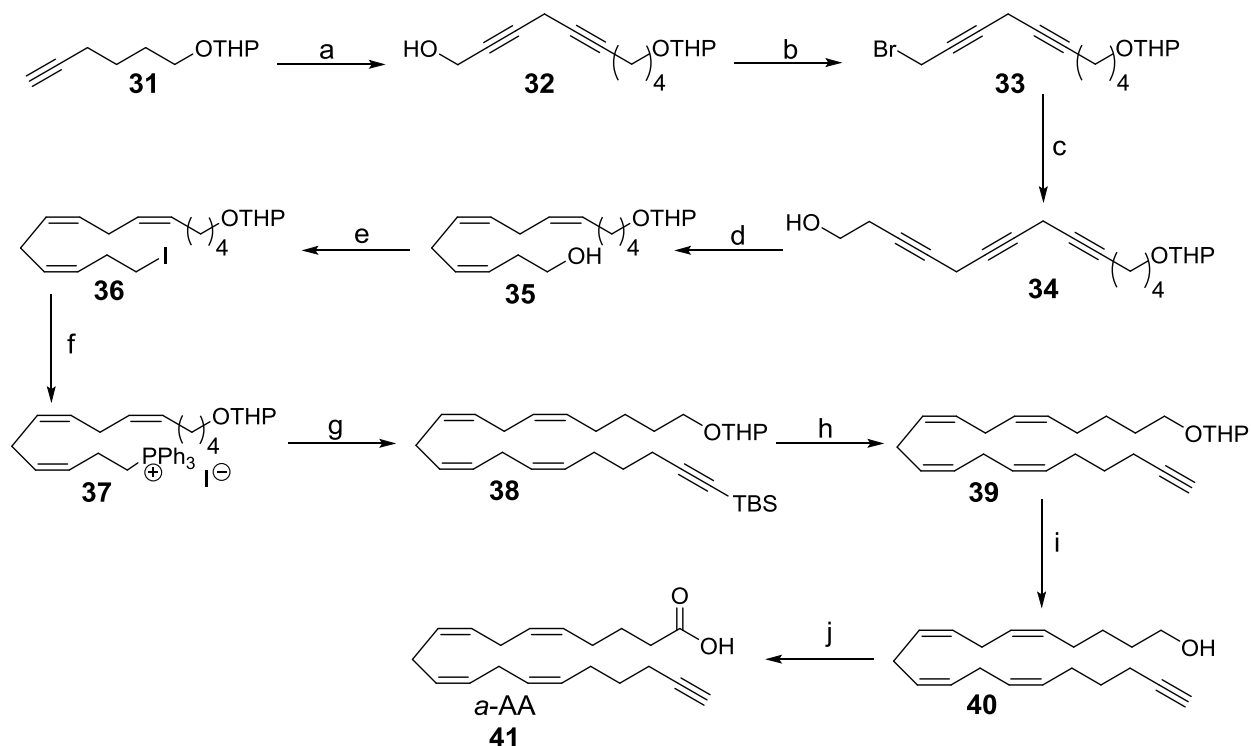


Reagents:  a) 4-chloro-2-butyn-1-ol, $K_2CO_3$, NaI, CuI, DMF; b) NBS, $PPh_3$, im, $CH_2Cl_2$ 0 °C; c) 3-butyn-1-ol, $K_2CO_3$, NaI, CuI, DMF; d) $H_2$, Pd/BaSO_4, quinoline, EtOAc; e) $I_2$, $PPh_3$, im, $CH_2Cl_2$; f) $PPh_3$, $CH_3CN$, reflux; g) i. nBuLi, THF/HMPA, -78 °C, ii. 6-TBS-5-hexynal; h) TBAF, THF; i) TsOH, MeOH; j) i. PCC, Celite, $CH_2Cl_2$, ii. Jones oxidation.

*Synthesis of THP-hexynol* **31**.  4-Toluenesulfonic acid (1.7 g, 0.0089 mol) was added to a solution of 5-hexyn-1-ol (5.0 mL, 0.045 mol) and 3,4-dihydro-2H-pyran (4.5 mL, 0.049 mol) in $CH_2Cl_2$ (100 mL).  After 1 h, the reaction mixture was washed with saturated $NaHCO_3$ and dried over $MgSO_4$.  The product was purified by column chromatography (10% EtOAc/hexanes) and isolated as a colorless liquid (6.9 g, 83%).  $^1$H NMR (CDCl$_3$) δ 4.54 (t, 1H, J = 2.7 Hz), 3.82 (m, 1H), 3.72 (dt, 1H, J = 6.2, 9.8 Hz), 3.46 (m, 1H), 3.37 (dt, 1H, J = 5.9, 9.7 Hz), 2.19 (dt, 2H, J = 2.6, 7.1 Hz), 1.91 (t, 1H, J = 2.6 Hz), 1.81-1.48 (m, 10H); $^{13}$C NMR (CDCl$_3$) δ 98.7, 84.3, 68.3,

66.8, 62.2, 30.7, 28.7, 25.4, 25.3, 19.5, 18.2; HRMS (ESI) calculated 205.1199 (M + Na), observed 205.1227.

*Synthesis of 4-chloro-2-butyn-1-ol* (7). Thionyl chloride (18 mL, 0.25 mol) was added dropwise to a solution of 2-butyne-1,4-diol (20 g, 0.23 mol) and pyridine (20 mL, 0.25 mol) in benzene (200 mL). After the reaction had stirred overnight, it was diluted with $H_2O$ and partitioned. The aqueous layer was extracted with ether. The combined organic layers were washed with saturated $NaHCO_3$, brine, and dried over $MgSO_4$. Purification by column chromatography (20% EtOAc/hexanes) yielded the product as a yellow liquid (16 g, 64%). The NMR data was consistent with the literature. $^{1}$H NMR ($CDCl_3$) δ 4.29 (dt, 2H, J = 1.8, 6.0 Hz), 4.15 (t, 2H, J = 2.0 Hz), 2.37 (t, 1H, J = 5.9 Hz).

*Synthesis of diynol* **32**. $K_2CO_3$ (7.9 g, 0.057 mol), NaI (8.5 g, 0.057 mol), and CuI (11 g, 0.057 mol) were added to a solution of 4-chloro-2-butyn-1-ol (6.0 g, 0.057 mol) and **31** (6.9 g, 0.038 mol) in DMF (100 mL). After stirring overnight, the reaction mixture was diluted with EtOAc and filtered through a pad of Celite. The filtrate was washed with saturated $NH_4Cl$, brine, and dried over $MgSO_4$. The product was purified by column chromatography (20% EtOAc/hexanes) and isolated in quantitative yield as a yellow liquid (10 g). The product contained some DMF, but was used in the following reaction without further purification. $^{1}$H NMR ($CDCl_3$) δ 4.55 (t, 1H, J = 2.8 Hz), 4.18 (t, 2H, J = 2.2 Hz), 3.80 (m, 1H), 3.69 (dt, 1H, J = 6.4, 9.6 Hz), 3.45 (m, 1H), 3.36 (dt, 1H, J = 6.1, 9.7 Hz), 3.11 (pentet, 2H, J = 2.3 Hz), 2.56 (br s, 1H), 2.14 (tt, 2H, J = 2.4, 7.0 Hz), 1.78-1.61 (m, 4H), 1.56-1.46 (m, 6H); $^{13}$C NMR ($CDCl_3$) δ98.6, 80.7, 80.3, 78.5, 73.7, 67.0, 62.1, 50.9, 30.6, 28.8, 25.4, 25.3, 19.4, 18.4, 9.7; HRMS (ESI) calculated 273.1461 (M + Na), observed 273.1481.

*Synthesis of bromodiyne* **33**.  A solution of **32** (9.4 g, 0.038 mol) in $CH_2Cl_2$ (20 mL) was added to a solution of $PPh_3$ (12 g, 0.046 mol), imidazole (3.9 g, 0.057 mol), and *N*-bromosuccinimide (8.1 g, 0.046 mol) in $CH_2Cl_2$ (200 mL) at 0 °C.  After 1 h, the reaction mixture was diluted with ether and filtered through a pad of silica.  Purification by column chromatography (10% EtOAc/hexanes) yielded the product as a colorless liquid (6.5 g, 55%).  $^1H$ NMR ($CDCl_3$) δ 4.52 (t, 1H, J = 2.7 Hz), 3.86 (t, 2H, J = 2.3 Hz), 3.80 (m, 1H), 3.69 (dt, 1H, J = 6.3, 9.7 Hz), 3.44 (m, 1H), 3.34 (dt, 1H, J = 6.1, 9.6 Hz), 3.16 (pentet, 2H, J = 2.4 Hz), 2.15 (tt, 2H, J = 2.4, 7.1 Hz), 1.79-1.73 (m, 1H), 1.69-1.60 (m, 3H), 1.55-1.46 (m, 6H) ; $^{13}C$ NMR ($CDCl_3$) δ 98.7, 82.0, 81.0, 75.2, 73.0, 66.9, 62.2, 31.5, 28.8, 25.42, 25.38, 19.6, 18.5, 14.8, 10.0; HRMS (ESI) calculated 335.0617 (M + Na), observed 335.0618.

*Synthesis of triynol* **34**.  $K_2CO_3$ (4.4 g, 0.032 mol), NaI (4.8 g, 0.032 mol), and CuI (6.2 g, 0.033 mol) were added to a solution of 3-butyn-1-ol (2.4 mL, 0.032 mol) and **33** (6.5 g, 0.021 mol) in DMF (50 mL).  After stirring overnight, the reaction mixture was diluted with EtOAc and filtered through a pad of Celite.  The filtrate was washed with saturated $NH_4Cl$, brine, and dried over $MgSO_4$.  The product was purified by column chromatography (30% EtOAc/hexanes) and isolated as a yellow liquid (3.9 g, 62%).  $^1H$ NMR ($CDCl_3$) δ 4.52 (t, 1H, J = 2.7 Hz), 3.80 (m, 1H), 3.68 (dt, 1H, J = 6.3, 9.6 Hz), 3.63 (t, 2H, J = 6.4 Hz), 3.44 (m, 1H), 3.34 (dt, 1H, J = 6.1, 9.6 Hz), 3.10-3.06 (m, 4H), 2.38 (tt, 2H, J = 2.4, 6.3 Hz), 2.28 (br s, 1H), 2.14 (tt, 2H, J = 2.3, 7.1 Hz), 1.80-1.70 (m, 1H), 1.65-1.46 (m, 9H); $^{13}C$ NMR ($CDCl_3$) δ 98.7, 80.5, 77.2, 75.9, 75.0, 74.3, 73.9, 66.9, 62.2, 61.0, 30.6, 28.8, 25.4, 23.0, 19.4, 18.5, 9.72, 9.66; HRMS (ESI) calculated 325.1774 (M + Na), observed 325.1780.

*Synthesis of trienol* **35**.  Pd/BaSO$_4$ (0.80 g, 20%/wt) and quinoline (0.40 mL, 10%/wt) were added to a solution of **34** (3.9 g, 0.013 mol) in EtOAc (65 mL), then the reaction mixture was charged with a balloon of H$_2$.  After 2 h, very little reaction was observed so additional Pd/BaSO$_4$ was added.  After 5 h, the reaction mixture was filtered through a pad of Celite.  The filtrate was washed with 10% HCl, saturated NaHCO$_3$, brine, and dried over MgSO$_4$.  Purification by column chromatography (20% EtOAc/hexanes) yielded the product as a pale yellow liquid (2.5 g, 63%).  ^{1}H NMR (CDCl$_3$) δ 5.53-5.45 (m, 1H), 5.41-5.30 (m, 5H), 4.54 (t, 1H, J = 2.7 Hz), 3.82 (m, 1H), 3.70 (dt, 1H, J = 6.7, 9.5 Hz), 3.60 (t, 2H, J = 6.5 Hz), 3.46 (m, 1H), 3.35 (dt, 1H, J = 6.4, 9.6 Hz), 2.81 (t, 2H, J = 6.4 Hz), 2.77 (t, 2H, J = 5.7 Hz), 2.32 (q, 2H, J = 6.6 Hz), 2.07 (q, 2H, J = 7.1 Hz), 1.85-1.66 (m, 3H), 1.65-1.32 (m, 8H); ^{13}C NMR (CDCl$_3$) δ 130.9, 130.0, 128.5, 127.8, 127.7, 125.6, 98.8, 67.4, 62.2, 62.1, 30.8, 30.7, 29.3, 27.0, 26.2, 25.7, 25.6, 25.4, 19.6; HRMS (ESI) calculated  331.2244 (M + Na), observed 331.2257.

*Synthesis of iodotriene* **36**.  Iodine (2.6 g, 10 mmol) was added in portions to a solution of **35** (2.5 g, 8.2 mmol), PPh$_3$ (2.6 g, 10 mmol), and imidazole (0.86 g, 13 mmol) in CH$_2$Cl$_2$ (40 mL).  After 1 h, the reaction mixture was diluted with ether and filtered through a pad of silica gel.  The product was purified by column chromatography (10% EtOAc/hexanes) and isolated as a colorless liquid (3.1 g, 90%).  ^{1}H NMR (CDCl$_3$) δ 5.54-5.45 (m, 1H), 5.40-5.27 (m, 5H), 4.55 (t, 1H, J = 2.7 Hz), 3.84 (m, 1H), 3.71 (dt, 1H, J = 6.6, 9.5 Hz), 3.47 (m, 1H), 3.36 (dt, 1H, J = 6.4, 9.6 Hz), 3.12 (t, 2H, J = 7.3 Hz), 2.78 (t, 4H, J = 6.1 Hz), 2.64 (q, 2H, J = 7.2 Hz), 2.07 (q, 2H, J = 7. Hz), 1.84-1.75 (m, 2H), 1.69-1.41 (m, 8H); ^{13}C NMR (CDCl$_3$) δ 130.4, 130.1, 128.7, 128.2, 127.7, 127.4, 98.8, 67.4, 62.3, 31.4, 30.7, 29.3, 27.0, 26.3, 25.8, 25.6, 25.5, 19.6, 5.2; HRMS (ESI) calculated 441.1261 (M + Na), observed 441.1243.

*Synthesis of phosphonium iodide* **37**.  PPh$_3$ (2.0 g, 7.4 mmol) was added to a solution of **36** (3.1 g, 7.4 mmol) in CH$_3$CN (15 mL), then the reaction mixture was heated to reflux.  After refluxing overnight, the reaction mixture was cooled, concentrated, and dried under high vacuum.  The product was isolated as a pale yellow oil (4.9 g, 98%).  The phosphonium iodide was used in the next reaction without purification.  HRMS (ESI) calculated 553.3230 (M - I), observed 555.3242.

*Synthesis of tetraene* **38**.  *n*BuLi (3.2 mL, 8.0 mmol) was added to a solution of the phosphonium iodide **37** (4.5 g, 6.6 mmol) in a mixture of THF (24 mL) and HMPA (8 mL) at -78 °C.  The solution turned dark orange upon formation of the ylide.  After 30 min, a solution of 6-TBS-5-hexynal (1.7 g, 8.1 mmol) in THF (5 mL) was added at -78 °C.  The synthesis of 6-TBS-5-hexynal is described above.  The reaction was allowed to warm to room temperature and stirred overnight.  The solution was then quenched with H$_2$O and extracted with EtOAc.  The organic layer was washed with brine and dried over MgSO$_4$.  The product was purified by column chromatography (5% EtOAc/hexanes) and isolated as a yellow liquid (1.7 g, 52%).  $^1$H NMR (CDCl$_3$) δ 5.40-5.29 (m, 8H), 4.55 (t, 1H, J = 2.7 Hz), 3.84 (m, 1H), 3.72 (dt, 1H, J = 6.6, 9.5 Hz), 3.47 (m, 1H), 3.36 (dt, 1H, J = 6.4, 9.5 Hz), 2.81-2.77 (m, 6H), 2.22 (t, 2H, J = 7.1 Hz), 2.21-2.13 (m, 2H), 2.11-2.04 (m, 2H), 1.84-1.71 (m, 2H), 1.64-1.39 (m, 10H), 0.90 (s, 9H), 0.052 (s, 6H); $^{13}$C NMR (CDCl$_3$) δ 130.0, 129.0, 128.7, 128.4, 128.3, 128.1, 127.94, 127.85, 107.7, 98.8, 82.6, 67.4, 62.2, 30.7, 29.3, 28.6, 27.0, 26.3, 26.2, 26.0, 25.6, 25.5, 19.6, 19.3, 16.5, -4.5.

*Synthesis of* **39**.  TBAF (5.0 mL, 5.0 mmol) was added to a solution of **38** (1.7 g, 3.4 mmol) in THF (17 mL).  After 6 h, the reaction mixture was diluted with EtOAc and washed with H$_2$O,

brine, and dried over MgSO$_4$.  Purification by column chromatography (5% EtOAc/hexanes)

yielded the product as a colorless liquid (1.1 g, 86%).  $^1$H NMR (CDCl$_3$) δ 5.42-5.29 (m, 8H),

4.55 (t, 1H, J = 2.7 Hz), 3.83 (m, 1H), 3.71 (dt, 1H, J = 6.6, 9.5 Hz), 3.47 (m, 1H), 3.36 (dt, 1H, J

= 6.4, 9.5 Hz), 2.80-2.76 (m, 6H), 2.16 (dt, 4H, J = 2.6, 7.1 Hz), 2.07 (q, 2H, J = 7.2 Hz), 1.92 (t,

1H, J = 2.6 Hz), 1.84-1.41 (m, 12H); $^{13}$C NMR (CDCl$_3$) δ 130.0, 128.9, 128.8, 128.4, 128.2,

128.0, 127.9, 127.8, 98.7, 84.3, 68.4, 67.4, 62.2, 30.7, 29.3, 28.3, 27.0, 26.3, 26.1, 25.6, 25.5,

19.6, 17.8; HRMS (ESI) calculated  393.2764 (M + Na), observed 393.2762.

*Synthesis of tetraenol* **40**.  4-Toluenesulfonic acid (0.11 g, 0.58 mmol) was added to a solution of

**38** (1.1 g, 2.9 mmol) in MeOH (15 mL).  After 4 h, the reaction mixture was diluted with EtOAc

and washed with saturated NaHCO$_3$, brine, and dried over MgSO$_4$.  The product was purified by

column chromatography (20% EtOAc/hexanes) and isolated as a colorless liquid (0.52 g, 62%).

$^1$H NMR (CDCl$_3$) δ 5.40-5.29 (m, 8H), 3.61 (t, 2H, J = 6.4 Hz), 2.82-2.77 (m, 6H), 2.16 (dt, 4H,

J = 2.6, 7.1 Hz), 2.07 (q, 2H, J = 7.2 Hz), 1.93 (t, 1H, J = 2.6 Hz), 1.62-1.51 (m, 4H), 1.45-1.38

(m, 2H); $^{13}$C NMR (CDCl$_3$) δ 130.0, 128.9, 128.8, 128.3, 128.2, 128.01, 127.97, 84.3, 68.4, 62.8,

32.3, 28.3, 26.9, 26.1, 25.7, 25.6, 17.8.

*Synthesis of a-AA* **41**.  PCC (0.50 g, 2.3 mmol) and Celite (1.8 g, 1 g/mmol) were added to a

solution of **40** (0.52 g, 1.8 mmol) in CH$_2$Cl$_2$ (9 mL).  After 1 h, the reaction mixture was diluted

with EtOAc and filtered through a pad of silica gel.  The crude aldehyde was used in the next

reaction without purification.  A solution of CrO$_3$ (0.20 g, 2.0 mmol) in H$_2$O/H$_2$SO$_4$ (2 mL, 3:1)

was added to a solution of the aldehyde (0.48 g, 1.7 mmol) in acetone (8 mL) at 0 °C.  After 1 h,

the reaction mixture was diluted with EtOAc and washed with H$_2$O, brine, and dried over

MgSO$_4$.  The product was purified by column chromatography (20% EtOAc/hexanes) and

isolated as a colorless liquid (0.26 g, 50%). $^1$H NMR (CDCl$_3$) δ 5.41-5.30 (m, 8H), 2.83-2.77

(m, 6H), 2.34 (t, 2H, J = 7.5 Hz), 2.17 (dt, 4H, J = 3.6, 7.1 Hz), 2.13-2.08 (m, 2H), 1.93 (t, 1H, J

= 2.6 Hz), 1.69 (pentet, 2H, J = 7.5 Hz), 1.57 (pentet, 2H, J = 7.3 Hz); $^{13}$C NMR (CDCl$_3$) δ

179.9, 129.0, 128.9, 128.8, 128.7, 128.3, 128.13, 128.09, 128.0, 84.3, 68.4, 33.4, 28.3, 26.4, 26.1,

25.6, 24.4, 17.8; HRMS (ESI) calculated 323.1982 (M + Na), observed 323.1965.

Scheme S7. Synthesis of *a*-POPC.
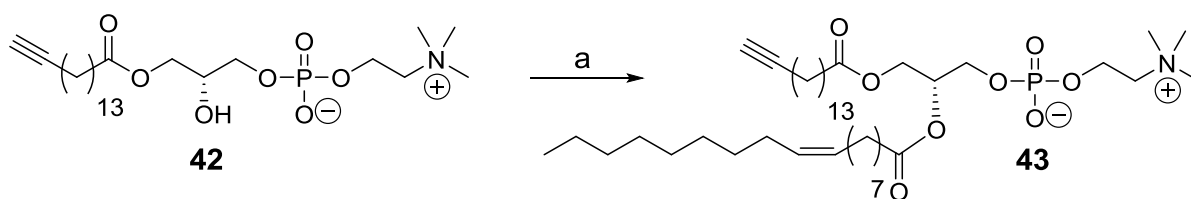


Reagents: a) oleic acid, DCC, DMAP, CHCl$_3$, glass, sonication.

*Synthesis of a-POPC* **43**. DCC (0.24 g, 1.2 mmol) and DMAP (0.13 g, 1.1 mol) were added to a

milky solution of the lyso-*a*-PC **42** (8) (0.26 g, 0.53 mmol) and oleic acid (0.22 g, 0.78 mmol) in

CHCl$_3$ (5 mL). Crushed glass was added and the reaction mixture sonicated. After 3 h, the

reaction mixture was filtered and concentrated. Purification by column chromatography (30%

MeOH/ + CH$_2$Cl$_2$ 5% H$_2$O) yielded the product as a white powder (0.14 g, 34%). $^1$H NMR

(MeOH-d$_4$) δ 5.34 (app t, 2H, J = 4.6 Hz), 5.24 (m, 1H), 4.43 (dd, 1H, J = 3.0, 12.0 Hz), 4.30-

4.23 (m, 2H), 4.16 (dd, 1H, J = 6.9, 12.0 Hz), 3.99 (t, 2H, J = 6.4 Hz), 3.66-3.63 (m, 2H), 3.22 (s,

9H), 2.32 (app q, 4H, J = 7.6 Hz), 2.17-2.12 (m, 3H), 2.03 (br q, 4H, J = 5.3 Hz), 1.65-1.55 (m,

4H), 1.52-1.45 (m, 2H), 1.40-1.25 (m, 38H), 0.90 (t, 3H, J = 7.0 Hz); $^{13}$C NMR (MeOH-d$_4$) δ

174.8, 174.5, 130.9, 130.8, 85.0, 76.1, 71.8, 71.7, 69.5, 67.4 (m), 64.9, 64.8, 63.7, 60.5, 60.4,

54.71, 54.66, 54.6, 35.1, 34.9, 33.1, 30.9, 30.8, 30.7, 30.5, 30.4, 30.3, 30.2, 30.1, 29.84, 29.76,

28.2, 26.0, 23.8, 19.1, 14.6; HRMS (ESI) calculated 778.5357 (M + Na), observed 778.5356.

# References

1.  Izzo, I., N. Maulucci, C. Martone, A. Casapullo, L. Fanfoni, P. Tecilla, and F. De Riccardis. 2006. On the importance of the pore inner cavity for the ionophoric activity of 1,3-alternate calix[4]arene/steroid conjugates. *Tetrahedron*. **62**: 5385-5391.

2.  Martin, R., E. V. Entchev, F. Däbritz, T. V. Kurzchalia, and H.-J. Knölker. 2009. Synthesis and Hormonal Activity of the (25S)-Cholesten-26-oic Acids – Potent Ligands for the DAF-12 Receptor in Caenorhabditis elegans. *European J Org Chem*. **2009**: 3703-3714.

3.  Bédard, A.-C., and S. K. Collins. 2011. Phase Separation As a Strategy Toward Controlling Dilution Effects in Macrocyclic Glaser-Hay Couplings. *J Am Chem Soc*. **133**: 19976-19981.

4.  Jiang, C.-S., R. Zhou, J.-X. Gong, L.-L. Chen, T. Kurtán, X. Shen, and Y.-W. Guo. 2011. Synthesis, modification, and evaluation of (R)-de-O-methyllasiodiplodin and analogs as nonsteroidal antagonists of mineralocorticoid receptor. *Bioorg Med Chem Lett*. **21**: 1171-1175.

5.  Dussault, P., and I. Q. Lee. 1995. A Chemoenzymic Approach to Hydroperoxyeicosatetraenoic Acids. Total Synthesis of 5(S)-HPETE. *J Org Chem*. **60**: 218-226.

6.  Hollingworth, G., G. Pattenden, and D. Schulz. 1995. Cascade Radical Cyclization-Fragmentation-Transannular-Ring Expansion Reactions Involving Oximes. A New Approach to Synthesis of Angular Triquinanes. *Aust J Chem*. **48**: 381-399.

7.  Qi, L., M. M. Meijler, S.-H. Lee, C. Sun, and K. D. Janda. 2004. Solid-Phase Synthesis of Anandamide Analogues. *Org Lett*. **6**: 1673-1675.

8.     Milne, S. B., K. A. Tallman, R. Serwa, C. A. Rouzer, M. D. Armstrong, L. J. Marnett, C. M. Lukehart, N. A. Porter, and H. A. Brown. 2010. Capture and release of alkyne-derivatized glycerophospholipids using cobalt chemistry. *Nat Chem Biol*. **6**: 205-207.

**6. Conclusions and future directions**

Cholesterol oxidation generates a variety of bioactive products, including hydroperoxides and aldehydes. Although their mechanisms of formation are not fully understood, they have been found elevated in several pathological conditions, such as atherosclerosis, Alzheimer's and Parkinson's disease. Several studies focusing on the biological effects of oxysterols have been published over the past decade, where it is shown a clear association between the accumulation of oxysterols and the occurrence of such diseases. However, it is not clear yet whether if the accumulation of oxysterols is a cause or a consequence of the disease. In the field of free radicals in biology and medicine there is not a clear understanding whether the unbalance in the redox state is a cause or a consequence of diseases and aging (Halliwell and Gutteridge 2007). Great effort is being directed to answer these questions, where we constantly try to understand the role of free radicals in the physiology and pathology of the cell. This is also true for the oxysterols and other lipid-derived oxidation products, where most of what is known is only their association with diseases.

On the other hand, very little in known about the chemistry underling the involvement of oxysterols in such diseases. The participation of ChOOH, for instance, could be associated with its capacity to react with metal ions and/or metallproteins, producing free radical species and a broad spectrum of bioactive products. In the study discussed in chapter one we suggest that the reaction of a single protein (cytc) with ChOOH leads to the production of lipid- and protein-derived carbon-centered radicals, which leads to protein inactivation and oligomerization. This reaction itself could have several implications to cell, including, for instance, an influence in the apoptosis signaling and cancer processes. Although this is just the tip of the iceberg, the understanding of such mechanisms is a critical step for unraveling the

involvement of ChOOH and other lipid-derived hydroperoxides in the development of pathological conditions. As perspectives for this study, it would be interesting to see what are the specific amino acid residues involved in the oligomerization process as well as the implications of such reactions to a living cell. Studies using mitoplasts and/or isolated mitochondria supplemented with ChOOH and other lipid-derived hydroperoxides might give regarding the relevance and implications of such reactions, which could, ultimately, help understanding their roles in the development of diseases.

In chapter two we discuss protein adduction promoted by cholesterol-derived aldehydes, particularly cytc adduction promoted by ChAld. Protein adduction promoted by other lipid-derived electrophiles has been extensively studied (Uchida and Stadtman 1992; Isom, Barnes et al. 2004; Sigolo, Di Mascio et al. 2007). Most studies show that α,β-unsaturated aldehydes, such as HNE, react with nucleophiles by two mechanisms: *i)* Michael addition to the double bond or; *ii)* formation of imine bonds with the aldehyde moiety (Schiff base formation) (Uchida and Stadtman 1992; Isom, Barnes et al. 2004). Aldehyde species such as ChAld or CSec can react only by the second mechanism, the formation of Schiff base adducts. This restriction is due to the absence of a double bond in the structure of the aldehyde. In our study, we were able to show that, indeed, these aldehydes react with nucleophilic amino acids (i.e. lysine residues) leading to the formation of Schiff base adducts. Interestingly, we were also able to show that, in the presence of membrane mimetics (i.e. SDS-micelles), ChAld modifies residues that interact directly with the membrane. Although we still do not understand the implications of these modifications, we hypothesized that they could improve the binding between cytc and the mitochondrial membrane, influencing the electron transport and apoptosis signaling. In the future, in

order to have a better understanding of the biological implications of these reactions one could use mitoplasts to address this question. A simple experimental design would be to deplete cytc from mitoplasts and then supplement with "normal" cytc and cytc adducted with ChAld. Such experiment could help understand whether or not the adduction affects mitochondrial respiration and cytc release.

Recently, we showed that such aldehydes, especially CSec, can react with His residues (Windsor, K. et al. *Submitted to Chem Res Toxic*). This result is quite unexpected, since His may not form imine bond due to the absence of the H-atom required for the dehydration. After many experiments, we were able to show that CSec might lose one water molecule and gain a double bond, rendering a species capable reacting with His through a Michael reaction. This is another example of the complex chemistry that underlies oxysterol-promoted protein adduction. Therefore, many studies are still necessary to fully understand the mechanisms and implications of such reactions.

In the last and third chapter of this study we designed alkynyl derivatives of 7-DHC, cholesterol and several cholesterol-derived oxidation products and probed them for protein adduction. Moreover, we searched for an association between the accumulation of 7-DHC and 7-DHC-promoted protein adduction in SLOS cells. Interestingly, alkynyl derivatives of both 7-DHC and cholesterol are incorporated and metabolized by Neuro2a cells. This gave us the support to use alkynyl-7-DHC as a probe to check for protein adduction using click chemistry. Using that, we were able to show that SLOS cells have elevated levels of protein adduction when compared to control cells (healthy cells), indicating that 7-DHC-derived oxysterols might be involved in the development of the disease. In this context, the use of the click chemistry approach can be extended to many biological studies, where it can help the

identification of other types of lipid-promoted protein adduction. In the future, the combined use of click chemistry and mass spectrometry can allow the identification of the specific proteins that were modified by the electrophiles, which might help understanding the progress of the disease as well as the development of therapeutic approaches.

## 7. References

Augusto, O. and S. Miyamoto (2011). Oxygen Radicals and Related species. Principles of Free Radical Biomedicine. K. Pantopoulos and H. M. Schipper, Nova Science Publishers, Inc. **I**.

Babior, B. M., C. Takeuchi, et al. (2003). "Investigating antibody-catalyzed ozone generation by human neutrophils." Proceedings of the National Academy of Sciences of the United States of America **100**(6): 3031-3034.

Barr, D. P., M. R. Gunther, et al. (1996). "ESR spin-trapping of a protein-derived tyrosyl radical from the reaction of cytochrome c with hydrogen peroxide." J Biol Chem **271**(26): 15498-15503.

Barr, D. P. and R. P. Mason (1995). "Mechanism of radical production from the reaction of cytochrome-c with organic hydroperoxides - an ESR spin-trapping investigation." The Journal of Biological Chemistry **270**(21): 12709-12716.

Belikova, N. A., Y. Y. Tyurina, et al. (2009). "Heterolytic reduction of fatty acid hydroperoxides by cytochrome c/cardiolipin complexes: antioxidant function in mitochondria." J Am Chem Soc **131**(32): 11288-11289.

Bieschke, J., Q. Zhang, et al. (2006). "Small molecule oxidation products trigger disease-associated protein misfolding." Acc Chem Res **39**(9): 611-619.

Bosco, D. A., D. M. Fowler, et al. (2006). "Elevated levels of oxidized cholesterol metabolites in Lewy body disease brains accelerate [alpha]-synuclein fibrilization." Nature Chemical Biology **2**(5): 249-253.

Brinkhorst, J., S. J. Nara, et al. (2008). "Hock cleavage of cholesterol 5alpha-hydroperoxide: an ozone-free pathway to the cholesterol ozonolysis products identified in arterial plaque and brain tissue." J Am Chem Soc **130**(37): 12224-12225.

Brunekreef, B. and S. T. Holgate (2002). "Air pollution and health." Lancet **360**(9341): 1233-1242.

Buettner, G. R. (1993). "The pecking order of free radicals and antioxidants: lipid peroxidation, alpha-tocopherol, and ascorbate." Arch Biochem Biophys **300**(2): 535-543.

Bukelis, I., F. D. Porter, et al. (2007). "Smith-Lemli-Opitz syndrome and autism spectrum disorder." Am J Psychiatry **164**(11): 1655-1661.

Colell, A., A. Fernandez, et al. (2009). "Mitochondria, cholesterol and amyloid beta peptide: a dangerous trio in Alzheimer disease." J Bioenerg Biomembr **41**(5): 417-423.

Criegee, R. (1975). "Mechanism of Ozonolysis." Angewandte Chemie-International Edition in English **14**(11): 745-752.

Feo, F., R. A. Canuto, et al. (1973). "Cholesterol and phospholipid composition of mitochondria and microsomes isolated from morris hepatoma 5123 and rat liver." FEBS Lett **33**(2): 229-232.

Foote, C. S. (1991). "Definition of Type-I and Type-Ii Photosensitized Oxidation." Photochemistry and Photobiology **54**(5): 659-659.

Frimer, A. A. (1979). "The reaction of singlet oxygen with olefins: the question of mechanism." Chemical Reviews **79**(5): 28.

Gaoua, W., F. Chevy, et al. (1999). "Oxidized derivatives of 7-dehydrocholesterol induce growth retardation in cultured rat embryos: a model for antenatal growth retardation in the Smith-Lemli-Opitz syndrome." J Lipid Res **40**(3): 456-463.

Garcia-Ruiz, C., M. Mari, et al. (2009). "Mitochondrial cholesterol in health and disease." Histol Histopathol **24**(1): 117-132.

Geletneky, C. and S. Berger (1998). "The mechanism of ozonolysis revisited by O-17-NMR spectroscopy." European Journal of Organic Chemistry(8): 1625-1627.

Girotti, A. W. (1992). "Photosensitized Oxidation of Cholesterol in Biological-Systems - Reaction Pathways, Cytotoxic Effects and Defense-Mechanisms." Journal of Photochemistry and Photobiology B-Biology **13**(2): 105-118.

Girotti, A. W. and T. Kriska (2004). "Role of lipid hydroperoxides in photo-oxidative stress signaling." Antioxidants & Redox Signaling **6**(2): 301-310.

Gumulka, J. and L. L. Smith (1983). "Ozonization of Cholesterol." Journal of the American Chemical Society **105**(7): 1972-1979.

Haas, D., S. F. Garbade, et al. (2007). "Effects of cholesterol and simvastatin treatment in patients with Smith-Lemli-Opitz syndrome (SLOS)." J Inherit Metab Dis **30**(3): 375-387.

Halliwell, B. and J. Gutteridge (2007). Free Radicals in Biology and Medicine, Oxford University Press.

Hang, H. C. and M. E. Linder (2011). "Exploring protein lipidation with chemical biology." Chem Rev **111**(10): 6341-6358.

Hermes-Lima, M. (2005). Oxygen in Biology and Biochemistry: Role of free radicals. Functional Metabolism: Regulation and Adaptation. K. B. Storey. New York, Wiley. **1**.

Ikonen, E. (2008). "Cellular cholesterol trafficking and compartmentalization." Nat Rev Mol Cell Biol **9**(2): 125-138.

Isom, A. L., S. Barnes, et al. (2004). "Modification of Cytochrome c by 4-hydroxy- 2-nonenal: evidence for histidine, lysine, and arginine-aldehyde adducts." Journal of the American Society for Mass Spectrometry **15**(8): 1136-1147.

Jaworski, K. and L. L. Smith (1988). "Ozonization of Cholesterol in Nonparticipating Solvents." Journal of Organic Chemistry **53**(3): 545-554.

Kawai, Y., A. Saito, et al. (2003). "Covalent binding of oxidized cholesteryl esters to protein: implications for oxidative modification of low density lipoprotein and atherosclerosis." J Biol Chem **278**(23): 21040-21049.

Kelley, R. I. and R. C. Hennekam (2000). "The Smith-Lemli-Opitz syndrome." J Med Genet **37**(5): 321-335.

Kettle, A. J., B. M. Clark, et al. (2004). "Superoxide converts indigo carmine to isatin sulfonic acid - Implications for the hypothesis that neutrophils produce ozone." Journal of Biological Chemistry **279**(18): 18521-18525.

Korytowski, W. and A. W. Girotti (1999). "Singlet oxygen adducts of cholesterol: Photogeneration and reductive turnover in membrane systems." Photochemistry and Photobiology **70**(4): 484-489.

Kulig, M. J. and L. L. Smith (1973). "Sterol Metabolism .25. Cholesterol Oxidation by Singlet Molecular-Oxygen." Journal of Organic Chemistry **38**(20): 3639-3642.

Mansano, F. V., R. M. Kazaoka, et al. (2010). "Highly sensitive fluorescent method for the detection of cholesterol aldehydes formed by ozone and singlet molecular oxygen." Anal Chem **82**(16): 6775-6781.

Montero, J., A. Morales, et al. (2008). "Mitochondrial cholesterol contributes to chemotherapy resistance in hepatocellular carcinoma." Cancer Res **68**(13): 5246-5256.

Nantes, I. L., A. Faljoni-Alario, et al. (2000). "Modifications in heme iron of free and vesicle bound cytochrome c by tert-butyl hydroperoxide: a magnetic circular dichroism and electron paramagnetic resonance investigation." Free Radic Biol Med **28**(5): 786-796.

Nieva, J., B. D. Song, et al. (2011). "Cholesterol secosterol aldehydes induce amyloidogenesis and dysfunction of wild-type tumor protein p53." Chem Biol **18**(7): 920-927.

Osada, K. and A. Sevanian (2000). "Cholesterol photodynamic oxidation by ultraviolet irradiation and cholesterol ozonization by ozone exposure." Singlet Oxygen, Uv-a, and Ozone **319**: 188-196.

Porter, F. D. and G. E. Herman (2011). "Malformation syndromes caused by disorders of cholesterol synthesis." J Lipid Res **52**(1): 6-34.

Pratt, D. A., J. H. Mills, et al. (2003). "Theoretical calculations of carbon-oxygen bond dissociation enthalpies of peroxyl radicals formed in the autoxidation of lipids." J Am Chem Soc **125**(19): 5801-5810.

Qian, S. Y., Y. R. Chen, et al. (2002). "Identification of protein-derived tyrosyl radical in the reaction of cytochrome c and hydrogen peroxide: characterization by ESR spin-trapping, HPLC and MS." Biochem J **363**(Pt 2): 281-288.

Resh, M. D. (2012). "Targeting protein lipidation in disease." Trends Mol Med **18**(4): 206-214.

Richards, M. J., B. A. Nagel, et al. (2006). "Lipid hydroperoxide formation in the retina: correlation with retinal degeneration and light damage in a rat model of Smith-Lemli-Opitz syndrome." Exp Eye Res **82**(3): 538-541.

Ronsein, G. E., F. M. Prado, et al. (2010). "Detection and characterization of cholesterol-oxidized products using HPLC coupled to dopant assisted atmospheric pressure photoionization tandem mass spectrometry." Anal Chem **82**(17): 7293-7301.

Sies, H. (2004). "Ozone in arteriosclerotic plaques: Searching for the "smoking gun"." Angewandte Chemie-International Edition **43**(27): 3514-3515.

Sigolo, C. A., P. Di Mascio, et al. (2007). "Covalent modification of cytochrome c exposed to trans,trans-2,4-decadienal." Chem Res Toxicol **20**(8): 1099-1110.

Smith, L. L. (1987). "Cholesterol Autoxidation 1981-1986." Chemistry and Physics of Lipids **44**(2-4): 87-125.

Smith, L. L. (1996). "Review of progress in sterol oxidations: 1987-1995." Lipids **31**(5): 453-487.

Smith, L. L. (2004). "Oxygen, oxysterols, ouabain, and ozone: A cautionary tale." Free Radical Biology and Medicine **37**(3): 318-324.

Tagiri-Endo, M., K. Nakagawa, et al. (2004). "Ozonation of cholesterol in the presence of ethanol: identification of a cytotoxic ethoxyhydroperoxide molecule." Lipids **39**(3): 259-264.

Tint, G. S., M. Seller, et al. (1995). "Markedly increased tissue concentrations of 7-dehydrocholesterol combined with low levels of cholesterol are characteristic of the Smith-Lemli-Opitz syndrome." J Lipid Res **36**(1): 89-95.

Tomono, S., N. Miyoshi, et al. (2009). "Formation of cholesterol ozonolysis products through an ozone-free mechanism mediated by the myeloperoxidase-H2O2-chloride system." Biochem Biophys Res Commun **383**(2): 222-227.

Tomono, S., N. Miyoshi, et al. (2011). "Formation of cholesterol ozonolysis products in vitro and in vivo through a myeloperoxidase-dependent pathway." Journal of Lipid Research **52**(1): 87-97.

Uchida, K. and E. R. Stadtman (1992). "Modification of Histidine Residues in Proteins by Reaction with 4-Hydroxynonenal." Proceedings of the National Academy of Sciences of the United States of America **89**(10): 4544-4548.

Uemi, M., G. E. Ronsein, et al. (2009). "Generation of cholesterol carboxyaldehyde by the reaction of singlet molecular oxygen [O2 (1Delta(g))] as well as ozone with cholesterol." Chem Res Toxicol **22**(5): 875-884.

van Meer, G., D. R. Voelker, et al. (2008). "Membrane lipids: where they are and how they behave." Nat Rev Mol Cell Biol **9**(2): 112-124.

Vila, A., K. A. Tallman, et al. (2008). "Identification of protein targets of 4-hydroxynonenal using click chemistry for ex vivo biotinylation of azido and alkynyl derivatives." Chem Res Toxicol **21**(2): 432-444.

Wang, K., E. Bermudez, et al. (1993). "The ozonation of cholesterol: separation and identification of 2,4-dinitrophenylhydrazine derivatization products of 3 beta-hydroxy-5-oxo-5,6-secocholestan-6-al." Steroids **58**(5): 225-229.

Wentworth, A. D., B. D. Song, et al. (2009). "The ratio of cholesterol 5,6-secosterols formed from ozone and singlet oxygen offers insight into the oxidation of cholesterol in vivo." Chem Commun (Camb)(21): 3098-3100.

Wentworth, P., Jr., J. Nieva, et al. (2003). "Evidence for Ozone Formation in Human Atherosclerotic Arteries." Science **302**(5647): 1053-1056.

Wentworth, P., J. E. McDunn, et al. (2002). "Evidence for antibody-catalyzed ozone formation in bacterial killing and inflammation." Science **298**(5601): 2195-2199.

Wentworth, P., A. D. Wentworth, et al. (2003). "Evidence for the production of trioxygen species during antibody-catalyzed chemical modification of antigens." Proceedings of the National Academy of Sciences of the United States of America **100**(4): 1490-1493.

Windsor, K., T. C. Genaro-Mattos, et al. (2013). "Probing lipid-protein adduction with alkynyl surrogates: application to Smith-Lemli-Opitz syndrome." J Lipid Res **54**(10): 2842-2850.

Xu, L., T. A. Davis, et al. (2009). "Rate constants for peroxidation of polyunsaturated fatty acids and sterols in solution and in liposomes." J Am Chem Soc **131**(36): 13037-13044.

Yin, H., L. Xu, et al. (2011). "Free radical lipid peroxidation: mechanisms and analysis." Chem Rev **111**(10): 5944-5972.

Zhang, Q., E. T. Powers, et al. (2004). "Metabolite-initiated protein misfolding may trigger Alzheimer's disease." Proc Natl Acad Sci U S A **101**(14): 4752-4757.

# APPENDIX

# Curriculum Vitae

**Thiago Cardoso Genaro de Mattos**

## 1. Personal Information

- Full name: Thiago Cardoso Genaro de Mattos
- Name used in bibliographic citations: Genaro-Mattos, T. C.
- Gender: Male
- Date of Birth: November 19th, 1984.
- Professional Address: Av. Prof. Lineu Prestes, 148. Bloco 9 superior, sala 951.
  Cidade Universitária – São Paulo-SP. Brazil. 05508-000.
- Phone: +551130919114
- E-mail: thiagocgmattos@gmail.com / thiagocgmattos@usp.br

## 2. Formal Education

- **Undergraduation**
  - Bachelor`s in Chemistry.
    University of Brasília – UnB.
  - Start year: 2002. End year: 2006.
- **Master`s degree**
  - Master`s in Analytical Chemistry.
    Institute of Chemistry. University of Brasília – UnB.
  - Start year: 2007. End year: 2009.
  - Research project: **Antioxidant mechanisms of Caffeic and Tannic acids in systems containing iron ions.**
  - Supervisor: Marcelo Hermes Lima, PhD.
- **PhD degree**
  - Doctorate in Biochemistry and Molecular Biology.
    Institute of Chemistry. Department of Biochemistry. University of São Paulo-USP.
  - Start year: 2010. End year: *In progress*.
  - Research project: **Characterization of cytochrome c modifications promoted by cholesterol aldehydes: mechanisms and biological implications.**
  - Supervisor: Sayuri Miyamoto, PhD.
  - One year as a visiting scholar at Vanderbilt University working with Ned A. Porter, PhD. Start year: 2013. End year: 2014.

Thiago C. Genaro-Mattos

# 3. Articles published in scientific journals.

- Genaro-Mattos, T. C. et al. **Reevaluation of the 2-deoxyribose assay for determination of free radical formation**. *Biochem Biophys Acta* **1790**, 1636-1642 (2009). *DOI*: 10.1016/j.bbagen.2009.09.003

- Mansano, F. V. et al. **Highly Sensitive Fluorescent Method for the Detection of Cholesterol Aldehydes Formed by Ozone and Singlet Molecular Oxygen**. *Anal Chem* **82**, 6775-6781 (2010). *DOI*: 10.1021/ac1006427

- Santos, P. et al. **Behavior of the thermal diffusivity of native and oxidized human low-density lipoprotein solutions studied by the Z-scan technique**. *J Biomedical Optics* **17**(10), 1050031-7 (2012). *DOI*: 10.1117/1.JBO.17.10.105003

- Genaro-Mattos, T. C. et al. **Covalent binding and anchoring of cytochrome c to mitochondrial mimetic membranes promoted by cholesterol carboxyaldehyde**. *Chem. Res. Toxicol.* **26**, 1536-1544 (2013). *DOI*: 10.1021/tx4002385

- Windsor, K. et al. **Probing lipid-protein adduction with alkynyl surrogates: application to Smith-Lemli-Opitz syndrome**. *J. Lipid. Res.* **54**, 2842-2859 (2013). *DOI*: 10.1194/jlr.M041061

# 4. Abstracts published in annals of events.

Genaro-Mattos, Thiago C. ; WINDSOR, K. ; KIM, H.-Y. H. ; LIU, W. ; TALLMAN, K. A. ; Miyamoto, Sayuri ; KORADE, Z. ; PORTER, N. A. . A click chemistry approach to identify protein adduction promoted by oxysterols. In: 17th biannual meeting of the Society for Free Radical Research International, 2014, Kyoto. 17th biannual meeting of the Society for Free Radical Research International, 2014.

Cunha, D. ; **Genaro-Mattos, T. C.** ; Miyamoto, Sayuri . Peroxidase Activity Induced by Cardiolipin Hydroperoxides in Cytochrome c Cardiolipin Complex. In: XLII Annual Meeting of The Brazilian Biochemistry and Molecular Biology Society, 2013, Foz do Iguaçu. Annals of the XLII Annual Meeting of The Brazilian Biochemistry and Molecular Biology Society, 2013.

**Genaro-Mattos, T. C.** ; Appolinário, Patricia ; MUGNOL, K. C. ; BLOCH JR, C. ; NANTES, I. L. ; Di Mascio, Paolo ; Miyamoto, Sayuri . Cytochrome c adduction promoted by cholesterol derived aldehydes - implications to protein-membrane binding. In: Antioxidants and Redox Process in Health - Bilateral Meeting Brazil - Japan, 2013, São Paulo. Antioxidants and Redox Process in Health - Bilateral Meeting Brazil - Japan, 2013.

**Genaro-Mattos, T. C.** ; QUEIROZ, R. F. ; APPOLINARIO, P. P. ; Cunha, D. ; PORTER, N. A. ; Augusto, Ohara ; Miyamoto, Sayuri . Cytochrome c reacts with cholesterol hydroperoxides producing protein and lipid carbon-centered radicals. In: Society for Free Radical Biology and Medicine - South American Group, 2013, Buenos Aires. Society for Free Radical Biology and Medicine - South American Group, 2013.

Thiago C. Genaro-Mattos

**Genaro-Mattos, T. C.** ; Appolinário, Patricia ; Nantes, Iseli ; Mascio, Paolo Di ; Miyamoto, Sayuri . Cytochrome C Modifications Promoted by Cholesterol Aldehydes - Implications to Electron Transport and Apoptosis. In: SFRBM's 19th Annual Meeting, 2012, San Diego. Free Radical Biology and Medicine, 2012. v. 53. p. S20-S20.

Appolinário, Patricia ; Medinas, Danilo ; **Genaro-Mattos, T. C.** ; Kazaoka, Rafaella M. A. ; CUSSIOL, J. R. R. ; NETTO, L. E. S. ; Augusto, Ohara ; Miyamoto, Sayuri . Characterization of Changes in the Apo Form of Enzyme Cu, Zn Superoxide Dismutase Promoted by Docosahexaenoic Acid and their Hydroperoxides. In: SFRBM's 19th Annual Meeting, 2012, San Diego. Free Radical Biology and Medicine, 2012. v. 53. p. S133-S133.

Kazaoka, Rafaella M. A. ; YAMAGUTI, T. H. ; Mansano, Fernando V. ; APPOLINARIO, P. P. ; DEROGIS, P. B. M. C. ; **Genaro-Mattos, T. C.** ; FREITAS, F. P. ; MEDEIROS, M. H. G. ; Miyamoto, Sayuri . Evaluation of cholesterol and its aldehydes in a transgenic rat model for amyotrophic lateral sclerosis. In: VII Meeting of the South American Group of the SFRBM, 2011, São Pedro. VII Meeting of the South American Group of the SFRBM, 2011.

APPOLINARIO, P. P. ; MEDINAS, D. B. ; **Genaro-Mattos, T. C.** ; AUGUSTO, Ohara. ; Miyamoto, Sayuri . Characterization of SOD1 aggregation induced by docosahexaenoic acid hydroperoxides. In: VII Meeting of the South American Group of the SFRBM, 2011, São Pedro. VII Meeting of the South American Group of the SFRBM, 2011.

**Genaro-Mattos, Thiago** ; Appolinário, Patricia ; Nantes, Iseli ; Bloch, Carlos ; Di Mascio, Paolo ; Miyamoto, Sayuri . Cytochrome c modifications promoted by cholesterol hydroperoxides and aldehydes. In: 52nd International Conference on the Bioscience of Lipids - Expanding the Horizons of Lipidomics, 2011, Varsóvia. Chemistry and Physics of Lipids, 2011. v. 164S. p. S44-S44.

Appolinário, Patricia ; Medinas, Danilo ; **Genaro-Mattos, Thiago** ; Augusto, Ohara ; Miyamoto, Sayuri . Docosahexaenoic acid induced SOD1 aggregation: The role of fatty acid conformation and the cysteine residues. In: 52nd International Conference on the Bioscience of Lipids - Expanding the Horizons of Lipidomics, 2011, Varsóvia. Chemistry and Physics of Lipids, 2011. v. 164S. p. S19-S19.

**Genaro-Mattos, T. C.** ; APPOLINARIO, P. P. ; NANTES, I. L. ; BLOCH JR, C. ; Mascio, Paolo Di ; Miyamoto, Sayuri . Cytochrome c modifications promoted by cholesterol hydroperoxides and aldehydes. In: VII Meeting of the South American Group of the SFRBM, 2011, São Pedro. VII Meeting of the South American Group of the SFRBM, 2011.

Genaro-Mattos, Thiago C. ; Mansano, Fernando V. ; Uemi, Miriam ; Mascio, Paolo Di ; Miyamoto, Sayuri . Characterization of Cytochrome C Modifications Promoted by Cholesterol Carboxyaldehyde. In: SFRBM's 17th Annual Meeting, 2010, Orlando. Free Radical Biology and Medicine. New York: Elsevier, 2010. v. 49. p. S165-S165.

**Genaro-Mattos, T. C.** ; DALVI, L. T. ; Bicalho, J. M. ; Hermes-Lima, M. . Fixing the Classical 2-Deoxyribose Assay. In: XXXVIII Reunião Anual da Sociedade Brasileira de Bioquímica e Biologia Molecular - SBBq, 2009, Águas de Lindóia. Anais da XXXVIII Reunião Anual da

Sociedade Brasileira de Bioquímica e Biologia Molecular - SBBq, 2009.

LOPES, A. C. F. ; **Genaro-Mattos, T. C.** ; ALONSO, A. ; Hermes-Lima, M. . Trivalent and Hexavalent Chromium as Mediators of Fenton-type Reactions. In: XXXVIII Reunião Anual da Sociedade Brasileira de Bioquímica e Biologia Molecular - SBBq, 2009, Águas de Lindóia. Anais da XXXVIII Reunião Anual da Sociedade Brasileira de Bioquímica e Biologia Molecular - SBBq, 2009.

**Genaro-Mattos, T. C.** ; LOPES, A. C. F. ; ALONSO, A. ; Hermes-Lima, M. . Chromium Mediated Hydroxyl Radical Formation: The longest-lasting Fenton-type reaction Reported so far. In: SFRBM 16th Annual Meeting, 2009, San Francisco. Free Radical Biology and Medicine, 2009. v. 47. p. S188-S188.

**Genaro-Mattos, T. C.** ; ALONSO, A. ; Hermes-Lima, M. . Antioxidant Activities of Caffeic and Tannic Acids os Iron Autoxidation.. In: XXXVII Reunião Anual da Sociedade Brasileira de Bioquímica e Biologia Molecular - SBBq, 2008, Águas de Lindóia - SP. Anais da XXXVII Reunião Anual da Sociedade Brasileira de Bioquímica e Biologia Molecular, 2008.

LOPES, A. C. F. ; **Genaro-Mattos, T. C.** ; Hermes-Lima, M. . In Vitro Oxidative Processes Mediated by Trivalent and Hexavalent Chromium. In: XXXVII Reunião Anual da Sociedade Brasileira de Bioquímica e Biologia Molecular - SBBq, 2008, Águas de Lindóia. Anais da XXXVII Reunião Anual da Sociedade Brasileira de Bioquímica e Biologia Molecular - SBBq, 2008.

**Genaro-Mattos, T. C.** ; MAURICIO, A. Q. ; Rettori, D ; Vautier-Giongo, C ; ALONSO, A. ; Hermes-Lima, M. . IN VITRO ANTIOXIDANT ACTIVITY OF THE IRON CHELATOR CAFFEIC ACID: MECHANISTIC CONSIDERATIONS. In: SFRBM's 15th Annual Meeting, 2008, Indianápolis. Annals of the SFRBM's 15th Annual Meeting, 2008.

**Genaro-Mattos, T. C.** ; DALVI, L. T. ; GINANI, J. S. ; Oliveira, R. G. ; Hermes-Lima, M. . Reevaluation of the 2-Deoxyribose assay for the study of metal-mediated free-radical formation. In: XXXVI Annual Meeting of the Brazilian Society for Biochemistry and Molecular Biology (SBBq), 2007, Salvador. XXXVI Reunião Anual da Sociedade Brasiliera de Bioquímica e Biologia Molecular (SBBq), 2007.

MAURICIO, A. Q. ; **Genaro-Mattos, T. C.** ; Gomes, C.S. ; GINANI, J. S. ; Hermes-Lima, M. . Effects of Caffeic Acid (CA) on Oxyradical Reactions Mediated by Fe(II) and Fe(III). In: Reunião Anual da Sociedade Brasileira de Bioquímica (SBBq), 2006, Águas de Lindóia. XXXV Reunião Anual Programa, 2006.

**Genaro-Mattos, T. C.** ; Gomes, C.S. ; Hermes-Lima, M. ; DUTRA, F. . In vitro oxidative processes mediated by trivalent Chromium. In: IV Meeting of The Brazilian Society of Biochemistry and Molecular Biology, 2005, Águas de Lindóia. Satellite Meeting of The Brazilian Society of Biochemistry and Molecular Biology, 2005.

Thiago C. Genaro-Mattos

Gomes, C.S. ; MAURICIO, A. Q. ; **Genaro-Mattos, T. C.** ; BONINI, M. ; AUGUSTO, Ohara. ; Hermes-Lima, M. . Effects of Pyridoxal Isonicotinoyl Hidrazone(PIH) on Fe(II) Autoxidation and Oxyradical formation.. In: Reunião Anual da Sociedade Brasileira de Bioquímica (SBBq), 2004, Caxambú. SBBq/ Programa e Resumos da XXXIII Reunião Anual/2004, 2004.

---

## 5. Lectures and oral presentations.

- Lecture at the Department of Nutrition at University of Brasília, **2009**, Brasilia – DF, Brazil. *Subject:* **Antioxidant mechanisms of caffeic acid, a compound present in coffee beans.**

- Oral presentation at the *XXXIII Annual Meeting of the Brazilian Society for Biochemistry and Molecular Biology - SBBq*, **2004**, Caxambú – MG, Brazil. *Subject:* **Effects of pyridoxal isonicotinoyl hidrazone (PIH) on Fe(II) autoxidation and oxyradical formation.**

- Oral presentation at the *Society for Free Radical Biology and Medicine - South American Group*, **2013**, Buenos Aires, Argentina. *Subject:* **Cytochrome c reacts with cholesterol hydroperoxides producing protein and lipid carbon-centered radicals.**

- Oral presentation at the *Antioxidants and Redox Process in Health - Bilateral Meeting Brazil - Japan*, **2013**, São Paulo, Brazil. *Subject:* **Cytochrome c adduction promoted by cholesterol derived aldehydes - implications to protein-membrane binding.**

---

## 6. Awards.

**2014** - Travel Award, Society for Free Radical Biology and Medicine - SFRBM.

**2013** - Young Investigator Award, Society for Free Radical Research International - SFRRI.

**2012** - Travel Award, Society for Free Radical Biology and Medicine - SFRBM.

**2011** - EPSCA Scholarship, FAPESP.

Thiago C. Genaro-Mattos

# Highly Sensitive Fluorescent Method for the Detection of Cholesterol Aldehydes Formed by Ozone and Singlet Molecular Oxygen

Fernando V. Mansano, Rafaella M. A. Kazaoka, Graziella E. Ronsein, Fernanda M. Prado, Thiago C. Genaro-Mattos, Miriam Uemi, Paolo Di Mascio, and Sayuri Miyamoto*

*Departamento de Bioquímica, Instituto de Química, Universidade de São Paulo, CP26077, CEP 05513-970, São Paulo, SP, Brazil*

**Cholesterol oxidation gives rise to a mixture of oxidized products. Different types of products are generated according to the reactive species being involved. Recently, attention has been focused on two cholesterol aldehydes, 3β-hydroxy-5β-hydroxy-B-norcholestane-6β-carboxaldehyde (1a) and 3β-hydroxy-5-oxo-5,6-secocholestan-6-al (1b). These aldehydes can be generated by ozone-, as well as by singlet molecular oxygen-mediated cholesterol oxidation. It has been suggested that 1b is preferentially formed by ozone and 1a is preferentially formed by singlet molecular oxygen. In this study we describe the use of 1-pyrenebutyric hydrazine (PBH) as a fluorescent probe for the detection of cholesterol aldehydes. The formation of the fluorescent adduct between 1a with PBH was confirmed by HPLC-MS/MS. The fluorescence spectra of PBH did not change upon binding to the aldehyde. Moreover, the derivatization was also effective in the absence of an acidified medium, which is critical to avoid the formation of cholesterol aldehydes through Hock cleavage of 5α-hydroperoxycholesterol. In conclusion, PBH can be used as an efficient fluorescent probe for the detection/quantification of cholesterol aldehydes in biological samples. Its analysis by HPLC coupled to a fluorescent detector provides a sensitive and specific way to quantify cholesterol aldehydes in the low femtomol range.**

Cholesterol (cholest-5-en-3β-ol) is a neutral lipid found in the cellular membranes of mammals.[1] Cholesterol is susceptible to oxidation mediated by enzymatic and nonenzymatic mechanisms.[2–5] The nonenzymatic oxidation can be mediated by reactive oxygen species.[2] Several oxidized products of cholesterol have been characterized including hydroperoxides, epoxides, and aldehydes.[2,6,7] These oxysterols have been detected in biological tissues and their formation has been associated to neurodegenerative and cardio-

vascular diseases.[2–5] Recently, attention has been focused on cholesterol aldehydes that can be formed by the oxidation of cholesterol by ozone[8] and singlet molecular oxygen.[9,10]

The ozonation of cholesterol produces several oxidized products, in special two aldehydes (Figure 1), the cholesterol 5,6-secosterols, 3β-hydroxy-5β-hydroxy-B-norcholestane-6β-carboxyaldehyde (1a) and 3β-hydroxy-5-oxo-5,6-secocholestan-6-al (1b).[11,12] Wentworth and co-workers showed the presence of **1a** and **1b** in atherosclerotic plaques[8] and LDL oxidized with several oxidants.[13] These aldehydes have been also detected in neurodegenerative diseases, like Lewy body dementia[14] and Alzheimer disease.[15] The role of **1a** and **1b** in the pathogenesis of cardiovascular and neurodegenerative diseases has been investigated. In vitro studies have shown that cholesterol aldehydes can covalently modify proteins, as well as, accelerate their aggregation, as in the case of amyloid β-peptide formation[15–17] and α-synuclein.[14] Further studies have shown that covalent modification of apo-B by **1b** causes this protein to misfold, rendering the LDL particle more susceptible to macrophage uptake.[18] Moreover, some reports have also shown that cholesterol aldehydes can induce apoptosis in macrophages and cardiomyoblasts.[19,20] The induction of apoptosis in cardi-

* To whom correspondence should be addressed. Phone: (55) (11) 3091-3810 (x261). Fax: (55) (11) 3815-5579. E-mail: miyamoto@iq.usp.br.

(1) Maxfield, F. R.; Tabas, I. *Nature* **2005**, *438*, 612–621.
(2) Brown, A. J.; Jessup, W. *Atherosclerosis* **1998**, *142*, 1–28.
(3) Björkhem, I.; Diczfalusy, U. *Arterioscler. Thromb. Vasc. Biol.* **2002**, *22*, 734–742.
(4) Garenc, C.; Julien, P.; Levy, E. *Free Radical Res.* **2010**, *44*, 47–73.
(5) Schroepfer, G. J., Jr. *Physiol. Rev.* **2000**, *80*, 361–554.
(6) Smith, L. L. *Lipids* **1996**, *31*, 453–487.
(7) Girotti, A. W. *J. Photochem. Photobiol. B* **1992**, *13*, 105–118.
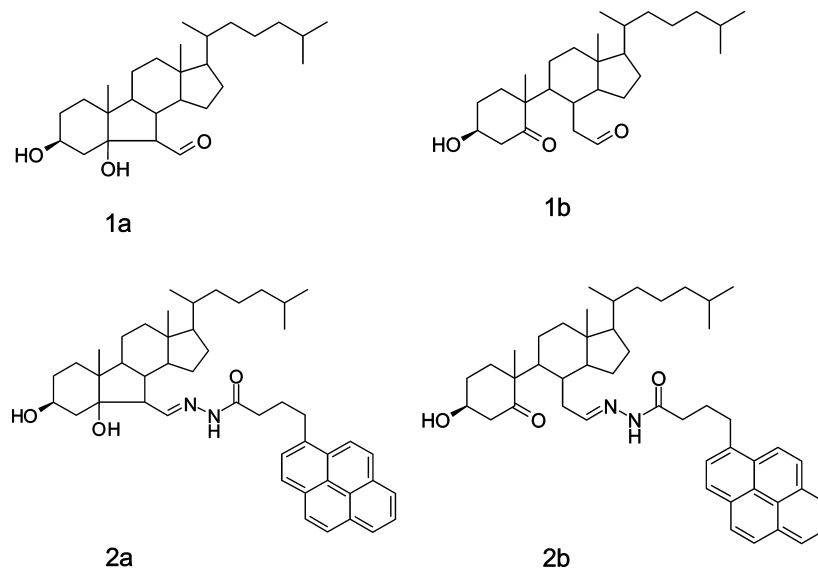
(8) Wentworth, P., Jr.; Nieva, J.; Takeuchi, C.; Galve, R.; Wentworth, A. D.; Dilley, R. B.; DeLaria, G. A.; Saven, A.; Babior, B. M.; Janda, K. D.; Eschenmoser, A.; Lerner, R. A. *Science* **2003**, *302*, 1053–1056.
(9) Brinkhorst, J.; Nara, S. J.; Pratt, D. A. *J. Am. Chem. Soc.* **2008**, *130*, 12224–12225.
(10) Uemi, M.; Ronsein, G. E.; Miyamoto, S.; Medeiros, M. H. G.; Di Mascio, P. *Chem. Res. Toxicol.* **2009**, *22*, 875–884.
(11) Gumulka, J.; Smith, L. L. *J. Am. Chem. Soc.* **1983**, *105*, 1972–1979.
(12) Jaworski, K.; Smith, L. L. *J. Org. Chem.* **1988**, *53*, 545–554.
(13) Wentworth, A. D.; Song, B. D.; Nieva, J.; Shafton, A.; Tripurenani, S.; Wentworth, P. *Chem. Commun.* **2009**, 3098–3100.
(14) Bosco, D. A.; Fowler, D. M.; Zhang, Q.; Nieva, J.; Powers, E. T.; Wentworth, P.; Lerner, R. A.; Kelly, J. W. *Nat. Chem. Biol.* **2006**, *2*, 249–253.
(15) Zhang, Q.; Powers, E. T.; Nieva, J.; Huff, M. E.; Dendle, M. A.; Bieschke, J.; Glabe, C. G.; Eschenmoser, A.; Wentworth, P., Jr.; Lerner, R. A.; Kelly, J. W. *Proc. Natl. Acad. Sci. U.S.A.* **2004**, *101*, 4752–4757.
(16) Scheinost, J. C.; Wang, H.; Boldt, G. E.; Offer, J.; Wentworth, P. *Alzheimer Dis.* **2008**, *47*, 3919–3922.
(17) Usui, K.; Hulleman, J. D.; Paulsson, J. F.; Siegel, S. J.; Powers, E. T.; Kelly, J. W. *Proc. Natl. Acad. Sci. U.S.A.* **2009**, *106*, 18563–18568.
(18) Takeuchi, C.; Galve, R.; Nieva, J.; Witter, D. P.; Wentworth, A. D.; Troseth, R. P.; Lerner, R. A.; Wentworth, P. *Biochemistry* **2006**, *45*, 7162–7170.
(19) Sathishkumar, K.; Gao, X.; Raghavamenon, A. C.; Parinandi, N.; Pryor, W. A.; Uppu, R. M. *Free Radical Biol. Med.* **2009**, *47*, 548–558.
(20) Gao, X.; Raghavamenon, A. C.; D'Auvergne, O.; Uppu, R. M. *Biochem. Biophys. Res. Commun.* **2009**, *389*, 382–387.

**Figure 1.** Structures of cholesterol carboxyaldehyde (**1a**), cholesterol secocholestanal (**1b**) and their corresponding fluorescent adducts formed upon derivatization with 1-pyrenebutyric hydrazide (**2a** and **2b**).

omyoblasts was associated with the induction of ROS generation and the activation of extrinsic and intrinsic pathway.[19]

Besides ozone, recent studies have evidenced the generation of cholesterol aldehydes in the reaction of cholesterol with singlet molecular oxygen. The proposed mechanisms involve Hock-cleavage of cholesterol 5α-hydroperoxide (5α-OOH) in the presence of acids[9] or cholesterol dioxetane decomposition.[10] In both cases, **1a** was detected as the major product. Supporting these studies, Tomono et al.[21] have also detected **1a** as the major product in the incubation of cholesterol with human myeloperoxidase in the presence $H_2O_2$ and chloride ions, a system that is suggested to generate singlet molecular oxygen in activated neutrophils.[22]

Several methods have been used for the determination of cholesterol aldehydes, including mass spectrometry,[10] UV–visible,[8,13,23] and fluorescence detection,[14,21] most of them coupled to liquid chromatography. Although mass spectrometry based methods have shown a good sensitivity, this technique requires specialized people and expensive equipment. UV–visible detection methods using 2,4-dinitrophenylhydrazine (DNPH) have been widely used to detect and quantify aldehydes derived from lipid peroxidation. However, this method is usually carried out in a strong acidic media, which is able to induce the cleavage of cholesterol 5α-OOH to form **1a** and **1b**,[9] therefore leading to an overestimation of the real aldehyde concentration in biological samples. An alternative method used to detect aldehydes involves their reaction with fluorescent probes and the detection of the fluorescent adducts formed. The fluorescent methods have been used to increase detection limits and exclude interferences. The fluorescent probe described in the literature for cholesterol 5,6-secosterols detection is dansyl hydrazine. Bosco and co-workers used this probe in acidic media to detect cholesterol aldehydes in brain.[14]

This manuscript describes a new fluorescence-based method to detect and quantify cholesterol aldehydes using the probe 1-pyrenebytiric hydrazine (PBH) (Figure 1). This method proved to be highly sensitive and has the advantage of minimizing the effect of interfering compounds and not requiring acidic media. The use of acid conditions showed to cause an overestimation of **1a** in a sample containing cholesterol 5α-OOH. Using PBH as the fluorescent probe we could detect **1a** in the low femtomolar range by HPLC coupled to fluorescence detector. Moreover, this methodology allowed detecting and calculating the ratio of **1a** and **1b** formed by the oxidation of cholesterol exposed to singlet molecular oxygen and ozone, respectively.

## EXPERIMENTAL SECTION

**Reagents.** Cholesterol, silica gel (200–400 mesh, 60 Å), 1-pyrenebutyric hydrazide (PBH), deuterated chloroform ($CDCl_3$), sodium phosphate monobasic and dibasic were purchased from Sigma (St. Louis, MO). Methylene blue was purchased from Merck (Rio de Janeiro, Brazil). All the other solvents were of HPLC grade and were acquired from Mallinckrodt Baker (Phillipsburg, NJ). The water used in the experiments was treated with the Nanopure Water System (Barnstead, Dubuque, IA).

**Synthesis of 3β-Hydroxy-5β-hydroxy-B-norcholestane-6β-carboxaldehyde (1a).** **1a** was synthesized by photooxidation of cholesterol in the presence of methylene blue as described previously.[10] Briefly, 200 mg of cholesterol dissolved in 20 mL of chloroform was mixed with 250 μL of methylene blue (10 mM in methanol). This solution was cooled at 4 °C and irradiated under continuous agitation using two tungsten lamps (500 W) during 2.5 h. The formation of cholesterol oxidation products were checked by thin-layer chromatography using ethyl acetate and isooctane (1:1, v/v) as the eluent. **1a** was purified from the reaction mixture by flash column chromatography, using silica gel and a gradient of hexane and ethyl eter. The purified **1a** was analyzed and quantified in $CDCl_3$ by NMR spectroscopy using DRX500 instrument, AVANCE series (Bruker-Biospin, Rhein-stetten, Germany) as described previously.[10] For the quantifica-

(21) Tomono, S.; Miyoshi, N.; Sato, K.; Ohba, Y.; Ohshima, H. *Biochem. Biophys. Res. Commun.* **2009**, *383*, 222–227.
(22) Kiryu, C.; Makiuchi, M.; Miyazaki, J.; Fujinaga, T.; Kakinuma, K. *FEBS Lett.* **1999**, *443*, 154–158.
(23) Wang, K. Y.; Bermudez, E.; Pryor, W. A. *Steroids* **1993**, *58*, 225–229.

tion, 2 $\mu$L of proprionaldehyde were added as the internal standard into 750 $\mu$L of the **1a** solution in CDCl$_3$. The $^1$H signal corresponding to the aldehyde group of the internal standard and **1a** appeared at 9.73 and 9.62 ppm, respectively. The relative signals of $^1$H of aldehydes were integrated by Mestre C software (Figure S1 in the Supporting Information (SI)).

**Synthesis of 3$\beta$-Hydroxy-5-oxo-5,6-secocholestan-6-al (1b).** **1b** was prepared by ozonation of cholesterol as described by Wentworth et al.[8] and Wang et al.[24] Ozone was produced at a rate of 100 mg/h by passing pure oxygen through AquaZone PLUS 200 instrument (Red Sea Fish Pharm. Ltd., Houston, TX). Oxygen flow rate was set to 10 mL/min. A solution of 10 mg/mL of cholesterol in chloroform was cooled at dry ice temperature and oxidized by bubbling ozone for 5 min. After oxidation, chloroform was evaporated with nitrogen gas and the residue was stirred for 2 h at room temperature with Zn powder (19.4 mg) in water-acetic acid (1:19 v/v; 3.1 mL). Dichloromethane (15 mL) was added and the mixture was washed five times with deionized water (5 × 15 mL). The organic phase was evaporated to dryness in vacuo. The residue was dissolved in isopropyl alcohol and kept at −80 °C for further analysis. The characterization of **1b** was performed by NMR spectroscopy using a DRX500 instrument, AVANCE series (Bruker-Biospin, Rheinstetten, Germany) operating at 11.7 T. Cholesterol ozonation followed by Zn reduction in acetic acid gave **1b** as a major aldehyde, as confirmed by $^1$H NMR analysis ($\delta$, ppm, CDCl$_3$): $\delta$ 9.607 (s, $J$ = 0.5 Hz, 1H, CHO), 4.466 (s, 1H, H-3), 3.097 (dd, $J$ = 13.5, 4.0 Hz, 1H, H-4e), 1.010 (s, 3H, CH$_3$-19), 0.671 (s, 3H, CH$_3$-18) (Figure S2 in the SI).

**Derivatization of Cholesterol Aldehydes with PBH.** The optimal conditions for the derivatization of cholesterol aldehydes were established using the purified **1a**. Time-course of PBH adduct formation with **1a** was monitored by incubating 100 $\mu$M **1a** with 2 mM PBH in isopropanol at 37 °C under continuous agitation for up to 8 h. Aliquots of 1 $\mu$L of the reaction mixture were taken at specified times and analyzed by HPLC coupled to fluorescence detector. The ideal concentration of the probe was determined by incubating 1 $\mu$M of **1a** in the presence of 1−1000 $\mu$M of PBH in isopropanol at 37 °C under continuous agitation for 6 h. The effect of the pH in the formation of **2a** was analyzed by incubating 1 $\mu$M of **1a** with 50 $\mu$M PBH in a reaction system consisted of isopropanol:10 mM phosphate buffer at pH 5.7, 7.4, and 8.0 (90:10, vol/vol). Quantitative analysis of **1a** was done by incubating an aliquot of sample with 600 $\mu$M of the probe in isopropanol containing 1 mM phosphate buffer at pH 7.4 (neutral condition) or 0.1 mM HCl (acid condition) at 37 °C for 6 h.

**Analysis of the Fluorescent Adduct by HPLC Coupled with Fluorescence Detector.** HPLC analysis was carried out on a Shimadzu Prominence system (Tokyo, Japan), consisted of LC-20AT pumps, SIL-20AV autosampler, RF-10Axl fluorescence detector, and a CBM-20A controller. One microliter of the sample was injected into a reversed-phase column Synergi C18 (50 × 4.6 mm, 2.5 $\mu$m particle size, Phenomenex, Torrance, CA). The HPLC mobile phase consisted of water (A) and methanol (B), and the flow rate was 1 mL/min. The separation of the fluorescent adducts was done using the following condition: 86% B for 5 min, 86−92% in 1 min, 92% B for 15 min, and 92−86% B in 1 min. The excitation and emission wavelengths were fixed at 339 and 380 nm,

respectively.[25] For the analysis 1 $\mu$L was injected through the autosampler. Data were acquired at high sensitivity and gain of 1× in the fluorescence detector. Fluorescence spectra were acquired by the fluorescence detector RF-551 (Shimadzu, Japan). HPLC data were processed using the LC solution software (Shimadzu, Japan).

**Analysis of the Fluorescent Adducts by HPLC-MS/MS.** The PBH fluorescent adducts formed with **1a** and **1b** were analyzed by a HPLC system connected to a UV−visible detector (SPD 10 AVVP, Shimadzu, Kyoto, Japan) and a Quattro II triple quadrupole tandem mass spectrometer (Micromass, Manchester, UK) (HPLC-MS/MS). HPLC separation was carried out as described above. The eluent from the column was monitored at 342 nm and 10% of the HPLC flow rate was directed into the mass spectrometer. The fluorescent adducts were detected using electrospray ionization (ESI) in the positive ion mode. The source and desolvation temperature of the mass spectrometer were set at 100 and 200 °C, respectively. The cone voltage was set to 50 V, the extractor cone voltage was set to 5 V and the capillary and the electrode potentials were set at 4.5 and 0.5 kV, respectively. Collision energy was set at 20 eV for **2a** and 30 eV for **2b**. Full-scan data was acquired over a mass range of 100−900 $m/z$. Data was processed by means of the MassLynx NT software.

**Cholesterol Oxidation Induced by Photooxidation, Ozone and HOCl/H$_2$O$_2$.** Cholesterol (10 mg/mL in chloroform) was photooxidized in the presence of methylene blue for 2.5 h. An aliquot of this sample was taken for cholesterol aldehyde determination. The ozonation of cholesterol (10 mg/mL in chloroform) was conducted essentially as described for the synthesis of **1b**. After 5 min ozonation, chloroform was evaporated by nitrogen gas and the residue was dissolved in isopropanol. An aliquot of this sample was diluted and used for cholesterol aldehyde determination. The oxidation of cholesterol by HOCl/H$_2$O$_2$ system was conducted by incubating a 10 mM cholesterol solution containing 1% ethanol in 10 mM phosphate buffer at pH 7.4 with 1 mM HOCl and H$_2$O$_2$, under continuous agitation at 37 °C for 5 min.

**Method Validation.** The limit of quantification (LOQ) was established as the amount of adduct formed that generated a signal 6-fold higher than baseline. The limit of detection (LOD) was established as the amount of adduct formed that generated a signal 3-fold higher than baseline. The reproducibility was checked by intra- and interday analysis. Interday analyses were conducted on three consecutive days.

## RESULTS

**Synthesis and Characterization of 1a.** Cholesterol carboxyaldehyde (**1a**) was synthesized by photooxidation of cholesterol.[10] After the reaction, the oxidized products were purified by flash column chromatography and **1a** was isolated. The identity of **1a** was confirmed by NMR spectroscopy as described by Uemi et al.[10] The $^1$H NMR analysis showed a doublet peak at 9.62 ppm consistent with the presence of the aldehyde group in **1a** structure (Figure S1 in the SI). **1a** was quantified by $^1$H NMR analysis using proprionaldehyde as the internal standard as described in the experimental section.

**Characterization of 2a Fluorescent Adduct.** Using the purified **1a** sample, several experiments were conducted to

(24) Wang, K. Y.; Bermudez, E.; Pryor, W. A. *Steroids* **1993**, *58*, 225–229.

(25) Morsel, J. T.; Schmiedl, D. *Freseniu*ś *J. Anal. Chem.* **1994**, *349*, 538–541.
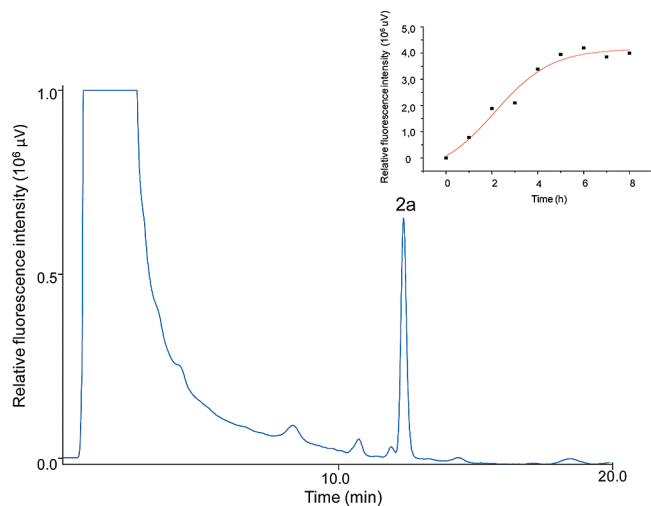
**Figure 2.** Analysis of **2a** fluorescent adduct, formed in the reaction of **1a** with PBH by HPLC coupled to fluorescence detector. HPLC/fluorescence chromatogram obtained for the analysis of **2a** using excitation at 339 nm and emission at 380 nm. For the derivatization, 5 pmol of **1a** was incubated with PBH 100 $\mu$M in a final volume of 100 $\mu$L isopropanol at 37 °C for 6 h under agitation. Analysis was done by injecting 1 $\mu$L of the reaction mixture into the HPLC. The inset shows the time dependent formation of **2a** during incubation of 100 $\mu$M of **1a** in the presence of 2 mM of PBH for up to 8 h.

establish the optimal conditions for the reaction with PBH. Incubations of **1a** with PBH were conducted in isopropanol at 37 °C under continuous agitation. HPLC analysis using fluorescence detection showed the appearance of an intense peak at 12.5 min, corresponding to the fluorescent adduct **2a** (Figure 2). The pH effect on **2a** adduct formation was analyzed. Incubations conducted at pH 5.7, 7.4, and 8.5 showed that this adduct was preferentially formed at pH 5.7 (Figure S3 in the SI), which is in accordance with favorable formation of Schiff base adduct at slightly acidic conditions.

A time-course analysis of **2a** showed a time-dependent increase of the peak area up to 4 h, reaching a *plateau* after this time (inset, Figure 2). Based on this, the incubation time for the derivatization was fixed to 6 h. The ideal concentration of PBH for the reaction was established by incubating **1a** (1 $\mu$M) in the presence of 1−1000 $\mu$M of PBH. The fluorescent adduct formation reached its maximum with PBH concentration higher than 50 $\mu$M.

The fluorescence of **2a** was characterized to establish the optimal excitation and emission wavelengths. Fluorescence analysis of **2a** showed a spectrum similar to the original probe with excitation and emission wavelengths maximum at 339 and 380 nm, respectively (Figure 3). Thus, indicating that adduct formation does not alter the fluorescence spectra of the probe.

The formation of **2a** was also confirmed by HPLC-MS/MS. The mass spectrum of **2a** acquired by ESI in the positive ion mode showed peaks corresponding to **2a** molecular ion ([M+H]$^+$) and its sodium adducts ([M+Na]$^+$) at $m/z$ 703 and 725, respectively (Figure 4A and 4B). Two other peaks at $m/z$ 685 and 667 were also detected, corresponding to the loss of one ([M+H−H$_2$O]$^+$) and two water molecules ([M+H−2H$_2$O]$^+$), respectively. These ions were also observed in the MS/MS spectrum of $m/z$ 703 (Figure 4C). The MS/MS spectrum also showed other fragment ions at $m/z$ 431, 398, 365, and 303. The first three, correspond to the ions formed by the loss of pyrene butyric (PB) group
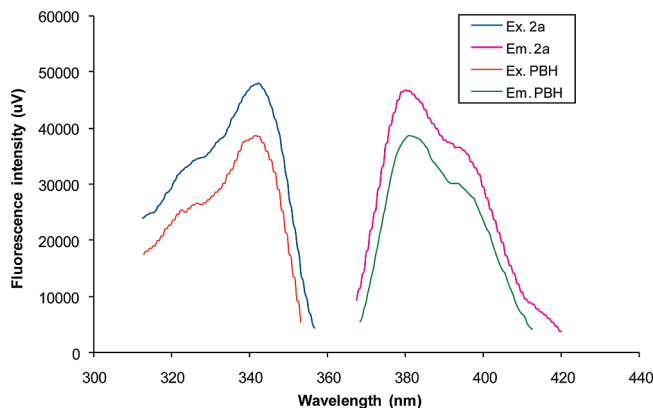


**Figure 3.** Fluorescence excitation and emission spectra of PBH and **2a**. Both compounds showed the same excitation and emission maximum wavelengths at 339 and 380 nm, respectively.

([M+H−PB]$^+$, $m/z$ 431), PBH and two protons ([M+H−PBH−2H]$^+$, $m/z$ 398) and PBH and two water molecules ([M+H−PBH−2H$_2$O]$^+$, $m/z$ 365), respectively. The fragment ion at $m/z$ 303 corresponds to the positively charged PBH ion.

**Reproducibility and Stability.** The intra- and interday reproducibility of the assay procedure was determined by evaluating three individual reactions containing **1a** (1 pmol; 1 $\mu$M final concentration) and PBH (50 $\mu$M). The relative standard deviation for the intra- and interday reproducibility at this concentration was 1.7% and 7.6%, respectively.

The stability of **2a** adduct was evaluated in triplicate reactions of **1a** (1 pmol; 1 $\mu$M final concentration) with PBH (50 $\mu$M). After derivatization, these samples were kept in vials inside the autosampler at 4 °C and the **2a** peak was monitored up to 6 h. There was no significant change in the peak area of the fluorescence signal during this period.

**Standard Curve, Limit of Detection and Limit of Quantification.** A calibration curve was constructed using 5−100 fmol (50−1000 nM) of **1a** in triplicate reaction in a final volume of 100 $\mu$L. Peak area of **2a** increased linearly over this concentration range with $R^2$ value of 0.9962 and $Y = 6.64 \times 10^3 X + 1.65 \times 10^4$. The limit of detection (LOD) and quantification (LOQ) of **1a** was 10 fmol (10 nM) and 20 fmol (20 nM), respectively.

**Application of PBH for Cholesterol Aldehyde Detection in Oxidized Cholesterol Samples.** The newly developed fluorescence-based method was applied for the detection and quantification of **1a** in cholesterol samples oxidized by photooxidation or ozone. Cholesterol photooxidation gave rise to a major peak at 12.5 min (Figure 5A). On the other hand, cholesterol ozonation yielded an intense peak at 10.3 min as well as some other smaller peaks, including the same peak at 12.5 min observed for the photooxidation (Figure 5B). Peak assignment was done by comparison of the retention times of the peaks with those obtained for the standard samples of **1a** (Figure 5C) and **1b** (Figure 5D). In this way, the peaks observed at 10.3 and 12.5 min were assigned to the fluorescent adducts **2b** and **2a**, respectively. Additionally, the identity of the peaks was confirmed by HPLC-MS/MS analysis (Figure S4 in the SI). It should be noted that the overall retention times for the analysis by HPLC-MS/MS were increased by almost 2 min compared to the analysis by HPLC/fluorescence detection. This retention time delay was due to the differences in room
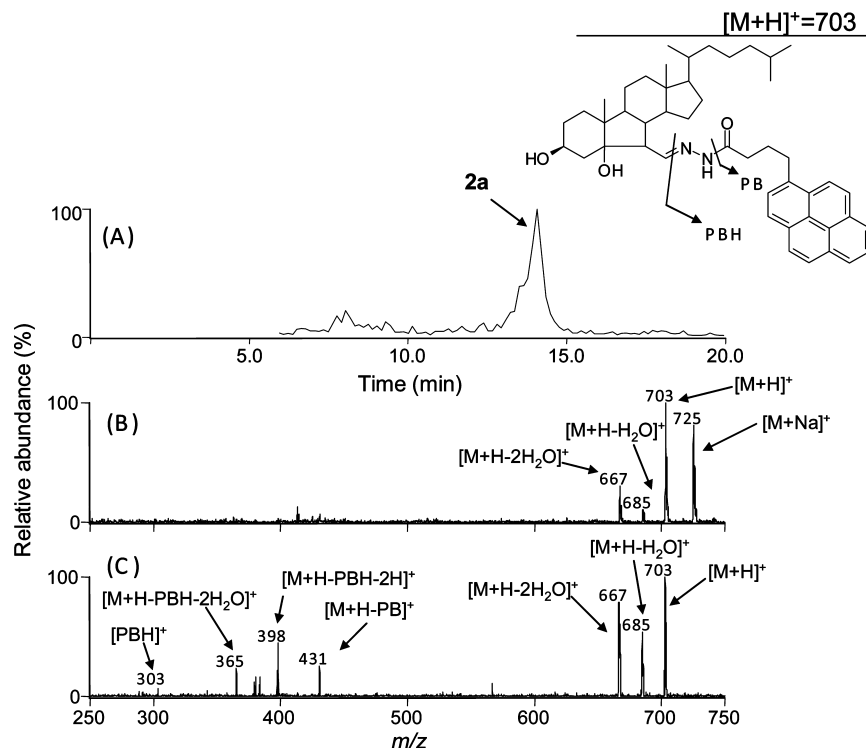
**Figure 4.** Analysis of **2a** by HPLC-MS/MS using ESI in the positive ion mode. The cone voltage and the collision energy were set to 50 V and 20 eV, respectively. Selected ion chromatogram of the ion at $m/z$ 703 (A). Spectrum of the peak corresponding to **2a** at 14 min (B). Fragment ion spectrum of $m/z$ 703 (C).
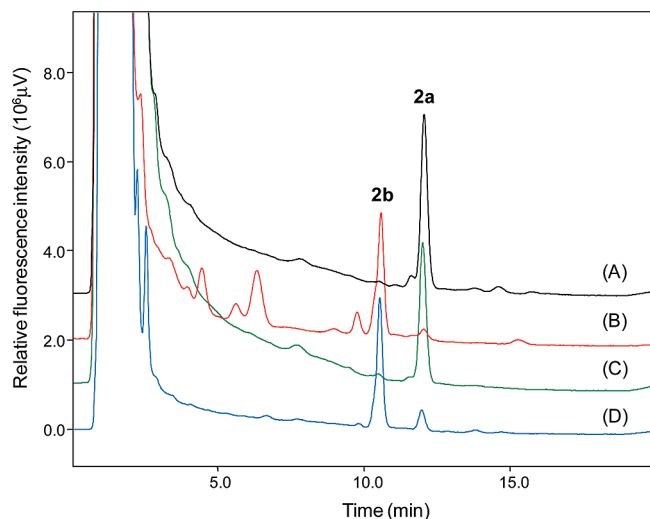


**Figure 5.** Analysis of cholesterol aldehydes formed in the photo-oxidation (A) and ozonation (B) of cholesterol using PBH. An aliquot of the sample was reacted with PBH (600 $\mu$M) for 6 h and analyzed by HPLC coupled to fluorescence detector. For peak assignment standard samples containing **1a** (C) or **1b** (D) were also reacted with PBH and analyzed.

temperatures, which was about 5 °C lower in the case of HPLC-MS/MS analysis.

The major fluorescent adduct detected in cholesterol ozonation was further characterized by HPLC-MS/MS analysis (Figure 6). Selected ion mass chromatogram of the ion at $m/z$ 703 showed a single peak at 12 min. (Figure 6A). Mass spectrum for this peak showed two major ions, one at $m/z$ 703 and other at $m/z$ 725 (Figure 6B), which corresponds to the molecular ion ([M+H]$^+$)

and the sodium adduct ([M+Na]$^+$) of **2b** (Figure 6B). Collision induced dissociation of the ion at $m/z$ 703, showed the same fragment ions observed for **2a**, suggesting that the peak corresponds to its isomer, **2b** (Figure 6C). Fragments ions observed at $m/z$ 685 and 667 are formed by the loss of one and two water molecules from **2b**, respectively. The ions at $m/z$ 431, 398, 383, and 365 are formed by the loss of PB, PBH and two protons, PBH and one water, and PBH and two water molecules from **2b**, respectively (Figure 6C).

Aiming to get a quantitative data on cholesterol aldehyde formation, a calibration curve constructed for **1a** was used to determine its concentration. For the quantification, oxidized cholesterol samples were diluted to get a final cholesterol concentration of 219 $\mu$M. The amounts of **1a** detected in the samples by PBH method at neutral pH were 19.1 ± 4.0 $\mu$M and 0.7 ± 0.3 $\mu$M for the photooxidation and ozonation, respectively. This corresponds to a **1a** yield of 8.7% for the photooxidation and 0.3% for the ozonation. For comparison, **1a** quantification was also done using dansyl hydrazine method in the presence of acid (0.1 mM HCl) (method in the SI). The concentrations of **1a** determined by this method were 35.2 ± 0.7 $\mu$M and 1.0 ± 0.1 $\mu$M in the photooxidation and ozonation, respectively. This provides **1a** yields of 16% for the photooxidation and 0.4% for the ozonation. As can be clearly noticed, the **1a** yield determined by the dansyl hydrazine method was overestimated by almost 2-folds for the photooxidation. The same result was obtained when PBH derivatization was conducted in the presence of acid. Under this condition, the **1a** concentration was 32.6 ± 0.7 $\mu$M, which corresponds to a **1a** yield of 15% in the photooxidation. These results are consistent with the fact that photooxidized cholesterol
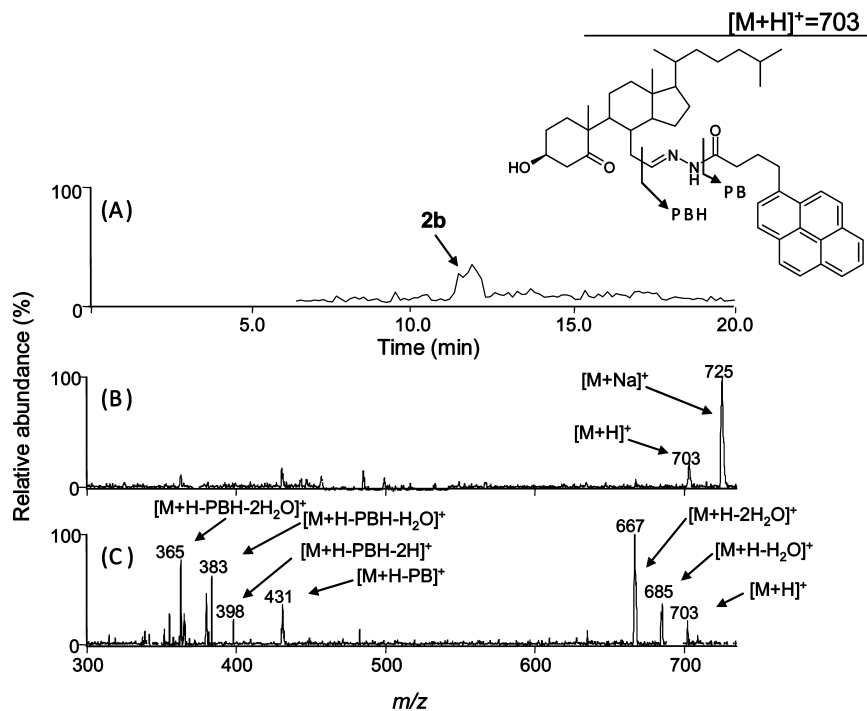
**Figure 6.** Analysis of **2b** by HPLC-MS/MS using ESI in the positive ion mode. The cone voltage was set to 50 V and the collision energy was set to 30 eV. Selected ion chromatogram for the ion at $m/z$ 703 (A). Mass spectrum of the peak corresponding to **2b** at 12 min (B). Fragment ion spectrum of $m/z$ 703 (C).

samples contain cholesterol $5\alpha$-OOH, which in the presence of acids is easily converted to **1a**.[9]

Moreover, the sensitivity of PBH and dansyl hydrazine methods were also compared (Figure S5 in the SI). PBH method conducted at neutral pH was almost 10 times more sensitive than dansyl hydrazine method. This difference was even larger when PBH reaction was carried out with acid, reaching a 90 times higher sensitivity.

PBH was also used for the quantification of ChAld formed during cholesterol oxidation promoted by the $HOCl/H_2O_2$ reaction system. This is a biologically relevant reaction system that is known to generate stoichiometric amounts of singlet molecular oxygen. The formation of **2a** was analyzed by HPLC coupled with fluorescence detector (Figure 7). The complete reaction system containing cholesterol and $HOCl/H_2O_2$ showed the appearance of an intense fluorescent peak corresponding to **2a**. The fluorescent adduct was quantified using the calibration curve and a value of 0.2 $\mu$M of **1a** was found. This corresponds to a yield of 0.2%.

## DISCUSSION

Cholesterol is oxidized in the presence of reactive oxygen species generating aldehydes, hydroperoxides and epoxides.[6,7] Recently, two cholesterol aldehydes have attracted attention, the cholesterol carboxyaldehyde (**1a**) and cholesterol secoaldehyde (**1b**). The formation of **1a** and **1b** was first described in the oxidation of cholesterol with ozone.[11,12] Wentworth and co-workers reported the presence of **1a** and **1b** in atherosclerotic plaques and related the detection of these aldehydes as an evidence for ozone generation in human tissues.[8] On the other hand, two recent studies identified the generation of **1a** in the reaction of cholesterol with singlet molecular oxygen.[9,10] Indeed, Brinkhorst and
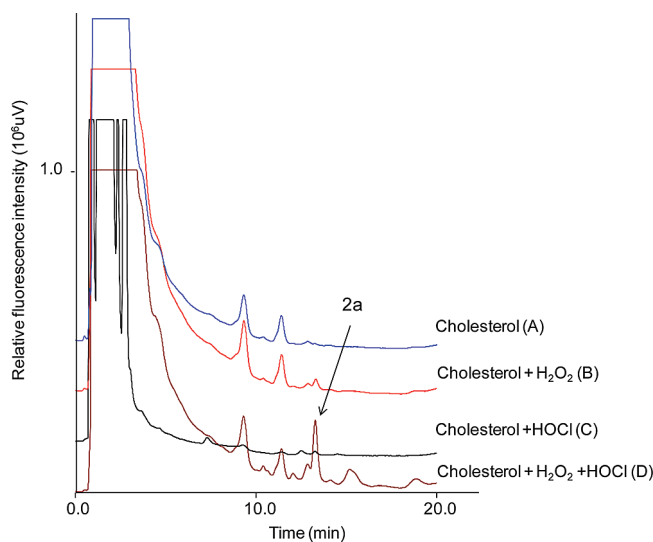


**Figure 7.** Analysis of cholesterol aldehydes generated by the reaction of cholesterol with $H_2O_2$ and HOCl using PBH. HPLC/fluorescence chromatograms obtained for cholesterol (A), and cholesterol incubated with $H_2O_2$ (B), HOCl (C), and $H_2O_2$ + HOCl (D). Reactions were carried out with 100 $\mu$M cholesterol in the presence of 1 mM HOCl, 1 mM $H_2O_2$ and 100 $\mu$M PBH for 6 h at 37 °C under continuous agitation.

co-workers reported the formation of **1a** from cholesterol $5\alpha$-hydroperoxide by Hock cleavage in acid media[9] and Uemi and co-workers reported the formation of **1a** in the reaction of cholesterol with singlet molecular oxygen generated either by photooxidation or by the thermodecomposition of endoperoxides.[10]

In this study, we have developed a new detection method for cholesterol carboxyaldehyde, **1a**, using the fluorescent probe PBH, which contains the highly fluorescent pyrene group. The

reaction of **1a** with PBH can be conducted in the absence of acids, which is important to avoid the formation of **1a** from acid catalyzed cholesterol 5α-OOH decomposition.[9] Bosco and co-workers[14] used dansyl hydrazine as a fluorescent label to detected **1a** and **1b** in a brain tissue sample from Lewy body disease. However, the derivatization of cholesterol aldehydes with dansyl hydrazine is conducted in the presence of strong acids, such as, 5 mM sulfuric acid.[14] In fact, we have done a comparative analysis of the two fluorescent probes (PBH and dansyl hydrazine) to detect **1a** in vitro and observed that the method using dansyl hydrazine can overestimate the basal level of **1a**, especially in samples containing cholesterol 5α-OOH. The **1a** yields in photooxidized cholesterol samples estimated by PBH (neutral pH) and dansyl hydrazine were 8.7% and 16.0%, respectively. This data indicates that the derivatization in the absence of acid is a critical point that should be considered when estimating **1a** basal level in samples, especially when they were oxidized by singlet molecular oxygen. When comparing dansyl hydrazine and PBH methods, the latter was approximately 10 times more sensitive for **1a** detection (Figure S5 in the SI). This difference was even larger when PBH derivatization was carried out at acid condition, clearly evidencing the superiority of PBH method compared to dansyl hydrazine in terms of sensitivity.

A number of studies has detected the formation of cholesterol aldehydes in vitro,[9,10,21] as well as in vivo.[8,14−16] In this study, we have used PBH to analyze the formation of **1a** during cholesterol oxidation mediated by ozone and singlet molecular oxygen. The reaction of cholesterol with ozone yielded **1a** and **1b** and also other minor unidentified products. We could not quantify exactly the amount of **1b** due to the lack of an appropriate pure standard for it. Nonetheless, the relative peak intensities suggest that cholesterol ozonation yields **1b** as a major product and a small amount of its aldolization product (Figure 5). The estimated ratio of **1a:1b** in the ozonation was 1:10. Similar results were described for the ozonation of human LDL, where a relative yield of 1:4 was found.[13] On the other hand, cholesterol oxidation promoted by singlet molecular oxygen yielded **1a** as the major product consistent with the data described by Brinkhorst et al.[9] and Uemi et al.[10] The estimated yield of **1a** in the photooxidation of cholesterol was approximately 8.7% and the ratio of **1a:1b** was 165:1. These values are in agreement with those reported for the photooxidation of human LDL using hematoporphyrin IX for 14 h where only **1a** was detected.[13] The incubation of cholesterol in

the presence of $H_2O_2$ and HOCl also gave **1a** as the major product, consistent with the oxidation of cholesterol promoted by singlet molecular oxygen. It is known that the reaction of $H_2O_2$ with HOCl generate stoichiometric amounts of singlet molecular oxygen[26] and this reaction is suggested to play an important role during inflammatory conditions.[22] The predominant formation of **1a** over **1b** by this reaction was also reported by Tomono and co-workers.[21] They incubated cholesterol (100 $\mu$M) in the presence of $H_2O_2$ (100 $\mu$M) and NaOCl (100 $\mu$M) and detected five times more **1a** than **1b** using dansyl hydrazine as a fluorescent probe.[21]

## CONCLUSIONS

We have developed a new sensitive method for the detection of cholesterol aldehydes using PBH as a fluorescent probe. This new methodology allows detecting and quantifying the relative amounts of **1a** and **1b** with high sensitivity, which is important to assess the relative contributions of ozone and singlet molecular oxygen to the oxidation of cholesterol in biological systems. Derivatization of cholesterol aldehydes using PBH can be conducted without the addition of strong acids, which is important for the determination of the basal level of cholesterol aldehydes present in biological tissues from different sources. In conclusion, the easy and reliable method developed in this study can help to investigate the formation cholesterol aldehydes in biological system, which is critical to clarify their relevance in disease progression.

## SUPPORTING INFORMATION AVAILABLE

NMR analysis of **1a** and **1b**. HPLC-MS/MS detection of **2a** and **2b**. HPLC-fluorescence data showing the pH effect on **2a** formation and the sensitivity of dansyl hydrazine and PBH methods. Dansyl hydrazine derivatization method. This material is available free of charge via the Internet at http://pubs.acs.org.

(26) Khan, A. U.; Kasha, M. *J. Am. Chem. Soc.* **1970**, *92*, 3293–3300.

# Highly sensitive fluorescent method for the detection of cholesterol aldehydes formed by ozone and singlet molecular oxygen

*Fernando V. Mansano, Rafaella M.A. Kazaoka, Graziella E. Ronsein, Fernanda M. Prado, Thiago C.Genaro-Mattos, Miriam Uemi, Paolo Di Mascio, Sayuri Miyamoto\**

Departamento de Bioquímica, Instituto de Química, Universidade de São Paulo,

CP26077, CEP 05513-970, São Paulo, SP, Brazil.

## SUPPORTING INFORMATION

Contents:

**Figure S1.** $^1$H NMR spectrum of **1a** acquired in CDCl$_3$. The doublet peak in 9.62 ppm corresponds to the hydrogen of the aldehyde group.
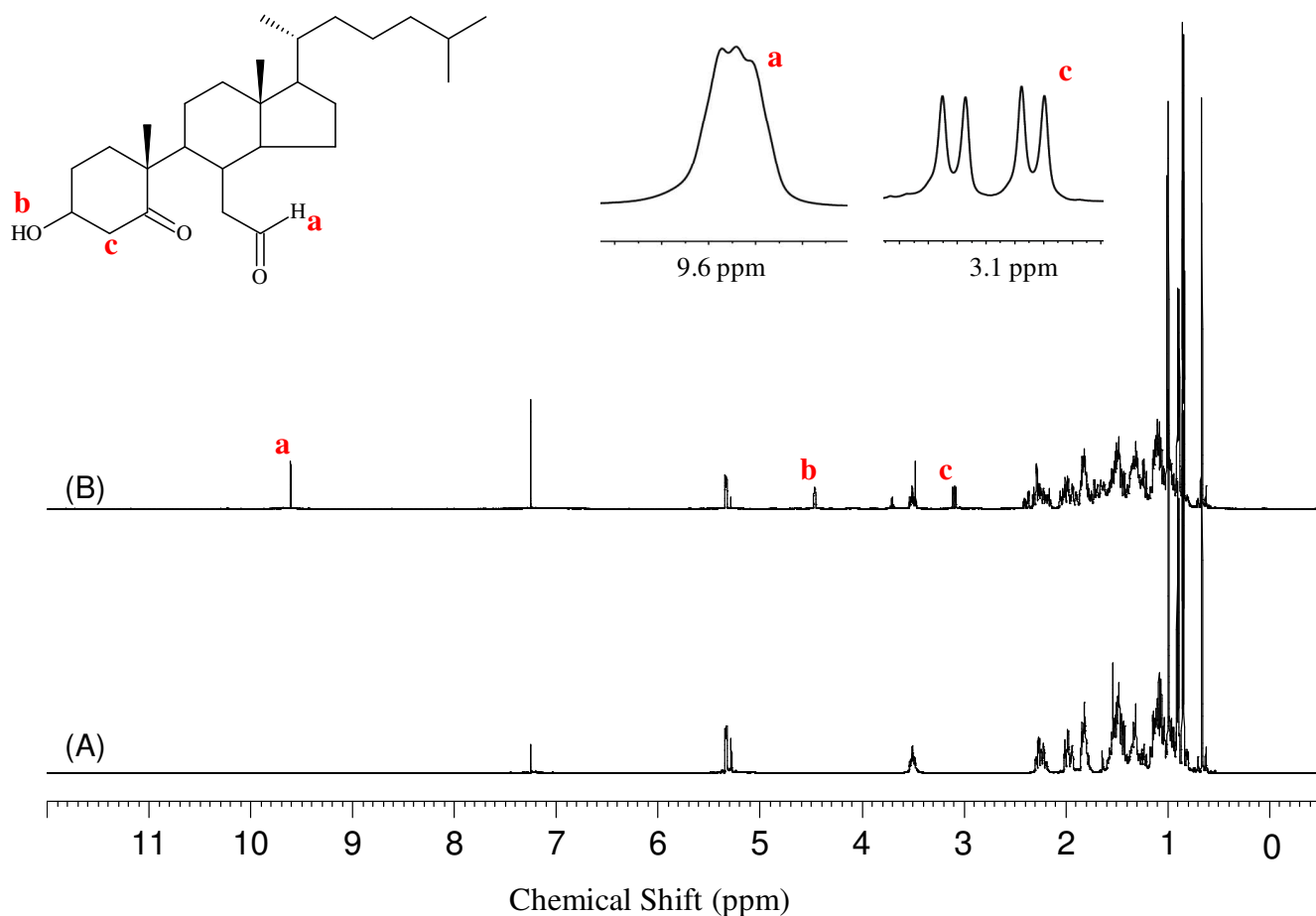
**Figure S2**. Comparative $^1$H NMR spectra (500 MHz; CDCl$_3$) of cholesterol before (A) and after ozonation and Zn reduction (B). Relevant protons observed for **1b** are indicated in the structure: (CDCl$_3$) **a**, δ 9.607 (s, J=0.5 Hz, 1H, CHO), **b**, 4.466 (s, 1H, H-3), **c**, 3.097 (dd, J=13.5, 4.0 Hz, 1H, H-4e).
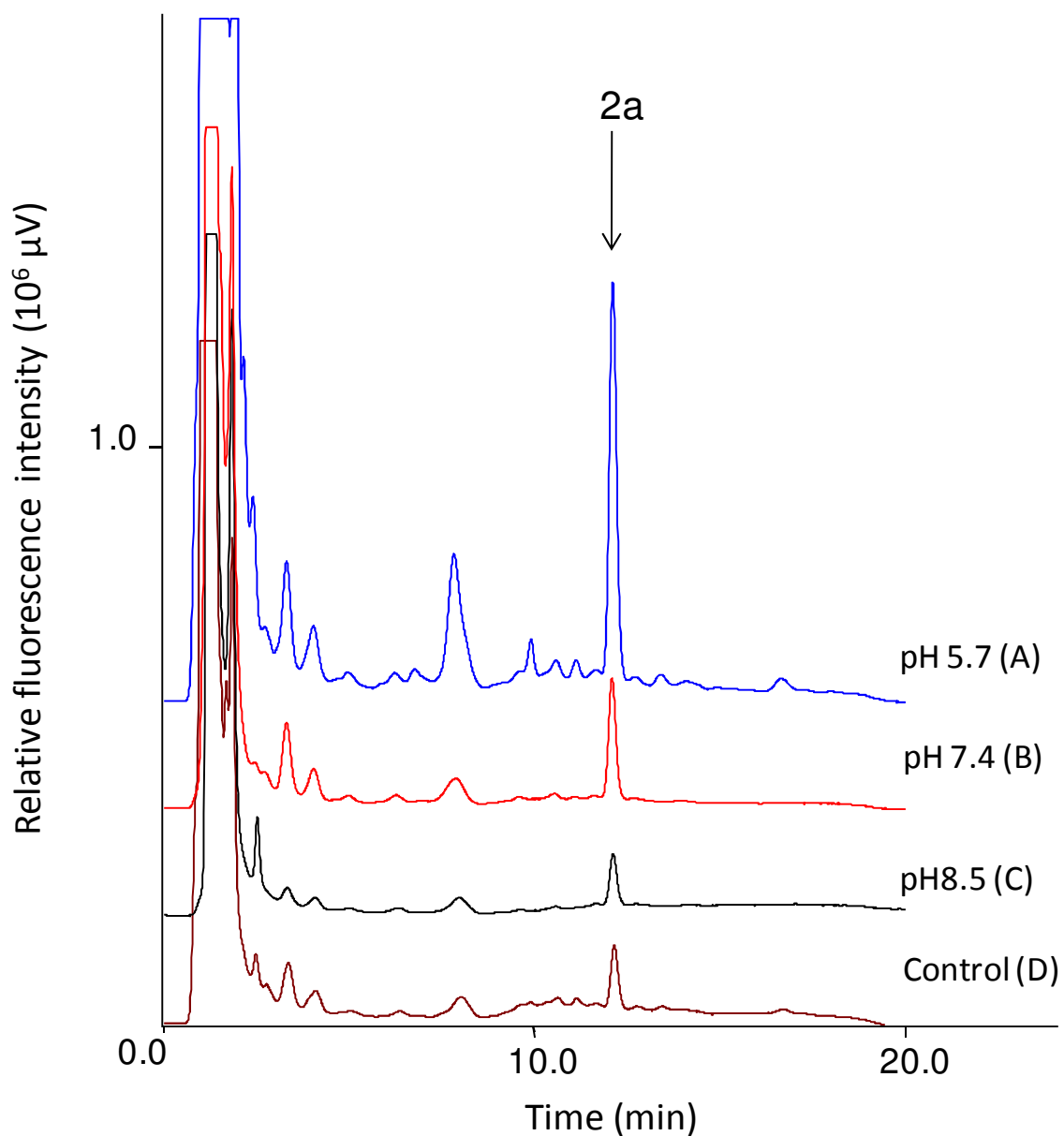
3

**Figure S3.** HPLC/fluorescence analysis of **2a** adduct formed at different pHs. For the reaction 0.1 pmol (final volume 100 μl) of **1a** was incubated with 100 μM PBH in 10mM phosphate buffer at pH 5.7 (A), 7.4 (B), 8.5 (C) and control without buffer (D) for 6 h at 37°C under continuous agitation. For the analysis 1μl was injected into the HPLC.
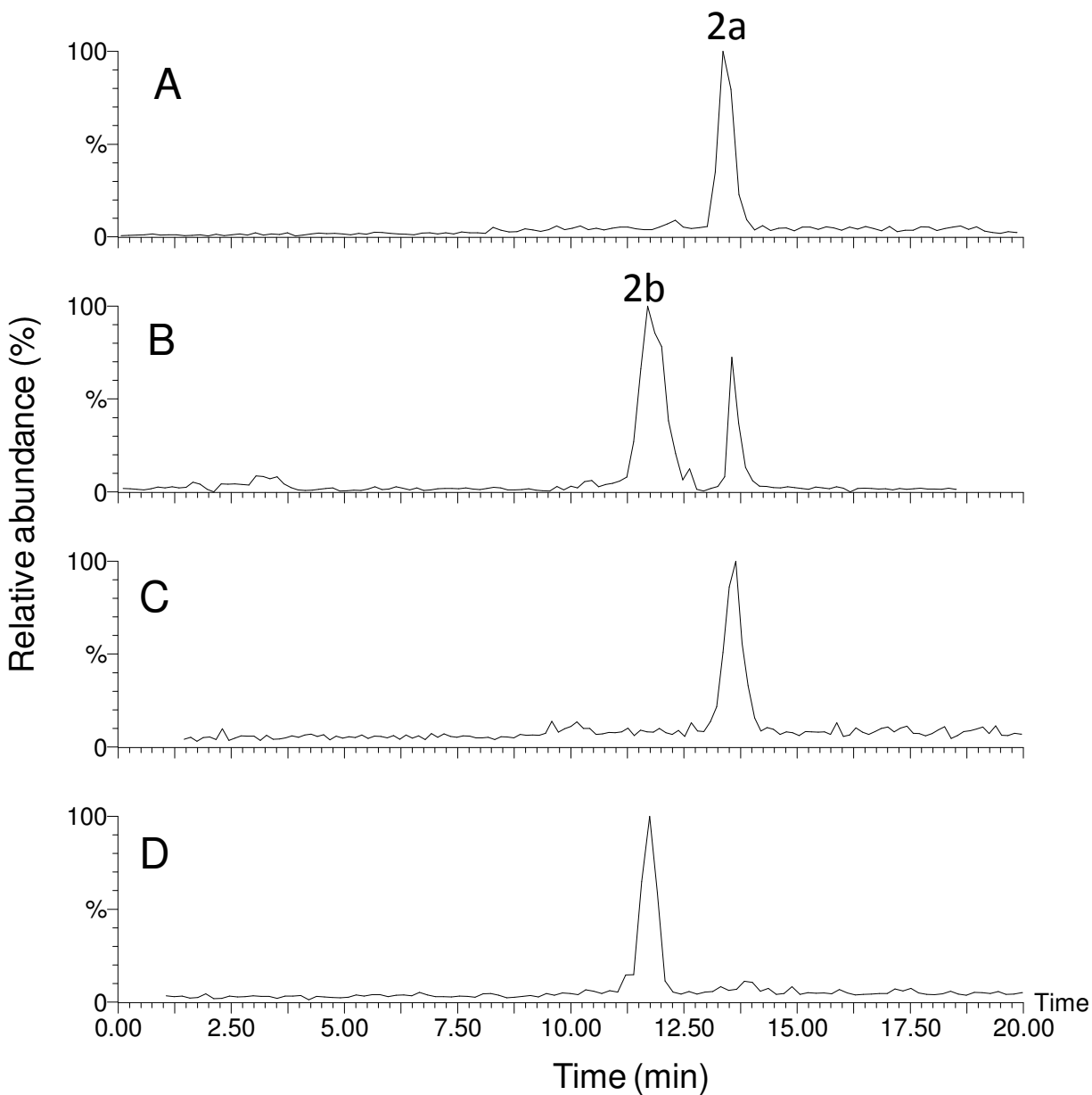
**Figure S4**. Analysis of cholesterol aldehydes formed in the photooxidation (A) and ozonation (B) of cholesterol using PBH by HPLC-MS/MS. Typical chromatograms obtained by selecting the ion at m/z 725, which corresponds to the sodium adduct of **2a** and **2b** ions ([M+Na]$^+$). For peak assignment standard samples containing **1a** (C) or **1b** ( D) were also derivatized with PBH and analyzed.
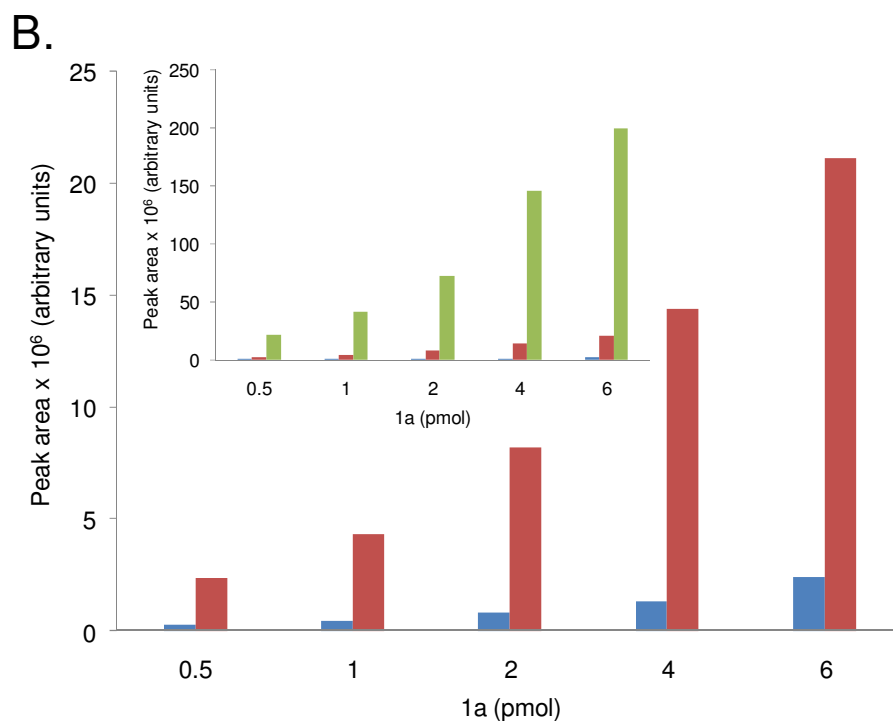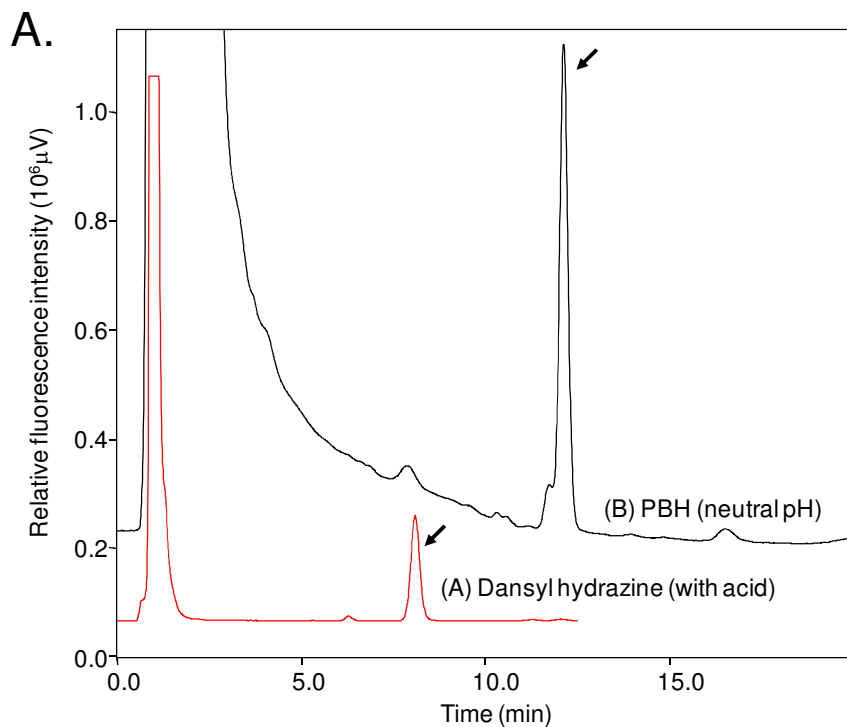
**Figure S5**. A. Comparative HPLC/fluorescence analysis of **1a** (4 pmol) derivatized with dansyl hydrazine (2 mM with HCl 0.1 mM) or PBH (600 μM at pH 7.4). B. Peak areas obtained for increasing concentrations of **1a** derivatized with dansyl hydrazine (blue bars) or PBH at neutral (red bars) and acid (green bars) conditions. The inset shows the comparative results between the three methods.

**Method**

**Cholesterol aldehyde derivatization with dansyl hydrazine**. Quantification of **1a** was conducted with dansyl hydrazine and PBH as fluorescent probes. Derivatization with dansyl hydrazine was done by incubating **1a** with 2 mM dansyl hydrazine solution containing 0.1 mM HCl in acetonitrile at 37 °C for 4h as described by Tomono and coworkers [21]. An aliquot of 1 µl of this solution was injected into the HPLC system (Shimadzu, Japan). Separation was done on a reversed-phase column Synergi™ C18 (50 mm x 4.6 mm, 2.5 µm particle size, Phenomenex, Torrance, CA), using a mobile phase consisted of 80 % acetonitrile in water at a flow rate of 1 ml/min. The excitation and emission wavelength were fixed at 336 nm and 534 nm, respectively.

# Behavior of the thermal diffusivity of native and oxidized human low-density lipoprotein solutions studied by the Z-scan technique

Priscila R. Santos
Thiago C. Genaro-Mattos
Andrea M. Monteiro
Sayuri Miyamoto
Antonio M. Figueiredo Neto

# Behavior of the thermal diffusivity of native and oxidized human low-density lipoprotein solutions studied by the Z-scan technique

**Priscila R. Santos,[a] Thiago C. Genaro-Mattos,[b] Andrea M. Monteiro,[a] Sayuri Miyamoto,[b] and Antonio M. Figueiredo Neto[a]**
[a]Universidade de São Paulo, Instituto de Física, Departamento de Física Experimental, Rua do Matão, Travessa R, 187, 05508-090, São Paulo, Brazil
[b]Universidade de São Paulo, Instituto de Química, Departamento de Bioquímica, Av. Prof. Lineu Prestes, 748, 05508-000, São Paulo, SP, Brazil, Brazil

**Abstract.** Modifications in low-density lipoprotein (LDL) have emerged as a major pathogenic factor of atherosclerosis, which is the main cause of morbidity and mortality in the western world. Measurements of the heat diffusivity of human LDL solutions in their native and *in vitro* oxidized states are presented by using the Z-Scan (ZS) technique. Other complementary techniques were used to obtain the physical parameters necessary to interpret the optical results, e.g., pycnometry, refractometry, calorimetry, and spectrophotometry, and to understand the oxidation phase of LDL particles. To determine the sample's thermal diffusivity using the thermal lens model, an iterative one-parameter fitting method is proposed which takes into account several characteristic ZS time-dependent and the position-dependent transmittance measurements. Results show that the thermal diffusivity increases as a function of the LDL oxidation degree, which can be explained by the increase of the hydroperoxides production due to the oxidation process. The oxidation products go from one LDL to another, disseminating the oxidation process and caring the heat across the sample. This phenomenon leads to a quick thermal homogenization of the sample, avoiding the formation of the thermal lens in highly oxidized LDL solutions. © *2012 Society of Photo-Optical Instrumentation Engineers (SPIE).* [DOI: 10.1117/1.JBO.17.10.105003]

## 1 Introduction

Atherosclerotic disease is the leading cause of death and morbidity in the western world.[1] It is a systemic, dynamic, progressive and essentially inflammatory disease. Since Steinberg and colleagues in 1989 suggested that modification of low-density lipoprotein (LDL) is involved in atherosclerosis,[2] a large number of studies have confirmed the hypothesis that the modification of LDL is the key for the formation and progression of atherosclerotic lesions in humans and experimental animals.[3,4] Furthermore, studies have shown that atherosclerosis is associated with higher concentrations of modified LDL (moLDL) in the bloodstream.[5,6] Recently, Haka et al.[7] used a combination of Raman and fluorescence spectroscopies to investigate the atherosclerotic plaque formation.

The difficulty in determine directly the amount of moLDL in the bloodstream, associated with the existence of few techniques for this purpose, led our group to use the Z-Scan technique (ZS)[8,9] and develop a new physical approach for the quantification of moLDL in a sample of LDL isolated from the human blood. The ZS technique was developed with the purpose of measuring the nonlinear optical response of a sample in a simple and direct way. Mainly, it is used to characterize the nonlinear response of inorganic materials,[10–12] however, nonlinear optics can play a significant role in the understanding of systems of biological interest. Recently, Vasudevan et al.[13]

reported an investigation about the death process of red blood cells by using the thermal lens technique. Lapotko et al.[14] used this technique to study the diameter, the degree of spatial heterogeneity of light absorbance and laser-induced damage thresholds in various types of cells.

Some years ago, we showed that there is a relationship between structural changes in LDL particle and its nonlinear optical response in the thermal time-scale regime (i.e., typical times of $\sim 10^{-3}$ s).[15] Moreover, we used the ZS to show that patients with periodontal disease had a higher amount of moLDL particles when compared to healthy individuals.[16] This conclusion was possible analyzing the amplitude the value of $\theta$)[15] of the peak-to-valley characteristic ZS curve of LDL solutions extracted from those individuals. LDL particles in solution present a value of $\theta$ that depends on this oxidation degree: the higher the oxidation degree, the smaller the value of $\theta$. Solutions of unmodified LDL (native LDL) present a pronounced ZS optical response with a high value of the parameter $\theta$. The ZS technique showed to be very sensitive, being able to differentiate solutions of minimally oxidized LDL from solutions of native LDL (naLDL), which cannot be distinguished with the biochemical techniques commonly used.

The parameter $\theta$ depends on different sample properties, namely, the thermo-optical coefficient, the density, heat capacity, linear optical absorption coefficient and thermal diffusivity. Despite the experimental fact that this parameter depends on the oxidative degree of the LDL particles, until now, there has not been an understanding of what occurs with the particles during

Address all correspondence to: Antonio M. Figueiredo Neto, Universidade de São Paulo, Instituto de Física, Departamento de Física Experimental, Rua do Matão, Travessa R, 187, 05508-090, São Paulo, Brazil. Tel: 55-11-3091-6638; Fax: 55-11-3091-6771; E-mail: afigueiredo@if.usp.br

this oxidation process that changes their nonlinear optical response, modifying the value of $\theta$. This knowledge is important not only from a fundamental point of view, but also may help in the understanding of LDL modification process and eventually propose new therapies.

Gómez et. al.,[17] showed that the linear absorbance coefficient of LDL solutions decreases (in the range between 250 and 550 nm) with the increasing of sample's oxidation degree. This decrease could be associated to the consumption of carotenoids during the oxidation process. The decrease in the sample absorbance is one of the responsible factors for the change in the nonlinear optical response. Other candidates to explain the observed behavior are the heat capacity, the thermo-optical coefficient and the thermal diffusivity. All these parameters are related with the nonlinear optical transmittance and influence the $\theta$ value.

In this paper, we focus on the different physical parameters of the sample that can influence on the amplitude of the nonlinear optical response. We report on measurements of the density, heat capacity, linear optical absorption coefficient, thermo-optical coefficient and thermal diffusivity of native and *in vitro* oxidized LDL (oxLDL) solutions. This type of oxidative process mimics, in some extent, what may happen in the human circulatory system.[18] Therefore, we aim to determine the role of each of these physical parameters in the nonlinear optical response of LDL samples due to the oxidation process. Different experimental techniques besides the ZS were employed in this study. In particular, in the case of the analysis of the ZS experimental results, we propose a fitting method, which takes into account the time-evolution of the transmittances measured and the typical peak-to-valley curve in the same fitting procedure. We used a high-performance liquid chromatography (HPLC) coupled to UV-Vis and fluorescence detectors to quantify the oxidation products, in particular the hydroperoxides and the $\alpha$-tocopherol, and correlate these quantities with the physical parameters measured.

## 2 Materials and Methods

### 2.1 Isolation of LDL

LDL was isolated from plasma by density differences in a sequential ultracentrifugation process at $10^5$ g, at 4℃, using a 75-rotor from Hitachi Ultracentrifuge.[19] The obtained solution was dialyzed for 24 h at 4℃ against phosphate buffered saline (PBS), pH 7.4. Protein concentration was determined using bicinchoninic acid (BCA) protein assay kit (Pierce, USA) with bovine serum albumin as standard.

### 2.2 LDL In Vitro Oxidation by Copper Ions

*In vitro* oxLDL was obtained by incubation of naLDL with 20 $\mu$M CuSO$_4$/mg protein at 37℃.[20] The samples were oxidized sequentially from 10 to 90 min, in steps of 10 min. At each predefined time, the oxidation reaction was inhibited with the addition of 1 mM of EDTA to the sample solution.

### 2.3 Spectrophotometry

Spectrophotometry setup was composed by a light source with a deuterium and a halogen lamps, a sample holder and two spectrophotometers from Ocean Optics, model USB4000. The lamps cover the light spectrum between 200 and 1100 nm. In this

set-up, light is lead from the source to the sample holder and then to the spectrophotometers by optical fibers.

### 2.4 Refractometry

To measure the thermo-optical coefficient of the samples we used a refractometer, from Atago, model 3T, connected to a heating/cooling system, from Julabo, model F12. Temperature was varied between 23℃ and 46℃. Measurements were performed with only the native and 90 min *in vitro* oxidized LDL.

### 2.5 Calorimetry and Densitometry

Heat capacity at constant volume ($c_v$) measurements were performed using a Differential Scanner Calorimeter (DSC) from Shimadzu, model DSC-60. Temperature was varied between 25℃ and 45℃ with a slope of 5℃/min. The density of the samples was measured using pycnometers made of glass, with volumes of approximately 500 $\mu$l.

### 2.6 Z-Scan Technique

ZS set-up was composed by a continuous-wave (CW) Nd:YVO$_4$ ($\lambda = 532$ nm) laser model Verdi V10 from Coherent, with a Gaussian profile beam. In this set-up the laser beam was chopped at 17 Hz and focused by a 25.4 mm lens with focal distance $f = 150$ mm, which gave a Rayleigh length $z_0 = 3.84 \pm 0.20$ mm.[21] Transmitted light was collected by a silicon photo detector model PDA36A from THORLABS, positioned at the far field (distance between the beam waist and the detector was about 1500 mm). All samples were measured using sample holders with 200 $\mu$m of width. The incident power of the laser on the samples varied between $121.9 \pm 1.0$ and $153.1 \pm 1.0$ mW. The power of the beam was set to obtain the ZS peak-to-valley dependence curve in the limit of the technique, i.e., the normalized transmittance lies between 1.2 and 0.8.

For each sample, we measured the time-dependent transmittance in 80 different $z$ positions around beam waist. At every position 10 independent measurements were performed.

To construct the ZS position-dependent transmittance curve it is necessary to make a normalization using the average time-dependent curve in every $z$ position. The normalization used is as follows $\Gamma_N(z) = I(0.03s, z)/I(0, z)$, where $I(t, z)$ stands for the transmittance measured at the time $t$ and position $z$. The value $t = t_s = 0.03$ s corresponds to the time when the thermal lens effect reaches the steady state. Our set-up allows concomitantly the measurement of the nonlinear optical absorption and refraction. The samples did not present any nonlinear optical absorption in all the experimental conditions investigated.

### 2.7 HPLC Measurements of Hydroperoxides

The lipid content of both naLDL and oxLDL was extracted according to the Bligh and Dyer method.[22] Briefly, methanol and chloroform containing 1 mM butylated hydroxytoluene (BHT) were added to each LDL sample. The resulting mixture was centrifuged at 1000 g for 10 min and the lower phase retrieved. Each sample was concentrated, resuspended in 50 $\mu$L and injected in the HPLC. The HPLC method consisted of gradient of water (solvent A) and methanol (solvent *B*). The gradient was: 90%B for 10 min; 90% to 100% *B* for 1 min; 100% *B* for 19 min; 100% to 90% *B* for 1 min; 90% *B* for

9 min. Determinations were made in a Nexera HPLC system (Shimadzu Co.) equipped with a photo diode array detector. A phenomenex column (Luna C8 4.6 mm × 15 cm) was used for the separations. The flow was adjusted to 1.0 mL/min and 10 $\mu$L was the injection volume. Maximum pressure was 250 Kgf/cm$^2$. Unoxidized cholesterol esters (Ch) and phospholipids (PL) were monitored in 205 nm. The respective hydroperoxides (ChOOH and PLOOH) were monitored in 235 nm.

## 2.8 Tocopherol Analyses by HPLC

The antioxidant content of the LDL samples was extracted and analyzed according to the method proposed by Hatam and Clayden.[23] Briefly, to 100 $\mu$L of each LDL sample a mixture containing NaOH 60%, ethanol and pyrogallol 6% was added. Samples were then incubated for 30 min at 70°C. At the end of this incubation, 1 mL of NaCl 1% and 1 mL of a mixture of ethylacetate:hexane (1:9 v/v) were added to each sample and the organic phase retrieved. The samples were dried with $N_2$, resuspended in 100 $\mu$L of methanol:ethanol (1:1 v/v) and injected in the HPLC. The HPLC method consisted of a gradient of water (solvent A) and acetonitrile (solvent B). The gradient was: 10% B for 0.5 min; 10% to 85% B for 2.5 min; 85% B for 3.5 min; 85% to 10% B for 0.2 min; 10% B for 3.3 min. Determinations were made in the same system as described in Sec. 2.7. A Shim-pack column (XR-ODS 75 × 2 mm) was used for the separations. The flow was adjusted to 0.45 mL/min and 10 $\mu$L was the injection volume. The $\alpha$-tocopherol content was monitored in 298 nm.

## 3 Results and Discussion

Figure 1 shows typical (average) time-dependent normalized transmittance curves in two different z positions of the sample (naLDL), before and after the focal point. From the set of time-dependent transmittance curves of each sample we construct the ZS characteristic position-dependent normalized transmittance curve (Fig. 2). Our results corroborate the fact that the bigger the oxidation time, the smaller the peak-to-valley amplitude. The asymmetry observed in some of the ZS curves seems to be caused by experimental errors, since the samples did not
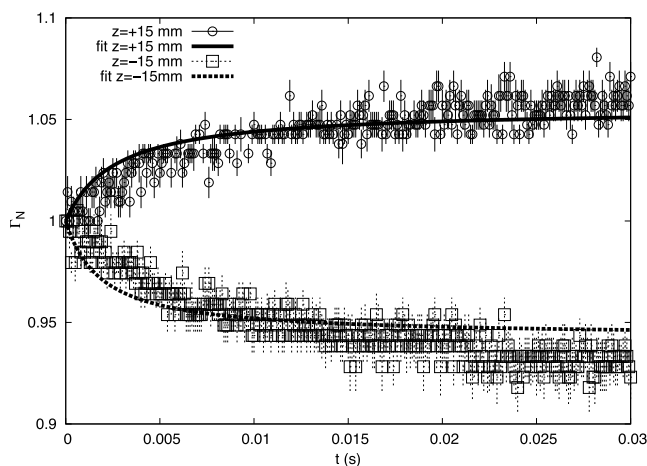


**Fig. 2** Position-dependent normalized transmittance curves as a function of z, from native (△), 60 min (■) and 90 min (○) copper oxidated LDL samples. Solid and dashed lines are fits with Eq. (4).

show nonlinear optical absorption in the experimental conditions of this work.

The time-dependent and position-dependent transmittance curves can be analyzed by using the thermal-lens model.[21] In this framework the normalized time and position-dependent transmittance is written as:

$$\frac{I(t,z)}{I(0,z)} = \left\{ 1 + \frac{\theta}{(1+t_c/2t)}\left[\frac{2(z/z_0)}{1+(z/z_0)^2}\right] + \left[\frac{\theta}{1+t_c/2t}\right]^2\left[\frac{1}{1+(z/z_0)^2}\right] \right\}^{-1}, \quad (1)$$

where $z_0$ is the Rayleigh length ($z_0 = \pi\omega_0^2/\lambda$), $\lambda$ is the laser wavelength, and $\omega_0$ is the spot radius at the beam waist. The parameters $\theta$ and $t_c$ are defined as:

$$\theta = \frac{2.303\,PA}{\lambda D\rho c_p}\left(-\frac{dn}{dT}\right), \quad (2)$$

$$t_c = \frac{\omega_0^2[1+(z/z_0)^2]}{4D}, \quad (3)$$

where $P$ is the beam power in the sample, $A = -\log_{10}(1-\alpha L)$ is the decadic absorbance, $\alpha$ is the linear optical absorption coefficient at $\lambda$, $L$ is the sample thickness, $c_p$ is the heat capacity at constant pressure, $dn/dT$ is the thermo-optical coefficient and $D$ is the thermal diffusivity.

Usually, to analyze the position-dependent normalized transmittance curve, Eq. (1) is written fixing $t = t_s$, and there are two fitting parameters, $\theta$ and $t_c$. In the same way, to analyze the time-dependent normalized transmittance curve at a given $z^*$ position, Eq. (1) is used fixing $z = z^*$, and again one has two fitting parameters $\theta$ and $t_c$. However, the fitting parameters $\theta$ and $t_c$ must be the best to fit the position-dependent and the time-dependent normalized transmittances. At this point, we propose an iterative method to fit all the time and position-dependent transmittance curves at the same time. With this



**Fig. 1** Typical (average) time-dependent normalized transmittance curves in two different z positions of the sample (naLDL) with the respective fit. The focal point is located at $z = 0$ mm.
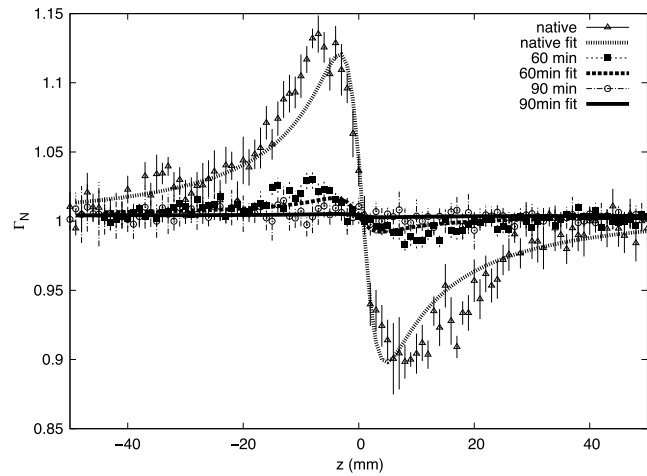
procedure we are able to determine the pair ($\theta$ and $t_c$) that best fit the whole set of curves (about 50 time-dependent curves and 1 position-dependent curve) for each sample investigated. Dr. F. Batalioto, an expert from our group, developed best-fit software to account for this task.

Gómez et al. showed that the linear absorption at $\lambda = 532$ nm of a completely oxidized LDL sample solution is much lower than that of a naLDL sample solution.[17] Figure 3(a) shows the linear absorption coefficient of the LDL sample solutions as a function of the oxidation time. The naLDL presents a yellowish aspect, which tends to disappear as a function of the oxidation process. Possible responsibles for this are the carotenoids present in the LDL structure, mainly inlaid in the phospholipid monolayer. To verify this hypothesis we measured the carotenoid content in the samples, as a function of the oxidation time, by using the HPLC. Figure 3(b) shows the carotenoids percentage extracted from the LDL solutions and linear absorption of the samples for each oxidation time. We see that the carotenoids are responsible for about 50% of the sample linear absorption, and after 90 min of oxidation, practically all the carotenoids are consumed.

Let us now analyze the samples nonlinear optical response represented by the parameter $\theta$. If the linear absorption was the only physical parameter, characteristic of the sample, responsible for the variation of $\theta$ [Eq. (2)], $\theta$/PA should be independent on the oxidation time. Figure 4 shows $\theta$/PA as a function of the oxidation time for all the samples investigated. As $\theta$/PA shows a decreasing behavior as a function of the

oxidation degree, at least, one more parameter in Eq. (2) is changing with sample's oxidation degree. The result shown in Fig. 4 must be interpreted at the moment as a tendency of $\theta$/PA decrease as the oxidation time increases. The actual errors in each measurement of $\theta$ are certainly larger than those depicted in Fig. 4 (obtained only from the fitting procedure). Biological samples are very complexes and the response of them to manipulation may introduce additional variations which increase the errors in the measured parameters. The values of $t_c$ encountered in the fitting process vary from about $4 \times 10^{-4}$ s to $8 \times 10^{-4}$ s, but with large fitting uncertainty, i.e., the curves are less sensitive to variations in this parameter when comparing to the sensitivity in $\theta$.

As the linear optical absorption is not the unique parameter changing with the oxidation time we will focus our attention to the other parameters present in Eq. (2).

The measured density, heat capacity at constant volume and thermo-optical coefficient as a function of the oxidation time are shown in Fig. 5(a) to 5(c), respectively. In Eq. (2) the heat capacity at constant pressure ($c_p$) is present. It is reasonable to assume that in our samples (liquid at the SATP) $c_p \approx c_v$. Figure 5(b) shows that $c_v$ does not present a significant variation as a function of the oxidation time. From these measurements we calculate the mean value $\bar{c}_v = 3.73 \pm 0.24$ J/(g · K) for the LDL samples, which is compatible within two standard deviations, with that of water [4.18 J/(g · K)].[24] In the same way, measurements of the density and thermo-optical coefficient presented an almost constant behavior as a function of the sample oxidation time [Fig. 5(a) and 5(b)]. The mean values of these parameters are $\bar{\rho} = 1.006 \pm 0.010$ g/cm³ and $\overline{dn/dT} = (-1.34 \pm 0.08) \times 10^{-4}$/K. These values are, likewise, compatible with those from water.

As the parameters $\rho$, $c_v$ and $dn/dT$ of LDL solutions were shown to be constants as a function of the oxidation time, the modification of the nonlinear optical response observed in our experiments with the LDL solutions seems to be due to variations in the thermal diffusivity. Taking into account the presence of these parameters in Eq. (2), we will rewrite Eq. (1) explicitly as a function of the thermal diffusivity D, which will be the unique fitting parameter. This procedure is more appropriate for the fitting process since $\theta$ and $t_c$ are not independent parameters [as can be seen in Eqs. (2) and (3)]:
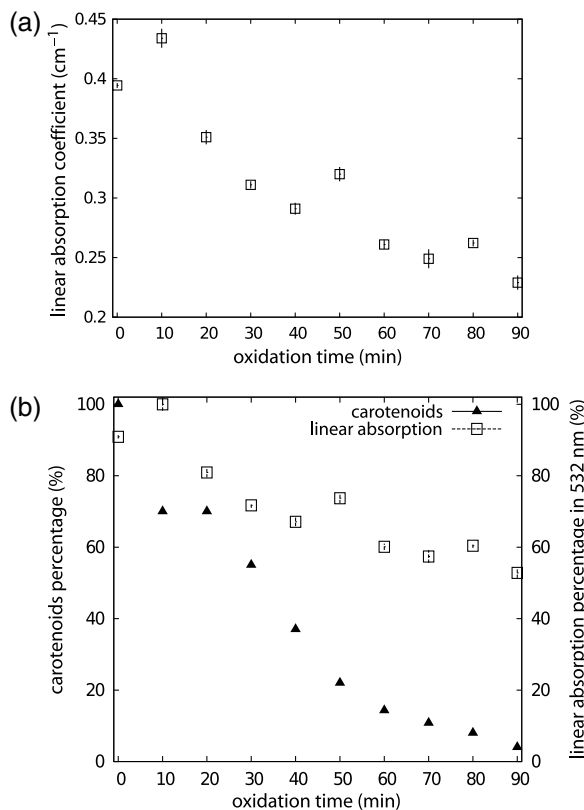


Fig. 3 (a) Linear absorption coefficient at 532 nm as a function of oxidation time. (b) The percentage of carotenoid content extracted from the LDL solutions (▲) present in the sample and the linear absorption coefficient at 532 nm (□) as a function of the oxidation time.
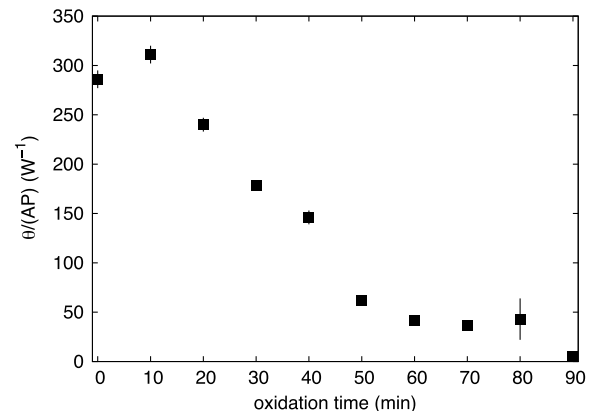


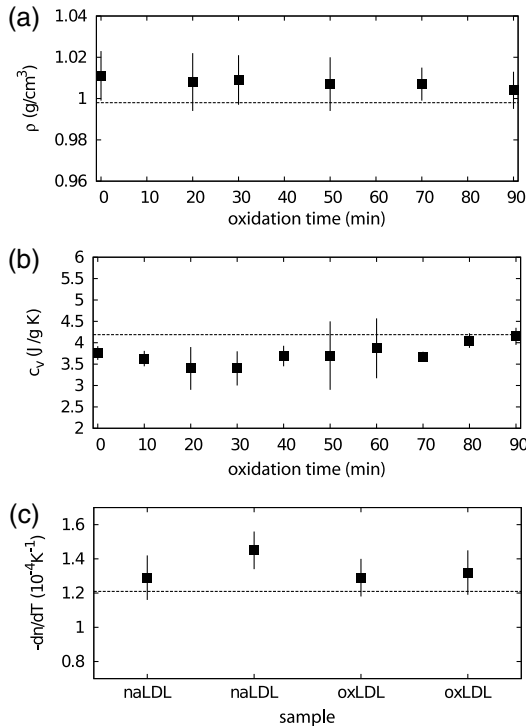Fig. 4 $\theta$/PA as a function of the oxidation time.

**Fig. 5** Experimental results of the (a) density; (b) heat capacity at constant volume; (c) thermo-optical coefficient, of the LDL samples, as a function of the oxidation time.

$$\frac{I(t,z)}{I(0,z)} = \left\{ 1 + \frac{2.303\,PA}{\lambda D \rho c_v}\left(-\frac{dn}{dT}\right) \right.$$
$$\times \frac{1}{\left(1 + \frac{\lambda z_0}{8\pi Dt}\left[1 + (z/z_0)^2\right]\right)}\left(\frac{2(z/z_0)}{1 + (z/z_0)^2}\right)$$
$$+ \left[\frac{2.303\,PA}{\lambda D \rho c_v}\left(-\frac{dn}{dT}\right)\frac{1}{\left(1 + \frac{\lambda z_0}{8\pi Dt}\left[1 + (z/z_0)^2\right]\right)}\right]^2$$
$$\left. \times \left(\frac{1}{1 + (z/z_0)^2}\right) \right\}^{-1}.$$
$$(4)$$

To determine $D$ through Eq. (4) we used the same fitting procedure as before, i.e., using the time and position-dependent normalized transmittance curves at the same time. Typical results of the fittings are shown in Figs. 1 and 2. The fit shown in Fig. 2 captures the overall physics of the system, however, the width of the peak and valley in the experiment is larger than that the fitting procedure furnishes. We verified that this deviation should be due to the error in the evaluation of the parameter $z_0$: The higher the $z_0$, the bigger the peak and valley widths. However, the amplitude of the nonlinear optical response, represented by the peak-to-valley amplitude does not present a significant variation changing a little the value of $z_0$. This aspect, which extrapolates the specific problem of the LDL solutions, is being faced by us theoretically, and will be the subject of a future publication. Figure 6 shows the thermal diffusivity as a function of the oxidation time.
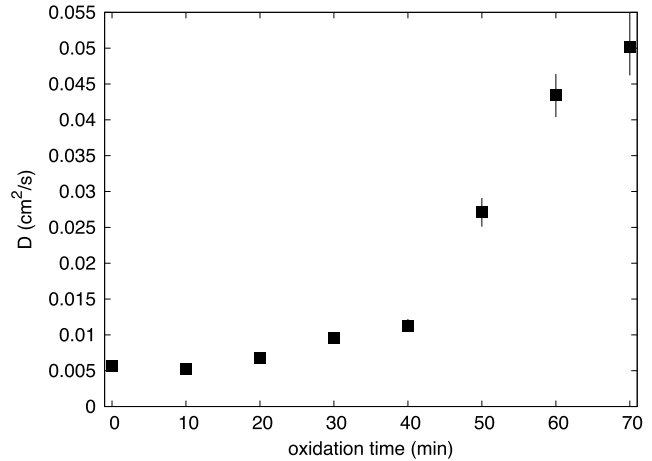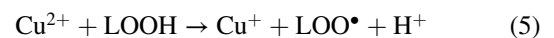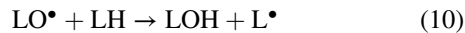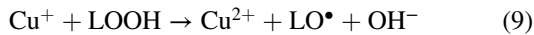


**Fig. 6** Thermal diffusivity of the LDL solutions as a function of the oxidation time.

We observe a tendency of $D$ to increase with the oxidation time. Samples oxidized for 80 and 90 min had very low linear absorption and low nonlinear transmittance. The normalized position-dependent ZS curves of these samples were flat, taking into account the experimental errors on the experimental points measured. In this way we could not determine a peak-to-valley and a reliable diffusivity value for these two samples. For that reason they do not appear in Fig. 6.

This result indicates that, with the sample oxidation procedure, the heat absorbed by the medium (mainly the LDL particles) diffuses more efficiently across the sample insofar as the oxidation time increases. In order to understand this process we have investigated the effect of the Cu-induced oxidation on lipid components in the LDL particles. Copper-mediated LDL oxidation process occurs in several steps [see scheme presented in the chemical Eqs. (5) to (10)].[25] It initiates with the reaction between $Cu^{2+}$ and preexisting lipid hydroperoxides (LOOH) generating peroxyl radicals [Eq. (5)]. These peroxyl radicals can react with $\alpha$-tocopherol (a membrane-integrating antioxidant, TOCH) or other lipid molecules (LH) present in the lipoprotein, yielding the respective radical species [Eqs. (6) and (7), respectively]. The reaction of $\alpha$-tocopherol with peroxyl radicals inhibits the progression of the oxidation. However, when almost all the $\alpha$-tocopherol content in LDL particle is consumed, the production of conjugated dienes and hydroperoxides begins to accelerate. This is the end of the initiation phase (or the lag stage). The major formation of hydroperoxides occurs in the propagation phase (or the log stage), in which the peroxyl radicals begin to react mostly with other lipid molecules producing more hydroperoxides [Eqs. (7) and (8)]. In addition, $Cu^+$ ions also can react with lipid hydroperoxides-in a Fenton-type reaction [Eq. (9)]-generating alkoxyl radicals ($LO^\bullet$). These radicals can lead, in a second reaction, to the formation of lipid radicals ($LO^\bullet$) [Eq. (10)], which enhances the propagation step and increases the formation of hydroperoxides. The process evolves until the hydroperoxides start to decompose into aldehydes, ketones, hydroxides and hydrocarbonates, reaching a stage, which is called the termination stage.[26] This whole process can take several hours.

$$Cu^{2+} + LOOH \rightarrow Cu^+ + LOO^\bullet + H^+ \qquad (5)$$

$$LOO^\bullet + TOCH \rightarrow LOOH + TOC^\bullet \qquad (6)$$

$$LOO^\bullet + LH \rightarrow LOOH + L^\bullet \qquad (7)$$

$$L^\bullet + O_2 \rightarrow LOO^\bullet \qquad (8)$$

$$Cu^+ + LOOH \rightarrow Cu^{2+} + LO^\bullet + OH^- \qquad (9)$$

$$LO^\bullet + LH \rightarrow LOH + L^\bullet \qquad (10)$$

Our ZS experiment shows that the nonlinear optical response of the sample drops to almost zero in less than 2 h, showing that ZS is sensitive to the beginning of the oxidation process.

To quantitatively investigate the oxidation process we measured, by using the HPLC, the $\alpha$-tocopherol consumption and the production of both cholesterol ester hydroperoxides



(ChOOH) and phospholipids hydroperoxides (PLOOH) along the oxidation process in LDL samples. Figure 7(a) and 7(b) shows an increase in the hydroperoxides content in the sample along with the oxidation time. On the other hand, the $\alpha$-tocopherol content in the samples decreases with increasing oxidation time [Fig. 7(c)]. Most of $\alpha$-tocopherol was consumed within 40 min of incubation and at this time a progressive increase in hydroperoxide content was observed. It is interesting to remark that the production of ChOOH and PLOOH present a time-dependent behavior very similar to that of the thermal diffusivity: a modest increasing rate until oxidation time of about 40 min and after that time a more pronounced increase in their amount. These results suggest a strong correlation between the hydroperoxides production and an increase of the sample's thermal diffusivity. It is important to point out that PLOOH, ChOOH and some other small molecules (therefore, more mobile in the solution) formed during the lipid peroxidation process can translocate from one LDL particle to another and, thereby, disseminate the oxidative damage.[26] This process of exchanging oxidation products between particles increases the heat diffusion across the sample. It is expected that the exchange of ChOOH and PLOOH increase with the oxidation time since more oxidation products are available in the solution. As a consequence of this oxidation products exchange between different LDL particles, the thermal diffusivity measured is expected to increase and the thermal lens response of the sample vanish as the oxidation time increases.

## 4 Conclusion

Our results show that native and oxidized LDL solutions present similar values of density, heat capacity and thermo-optical coefficient. On the other hand, the linear optical absorption decreases as a function of the oxidation time. The Z-scan experiment was used to measure the thermal diffusivity of native and oxidized LDL solutions with different oxidation times. The thermal diffusivity of oxidized LDL samples was shown to be bigger than that of native samples. The higher the oxidation time, the higher the thermal diffusivity of the sample. The linear optical absorption decrease observed in oxLDL is partially explained by the consumption of LDL's carotenoids, which is a consequence of lipid peroxidation processes. The increase in the thermal diffusivity, in turn, seems to be related to the production of lipid hydroperoxides. These hydroperoxides, PLOOH and ChOOH, are exchanged among the LDL particles, disseminating the oxidation process and spreading the heat across the sample. This hypothesis is reinforced by the HPLC measurements, in which the production of hydroperoxides correlates itself with the increase in the thermal diffusivity. In this sense, the higher the PLOOH and ChOOH production, the more efficient the heat diffuses across the solution. This phenomenon leads to a faster thermal homogenization at the solution, inhibiting the thermal lens formation observed prior to the LDL oxidation. The results reported herein indicate that the ZS technique can be a complementary tool to estimate the LDL oxidation state in human plasma.
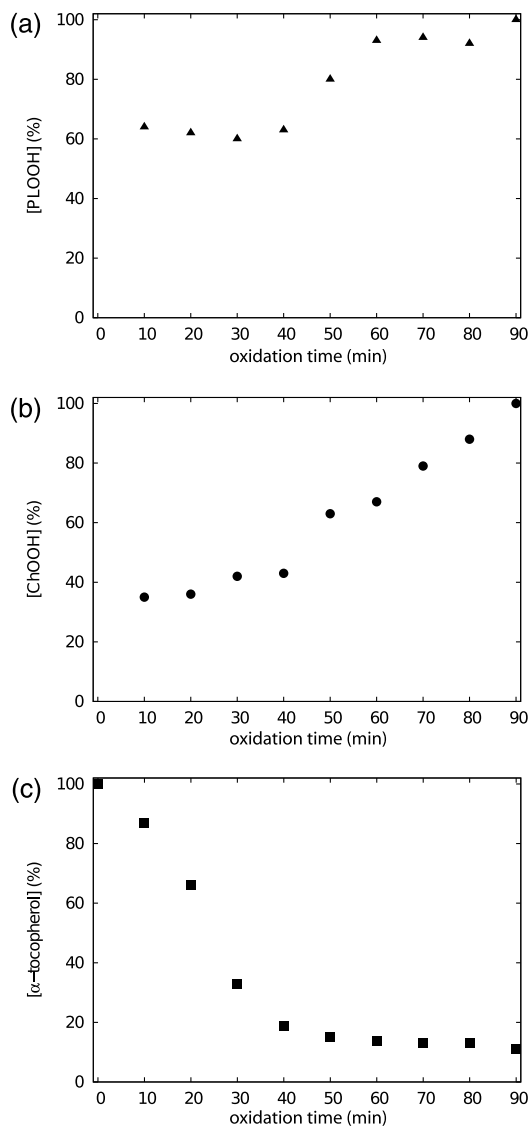
**Fig. 7** (a) Increase of phospholipids hydroperoxides content extracted from LDL solutions as a function of time. (b) Increase of cholesterol ester hydroperoxides content extracted from LDL solutions as a function of time. (c) Decrease of $\alpha$-tocopherol content extracted from LDL solutions as a function of oxidation time. The percentages were calculated considering the final incubation time (90 min) as 100% for phospholipid and cholesterol hydroperoxides. For $\alpha$-tocopherol the initial time was considered as 100%.

## References

1. A. D. Lopez et al., "Global and regional burden of disease and risk factors, 2001: systematic analysis of population health data," *Lancet* **367**(9524), 1747–1757 (2006).
2. D. Steinberg et al., "Beyond cholesterol. Modifications of low-density lipoprotein that increase its atherogenicity," *N. Engl. J. Med.* **320**(14), 915–924 (1989).
3. R. Stocker et al., "Role of oxidative modifications in atherosclerosis," *Physiol. Rev.* **84**(4), 1381–1478 (2004).
4. J. L. Witztum et al., "The oxidative modification hypothesis of atherosclerosis: does it hold for humans?," *Trends. Cardiovasc. Med.* **11**(3–4), 93–102 (2001).
5. S. Ehara et al., "Elevated levels of oxidized low density lipoprotein show a positive relationship with the severity of acute coronary syndromes," *Circulation* **103**(15), 1955–1960 (2001).
6. P. Holvoet et al., "Circulating oxidized LDL is a useful marker for identifying patients with coronary artery disease," *Arterioscler. Thromb. Vasc. Biol.* **21**(5), 844–848 (2001).
7. A. S. Haka et al., "Mechanism of ceroid formation in atherosclerotic plaque: in situ studies using a combination of Raman and fluorescence spectroscopy," *J. Biomed. Opt.* **16**(1), 011011 (2011).
8. M. Sheik-Bahae et al., "High-sensitivity, single-beam $n_2$ measurements," *Opt. Lett.* **14**(17), 955–957 (1989).
9. M. Sheik-Bahae et al., "Sensitive measurement of optical nonlinearities using a single beam," *IEEE J. Quantum Electron.* **26**(4), 760–769 (1990).
10. B. Gu et al., "Determination of the nonlinear refractive index in multiphoton absorbers by Z-scan measurements," *J. Opt. Soc. Am. B* **27**(11), 2438–2442 (2010).
11. S. Liu et al., "Optical nonlinear absorption characteristics of crystalline $Ge_2Sb_2/Te_5$ thin films," *J. Appl. Phys.* **110**(3), 033503 (2011).
12. T. R. Tsai et al., "Nonlinear optical properties of lanthanum-modified lead zirconate titanate investigated by the femtosecond Z-scan technique," *Appl. Phys. Lett.* **99**(24), 241101 (2011).
13. S. Vasudevan et al., "Application of thermal lens response to monitor health status of red blood cells: a quantitative study of the cell death process by extracting thermal diffusivity and size," *Appl. Phys. Lett.* **96**(11), 113703 (2010).
14. D. Lapotko et al., "Photothermal responses of individual cells," *J. Biomed. Opt.* **10**(1), 014006 (2005).
15. S. L. Gómez et al., "Cu and Fe metallic ions-mediated oxidation of low-density lipoproteins studied by NMR, TEM and Z-scan technique," *Chem. Phys. Lipids* **163**(6), 545–551 (2010).
16. A. M. Monteiro et al., "Cardiovascular disease parameters in periodontitis," *J. Periodontol* **80**(3), 378–388 (2009).
17. S. L. Gómez et al., "Characterization of native and oxidized human low-density lipoproteins by Z-scan technique," *Chem. Phys. Lipids* **132**(2), 185–195 (2004).
18. I. Levitan et al., "Oxidized LDL: diversity, patterns of recognition, and pathophysiology," *Antioxid. Redox Signal.* **13**(1), 39–75 (2010).
19. R. J. Havel et al., "The distribution and chemical composition of ultracentrifugally separated lipoproteins in human serum," *J. Clin. Invest.* **34**(9), 1345–1353 (1955).
20. E. C. Fernvik et al., "The autoantibody repertoire against copper- or macrophage-modified LDL differs in normolipidemics and hypercholesterolemic patients," *J. Clin. Immunol.* **24**(2), 170–176 (2004).
21. C. A. Carter et al., "Comparison of models describing the thermal lens effect," *Appl. Opt.* **23**(3), 476–481 (1984).
22. E. G. Bligh et al., "A rapid method of total lipid extraction and purification," *Can. J. Biochem. Physiol.* **37**(8), 911–917 (1959).
23. L. J. Hatam et al., "A high-performance liquid chromatographic method for the determination of tocopherol in plasma and cellular elements of the blood," *J. Lipid Res.* **20**(5), 639–645 (1979).
24. D. R. Lide, *Handbook of Chemistry and Physics*, CRC Press, Boca Raton, Florida (1998).
25. H. Esterbauer et al., "The role of lipid peroxidation and antioxidants in oxidative modification of LDL," *Free Radic. Biol. Med.* **13**(4), 341–390 (1992).
26. A. W. Girotti, "Translocation as a means of disseminating lipid hydroperoxide-induced oxidative damage and effector action," *Free Radic. Biol. Med.* **44**(6), 956–968 (2008).